Ph.D. course in:

"Food and Human Health"

XXXVII cycle

Dissertation title

"Application of an Eco-sustainable technology: use of direct and photodynamic UV light for the microbial inactivation in food industries"

Ph.D student

Alessia Lena

Supervisor

Michela Maifreni

2025

La presente pubblicazione è il risultato del progetto realizzato con il cofinanziamento dell'Unione Europea - FSE REACT-EU, PON Ricerca e Innovazione 2014-2020, UniUD

Table of Contents

List of abbreviations 7
Summary 9
Chapter 1 11
Introduction 11
1.1 The prevalence of food pathogens and spoilage bacteria and non-thermal technology as a strategy for safety and quality 12
1.2 Light sources and parameters 14
1.2.1 Light Emitting Diodes 14
1.2.2 Wavelength 15
1.2.3 Irradiance 15
1.2.4 Dose 16
1.2.5 Microbial inactivation calculation 16
1.3 Microbial inactivation 16
1.3.1 Mode of action 16
1.3.2 Endogenous Photosensitizers 18
1.3.3 Exogenous Photosensitizers 24
1.3.4 Fungi 25
1.3.5 Microbial biofilms 26
1.4 Parameters that influence the Blue Light microbial inactivation 30
1.4.1 Microbial concentration, oxygen consumption and growth phase of the microbes 30
1.4.2 Temperature 31
1.4.3 pH 32
1.4.4 Water Activity (a_w) 32
1.5 Microbial resistance to Blue Light 32
1.6 Blue Light and food contact surfaces decontamination 33
1.7 Blue Light and food products 34
1.7.1 Milk and dairy products 34
1.7.2 Horticultural products 34
1.7.3 Meat and fishery food products 35
1.8 Blue Light and synergy with other applications 35
1.8.1 Free and immobilized PS 35
1.8.2 Natural and Synthetic compounds 37
1.8.3 Technologies 38
1.9 Safety of Blue Light 38
Section 1 40
Chapter 2 41
Qualitative and quantitative screening of Blue Light microbial inactivation 41

2.1 Introduction 42
2.2 Aim of the study 42
2.3 Material and Methods 43
2.3.1 Blue Light Source 43
2.3.2 Screening of microbial inactivation capacity of Blue Light 44
2.3.3 Quantitative assessment of microbial inactivation capacity of Blue Light 45
2.3.4 Inactivation kinetic of blue light against microorganism 46
2.3.5 Data analysis 47
2.3.6 Microbial Strains and Culture Conditions 48
2.4 Results and Discussion 48
2.4.1 Characterisation of different parameters for photodynamic inactivation 48
2.4.2 Assessment of Photodynamic Inactivation on microbes based on endogenous photosensitizers 51
2.4.3 Kinetics of inactivation of food-related microbes with Blue Light 59
2.5 Conclusions 67
Chapter 3 68
Reactive oxygen species formation by light technologies and microbial damages 68
3.1 Introduction 69
3.2 Aim of the study 70
3.3 Material and methods 71
3.3.1 Microbial Strains and Culture Conditions 71
3.3.2 Light irradiation 71
3.3.3 Bacterial cell culture preparation and light treatment 71
3.3.4 Cell Viability 72
3.3.5 Live/Dead PCR 73
3.3.5.1 DNA extraction 73
3.3.5.2 Real-Time PCR 73
3.3.5.3 Viable cell quantification through Live/Dead qPCR 74
3.3.6 DCFH-DA assay 75
3.3.7 TBAR assay 75
3.3.8 Data Analysis 75
3.4 Results and discussion 76
3.5 Conclusion 88
Chapter 4 89
Inactivation of microbial Biofilm with Blue Light 89
4.1 Introduction 90
4.2 Aim of the study 90
4.3 Material and Methods 92

4.3.1 Microbial Strains and Culture Conditions 92
4.3.2 Blue Light source 92
4.3.3 Biofilm formation 92
4.3.3.1 5-days biofilm formation 92
4.3.3.2 Biofilm formation on glass surfaces 93
4.3.4 5-days biofilm Blue Light treatment 93
4.3.5 13-days biofilm Blue Light treatment 94
4.3.5.1 Confocal Laser Scanning Microscope (CLSM) Visualization 95
4.3.6 Sample quantification 95
4.4 Statistical analysis 95
4.5 Results and Discussion 96
4.5.1 5-days biofilms 96
4.5.2 13-days biofilm 100
4.6 Conclusions 109
Chapter 5 110
Application of Light technologies to domestic furniture: Blue Light vs UVA 110
5.1 Introduction 111
5.2 Aim of the study 112
5.3 Material and Methods 113
5.3.1 Microbial Strains and Culture Conditions 113
5.3.2 Light Source 113
5.3.3 Light treatment 114
5.3.4 Data analysis 115
5.4 Result and Discussion 116
5.4.1 Irradiance measurements 116
5.4.2 Effectiveness of light treatment at different wavelengths (UVA and Blue Light) 120
5.5 Conclusions 125
Section 2 126
Exploitation of Exogenous Photosensitizers for Photodynamic Inactivation 127
Chapter 6 128
Exploitation of a synthetic photosensitizer: Methylene Blue 128
6.1 Introduction 129
6.2 Aim of the study 130
6.3 Material and methods 131
6.3.1 Microbial culture 131
6.3.2 Photosensitizer 131
6.3.3 Lamp characterisation 132
6.3.4 Photodynamic inactivation tests in transparent liquid substrate 132

6.3.5 Photodynamic inactivation test in an organic substrate 133
6.3.6 Biofilm preparation on culture media and milk 134
6.3.7 Biofilm treatment 134
6.3.8 Statistical Analysis 135
6.4 Results and Discussion 136
6.4.1 Photodynamic Inactivation (PDI) in a liquid substrate 136
6.4.2 Photodynamic Inactivation (PDI) treatment on milk 138
6.4.3 Photodynamic Inactivation (PDI) treatment on microbial biofilm formed in culture media 141
6.4.4 Photodynamic Inactivation (PDI) treatment on microbial biofilms formed in milk 143
6.5 Conclusions 146
Chapter 7 147
Exploitation of a natural photosensitizer: Curcumin 147
7.1 Introduction 148
7.2 Aim of the study 149
7.3 Material and Methods 150
7.3.1 Microbial Strains and Culture Conditions 150
7.3.2 Blue Light Source 150
7.3.3 Curcumin solution preparation 150
7.3.4 Blue Light treatment 151
7.3.5 Data analysis 152
7.4 Results and Discussion 153
7.5 Conclusions 156
Chapter 8 157
Microbial inactivation by Photoactive Materials 157
8.1 Introduction 159
8.2 Aim of the study 161
8.3 Material and Methods 162
8.3.1 Experimental set-up 162
8.3.2 Microbial Strains and bacterial cell culture preparation 162
8.3.3 Material preparation 162
8.3.3.1 Preparation of the vanillin dimer 162
8.3.3.2 Preparation of Valpol material 163
8.3.4 Synthesis of the photoactive material 164
8.3.4.1 Pretreatment of Valpol for the preparation of composite blends 164
8.3.4.2 Preparation of composite blends to obtain active materials 164
8.3.4.3 Preparation of polymeric material tablets 164
8.3.5 Blue Light source 165

8.3.6 Blue Light Treatment 165
8.3.7 Photodynamic Inactivation of microorganisms on Valpol material at different 4MeP concentrations 165
8.3.8 Photodynamic Inactivation of microorganisms on glass 168
8.3.9 Microbial Biofilm 168
8.3.10 Biofilm formation 168
8.3.11 Biofilm Blue Light treatment 169
8.3.12 Reutilisation of the Valpol material 170
8.3.13 Data analysis 170
8.4 Results and Discussion 171
8.4.1 Characteristics of the Valpol material 171
8.4.2 Photodynamic inactivation of *E. coli* with Valpol at different porphyrin (4MeP) concentrations 172
8.4.3 Photodynamic inactivation of *L. monocytogenes* with Valpol at different porphyrin (4MeP) concentrations 176
8.4.4 Photodynamic inactivation of *E. coli* and *L. monocytogenes* biofilms grown in Valpol and glass surfaces 179
8.5 Conclusion 183
Chapter 9 184
General Discussion 184
9.1 Brief Introduction 185
9.2 Discussion 188
9.2.1 Section 1 188
9.2.2 Section 2 192
References 196

List of abbreviations

4MeP	5,10,15,20-tetrakis(4-methylphenyl)-21H,23H-porphine
AgNPs	Silver nanoparticles
ALA	5-aminolevulinic acid
ANOVA	Analysis of variance
a_w	Water Activity
BCFAs	Branched-Chain Fatty Acids
BHI	Brain Heart Infusion broth/agar
BL	Blue Light
CCPs	Critical Control Points
CDots	Carbon Dots
Ce6	Clorine e6
CFU	Colony Form Units
D	Dose
DC	Dark Control
DCFH-DA	2′,7′-Dichlorofluorescin Diacetate
DMSO	Dimethyl sulfoxide
LB	Luria Bertani broth
LDPE	Low-Density Polyethylene
LED	Light-Emitting Diode
Log	Logarithm
EDOT	Ethylenedioxythiophene
FCS	Food Contact Surfaces
GMP	Good Manufacturing Practice
GRAS	Generally Recognized as Safe
H_2O_2	Hydrogen Peroxide
ICNIRP	Non-Ionizing Radiation Protection
MDA	Malondialdehyde
MDRAB	Multidrug-resistant *A. baumannii*
MRD	Maximum Recovery Diluent
MRSA	Methicillin-Resistant *Staphylococcus aureus*
NB	Nutrient Broth
OD	Optical Density
PBS	Phosphate Buffer Solution
PCA	Plate Count Agar
PDI	Photodynamic Inactivation
PS	Photosensitizer

PVC	Poly(vinyl) Chloride
QS	Quorum Sensing
ROS	Reactive Oxygen Species
SCCS	Scientific Committee on Consumer Safety
SD	Standard Deviation
T	Temperature
t	time
TBAR	Thiobarbituric Acid Reactive Substances
TBO	Toluidine Blue
Tf	Final Temperature
TSA	Tryptone Soy Agar
TSB	Tryptone Soy Broth
UHT	Ultra-High-Temperature
UV	Ultraviolet
VBNC	Viable But Non Countable
WHO	World Health Organization

Summary

Visible light, particularly blue light (BL), has emerged as a non-thermal, chemical-free method for microbial inactivation in food-related contexts. By ensuring product safety and extending shelf life without compromising quality, BL not only enhances food preservation but also aligns with sustainable and consumer-friendly practices. Due to the novelty of this technique, the mechanism of action and the bacterial response in not fully elucidated.

This PhD thesis investigates the application of BL for microbial inactivation. The research initially concentrated on leveraging endogenous photosensitizers (PS) inherently present within bacterial cells. By optimizing treatment parameters and determining the optimal dose range, subsequent experiments were conducted in various substrates, including agar and liquid media (Chapter 2), as well as on mature biofilms (Chapter 4), to replicate scenarios relevant to food-related environments.

Tests conducted on agar and liquid substrates highlighted the greater susceptibility of Gram (+) bacteria compared to Gram (-) bacteria. However, variability was observed even within the same bacterial class. This heterogeneity could be attributed to differences in the quantity, type, and intracellular localization of the PS, as well as to the bacteria's specific oxidative stress response mechanisms.

Biofilms were cultivated over periods of 5 and 13 days on different surfaces, and their reduction, along with morphological alterations post-irradiation, was validated using confocal laser scanning microscopy. The findings consistently demonstrated that lower BL wavelengths exhibit greater antimicrobial efficacy than higher wavelengths. Furthermore, Gram (+) bacteria were found to be significantly more susceptible to BL treatment compared to Gram (-) bacteria.

Along this research, we also compared the effects of 365 nm (UVA) and 405 nm (BL) wavelengths on the production of reactive oxygen species (ROS), which are known to mediate cellular damage and death following light irradiation (Chapter 3). Two key types of cellular damage were assessed: lipid peroxidation and membrane permeabilization. The microbial reduction results suggested that, in addition to membrane permeabilization, other ROS-mediated mechanisms contribute to microbial inactivation.

In collaboration with Electrolux Italia S.p.A., a moke-up system for 365 nm and 405 nm light irradiation was designed, developed, and optimized for potential integration into consumer appliances (Chapter 5). The system's performance was evaluated across two configurations, focusing on the uniformity of emitted irradiance, light dosage, microbial inactivation, and

energy efficiency. Results indicated that at both room and refrigerated temperatures, microbial inactivation was consistent between the two wavelengths, emphasizing that the emitted light dose was the most critical parameter for achieving effective inactivation.

The study advanced by investigating exogenous PS in solution, utilizing Methylene Blue (MB) as a synthetic PS and curcumin as a natural alternative (Chapters 6 and 7). Experimental findings with MB highlighted that factors such as the liquid substrate's characteristics—particularly its opacity and the presence of organic matter—and the microbial gram-type significantly influence the required PS concentration. These variations are necessary to achieve comparable microbial reductions in both planktonic cells and biofilms.

The application of curcumin demonstrated a similarly high level of microbial reduction across both Gram (+) and Gram (-) bacteria, albeit with distinct kinetic profiles. In this context, the use of monochromatic light enabled effective microbial inactivation with a low concentration of photosensitizer and minimal light dosage, highlighting its efficiency.

The study also investigated an exogenous PS, 4MeP porphyrin, supported within a vanillin-based material, Valpol (Chapter 8). Materials containing different porphyrin concentrations (5% and 10%) demonstrated a greater susceptibility of Gram (+) bacteria compared to Gram (-) bacteria in planktonic form. With equivalent PS concentrations, Gram (+) bacteria required a lower light dose for effective inactivation. Reuse of the material, at both porphyrin concentrations, enhanced microbial inactivation due to increased PS exposure to light following the formation of pores in the material. Notably, the relationship between increased PS content and microbial inactivation was nonlinear. For microbial biofilms formed on the material's surface, the reduction was minimal regardless of the 4MeP concentration or bacterial gram type.

In conclusion, this thesis advances the study of light-based technologies within the food sector by exploring various applications relevant to food-related contexts and initiating the technological transfer necessary for implementation. The findings underscore the importance of several critical parameters for the effective application of this technology, including light dose, microbial type, light wavelength, and substrate characteristics. These factors were identified as the most influential in achieving microbial reduction. Consequently, the selection of optimal conditions tailored to the specific application is essential for the successful deployment of light-based treatments in this field.

Chapter 1

Introduction

1.1 The prevalence of food pathogens and spoilage bacteria and non-thermal technology as a strategy for safety and quality

The World Health Organization (WHO) approximates that annually, nearly 600 million people, or almost 1 out of every 10 individuals, become sick from ingesting contaminated food. Moreover, globally, approximately 33 million deaths occur each year due to the consumption of unsafe food, though this figure is likely underestimated (World Health Organization, 2015). In order to avoid any possible contamination, the maintenance of a sanitised and disinfected environment is crucial. Food companies are always seeking innovative technologies to assure food safety for the consumer, to avoid cross-contaminations along the food chain, which could also maintain the sensorial characteristics of the food products. Cross-contaminations are the main cause of food contamination during food production. Therefore, to prevent them, it is crucial to uphold a sanitized environment, particularly on surfaces that come into contact with food.

Some of the most prevalent bacteria known to cause illness include *Bacillus* spp., *Escherichia coli*, *Listeria monocytogenes*, *Salmonella* spp., and *Staphylococcus aureus*. *Bacillus cereus*, a Gram (+) bacterium, can lead to food poisoning if present in food. *E. coli* and *Salmonella* spp., both Gram (-) bacteria belonging to the *Enterobacteriaceae* family, naturally reside in the human gut microbiota. However, certain strains of these bacteria can cause severe illness in humans and are commonly found in water and soil, often due to contamination from animal faeces (Andino & Hanning 2015; Eng et al., 2015; Knodler & Elfenbein 2019; Yang et al., 2017). Salmonellosis and Shiga Toxin produced by *E. coli* (STEC) were the second and third most commonly reported foodborne gastrointestinal infections in humans in the European Union in 2023, respectively (EFSA & ECDC 2023). *L. monocytogenes*, a Gram (+) bacterium, poses a significant threat as a foodborne pathogen due to its ability to infect both humans and animals, being the fifth zoonosis responsible for hospitalization and death in 2023 (EFSA & ECDC 2023). This bacterium is widespread and challenging to eradicate because of its resistance to low temperatures, high salt concentrations, and its capacity to form biofilms (Thakur et al. 2018). For this reason, the European Commission regulated its presence on foodstuffs with the Commission Regulation (EC) No. 2073/2005. *S. aureus* is a pathogen affecting humans and animals and is a major cause of foodborne illness globally, affecting mainly meat and meat products, poultry and egg products, milk and dairy products, salads and bakery products (Kadariya et al., 2014). Food poisoning can also occur due to ingestion of

staphylococcal enterotoxins produced in food during its growth, or through the consumption of raw milk or raw milk cheese from dairy animals with *S. aureus* mastitis (Fetsch & Johler 2018). The issue of antimicrobial resistance, particularly Methicillin-Resistant *Staphylococcus aureus* (MRSA), is of considerable concern since could also colonize food-producing animals (EFSA 2009).

In addition to pathogenic bacteria, the food industry faces challenges from spoilage microorganisms, which can degrade the quality of raw and ready-to-eat products. One such microorganism is *Pseudomonas fluorescens*, a psychrotrophic Gram (-) bacterium. This versatile microorganism can thrive across various temperatures and contaminate various food products, including meat and dairy, whether stored at room temperature or refrigerated. Its enzymatic activities, particularly the production of lipases and proteases, contribute to spoilage. Furthermore, the formation of biofilms by *P. fluorescens* presents a significant challenge for the food industry, as biofilms facilitate cross-contamination (Kumar et al., 2019; Rajmohan et al., 2002).

Non-thermal technologies, such as light treatments (Ultraviolet, UV), have been studied in the past years for microbial inactivation. Presently, the rise of bacterial resistance to disinfectants and antibiotics poses a significant concern, prompting researchers to explore new decontamination methods. Various approaches exist to sanitize industrial settings, with some relying on light-based technologies. Light technologies, such as UV light categorized into UVA, UVB, and UVC (**Figure 1.1**), have been extensively studied for their efficacy against pathogens and spoilage microbes in water, surfaces, air, and food products without leaving residues (Bhardwaj et al., 2021; Kebbi et al., 2020; Kim & Kang, 2018; Manzocco et al., 2011). However, their use for microbial decontamination presents several drawbacks, including limited penetration, the need to position the target sample close to the light source, and potential hazards for operators due to prolonged exposure leading to conditions like skin cancer, facial erythema, and eye problems such as keratoconjunctivitis, ground-glass eyeballs, welder's flash, and snow blindness (Guerrero-Beltrán & Barbosa-Cánovas, 2004; Trevisan et al., 2006; Zaffina et al., 2012).

The quest for innovative sanitation solutions in the food industry, coupled with growing interest in light technologies, has led researchers to explore other parts of the electromagnetic spectrum.

The visible region (400-700 nm) is subdivided into four parts (**Figure 1.1**): blue (400-480 nm), green (480-560 nm), yellow/orange (560-610 nm), and red (610-760 nm) (Zwinkels, 2015).

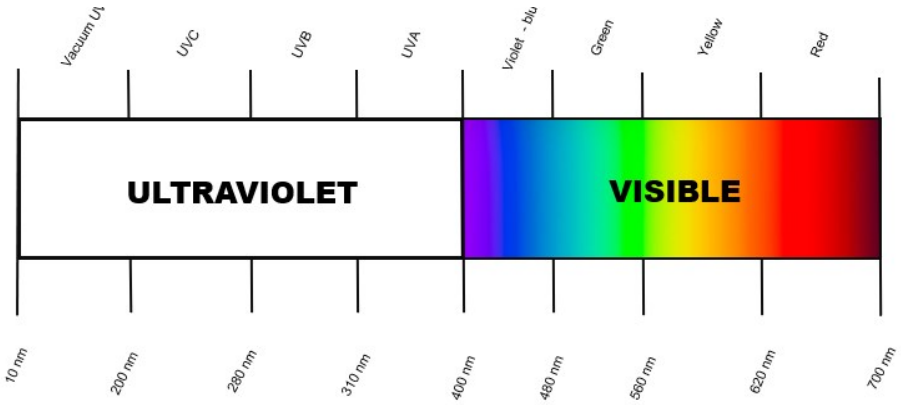


Figure 1.1 Ultraviolet (UV) and visible parts of the light electromagnetic spectra (Lena et al., 2024)

Among light-based technologies, Blue Light (BL) appears to hold the most promise for microbial inactivation. BL technology was born a few times ago and it was applied largely in the medical field due to its ability to target microbial cells while minimizing damage to mammalian cells, making it suitable for treating various localized infections, including superficial and deep-seated ones (Bumah et al., 2020; Liu et al., 2020; Tsutsumi-Arai et al., 2022; Wang et al., 2019; Zhang et al., 2023). BL has also been shown, to a lesser extent, to be the potential for surface decontamination, and, in some cases, for sanitizing food contact surfaces (FSC) and food products (Aurum & Nguyen, 2019; Bache et al., 2018; Prasad et al., 2020; Weber et al., 2019). The application of BL seems a promising technology to control microbes, as bacteria seem less likely to develop resistance to it (this aspect will be addressed in Paragraph 5). However, due to the relatively recent application of this technology, most studies have been conducted in laboratory culture media. Consequently, research on its application to surfaces or food products remains limited, and various factors, such as its penetration depth on different surfaces, have not been thoroughly investigated.

1.2 Light sources and parameters

1.2.1 Light Emitting Diodes

In the past, light technology (i.e., UV light) relied on low-pressure and medium-pressure mercury lamps but, the recent advancement of light-emitting diodes (LED) technology has emerged as a preferable alternative for light treatments. LED are solid-state semiconductor

diodes comprised of a p-n junction that emits light at a specific wavelength through the phenomenon of electroluminescence (Dutta Gupta & Jatothu, 2013). Conventional mercury lamps come with various drawbacks, including mercury toxicity, high energy consumption, the need for warming up, overheating, and a relatively short lifespan (<12,000 hours) (Jo & Tayade 2014; Martín-Sómer et al., 2017; Vilhunen et al., 2009; Würtele et al., 2011). In contrast, LED lamps offer several advantages from both an energy and economic perspective. LEDs have a lifespan exceeding 100,000 hours, allow for the use of specific wavelengths, are low-cost and do not require special disposal methods after use (Crawford et al., 2005; Ghate et al., 2015; Josewin et al., 2018a; Singh et al., 2021).

In order to work with light, it is important to have a thorough understanding of some light and processing parameters, such as the following.

1.2.2 Wavelength

BL represents the initial segment of the visible spectrum following the UV section, spanning from 400 nm to 480 nm. Some researchers (Angarano et al., 2020; Hoenes et al., 2021a,b; Murdoch et al., 2013) define the wavelength range from 400 nm to 450 nm as violet light. Thus far, a majority of scientific investigations have focused on 405 nm blue LED lamps, with lesser attention given to those emitting wavelengths within the 450 - 460 nm range. The prevalence of 405 nm LED usage may be attributed to its proximity to the UV spectrum, potentially enhancing microbial inactivation. Additionally, the specific wavelength of emitted light can influence microbial inactivation rates for the specificity with photosensitizer (PS) absorption wavelength (Hoenes et al., 2018).

1.2.3 Irradiance

Irradiance (I) is defined as the radiant power received by a surface per unit area of the sample, expressed in watts per square centimetre (W cm^{-2}). Essentially, it quantifies the rate at which energy is transmitted to the surface, and its estimation is crucial for setting up a light treatment. The irradiance of LED emitting light at different wavelengths, at a specific distance from the surface, is typically measured using radiometers, which are devices equipped with probes. These probes consist of an electronic ammeter connected to a light sensor head, generating a current proportional to the incident irradiance (Bolton & Linden 2003). Irradiance is influenced by light intensity, which is contingent upon photon fluence (∅), and it is inversely proportional

to the distance from the light source to the sample: as the distance increases, irradiance decreases (Bolton & Linden 2003; Prasad et al., 2020).

1.2.4 Dose

Energy dose (D), or fluence, is defined as the total radiant energy incident from all directions onto a small sphere divided by the cross-sectional area of that sphere. The energy dose is equal to the product of the irradiance and the exposure time, as reported in (1):

(1)

$$D = I \cdot t$$

where D represents the energy dose of the LED light per unit of area (J cm^{-2}), I represents the irradiance of the LED light (W cm^{-2}) and t represents the exposure time to LED light (s)(Bolton et al., 2015). The dose value required for disinfection may vary according to the microorganisms' species (both species and strains could exhibit differences) and on the final effect required for each food product.

1.2.5 Microbial inactivation calculation

The microbial inactivation produced by BL may be expressed as reported in Equation (2):

(2)

$$\frac{N_t}{N_0} = e^{-k \cdot I \cdot \Delta t} = e^{-k \cdot D}$$

Where N_t is the final microbial population after Δt, N_0 is the initial microbial population, k is the microbe-dependent inactivation constant, and I is the irradiance received by the microbes (μW cm^{-2}). The equation may also be expressed in terms of dose, since it corresponds to the multiplication of I for Δt, as reported in Equation 2 (Singh et al., 2021).

1.3 Microbial inactivation

1.3.1 Mode of action

The utilization of visible light wavelengths as an antimicrobial requires three primary actors: oxygen, a PS (either endogenous or exogenous), and light with an appropriate wavelength that matches the absorption spectrum of the photosensitizer (Dai et al., 2012; Kim et al., 2015). Upon light absorption (**Figure 1.2**), the PS passes from a low ground energy state to an excited

singlet state (with a lifetime of 10^{-9} to 10^{-6} seconds) and then to an excited triplet state (with a lifetime of 10^{-3} to 10 seconds). In this triplet state, it can interact with the surrounding environment through two reactions. The first pathway, known as the type I reaction, involves an electron transfer from the substrate to the PS, resulting in the formation of unstable ions that can generate reactive oxygen species (ROS) upon further interaction with the substrate. These ROS include superoxide anions (O^{2-}), hydroxyl radicals (•OH), and hydrogen peroxide (H_2O_2). Indeed, the type II reaction relies on the production of singlet oxygen radicals ($^1O_2$) through energy transfer from the triplet-state PS to ground-state molecular oxygen (Cossu et al., 2021). Both reactions occur during photoactivation in bacterial cells, although one may predominate over the other depending on the intracellular oxygen levels. Indeed, the availability of oxygen serves as a limiting factor in singlet oxygen production (Ghate et al., 2019; Maclean et al., 2008b). Recently, Hamblin & Abrahamse (2020) proposed a "type III photochemical pathway," which involves three oxygen-independent PS (psoralens, tetracyclines, and inorganic salts) that lead to bacterial death. In the case of psoralens and tetracyclines, cell death occurs through the binding of the PS to a molecular structure within bacterial cells. For inorganic salts, the process may involve the formation of a PS radical anion and an inorganic radical, which subsequently attack microbial cells. However, many mechanisms involving organic salts still rely on the presence of oxygen.

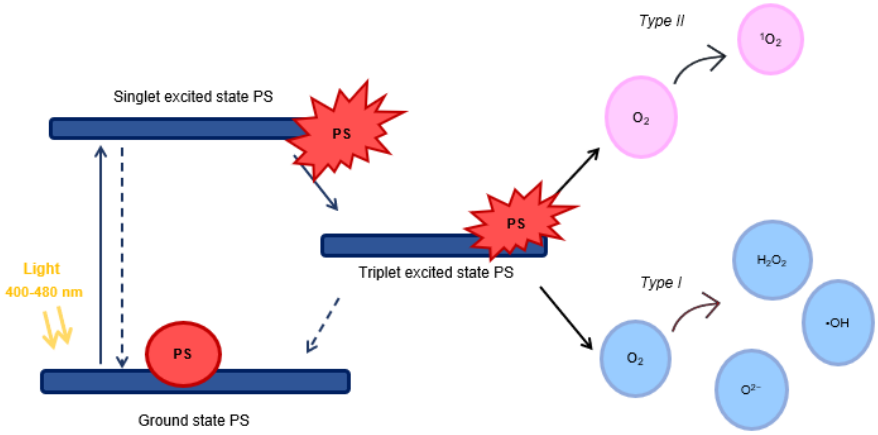


Figure 1.2. Schematic representation of photoactivation. The photosensitizer (PS) is in a ground state. When it absorbs energy from light, it is promoted to a singlet excited state. Here it can emit all the energy, in the phenomena called fluorescence, or it can pass to a triplet energy state. Now, the excited PS can undergo type I and type II reactions forming different Reactive Oxygen Species (ROS) (Lena et al., 2024).

In response to environmental stresses, ROS are naturally produced and accumulated in microbial cells causing oxidative stress (Ray et al., 2012). Under normal conditions, microbial cells employ various antioxidant systems to counterbalance ROS, including superoxide dismutase, catalases, glutathione peroxidases, glutathione reductases, thiol peroxidases, thioredoxins, glutaredoxins, and peroxiredoxins (Belozerskaya & Gessler 2007; Bishai et al., 1994; Fang 2004; Fang et al., 1999; Seyler et al., 2001). In the case of biofilms, the promotion of the extracellular polymeric substance (EPS) matrix and adjustments to biofilm heterogeneity also serve as defence mechanisms against oxidative stress (Wang et al., 2021). However, if ROS accumulate faster than the defence mechanisms can detoxify cells, they may cause damage to various cell components, including the bacterial membrane, DNA, proteins, and lipids, ultimately leading to cell death via necrosis or apoptosis (**Figure 1.3**) (Amin et al., 2016; Cabral & Rodrigues, 2019; Choby & Skaar, 2016; Kim et al., 2015; Luksiene & Paskeviciute, 2011; Plavskii et al., 2018).

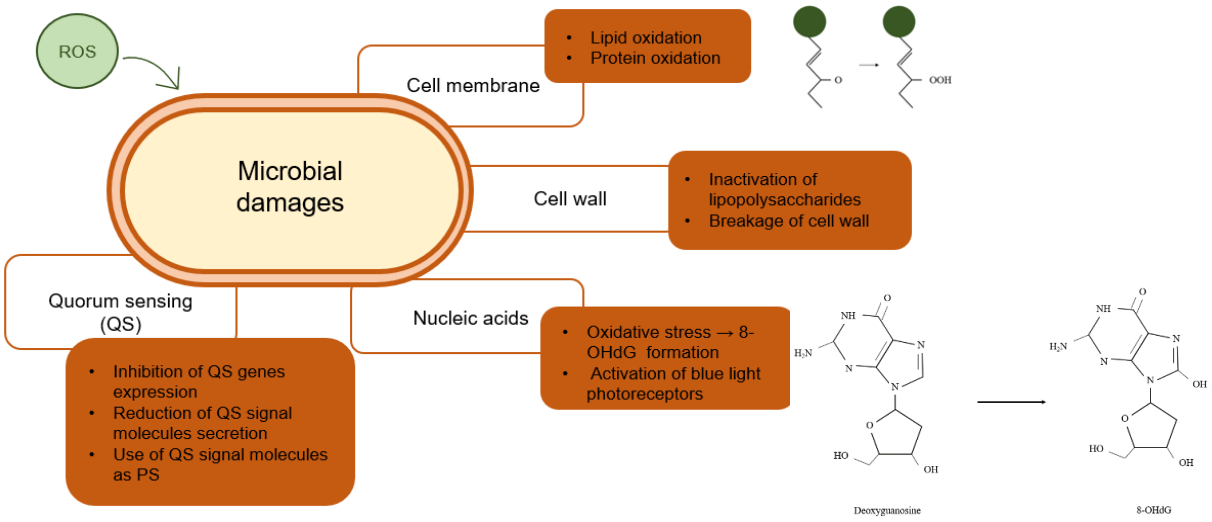


Figure 1.3. Schematic representation of the microbial damages operated by ROS in the cell membrane, cell wall, nucleic acids and on the quorum sensing (QS) system (Lena et al., 2024).

1.3.2 Endogenous Photosensitizers

Microbes possess intracellular PS (i.e., porphyrins, flavins, cytochromes, and NADH) that can be activated by BL (**Figure 1.4**). Porphyrins, including coproporphyrin III, protoporphyrin IX, zinc protoporphyrin, and uroporphyrin III, exhibit peak absorption around 405 nm, declining towards 450 nm. Therefore, at higher wavelengths, other endogenous PS like FAD or flavins

become involved in photoinactivation, as they demonstrate significant absorbance around 450 nm and also at 470 nm (Hoenes 2017; Hoenes et al., 2018; Plavskii et al., 2018). The use of endogenous PS activated by light is termed antimicrobial BL.

The effectiveness of BL treatment is influenced by microbial characteristics. Gram (+) and Gram (-) bacteria exhibit notably different susceptibility to photosensitization, likely due to structural differences in their cell walls. Gram (+) microbes are characterized by a thick and porous peptidoglycan layer (15 – 80 nm thickness), which facilitates the penetration of PS into the inner plasma membrane. In contrast, Gram (-) bacteria have inner and outer membranes separated by a thin layer of peptidoglycan. The outer membrane of Gram (-) cells presents a highly organized, compact structure, hindering the binding of porphyrins and similar molecules and rendering them less sensitive to certain porphyrin-mediated photodynamic inactivation (PDI) (Luksiene 2005; Malik et al., 1992; Yin et al., 2013). Gram (-) bacteria show resistance to anionic and neutral porphyrins since ROS are not effectively produced in sensitive regions upon illumination; however, they appear to be susceptible to cationic ones. Alves et al. (2009) demonstrated that a photo-treatment with cationic porphyrins, using a light dose of 64.8 J cm^{-2}, reduced > 7 log of *E. coli* and *Enterococcus faecalis* bacterial suspensions. Similarly, in a study by Minnock et al. (1996), suspensions of *E. coli* and *P. aeruginosa* were effectively photo-inactivated in the presence of a cationic water-soluble zinc pyridinium phthalocyanine (PPC).

Gram (-) species typically require longer exposure times compared to Gram (+) species. A 180-minute (108 J cm^{-2}) exposure was necessary to achieve a 4.2 log reduction of *Acinetobacter baumannii* suspension, and a 300-minute (180 J cm^{-2}) exposure was needed to achieve a 3.1 log reduction of *E. coli* suspension with 405 nm BL. In contrast, *Staphylococcus* spp., *Streptococcus pyogenes*, and *Clostridium perfringens* strains were reduced by up to 5 log colony-forming units (CFU) after exposures ranging between 60 and 90 minutes with 405 nm BL, using doses of 36, 54, and 45 J cm^{-2}, respectively (Maclean et al., 2009).

Table 1.1 presents several examples of microbial inactivation following exposure to BL irradiation. Upon reviewing the data presented in the table, it becomes apparent that a significant portion of the studies conducted thus far have utilized wavelengths near the UV spectra. This choice is likely due to the confirmed efficacy of UV light in microbial inactivation, prompting researchers to explore similar wavelengths within the visible light spectrum for their antimicrobial properties.

Table 1.1 Effect of the blue light to inactivate planktonic cells in different conditions: in vitro, packaging and food. Microbial inactivation results are reported as in the references, with any modifications.

Wavelength	Microorganism	Substrate	Dose (J cm^{-2})	Microbial inactivation	Temperature (°C)	Reference
415	*Pseudomonas aeruginosa* ATCC 19660	Brain Heart Infusion (BHI) broth	48	3.54 log	Not mentioned	(Amin et al., 2016)
400	*P. aeruginosa* ATCC 15692	Phosphate Buffere Saline (PBS)	108	5.59 log	Not mentioned	(Halstead et al., 2016)
405	*P. aeruginosa* ATCC 27853	Tryptic Soy Agar (TSA)	15	89.5%	Not mentioned	(Guffey & Wilborn, 2006)
470				39.3%		
413	*P. aeruginosa* ATCC 27853	Milk	720	5.0 log	Not mentioned	(dos Anjos et al., 2020)
400	*Staphylococcus aureus* ATCC 29213	PBS	108	6.76 log	Not mentioned	(Halstead et al., 2016)
461	*S. aureus* ATCC 6538	Tryptic Soy Broth (TSB)	596.7	4.7 log	10	(Ghate et al., 2013)

405 ***470***	*S. aureus* ATCC 25923	TSA	15	87.9% 62.0%	Not mentioned	(Guffey & Wilborn, 2006)
400	*Stenotrophomonas maltophilia* QEHB	PBS	108	7.21 log	Not mentioned	(Halstead et al., 2016)
400	*Escherichia coli* EPEC CFT_073	PBS	108	4.71 log	Not mentioned	(Halstead et al., 2016)
461	*E. coli* O157:H7 EDL933	TSB	596.7	5.1 log	10	(Ghate et al., 2013)
405	*E. coli* K-12	Luria Bertani (LB) Broth	67.49	100%	Not mentioned	(Barneck et al., 2016)
435	*E. coli* ATCC 25922	Cucumbers, tomatoes, lettuce,	33.8	3.0 log	Not mentioned	(Glueck et al., 2017)
461	*Salmonella* Typhimurium ATCC 14028	TSB	596.7	4.6 log	10	(Ghate et al. 2013)
413	*S.* Typhimurium ATCC 14028	Milk	720	5.0 log	Not mentioned	(dos Anjos et al., 2020)
464	*S.* Typhimurium	Cucumber	18	7.5×10^3 CFU/mL	Not mentioned	(Guffey et al., 2016)
405	*Salmonella Enteritidis PT4*	TSB	Not mentioned	5.82 log	4	(Keyvan et al., 2022)

405	*Salmonella spp.*	Fresh-cut papaya	1.7 x 10^3	1.0 - 1.2 log	4	(Kim et al., 2017b)
405	*Salmonella* spp.	Cantaloupe rinds	1210	2.3 log CFU/cm^2	4	(Josewin et al., 2018b)
460	*Listeria monocytogenes*	Smoked salmon	Not mentioned	1.2 log 1.1 log	4 12	(Josewin, et al., 2018a)
405	*L. monocytogenes*	Stainless steel coupons contaminated by salmon exudates	748.8	2.4 log 2.4 log 1.9 log	4 15 25	(Li et al., 2018)
405	*L. monocytogenes*	Acrylic coupons contaminated by salmon exudates	748.8	2.8 log 2.4 log 2.4 log	4 15 25	(Li et al., 2018)
405	*Campylobacter jejuni*	Stainless steel coupon contaminated with bacteria chicken exudate	183.4	4.9 log	56	(Gunther et al., 2016)
405	*Campylobacter coli*	Stainless steel coupon contaminated with bacteria chicken exudate	180.8	5.1 log	53.6	(Gunther et al., 2016)
405	*Bacillus cereus* ATCC 12826	Polyolefine, a mixture of polyethylene/polypropylene	Not mentioned	4.5 log	Not mentioned	(Luksiene e Paskeviciute 2012)

402	*Acinetobacter baumanii*	PBS	84	1.8 log	Not mentioned	(Buchovec et al., 2023)
402	*Stenotrophomonas maltophilia*	PBS	50.4	1.3 log	Not mentioned	(Buchovec et al., 2022)
410	*Aeromonas bestiarum*	Anchovy and sardine skin	200	3 log	Not mentioned	(Orlandi et al., 2024)

1.3.3 Exogenous Photosensitizers

To enhance the antimicrobial effect of BL, exogenous PS can be added to the microbial suspension, a process known as photodynamic inactivation (PDI). Some commonly used exogenous PS (**Figure 1.4**) include curcumin, porphyrins, riboflavin, hypericin (natural), as well as synthetics like Rose Bengal, methylene blue (MB), Clorine e6 (Ce6), toluidine blue (TBO), expanded porphyrins, methylene blue, and eosin Y (Alberto et al., 2016; Alhenaki et al., 2021; Bonin et al., 2018; He et al., 2022; Makdoumi et al., 2017; Song et al., 2020). The efficacy of PDI is highly dependent on the microbe being targeted and the type of PS utilized. Considering the type of PS, when applying BL in combination with eosin cumin (5 μM), Rose Bengal (1 μM), and curcumin (5 μM) to *E. faecalis*, were observed reductions from 7.8 ± 0.70 CFU/mL to 2.9 ± 0.30 CFU/mL, 0.5 ± 0.30 CFU/mL, and 0.15 ± 0.36 CFU/mL, respectively (Pileggi et al., 2013).

Another approach involves inducing the synthesis of porphyrins inside bacterial cells by adding their precursor, δ-aminolevulinic acid (ALA), a metabolite naturally occurring in cellular heme synthesis. Oriel & Nitzan (2010) induced porphyrin synthesis by adding ALA and its hydrophobic derivative ALA methyl ester (m-ALA) to inactivate *C. albicans* suspension after visible light treatment. They found that an initial concentration of 100 mg/ml ALA or m-ALA, associated with a light dose of 36 J cm^{-2}, caused reductions of 1.6 or 2.1 orders of magnitude, respectively. Similarly, Buchovec et al. (2010) observed that *L. monocytogenes* cell suspension decreased from 2.3 log to 3.7 log, and biofilm on packaging material decreased from 1.7 log to 3 log, depending on the concentration of ALA used (7.5 - 10 mM).

The use of exogenous PS in PDI could be advantageous by reducing the inactivation time or light dose needed, or enhancing the inactivation rate of microbes, decreasing the energy consumption of the lamps. However, in food environments and food products, several considerations must be taken into account. Firstly, any added compound should be generally recognized as safe (GRAS), ensuring that it poses no harm to consumers. Additionally, it's crucial that the added PS does not alter the quality characteristics of the food product, including its organoleptic and visual appearance. Maintaining the safety and quality of food products is fundamental, and any antimicrobial treatment applied should not compromise these aspects. Therefore, when selecting exogenous PS for PDI in food applications, their safety profile and potential impact on food quality must be carefully evaluated.

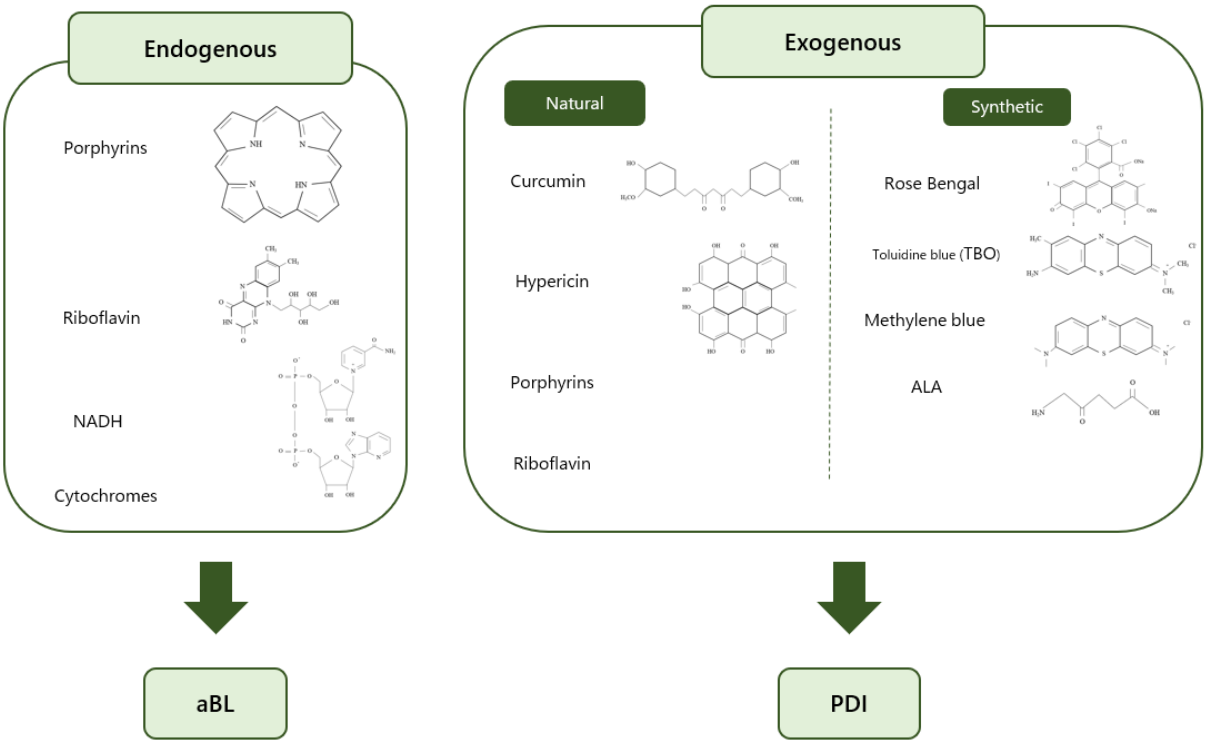


Figure 1.4. Representation of the common endogenous and exogenous photosensitizer (PS) molecules. In the case of the activation of endogenous PS, the process is called antimicrobial Blue Light (BL); differently, the addition of exogenous photosensitizers takes the name of Photodynamic Inactivation (PDI). Furthermore, the exogenous PS could be natural or synthetic (Lena et al., 2024).

1.3.4 Fungi

While there are some publications on the use of PS and light to eradicate yeasts and other fungi, fewer studies have focused on the physiochemical properties of the PS used in these treatments. Unlike bacteria, fungi possess complex targets for photosensitizers in their external wall (i.e., glucan, mannan, chitin, and lipoprotein). However, they seem to be less susceptible to PDI. Studies have indicated that fungi primarily suffer damage to their plasma membrane and mitochondria, where endogenous porphyrins are located. The lower sensitivity of fungi to PDI is attributed to factors such as the presence of a nuclear membrane acting as an additional barrier, larger cell size, and reduced number of targets for singlet oxygen per unit volume of the cell (Donnelly et al., 2008; Fraikin et al., 1996; Murdoch et al., 2013).

When considering exogenous PS, fungi tend to favour hydrophilic compounds with charged groups over lipophilic ones. Upon absorption, exogenous PS are distributed to subcellular targets, and the effectiveness of treatment depends on oxygen availability, singlet oxygen formation, its short lifetime (10^{-6} s), limited diffusivity (movement capability of ca. 0.1 μm),

and reaction with cell targets (e.g., nucleic acids, membrane lipids or cytoplasmic enzymes). Generally, the closer the target is to the PS, the higher the likelihood of cellular damage.

In the literature, there are few examples from *in vitro* studies to demonstrate the potential effectiveness of BL inactivating various fungi. *S. cerevisiae* and *C. albicans* suspensions exposed to 405 nm light (dose of 288 and 576 J cm^{-2}, respectively) exhibited significant reductions in microbial load (5 log CFU) (Murdoch et al., 2013). Fluorescence spectroscopy revealed the presence of intracellular free porphyrins, indicating susceptibility to PDI, when excited at 405 nm. In particular, the most important PS are protoporphyrin IX and zinc protoporphyrin, and not coproporphyrin. Indeed, at 450 nm, fluorescence spectra analysis showed that no porphyrins are involved in 450 nm PDI: at this wavelength, flavins appear to be the key PS (Hoenes et al., 2018).

Similarly, studies on *Fusarium oxysporum*, *Botrytis cinerea*, and *Rhizopus stolonifera* demonstrated varying degrees of susceptibility to BL treatment, with differences observed based on the substrate (Trzaska et al., 2017). Additionally, the use of exogenous PS like curcumin (800 mM) has shown promise in inactivating fungi such as *Botrytis cinerea* spores: Huang et al. (2021) used 120 J cm^{-2} BL (430 nm) combined of curcumin resulted in no spore germination, meaning that BL treatment inactivated 10^4 CFU/mL of spores. However, further research is needed to explore the efficacy and safety of these treatments in food applications.

1.3.5 Microbial biofilms

A biofilm refers to a structured assembly of microorganisms firmly attached to a surface and enclosed within a matrix primarily composed of polysaccharide material, which is secreted by the microorganisms (Costerton et al., 1987; Donlan, 2002; Kokare et al., 2009). Its development involves several stages, including bacterial attachment to a surface, microbial growth, formation of microcolonies, maturation of the biofilm, and eventual detachment and dispersal of biofilm cells (Donlan 2002; Kokare et al., 2009; Kumar & Anand 1998). Biofilms are found on various surfaces where viable microorganisms exist, such as plastics, metals, glass, living tissues, natural aquatic systems, and food products. While single-species biofilms have been extensively studied *in vitro*, the majority exist as complex communities of multiple microbial species, offering advantages like metabolic cooperation, resistance mechanisms, increased genetic diversity through DNA sharing, and *quorum sensing* (QS) (Peters et al., 2012; Wolcott et al., 2013).

Controlling biofilms poses a challenge in environments where microbial communities are problematic, such as the food industry, where biofilm eradication is crucial to prevent cross-contamination. Various strategies, including chemical disinfection, have conventionally been used for biofilm elimination, but due to concerns related to antibiotic resistance and environmental and human health, alternative physical methods have been developed (Dai et al., 2012; Kumar & Anand 1998; Marino et al., 2018; McKenzie et al., 2013). BL has emerged as a potential tool against microbial biofilms which can be employed to prevent its formation, serving as a good manufacturing practice (GMP). ROS produced by BL can disrupt biofilms by destabilizing the microbial community, causing cell lysis, disrupting the matrix structure, and interfering with cell motility and *quorum sensing* (Cheng et al., 2020; Fekrirad et al., 2019; Halstead et al., 2016; Huang et al., 2020).

Studies on biofilm were done exploiting both endogenous and exogenous PS (i.e., curcumin, rutium gallium(III), Ce6, vitamin K3, octyl gallate, etc) (Martegani et al., 2020; Minhaco et al., 2023; Negri et al., 2023; Nie et al., 2021; Pourhajibagher et al., 2024; Shi et al., 2022a). Yang et al. (2017) demonstrated that irradiation with 460 nm light, at doses of 240 J cm^{-2} or 360 J cm^{-2}, effectively killed most *S. aureus* MRSA biofilm cells by disrupting their structure, as evidenced by live/dead staining analysis. Ferrer-Espada et al. (2020) exposed biofilms of *Acinetobacter baumannii*, *C. albicans*, *E. coli*, *E. faecalis*, *S. aureus*, *Neisseria gonorrhoeae*, *Pseudomonas aeruginosa,* and *Proteus mirabilis* to 405 nm light on microtiter plates for 30 or 60 minutes, with doses of 108 J cm^{-2} or 216 J cm^{-2}, respectively. While *E. faecalis*, *E. coli*, and *S. aureus* are relevant to both the medical and food sectors, *P. aeruginosa* is less common in food products but may be encountered due to errors along the food chain. **Table 1.2** provides additional examples of BL applications for microbial biofilms.

Table 1.2. Conditions of Blue Light inactivation of microbial biofilm in different substrates. Microbial inactivation results are reported as in the references, with any modifications.

Wavelength	Microorganism biofilm	Substrate	Dose (J cm^{-2})	Irradiance (mW/cm^2)	Microbial inactivation (CFU/mL)	Reference
405	*L. monocytogenes*	Stainless steel coupons contaminated by salmon exudates	748.8	26	1.5 log	(Li et al., 2018)
405	*L. monocytogenes*	Acrylic coupons contaminated by salmon exudates	748.8	26	1.6 log	(Li et al., 2018)
405 ***420*** ***460***	*L. monocytogenes*	Stainless steel coupons	2672 960 800	50	3.0 log CFU cm^{-2} 1.9 log CFU cm^{-2} 1.6 log CFU cm^{-2}	(Olszewska et al., 2023)
400	*Stenotrophomonas maltophilia* QEHB	Mueller Hinton Broth	192	60	92.4%	(Halstead et al., 2016)
400	*P. aeruginosa* PAO1	Mueller Hinton Broth	192	60	82.8%	(Halstead et al., 2016)
410	*Staphylococcus aureus* NCTC 10788	M9 medium supplemented with glucose 10 mM and 0.2% W/V casamino acid	450	100	6.0 log	(Martegani et al., 2020)
400	*Klebsiella pneumoniae* QEHB	Mueller Hinton Broth	192	60	36.3%	(Halstead et al., 2016)

455-460	*Vibrio parahaemolyticus*	TSB	13.68	380	8.0 log	(Chen et al., 2020)
440	*Acinetobacter baumannii*	PBS	158.4	44	1.3 log	(Buchovec et al., 2022)
440	*A. baumannii*	PBS	252	35	1.7 log	(Buchovec et al., 2022)
402	*A. baumannii*	PBS	151.2	42	2.9 log	(Buchovec et al., 2022)
402	*A. baumannii*	PBS	189	35	1.9 log	(Buchovec et al., 2023)

1.4 Parameters that influence the Blue Light microbial inactivation

There are several parameters which can modify the BL effect on microbial inactivation (i.e., initial inoculum, oxygen consumption and the growth phase of the microbes) and parameters that are used to evaluate the shelf-life of the food products. These could be characteristics of the matrix, such as pH and water activity (a_w), or conservation parameters, like temperature.

1.4.1 Microbial concentration, oxygen consumption and growth phase of the microbes

The initial concentration of microorganisms in a sample significantly influences the effectiveness of BL treatment since a higher microbial density, indicated by a higher optical density (OD) of the suspension, can lead to reduced microbial inactivation due to the Beer-Lambert law. Vollmerhausen et al. (2017) investigated how different concentrations of *E. coli* respond to 420 nm BL treatment, underling how the inactivation rate changed (from a complete inactivation to no inactivation) by passing from 10^3 CFU mL^{-1} to 10^7 CFU mL^{-1}. The higher *inoculum* concentration also led to greater oxygen consumption, further lowering bacterial PDI, since it is a crucial parameter for PDI function. Dissolved oxygen levels decreased notably after 2 hours of irradiation, indicating the importance of oxygen in the PDI process (Vollmerhausen et al., 2017). Similarly, Maclean et al. (2008a) demonstrated the oxygen dependency of *S. aureus* by observing a 3 log CFU difference in samples where extra oxygen was provided during BL treatment.

In addition, factors like packaging type and the presence of antioxidants in the food sector, such as β-carotene or ascorbic acid, can compromise oxygen availability, thus reducing the efficacy of BL treatment (Ghate et al., 2019).

Most studies on the antimicrobial effects of BL have focused on bacteria in the logarithmic (log) growth phase. However, bacteria in the stationary phase exhibit different characteristics compared to those in the log phase. *E. coli* and *S. aureus* in the lag phase contain a higher proportion of "persister" cells, which increase in the stationary phase. These persister cells share the same genotype as active cells but differ phenotypically, exhibiting dormancy and resistance to some treatments and antibiotics. Keshishyan et al. (2015) compared the effects of BL on lag and log phase *E. coli*, *S. aureus*, and *P. aeruginosa*. They found that irradiation with 450 nm light (117 J cm^{-2}) resulted in lower microbial inactivation in the log phase (14-50%) compared to the lag phase, where complete inactivation was observed. Abana et al. (2017) further

investigated the susceptibility of five *E. coli* strains in log, transition, and early stationary phases to 455 nm BL. They observed that only *E. coli* DH5α maintained a reduction of 1.5-2.5 CFU/mL across all phases, highlighting the complex dynamics of bacterial susceptibility to BL irradiation.

1.4.2 Temperature

There are contradictory findings regarding the role of temperature in bacterial inactivation by BL. On one hand, it could significantly influence microbial inactivation by BL. Lower temperatures can enhance bacterial inactivation due to the increased proportion of unsaturated fatty acids in the cell membrane, making the membrane more susceptible to damage by ROS generated during PDI. Microorganisms adjust their membrane lipid composition in response to temperature changes to maintain membrane function, often increasing the unsaturation of fatty acid chains to increase membrane fluidity. This increased unsaturation can make the membrane more vulnerable to oxidation by ROS, making it more easily damaged by BL illumination at lower temperatures (Beales 2004; Ghate et al., 2013; Hyun & Lee 2020a).

Studies have shown that the efficacy of BL treatment is higher at lower temperatures. Hyun & Lee (2020a) found that treatment with 460 – 470 nm LED light at a dose of 286.8 J cm^{-2} resulted in higher reductions in the number of *L. monocytogenes* and *P. fluorescens* cells at 4 °C compared to 25 °C. Similarly, Ghate et al. (2013) observed significant inactivation of bacterial suspensions at 10°C and 15°C after illumination with 461 nm light, whereas illumination at 20 °C was ineffective.

On the other hand, some studies have reported no significant effect of temperature on microbial inactivation. Kumar et al. (2016) found that varying the temperature from 4 to 10 and 25°C did not have a noticeable effect on the reduction of *Lactobacillus plantarum*, *S. aureus*, and *V. parahaemolyticus* populations irradiated with 405 nm BL.

Further complicating matters, the temperature-dependent behaviour of bacteria may vary depending on the specific microbial strain and other factors. Kumar et al. (2015) observed different inactivation rates for various bacterial strains at different temperatures. *S. aureus* and *S. Typhimurium* showed higher reductions at 25°C compared to 10 and 4 °C, while *B. cereus* and *L. monocytogenes* showed similar reductions across all temperatures.

Overall, the susceptibility of planktonic cells to BL treatment and its temperature dependence may be influenced by a variety of factors, including the microbial strain and its metabolic activity at different temperatures.

1.4.3 pH

Different pH values can indeed have varying effects on microbial inactivation by BL. Ghate et al. (2015) examined the impact of pH on the effectiveness of 461 nm light against suspensions of *E. coli* O157:H7, *S. Typhimurium*, and *L. monocytogenes* finding that at pH 4.5 and 9.5, the decimal reductions (D-values) differed significantly. The log reductions for *E. coli* O157:H7 were 5.75 and 2.82 at pH 4.5 and 9.5, respectively. Similarly, *S. Typhimurium* showed log reductions of 5.74 and 2.38 at the same pH values, while *L. monocytogenes* exhibited log reductions of 1.46 and 6.04.

Oriel & Nitzan (2010) also investigated the effect of pH changes on *C. albicans* suspensions following BL treatments. They observed that the initial pH of 8.0 decreased to 6.5 before light treatment and further decreased to 5.8 after illumination with a dose of 36 J cm^{-2}. Their findings suggested that a pH of around 6.5 was favourable for photosensitization, as lower or higher pH values resulted in lower inactivation rates.

These studies highlight the importance of considering pH conditions when using BL for microbial inactivation. Optimal pH levels can enhance the efficacy of photodynamic treatment, while extreme pH values may impair the process, potentially affecting its overall effectiveness.

1.4.4 Water Activity (a_w)

The water activity (a_w) is a critical factor influencing the growth of microorganisms in food items. Surprisingly, there is a lack of research exploring the impact of varying a_w levels on the efficacy of BL decontamination treatments. Despite its significance in microbial growth, this aspect has not been addressed in existing studies. Therefore, there is an opportunity to investigate how different aw values might influence the effectiveness of light treatment, alongside other previously mentioned parameters.

1.5 Microbial resistance to Blue Light

An important question that is yet to be deeply investigated is whether microorganisms can develop some form of resistance against BL treatment.

Firstly, it is necessary to understand the difference between the terms "*resistance*" and "*tolerance*". According to the Scientific Committee on Consumer Safety (SCCS), the word "resistance", related to non-antibiotic agents, is used when a strain is not killed or inhibited by an agent in-use concentration at killing concentrations (SCCS, 2010). "Tolerance", differently, defines the character of a bacterial population that dies very slowly following antimicrobial

treatment. Under stressful conditions, cells slow down a lot of their metabolic activity and grow very slowly (Ciofu et al., 2022).

BL technology has attracted attention for its potential in combating drug resistance, with studies suggesting effectiveness against resistant strains due to multi-target damage (Dai et al., 2009; Ferrer-Espada et al., 2019; Yin et al., 2013). However, contradictory findings exist regarding the development of resistance or tolerance. Some studies observed no evidence of development after repeated exposure (Amin et al., 2016; Zhang et al., 2014), while others noted resistance in bacteria like *S. aureus*, which may be mitigated by adjusting dose and wavelength combinations (Guffey et al., 2013). Sublethal BL exposure in *S. aureus* activates genes involved in mutation and repair processes (RecA gene and SOS response), potentially leading to increased mutation rates (Rapacka-Zdonczyk et al., 2019). Further research is needed to fully understand the development of resistance and tolerance to BL treatment.

1.6 Blue Light and food contact surfaces decontamination

The majority of studies assessing the efficacy of BL have been conducted *in vitro*, demonstrating higher effectiveness compared to treatments on food contact surfaces (FCS) and food products (Barneck et al., 2016; Bumah et al., 2020; Josewin et al., 2018a; Oriel & Nitzan 2010; Pileggi et al., 2013). FCS sanitation, crucial for preventing pathogen transmission to food products during production and processing, has not been thoroughly investigated for BL effects *in vivo*. However, some *in vitro* studies have used coupons of materials like stainless steel, acrylic, high-density polyethylene, polypropylene, polished stainless steel, and glass coupons to simulate real conditions (Gunther et al., 2016; Lang et al., 2022; Li et al., 2018). Variances in antimicrobial outcomes may arise from surface characteristics like absorption coefficient, reflectivity, specific heat capacity, colour, porosity, texture, and thickness (Lang et al., 2022; Luksiene & Paskeviciute 2011; Tortik et al., 2014). However, studies assessing these factors have not explored the penetration depth of BL wavelengths in different materials. While the penetration depth of visible light ranges from micro to millimetres, BL penetration, evaluated on human skin, is approximately 1 mm (Ash et al., 2017). Further research is warranted to investigate whether specific surface characteristics, such as hydrophobicity or hydrophilicity, could enhance the efficacy of BL treatments.

1.7 Blue Light and food products

The utilization of photoinactivation is now extending to the food industry, with a focus on various food products. **Tables 1.1** and **1.2** provide assessments of BL effectiveness against microbes on select food products. Different quality parameters were examined based on the treated food commodities.

1.7.1 Milk and dairy products

Numerous studies on milk and dairy products have demonstrated the antimicrobial efficacy of BL without notable changes in milk constituents like sugars, proteins, and lipids, while also extending shelf life (dos Anjos et al., 2020; Hyun & Lee, 2020b; Ricciardi et al., 2020; Saraiva et al., 2024). Srimagal et al. (2016) achieved a 5-log reduction, equivalent to pasteurization standards, with minimal colour alteration using specific parameters: 406 nm wavelength, 13.8°C, and 37.8 min of treatment. Light-treated milk exhibited comparable composition and physicochemical properties to untreated samples. Milk stored in low-density polyethylene (LDPE) pouches under refrigeration showed a shelf life of approximately 9 days post-treatment, nearly double that of untreated milk (5 days).

1.7.2 Horticultural products

BL has been employed for microbial inactivation on various horticultural products such as cucumber, tomato, lettuce, mangoes, pineapple, grapes, cantaloupe rinds, fenugreek seeds, mung beans, and mung bean germlings (Aurum & Nguyen 2019; Bhavya & Umesh Hebbar 2019; Glueck et al., 2017; Josewin et al., 2018b; Kim et al., 2017c; Olszewska et al., 2024; Luksiene & Paskeviciute 2011). Studies have demonstrated antimicrobial effects ranging from 1.0 to 5.0 log reductions, influenced by factors like initial microbial populations, the addition of exogenous PS, and process parameters like wavelength, light dose, and temperature. Assessments of physicochemical properties post-light treatment often showed no significant differences in anthocyanins, phenols, flavonoids, surface colour, and antioxidant activity, with generally extended shelf-life (Bhavya & Umesh Hebbar 2019; Kim et al., 2017c; Luksiene & Paskeviciute 2011). Aurum & Nguyen (2019) found that exposure to 465 nm light combined with curcumin led to a 2.4 log CFU/g reduction in *E. coli* on grapes after light exposure of 36.3 J cm^{-2} and less textural degradation, better firmness retention, and reduced weight loss compared to untreated samples.

1.7.3 Meat and fishery food products

Limited research has been conducted on the application of BL treatments to meat and seafood products (Josewin et al., 2018a; Li et al., 2018; Luo et al., 2021; Orlandi et al., 2024; Shirai et al., 2022). Compared to laboratory settings, light treatments appear to be less effective on the surfaces of meat and seafood, likely due to their opaque and uneven surfaces which create shadows and the presence of proteins that attenuate ROS species (Kim et al., 2017a; Shirai et al., 2022). Some studies showed that the PDI was more effective when operated in culture media (i.e., PBS) or smooth surfaces (i.e., stainless steel) at low dosages, compared to chicken at higher dosages (Kim et al., 2017a; Gunther et al., 2016). Luo et al. (2021) noted minimal changes in fresh beef quality following light treatment, with only slight alterations in colour, total free amino acids, and taste after applying 44 J cm^{-2} light. To enhance microbial inactivation, some studies explored the use of external photosensitizers, such as riboflavin or curcumin (Josewin et al., 2018a; Gao & Matthews 2020).

1.8 Blue Light and synergy with other applications

1.8.1 Free and immobilized PS

As mentioned in the previous paragraphs, the PS required for BL inactivation could be endogenous (i.e., porphyrins, flavins, cytochromes, and NADH) or exogenous. The exogenous PS could be natural or synthetic, as reported in Paragraphs 1.3.2 and 1.3.3.

Over the past few, self-disinfecting surfaces have been studied to control pathogens. Some of the most recent strategies include surfaces with anti-adhesive and antimicrobial properties. Antimicrobial surfaces can exert their properties by adding specific additives, which can be stably incorporated into or be slowly released from the material. However, in a food-context application, the release of the PS should be avoided. One class of these antimicrobial surfaces is represented by photoactive materials that perform the disinfection activity through a photodynamic mechanism. They are synthesized by the direct polymerization of the PS agent or are the result of the immobilization of a photosensitizer into a support (Castro et al., 2019; Reynoso et al., 2021; Santamarina et al., 2022). For this purpose, several supports are available, for instance, resins, polymers, and nanoparticles (Alhenaki et al., 2021; Comuzzi et al., 2020, 2022; Page et al., 2015; Thandu et al., 2014). There is a plethora of photoactive materials that could be activated by visible light (Mesquita et al., 2018); for instance, 5-[4-(1-dodecanoylpyridinium)]-10,15,20-triphenyl-porphyrin was tested against *S. aureus* MRSA at 416 nm irradiation. Thandu et al. (2021) completed the inactivation of *S. aureus* (10^8 CFU/mL)

in 60 min by irradiating dioctyl adipate (OA20) added with porphyrin and expanded porphyrins (460 nm, 50 W m^{-2}). In a further study, OA20 was added with four porphyrins (5,10,15,20-tetrakis(4-methylphenyl)-21H,23H-porphine (4MeP, 1), 5,10,15,20-tetra- kis(4-methoxyphenyl)-21H,23H-porphine (4OMeP, 2), 5,10,15,20-tetra-4-pyridinyl-21H,23H-porphine (4PyP, 3), and 5,10,15,20-tetrakis(4-aminophenyl)-21H,23H-porphine (4NH2P, 4)). The results show that 5,10,15,20-tetrakis(4-aminophenyl)-21H,23H-porphine 5,10,15,20-tetrakis(4-aminophenyl)-21H,23H-porphine octyl adipate (4NH2P5-OA20) and 5,10,15,20-tetra-4-pyridinyl-21H,23H-porphine octyl adipate (4PyP5-OA20) were the most active components, determining about 4 log CFU/mL and 3 log CFU/mL reductions. 4PyP, which shows the worst photosensitizing ability in solution, became an active additive by immobilization into PVC. Considering photoactive materials, the author underlined that the antimicrobial properties derived from the honeycomb-shaped morphology of the composite surface, suggesting that the molecular assembly and the surface organization of the material should be taken into account to designing new photoactive materials (Comuzzi et al., 2022). Also, some studies investigated the use of poly(vinyl) chloride (PVC), a plastic material used for drinking bottles and food packaging (Muhib et al., 2023), added with curcumin (Saltos et al., 2014) or a gelatin/chitosan film incorporated with curcumin (GEL/CS/Cur), which reduced > 4 log of *L. monocytogenes*, *E. coli* and *Shewanella putrefaciens* after 455 nm light irradiation (Wang et al., 2022). Lopez et al. (2022) developed an antimicrobial coating by the electropolymerization of a porphycene able to inactivate 105 CFU/mL of MRSA and *E. coli* EC7 after being irradiated with 455-800 nm light (30 mW cm-2). Another light-activated antimicrobial coating was developed by Gusev et al. (2022) by using electrodeposited phthalocyanine (Pc)-based photoactive layer with zinc (tetraamino)phthalocyanine (ZnPcNH2) as PS. This coating was able to inactivate ca. 3 log of S. aureus (400-800 nm light).

The photoactivation of π-conjugated photoactive polymeric films (FDP 5), a self-sterilizing film, determined a complete inactivation of *S. aureus* and > 2 log of *E. coli*, while microbial biofilms formed on it were reduced by > 4 log (Heredia et al., 2019). The photoactivation of these antimicrobial films in aqueous solutions produced an inactivation of ca. 3 log of *E. coli* and ca. 2 log of *C. albicans* (Funes et al., 2009).

Thandu et al. (2017) studied the effect of a magnetic porphyrin nanoconjugate (SPION-TPP) against two Gram (+) bacteria evaluating that 0.5 μM of SPION-TPP was sufficient to kill 10^7-10^8 CFU/mL of *S. aureus* and, in a lower amount, *Streptococcus mutans*. Feese et al. (2011) built a crystalline material made of cellulose nanocrystals modified on the surface with a cationic porphyrin (CNC-Por) and demonstrated its capability to photo-kill *Mycobacterium*

smegmatis and *S. aureus*. Its decontaminating efficacy after light irradiation was also demonstrated towards *A. baumannii*, multidrug-resistant *A. baumannii* (MDRAB) and MRSA, achieving a reduction of 5–6 log CFU (Carpenter et al., 2012). Also Comuzzi et al. (2020) studied the photokilling effect of modified PET-ITO electrodes, a regenerable material, against *S. aureus*. The electropolymerization of ZnPc-EDOT and CuPc-EDOT with ITO added with iodide salt (KI), reduced *S. aureus* and *E. coli* of ca. 4 log CFU (Baigorria et al., 2021).

Reynoso et al. (2021) developed a material by the combination of fullerene C60 and 3,4-ethylenedioxythiophene (EDOT) that, after being photoactivated, was able to kill > 99.9% of planktonic *S. aureus* and biofilms formed on it. In another study, a porphyrin-fullerene C60 dyad (TCP-C6) was made by attaching a carbazoyl porphyrin derivative to fullerene C60. The irradiation of the film was effective in the inactivation of 4 log of *S. aureus* and *E. coli* (Ballatore et al., 2015). *E. coli* and *S. aureus* were reduced by 99% and 98% respectively by a modified fabric, composed of a bottom layer of ε-polylysine, able to kill bacterial membrane, and a second layer of zinc phthalocyanine, a PS (Chen et al., 2017). In order to be applied in a food-related context, photoactive materials should not release the PS that they support.

1.8.2 Natural and Synthetic compounds

The use of exogenous PS could enhance microbial inactivation when combined with BL by increasing ROS production. Essential oils, derived from aromatic plants, possess strong antibacterial and antifungal properties due to their hydrophobic nature, which disrupts bacterial cell membranes, leading to cell death (Diao et al., 2013; Dorman & Deans 2000). Combining essential oils with BL can further enhance microbial inactivation, but the effectiveness depends on factors such as oil type and concentration, light wavelength, and microorganism species (Marqués-Calvo et al., 2017). For example, clove and thyme oils, at a 5% concentration combined with 470 nm light, reduced the presence of *Staphylococcus epidermidis*, *P. aeruginosa*, and *C. albicans*. Plant-derived compounds, particularly polyphenols or other hydrophobic components found in essential oils, are known to have antiseptic qualities. Among them, flavan-3-ols, flavonols, and tannins exhibit antimicrobial activity by inhibiting biofilm formation and neutralizing bacterial toxins (Daglia 2012; Dorman & Deans 2000; Gwynne & Gallagher 2018; Lai & Roy 2012). When exposed to BL, polyphenols such as caffeic acid and chlorogenic acid (1 mg/mL) can significantly reduce bacterial populations (Gram + and Gram -) up to 4 log CFU/mL, highlighting their synergistic effect with light treatment for microbial inactivation (Nakamura et al., 2015).

In the scientific literature, some articles report the combined effects of BL and some chemicals or other technologies. Here there will be reported briefly some examples. Chlorinated disinfectants are commonly used in the food industry for surface cleaning. When combined with BL, they effectively deactivate *Clostridium difficile*, especially its spores, even at lower concentrations. Similarly, combining BL with hydrogen peroxide (H_2O_2) or chlorin e6 shows promising results against bacteria like *S. mutans* and in eradicating multi-species biofilms (Nie et al., 2021; Feuerstein et al., 2006).

Silver nanoparticles (AgNPs) are effective antimicrobials against various bacteria, with triangular-shaped nanoparticles being particularly potent against *E. coli*. When combined with BL, their antimicrobial effects are enhanced against MRSA and *P. aeruginosa*. Adding non-toxic inorganic salts can enhance the action of PS under BL, reducing populations of bacteria like *S. aureus* and *E. fecalis*. Carbon dots (CDots) activated by BL also show antibacterial properties (Akram et al., 2016; Caires et al., 2020; Chen & Yeh, 2019).

1.8.3 Technologies

Regarding the combination of BL and other technologies, the studies focused on ultrasounds (US) and magnetic fields. A recent study on *S. aureus* biofilms showed significant reduction with 450 nm light Combining US (1 MHz) with BL increases cell damage and inhibits microbial growth (3.48 log) (Alves et al., 2021; Li et al., 2014). Studies on *E. coli* under magnetic fields using various wavelengths have shown promising reductions in bacterial populations since they can enhance BL treatments by inducing stress in bacterial cells and stimulating porphyrin synthesis (Astuti et al., 2017; Utsunomiya et al., 2003).

1.9 Safety of Blue Light

BL is generally considered as safe for the operator. However, there are some indications of exposure. The Italian Legislation (Legislative Decree 81/2008, Chapter V, Art. 213 -218 and Annex XXXVII), in accordance with Directive EU 2006/25, has set the limit values for exposure to BL radiations: $L_B = 10^6 \cdot t^{-1}$ W/m^{2}sr (watt per steradian per square meter, for the International System is the unit of radiance) and $L_B = 100$ W/m^2·sr for $\alpha \geq 11$ mrad (L_B is the effective radiance and α the angular subtense)(Italian Government, 2008; Leccese et al., 2015). The International Commission for Non-Ionizing Radiation Protection (ICNIRP 2013) has stated

that the maximal exposure duration to BL should be 100 J/cm^2·sr for about 167 min per day (Sheng et al., 2022). Other guidelines were provided by the American Conference of Governmental Industrial Hygienists (1994), that recommend daily exposure of personnel to BL with these limits: for 10,000 s (2.8 h) or more exposure, the maximum intensity of the light source is ≤0.01 W/cm^2·sr and the maximum dose of light is 100 J/cm^2·sr. It is therefore of fundamental importance to use a tested protective filter to cover the eyes completely, such as the use of specific glasses that guarantee adequate protection for the workers (Soares et al., 2017).

An *in vitro* study showed that the application of 1.13 -1.16 mW cm^{-2} on human eyes, decreased the corneal cells' viability, changed the cellular morphology, and other alterations caused by oxidative stress and ROS accumulating (Marek et al., 2018). Regarding the human skin, a study conducted by Kleinpenning et al. (2010) tested the effect of 420 nm BL (100 J cm^{-2} per day) on eight healthy volunteers by illuminating them over five consecutive days. The results did not show DNA damage, inflammatory processes, and sunburn before and after the test. Although, they observed transient melanogenesis and vacuolization of keratinocytes.

Most of the information present in the introduction can be found in:

Lena, A., Marino, M., Manzano, M. *et al.* An Overview of the Application of Blue Light-Emitting Diodes as a Non-Thermic Green Technology for Microbial Inactivation in the Food Sector. *Food Eng Rev* 16, 59–84 (2024). https://doi.org/10.1007/s12393-023-09355-1

Section 1

Chapter 2

Qualitative and quantitative screening of Blue Light microbial inactivation

2.1 Introduction

In recent years, BL technology has been introduced for microbial inactivation. It is regarded as an environmentally friendly, affordable, safe, and flexible method. While initially utilized mainly in the medical field, its application has recently expanded to the food industry as a potential approach for decontaminating food contact surfaces or food itself (Cabral & Rodrigues, 2019; do Prado-Silva et al., 2022; Hinds et al., 2019).

The exploitation of BL for microbial inactivation is gaining significant attention in the food industry because it leaves no residues, is non-toxic and seems to not favour the development of microbial resistance (Dai et al., 2012; Trinetta et al., 2011). Due to its novelty, most of the tested microbes belong to the medical sector and the tested conditions were limited. It is therefore essential to evaluate the impact of BL on foodborne pathogens and spoilage bacteria, which are commonly targeted by traditional sanitization and disinfection methods, such as *Bacillus* spp., *Enterobacteriaceae*, *Listeria monocytogenes*, *Pseudomonas* spp., and *Staphylococcus* spp. (Kumar et al., 2019; Rajmohan et al., 2002). Additionally, various operational conditions that could be applicable in the food sector should also be tested.

2.2 Aim of the study

This research aims to investigate the potential of BL to inactivate key foodborne pathogens and spoilage bacteria, including *E. coli*, *L. monocytogenes*, *S. enterica*, *S. aureus*, *B. subtilis*, and *P. fluorescens*. The study focuses on identifying optimal treatment conditions, taking into account scenarios commonly encountered in the food industry, such as solid and liquid substrates. The goal is to maximize the photochemical effects of BL, facilitating its practical application in food safety and preservation. Furthermore, this work evaluates the efficacy of different regions within the BL spectrum against these significant bacterial species, providing insights for effectively integrating BL technology into food industry practices.

2.3 Material and Methods

2.3.1 Blue Light Source

For the BL irradiation, three customized light-emitting diode (LED) lamps were used. Each lamp had the following dimensions, 159 mm x 88 mm x 62 mm, and was made of five LED stripes connected in parallel, with 8 LED in each one. Lamps had different emission peaks (**Figure 2.1**): 405 nm, 420 nm and 450 nm (C-LED, Imola, Italy). Each LED emitted monochromatic light and had an irradiation angle of 120°.

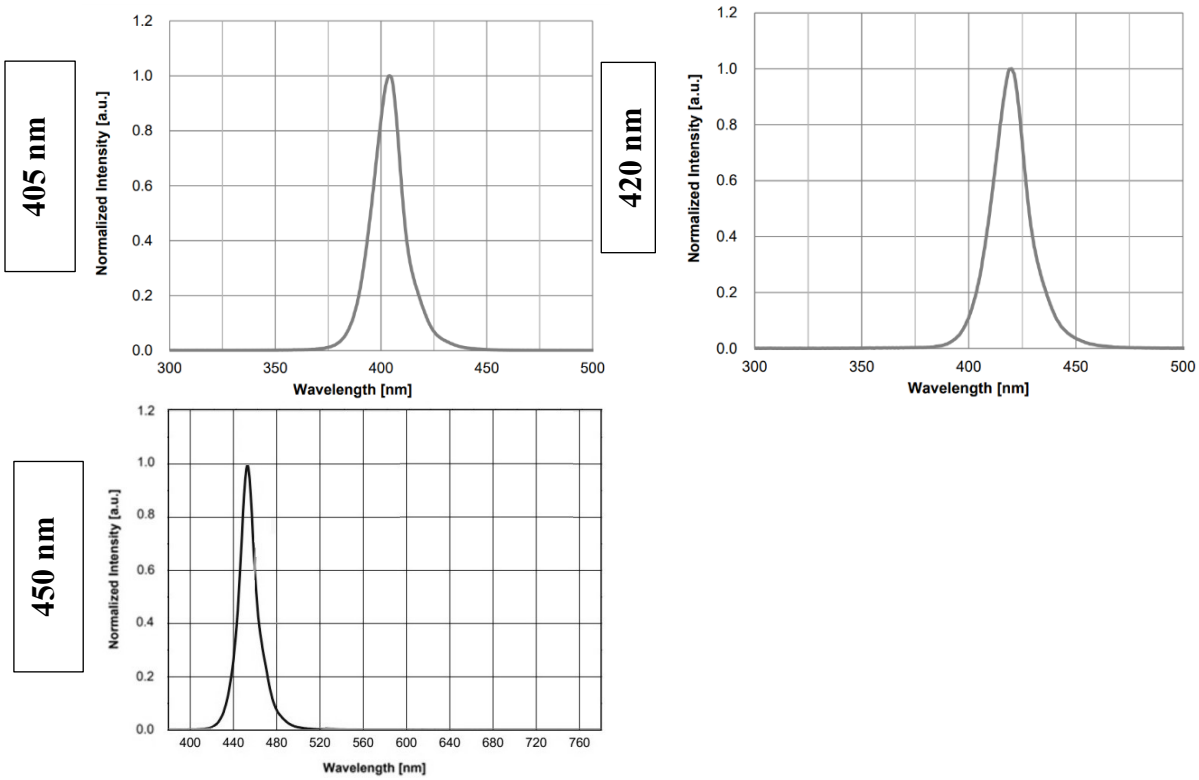


Figure 2.1. Emission spectra of the three lamps provided by the manufacturer.

The irradiance received by the samples was measured through a radiometer HD2302.0 (Delta Ohm, Caselle di Selvazzano, Italy) combined with a probe LP471 (Delta Ohm, Caselle di Selvazzano, Italy). For each treatment, the final dose (D, J cm^{-2}) was calculated using Equation (1), reported in Chapter 1:

$$(1)\ D = I \cdot t$$

Table 2.1. Specifics of the three lamps used during the experimentation provided by the manufacturer.

Wavelength (nm)	Electric Power (W)	Radiometric Power (W)
405	70	35
420	70	35
450	70	40

2.3.2 Screening of microbial inactivation capacity of Blue Light

To assess the sensitivity and resistance of different bacterial strains to BL, a qualitative screening was conducted. Sample preparation followed the protocol illustrated in **Figure 2.2**. On each agar plate, two microorganisms were potentially streaked together, as described by Kim & Yuk (2017d). Colonies were transferred using a sterile loop from a pre-prepared plate (**Paragraph 2.2.1**). Two identical plates were prepared: one was divided in two parts, served as the BL treatment and dark control, and the other was the overnight colony growth control. For the BL treatment plate, half was covered to shield it from exposure, while the other half was exposed to BL for one hour.

The BL treatment was performed at three dose ranges: 1000-700 J cm^{-2}, 700-300 J cm^{-2}, and below 300 J cm^{-2}, using three wavelengths (405 nm, 420 nm, and 450 nm). Lamp voltage was maintained at a constant 10 V throughout the experiment. Following the BL exposure, both the treated and control plates were incubated at 37 °C for 24 hours. Growth or absence of the microbial line thereof was visually evaluated, resulting in three outcomes: no effect of BL exposure, indicated by a confluent line across the plate (**Figure 2.2 A.**); partial microbial load reduction, evidenced by diminished but present colony growth (**Figure 2.2 B.**); and complete microbial inactivation in the exposed region of the plate (**Figure 2.2 C.**).

During the treatment, the temperature was monitored every 30 minutes through a probe Checktemp 1 (HI98509, Hanna, Ronchi di Villafranca Padovana, Italy).

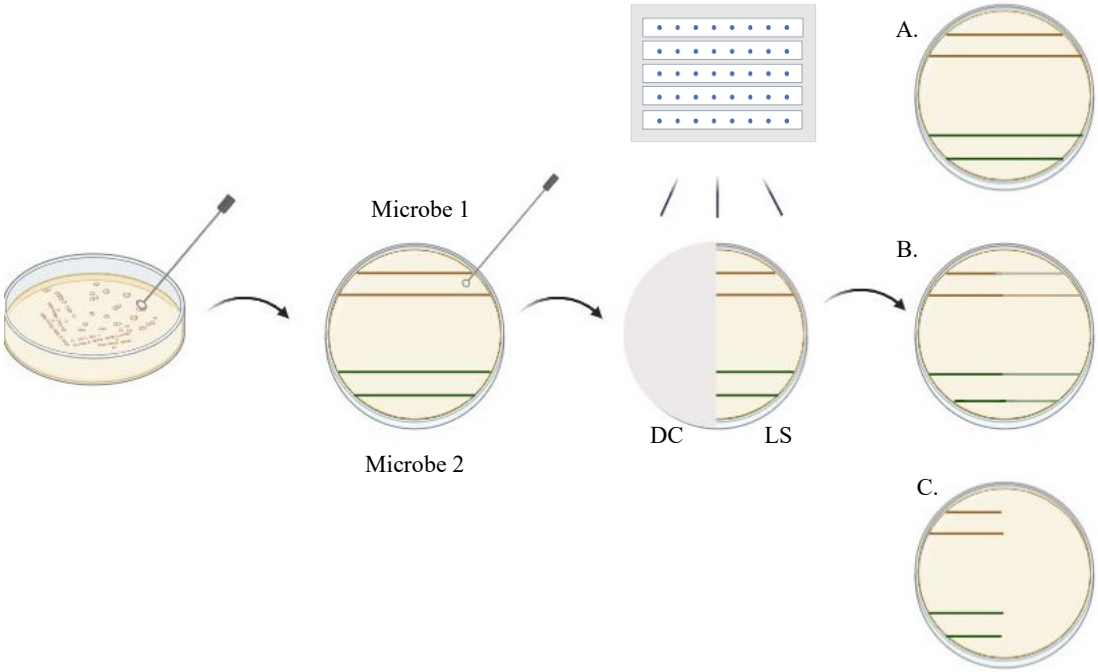


Figure 2.2. Experimental set-up of the qualitative assessment. DC, Dark control; LS, Light sample. **A.** No photoinactivation effect; **B.** partial photoinactivation effect; **C.** photoinactivation effect.

2.3.3 Quantitative assessment of microbial inactivation capacity of Blue Light

The direct assessment on agar plates was done by exposing bacteria seeded in an agar plate to BL. The bacterial strains were grown overnight in BHI broth. The microbial suspensions were then washed three times with Phosphate Buffer Solution (PBS, Oxoid, Milano), centrifuged at 13,000 x *g* and serially diluted. Each plate was divided into 6 parts, and, in each part, bacterial cultures were plated with the drop plate method (Herigstad et al., 2001). Then, half of the plate was covered as a control (**Figure 2.3**). Plates were then subjected to BL treatment, with 405 nm, 420 nm and 450 nm lamps for 60 minutes at a light dose between 700 J cm^{-2} and 300 J cm^{-2} (light-sample distance of 5 cm) and a dose < 300 J cm^{-2} (light-sample distance of 10 cm). For each sample, a plate was done and left in dark conditions for 60 min. During the quantitative screening, the temperature was taken every 30 minutes with a probe Checktemp 1 (HI98509, Hanna, Ronchi di Villafranca Padovana, Italy). The voltage of the lamps was kept constant at

10 V. After the BL treatments, treated plates and controls were let grown at 37 °C or 30 °C for 24h – 48 h.

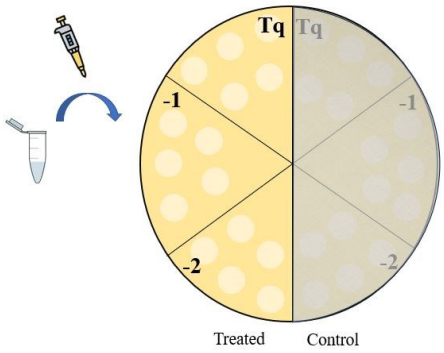


Figure 2.3. Experimental set-up of the quantitative assessment on agar plates.

2.3.4 Inactivation kinetic of blue light against microorganism

A 24-well microtiter plate was used for the BL treatment in liquid media. Bacterial strains were grown overnight in BHI broth. The cell suspensions were washed three times with Phosphate Buffer Solution (PBS, Oxoid, Basingstoke, United Kingdom), centrifuged at 13,000 x *g*, and diluted to reach a concentration of 10^7 CFU/mL (*inoculum*). The set-up of the experiment is reported in **Figure 2.4**. Briefly, 1 mL of the *inoculum* was added to each well; then, half of the plate was covered and used as a dark control and the other part was exposed to BL. The BL treatment was performed for two hours, keeping the dose constant at 216 J cm^{-2} (approximately a light-sample distance of 10 cm) during which the plate was kept in movement (120 rpm) to guarantee the homogenization and oxygenation of the samples. Every 15 min, 1 mL of the culture was taken from the well exposed to the BL and from the covered one, serially diluted and plated in BHI agar plates. Finally, plates were incubated for 24 h at 37°C or 30°C (based on the tested microbe) and viable cells were counted and expressed in the logarithmic form. During the tests on the liquid substrate, the temperature was taken every 30 minutes with a probe.

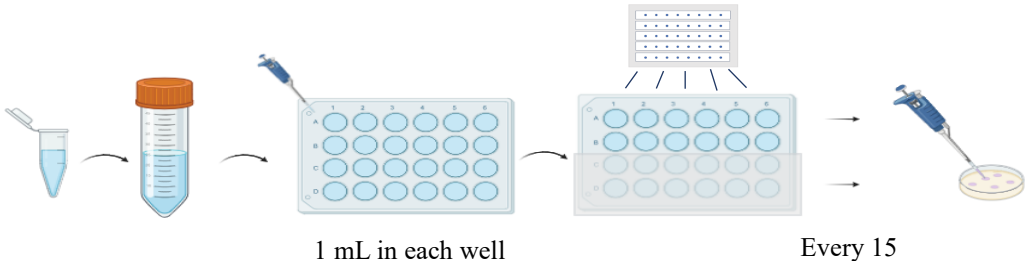


Figure 2.4. Experimental set-up of the quantitative assessment on a liquid substrate.

2.3.5 Data analysis

Results were expressed as CFU/mL and transformed in the logarithm CFU/mL. The Log (N/N0) were then calculated, where N is the log CFU/mL after the BL treatment and N0 is the log CFU/mL of the control. The data were elaborated with Microsoft Excel, represented as the mean of two biological replicates ± standard deviation (SD) with GraphPad Prism 9.0.0 and subjected to statistical analysis by IBM SPSS Statistics for Windows version 23.0 (IBM Corp., Armonk, N.Y., USA). The statistical methods used to determine the significant differences between the samples were One-way Analysis of Variance, ANOVA ($p \leq 0.05$), Two-way ANOVA ($p \leq 0.05$) and post-hoc Tuckey-B test.

2.3.6 Microbial Strains and Culture Conditions

For this study, the strains used were *Escherichia coli* DSMZ_8739, *Staphylococcus aureus* DSA_226, *Listeria monocytogenes* DSMZ_7644, *Salmonella enterica* DSA_52*, Pseudomonas fluorescens* DSA_L22*,* and *Bacillus subtilis* DSM_1092, part of the University of Udine collection. Stock cultures of each strain were stored at −80 °C in Brain Heart Infusion broth (BHI, Oxoid, Basingstoke, United Kingdom) supplemented with 30% (v:v) glycerol. An aliquot of the stock suspensions was plated in BHI agar (Technical Agar, Oxoid, Basingstoke, United Kingdom) and incubated at 37°C or 30 °C, based on the tested microbes. Before each test, microbes were cultured overnight twice in BHI broth at 37 °C or 30 °C, based on the tested microbe (*overnight* culture).

2.4 Results and Discussion

2.4.1 Characterisation of different parameters for photodynamic inactivation

In the present work, experiments were designed to assess the best conditions to inactivate microbes with BL *in vitro*. It is known that the effect of BL is strictly dependent on the light dose received by the sample (Lena et al., 2024). For that reason, the first experiments were divided into three ranges of dose emitted by 405, 420 and 450 nm lamps.

These analyses showed that at the higher dose (between 1000 J cm^{-2} and 700 J cm^{-2}) all the microbes showed great microbial inactivation.

Table 2.2 reports the inactivation obtained with BL treatment and the temperature effect. At 405 and 420 nm, *E. coli*, *S. aureus*, *L. monocytogenes*, *S. enterica* and *P. fluorescence* were completely inactivated. However, the inactivation was associated with a high temperature that was supposed to influence microbial reduction. T was > 47.9 °C for all the wavelengths, reaching 68.4 °C for 405 nm, 70.1 °C for 420 nm, and 87 °C for 450 nm. Considering the tested microbes, they have all an optimum growth T of around 37 °C, except for *P. fuorescens* which has an optimum growth T of around 22-25 °C (Guillou & Guespin-Michel, 1996). Therefore, it was not possible to associate microbial reduction with the BL-only effect. At high dosages (between 1000 and 700 J cm^{-2}) probably the effect of BL is the result of a combination of photothermal and photochemical effects and reducing the light dose could be a strategy to appreciate the photochemical effect and lower photothermal effect. A similar increase in the temperature was achieved in a study by Gunther et al. (2016), where a temperature > 50°C was associated with ca. 5 log inactivation of *Campylobacter jejuni* and *Campylobacter coli*. Since

Campylobacter was subjected to heat inactivation above 48°C, the authors suggested that those reductions were due to the combination of BL and temperature.

Among the tested microbes, *B. subtilis* seem to be the most resistant; this could be explained by the presence of Yvta, a positive regulator in the environmental signalling branch of the σ^B signal transduction network of *B. subtilis*. YtvA functions as a blue-light-responsive positive regulator in the environmental signalling pathway that activates *B. subtilis* σ^B. This capability could contribute to the survival of *B. subtilis* in the environment (Gaidenko et al., 2006).

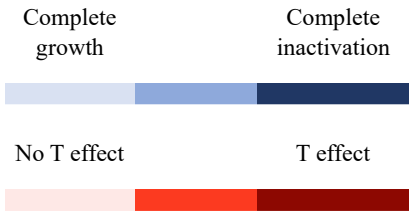
Due to the temperature reached during the experiments, and comparing the treated parts with the controls, for further tests, it was chosen to reduce the applied light dose and proceed with the other two tested conditions.

A dosage between 300 and 700 J cm^{-2} guarantees a lower T for all the wavelengths: 54.2 °C for 405 nm, 52.1°C for 420 nm, and 59.0 °C for 450 nm, on average. Indeed, a dose < 300 J cm^{-2} leads to a more controlled temperature, an average of 36.1 °C at 405 nm, 37.4 °C at 420 nm, and 38.5 at 450 nm. The correlation between higher dosage and higher temperature was found in other studies. Minor & Sabillón (2023) hypothesized that the BL treatments may increase the temperature of target surfaces: they saw that the temperature increase was linear with the increase of energy dose.

For the same dose range, 405 nm, 420 nm, and 450 nm showed different temperature increases. Therefore, by setting up all the variables equal, the temperature increase could be considered a wavelength-dependent feature. This point was evidenced also by Prasad et al. (2021), who, in his study, noticed that LED may increase the temperature and register a difference in surface temperature, providing the same energy dose, when irradiating with 405 or 460 nm.

Table 2.2. Microbial inactivation and temperature effect of BL treatment using three ranges of dose (700 < D < 1000 J cm^{-2}, 300 < D < 700 J cm^{-2}, and <300 J cm^{-2}). Complete growth (light blue) means that in both covered and exposed parts microbes grow with no differences, complete inactivation (dark blue) means that in the exposed part, no microbes were detected. If the microbial inactivation was not complete but it was not completely grown, the blue colour was selected. Similarly, no T effect means (light red) that in the covered part microbes grew as in the control plate; T effect (dark red) means that under the covered part microbes did not grow. If there was a partial inactivation the red colour was selected. The results are the average of two biological replicates.

Legend



λ (nm)	Microbe	Dose (J cm^{-2})		
		1000 - 700	700 - 300	< 300
405	*E. coli*			
	S. aureus			
	L. monocytogenes			
	S. enterica			
	B. subtilis			
	P. fluorescens			
420	*E. coli*			
	S. aureus			
	L. monocytogenes			
	S. enterica			
	B. subtilis			
	P. fluorescens			
450	*E. coli*			
	S. aureus			
	L. monocytogenes			
	S. enterica			
	B. subtilis			
	P. fluorescens			

2.4.2 Assessment of Photodynamic Inactivation on microbes based on endogenous photosensitizers

Based on the previous results, the direct inactivation on agar plates was done at doses between 700 and 300 J cm^{-2} and < 300 J cm^{-2}.

For all the tested conditions the covered part control did not show any temperature effect, remaining constant at $10^7/10^8$ CFU/mL. In the first case, a light dose higher than 300 J cm^{-2} determined no colonies detected for all the microbes, with the only exception being *E. coli* using 450 nm lamp, which resulted in a –1.06 ± 0.04 log.

The result obtained by using a light dose higher than 300 J cm^{-2} could be related to the combination of BL and high temperature (**Table 2.3**). During the 60 min of treatment, T was > 47.9 °C for all the wavelengths, reaching a peak of 68.4 °C, 70.1°C and 87°C for 405, 420, and 450 nm, respectively. These results were in accordance with other studies, where the photodynamic effect was combined with the photothermal caused by the heat dissipated by LED (Gunther et al., 2016; Izzo & Walsh, 2004; Lang et al., 2022; Prasad et al., 2021; Trzaska et al., 2017). Therefore, the emission of a light D > 300 J cm^{-2} increased the temperature, which had no effect alone. However, the combination of BL and high temperature increased the microbial inactivation of the exposed part. This could be due to due to the expression of some protective pathways (e.g. SOS response) which are activated when the temperature rises, and this could make bacteria more vulnerable (Shapiro & Cowen, 2012).

Table 2.3. Final dose (J cm^{-2}) and registered temperature (°C) for the tested microbes with the three different wavelengths in the case of D > 300 J cm^{-2}. The results are the average of two biological replicates.

Microbe	λ (nm)	Tf (°C)	Dose (J cm^{-2})
S. aureus	405	42.5	468
	420	47.2	450
	450	44.9	414
E. coli	405	40.4	414
	420	51.3	450
	450	43.4	432
L. monocytogenes	405	48.5	396
	420	45.9	504
	450	47.5	594
S. enterica	405	41.3	468
	420	47.8	432
	450	53.1	612
B. subtilis	405	45.9	558
	420	42.9	540
	450	45.8	666
P. fluorescens	405	43.3	540
	420	48.4	540
	450	46.0	648

In this study, BL antimicrobial capacity was evaluated by exploiting only endogenous PS. In order to exclude the photothermal effect, a lower light dose (D < 300 J cm^{-2}) was tested. As expected, the temperature increase produced by the BL LED lamps was lower than the one associated with a D > 300 J cm^{-2}. At D < 300 J cm^{-2}, temperature ranges between 30.5 °C and 39.5 °C: these temperatures are part of the optimum temperature of growth for all the microbes (**Table 2.4**).

Table 2.4. Final dose (J cm^{-2}) and registered temperature (°C) for the tested microbes with the three different wavelengths in the case of D < 300 J cm^{-2}. The results are the average of two biological replicates.

Microbe	λ (nm)	Tf (°C)	Dose (J cm^{-2})
S. aureus	405	34.7	144
	420	37.5	162
	450	36.5	198
E. coli	405	38.2	162
	420	38.7	180
	450	34.9	162
L. monocytogenes	405	37.1	198
	420	37.7	198
	450	39.4	216
S. enterica	405	37.8	162
	420	37.1	180
	450	39.5	216
B. subtilis	405	28.4	162
	420	32.9	162
	450	30.5	180
P. fluorescens	405	30.9	198
	420	32.7	216
	450	34.2	144

Looking at the microbial reductions, *S. aureus*, *E. coli,* and *L. monocytogenes* showed a significant difference ($p < 0.05$) among the three wavelengths used (**Figure 2.5, 2.6**).

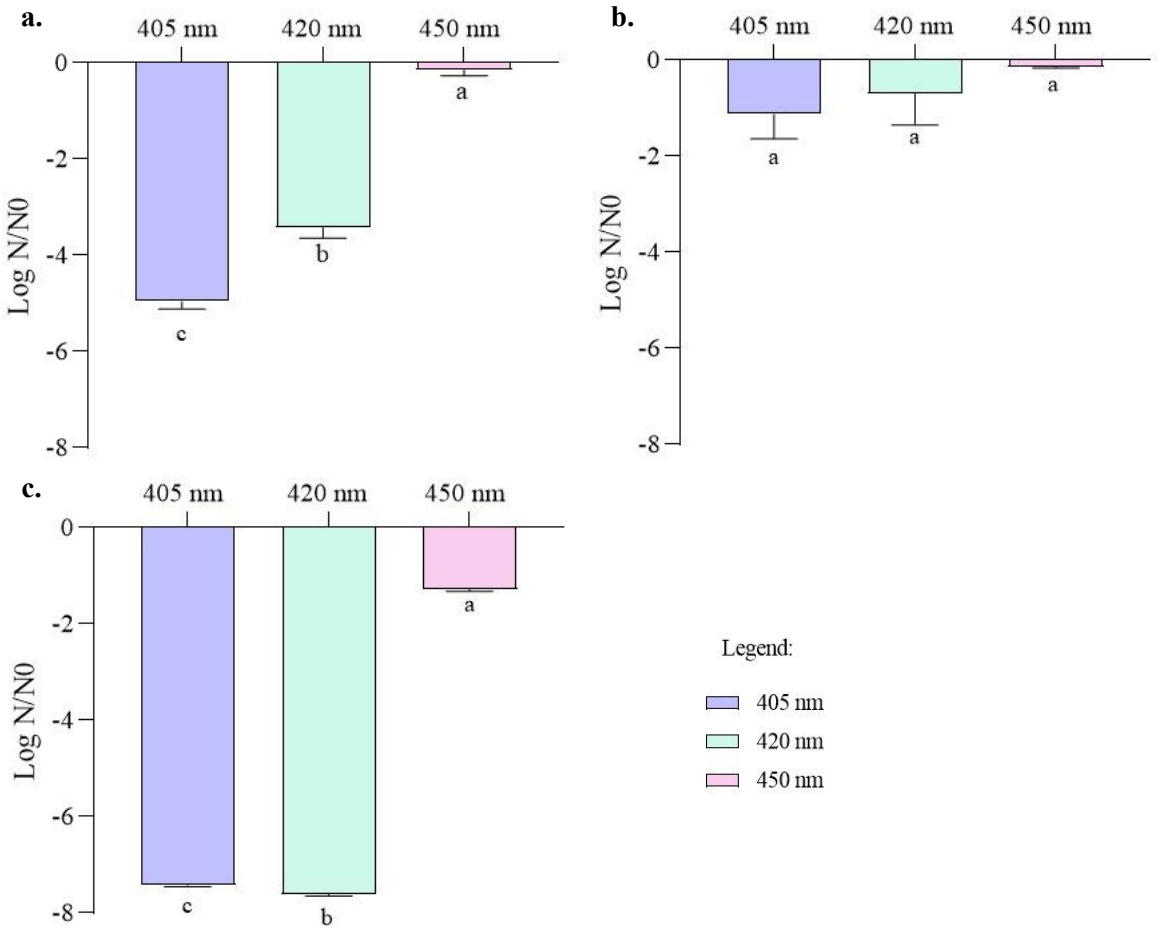


Figure 2.5. Microbial inactivation of the Gram (-) microbes (**a.**) *E. coli*, (**b.**) *S. enterica* and (**c.**) *P. fluorescens* in agar media exposing them to a light dose < 300 J cm^{-2} with 405, 420 and 450 nm. Different lowercase letters indicate significant differences ($p < 0.05$) between the same microbe irradiated with different wavelengths. The results are the average of two biological replicates.

Among the tested microbes, *S. enterica* was the one more resistant to the BL effect, especially at 420 and 450 nm. *S. enterica* is a Gram (-) bacteria that can be transmitted by ingestion of contaminated food or water or by direct contact with infected individuals or animals (Knodler & Elfenbein, 2019). As reported in numerous studies, Gram (-) bacteria, due to their cell wall, are known to be more resistant to BL and therefore require much light dose to be inactivated (Maclean et al., 2009; Malik et al., 1992; Murdoch et al., 2012). However, among Gram (-) bacteria, there are differences in microbial inactivation. For instance, in the present work, the same dose (405 nm, D = 162 J cm^{-2}; 420 nm, D = 180 J cm^{-2}), produced a greater reduction of *E. coli* cells (405 nm, -4.96 ± 0.15; 420 nm, -3.42 ± 0.22) compared to *S. enterica* (405 nm, -1.13 ± 0.5; 420 nm, -0.70 ± 0.65). Indeed, at 450 nm, *E. coli* received 54 J cm^{-2} less than *S.*

enterica, but the microbial reduction was for both microbes of ca. 0.15 log. This difference could be explained by the fact that despite light dose and wavelength, there are other factors influencing microbial inactivation, such as different porphyrin concentration, types and porphyrin wavelength absorption maxima, and oxygen concentration (Hamblin & Hasan, 2004; Lena et al., 2024; Maclean et al., 2008b; Murdoch et al., 2012; Plavskii et al., 2018). Buchovec et al. (2017) studied the inactivation of Gram (-) *S. enterica* with the addition of an external PS and they observed that, after treatment with BL, oxidative stress-resistant genes (OxyR, AhpC, GrxA, SulA, AtpC, groEL, STM0225) were expressed; therefore, the produced ROS were not able to induce cell death. For *E. coli*, all three wavelengths determined a significantly different ($p < 0.05$) microbial reduction, and 405 nm was again the most effective wavelength while 450 nm, as in the case with D > 300 J cm^{-2}, did not show any inactivation effect against *E. coli*. It is known that porphyrins (i.e., protoporphyrin IX, coproporphyrin I and III) have a peak of light absorption between 400 and 420 nm, determining a higher production of ROS and resulting in a higher microbial inactivation, while the flavins absorption peak is around 450 nm. This could explain why 450 nm was the lower effective wavelength. In confirmation of this, Plavskii et al. (2018) showed that *E. coli* was sensitive to 405 nm but resistant to 455 nm, compared to other microorganisms. Also, they evidenced that together with porphyrins, flavins act as PS in *E. coli*, and their contribution is more accentuated with 455 nm irradiation. Therefore, a lower inactivation at 450 - 455 nm could be associated with a lower amount of flavins inside *E. coli* cells, favouring the presence of endogenous porphyrins. Also, Huang et al. (2023) evidenced that notwithstanding that in *E. coli* flavins and porphyrin fluorescence intensities were analogous, porphyrins had a more crucial role in the photo inactivation, which could also be caused by the faster degradation of flavins.

Similarly, *P. fluorescens,* a Gram (-) bacteria, by using a dose < 300 J cm^{-2}, was affected by 405 nm and 420 nm, but the application of 450 nm produced a lower microbial inactivation. Similarly to what was observed for *E. coli*, the inactivation effect produced by the three wavelengths was significantly different. It has been demonstrated that *P. fluorescens* is able to produce endogenous porphyrins, principally coproporphyrin III (Amin et al., 2016). Dai et al. (2013) evidenced that, through the emission spectra of fluorescence spectroscopy, coproporphyrin III and/or uroporphyrin III could be the intra-cellular photosensitive chromophores associated with the BL inactivation of *P. aeruginosa*. Therefore, the same chromophore could be associated also with *P. fluorescens*. Additionally, it's noteworthy that the Gram (-) bacteria tested in this study showed less vulnerability to higher wavelengths of BL spectra (450 nm) but were more sensitive to wavelengths at the lower end of the spectrum (405

nm and 420 nm). This observation aligns with findings from a study by Hoenes et al. (2021a), where Gram (-) bacteria exhibited less susceptibility to 450 nm compared to 405 nm due to the endogenous porphyrins present. However, not only the amount but also the type and the cellular localization of the PS are crucial for bacterial inactivation (Gábor et al., 2001).

Between Gram (+), *L. monocytogenes* was the most susceptible bacteria among the tested ones. *L. monocytogenes* is a ubiquitous food-born pathogen, and its control in food products is regulated by the Commission Regulation (EC) No 2073/2005. *L. monocytogenes* obtained already good inactivation results from preliminary tests. The greatest reduction was observed at 405 nm, when it was almost completely inactivated, followed by 420 nm, where the reduction consisted of around -4.00 log. The reduction obtained with 405 nm and 420 nm was not significantly different ($p < 0.05$) while it differs with the microbial inactivation resulting after 450 nm treatment. In particular, 405 and 420 nm showed no significant difference in terms of microbial reduction while at 450 nm, a higher dose determined the lower microbial inactivation, which was significantly different compared to the one obtained with the other two wavelengths. This was observed by Murdoch et al. (2012), who obtained 100% inactivation on agar plates using 128 J cm^{-2}. However, they did not notice a difference between *L. monocytogenes* inactivation at 405 nm and 460 nm.

Considering *S. aureus*, the microbial inactivation obtained by 405 nm and 450 nm wavelengths were significantly different ($p < 0.05$) and consisted of -4.76 ± 0.87 and -1.47 ± 0.48 log. This was similar to what was underlined by Guffey & Wilborn (2006), who observed that *S. aureus* required a higher dose to achieve the same inactivation at 470 nm compared to the one needed at 405 nm. Also Maclean et al. (2008a, 2009) confirmed the photodynamical inactivation of *S. aureus* at 405 nm due to an oxygen-dependent process and the predominant porphyrin produced in *Staphylococcus* spp. were coproporphyrins, in a five to six-fold higher than in Gram (-) bacteria (Nitzan et al., 2004). The 420 nm wavelength determined a reduction of -2.80 ± 0.78, lower compared to the reduction obtained at 405 nm. This result is coherent with what was observed by Maclean et al. (2008a), who observed that the use of 420 nm wavelength caused 0.30 log reduction, lower compared to the use of 405 nm, which provided 2.40 log reduction. Additionally, they demonstrated that 400-420 ± 5 nm wavelength was more efficient in bacterial inactivation compared to 430 – 500 ± 5 nm wavelength.

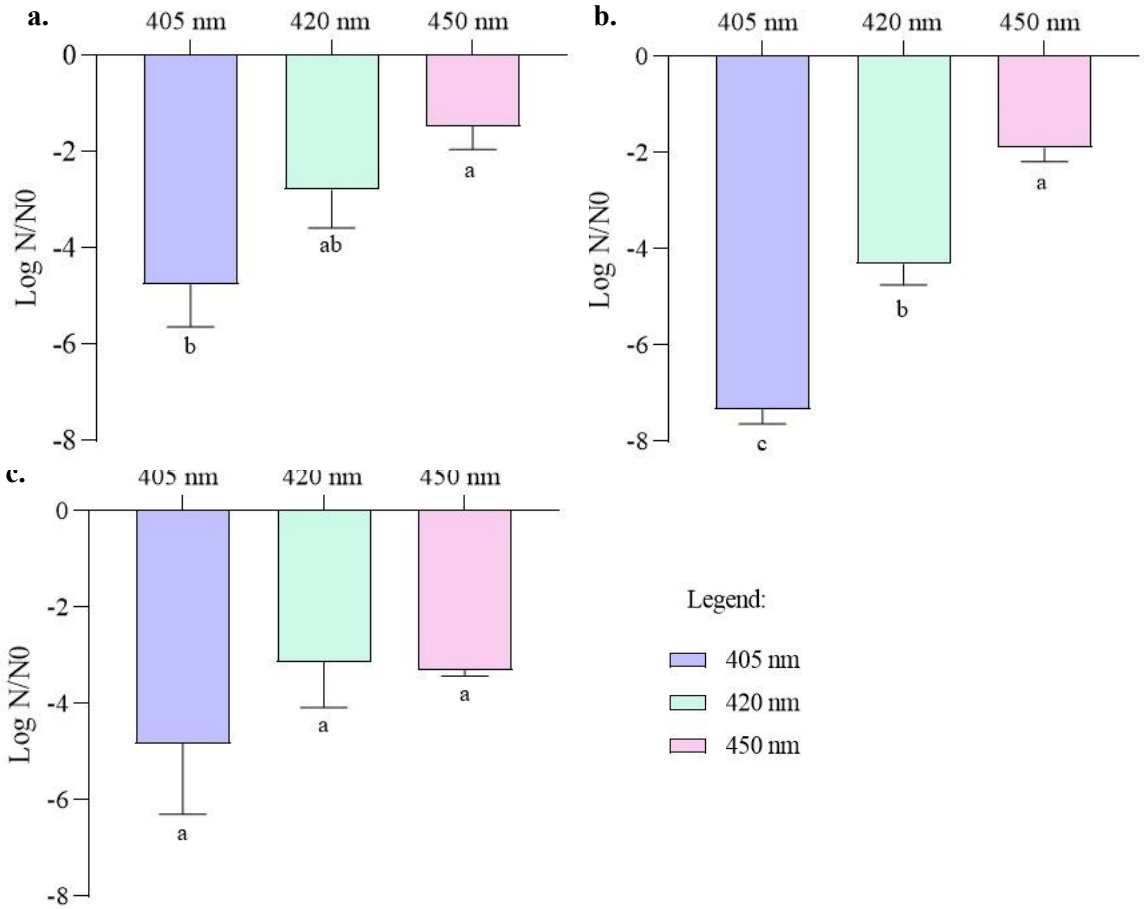


Figure 2.6. Microbial inactivation of the Gram (+) microbes (**a.**) *S. aureus*, (**b.**) *L. monocytogenes* and (**c.**) *B. subtilis* in agar media exposing them to a light dose < 300 J cm^{-2} with 405, 420 and 450 nm. Different lowercase letters indicate significant differences ($p<0.05$) between the same microbe irradiated with different wavelengths. The results are the average of two biological replicates.

Differently from what was observed from the qualitative tests, *B. subtilis* was more resistant. In the previous tests, the high temperature reached could have made *B. subtilis*, known to be a sporogenous bacteria, in a stress condition. From these tests it is clear that *B. subtilis* is more susceptible to 405 nm, nonetheless, 420 and 450 nm resulted in a good inactivation, -3.14 ± 0.94 and -3.31 ± 0.12, respectively. A study by Olsson et al. (2002) described that this bacterium has 5-aminolevulinic acid (ALA) and uses it for the synthesis of the heme group. The terminal step of this pathway involves protoporphyrin IX. ALA is a precursor of endogenous porphyrins in bacteria. Therefore, *B. subtilis* is characterized by the presence of endogenous porphyrins which are activated by 405 nm BL. Despite 450 nm wavelength providing the lower results in terms of microbial inactivation, in the case of Gram (+) bacteria, it can be still considered a good result since it provides ca. -1.50, -1.90 and -3.31 log respectively, for *S. aureus*, *L.*

moncytogenes and *B. subtilis* which are good results in terms of sanitation. Considering an industrial application, it could be necessary to find a compromise between the maximum bacterial inactivation, the temperature rise and the costs. Therefore, applying BL technology after regular cleaning could represent a way to have more sanitize food-related surfaces in food companies.

The obtained results confirmed that Gram (+) bacteria are more susceptible to BL compared to Gram (-) after exposure to all the used wavelengths. This result is consistent with the other studies (Alves et al., 2009; Halstead et al., 2016; Maclean et al., 2009), which explain that this difference is a consequence of the diversity between Gram (+) and Gram (-) cell wall. In fact, Gram (+) microbes have a thick and porous peptidoglycan layer (15 – 80 nm thickness), which allows PS to flow into the inner plasma membrane, while Gram (−) has a thin layer of peptidoglycan between inner membranes and an outer membrane (Lena et al., 2024; Vieira et al., 2018). Murdoch et al. (2012) in his study observed that the inactivation of 3.5 log CFU mL^{-1} of *S. enterica* required 2.5 times the dose needed to inactivate 5 log CFU mL^{-1} of *L. monocytogenes*, under the same conditions. Also, Josewin et al. (2018b) showed that *L. monocytogenes* inactivation was higher compared to *S. enterica*.

In general, evaluating the obtained results, by fixing the light dose < 300 J cm^{-2}, the microbial inactivation was dependent on two main factors, the light wavelength and the type of tested microbe (**Table 2.5)**. The statistical analysis showed that the microbial inactivation was influenced significantly ($p < 0.01$) by the three used different wavelengths (405 nm, 420 nm, and 450 nm), showing that 405 nm produced the highest microbial inactivation, while 450 nm produced the lowest, but still good in terms of sanitation. The BL wavelength alone influenced the microbial inactivation for 67.7% while, the type of microorganism, accounts for 26.2%. Indeed, the interaction between the type of microorganism and the wavelength influenced microbial inactivation only for 6.1%.

Table 2.5. Two -Way Analysis of variance (ANOVA) of the effect of two variables, the microorganism (M) and the wavelength (W).

Variables	SS%	$p \leq 0.05$
M	26.2	***
W	67.7	***
M x W	6.10	***

SS, sum of squares; p, significance; * $p \leq 0.05$; ** $p \leq 0.01$; *** $p \leq 0.001$.

This statistical result finds again a confirmation of scientific literature, where the majority of the authors that exploited endogenous PS found out that near-UV wavelengths, i.e. 405 nm and 420 nm, produced a higher microbial inactivation compared to higher BL wavelength (i.e., 450 nm, 460 nm) for the excitation of endogenous PS. Also, these results clarify that by fixing a light dose, the most important factors to take into account are the wavelength and the type of microorganisms that are going to be inactivated with BL treatment. Using an exogenous PS could be beneficial in order to get a more intense and faster inactivation effect with BL, but its selection should be carefully evaluated considering the final application.

2.4.3 Kinetics of inactivation of food-related microbes with Blue Light

The results of tests on liquid media are reported in **Figures 2.7** and **2.8**. For all the tested microbes, the controls remained constant at 10^7 CFU/mL. Considering Gram (-) bacteria, for *E. coli*, *S. enterica* and *P. fluorescens*, 405 nm and 420 nm were the most effective wavelengths, consisting of -1.43±0.80, -2.08±0.90 and -5.08±0.09 log for 405, respectively, and -1.56±0.47, -0.92±0.60 and -4.78±0.37 log for 420 nm, respectively. After 120 min of treatment (D= 216 J cm^{-2}), *E. coli* had a similar inactivation for 405 and 420 nm, which was significantly different to the inactivation obtained at 450 nm ($p= 0.01$). In general, its inactivation kinetics seems to be linear for all the wavelengths used. The same strain used in this study, *E. coli* ATCC 8739, was used also by Plavskii et al. (2018), who found that the amount of porphyrins and flavins are the same but the porphyrins are more determinant in the effectiveness of BL (Bumah et al., 2020; Chen et al., 2021) probably because flavins are degraded faster than porphyrins into lumichrome, as some studies underlined (Hessling et al., 2020; Huang et al., 2023). Lumichrome is a PS that can be excited at 405 nm, and praecipe to the inactivation process.

Similarly, the *P. fluorescens* inactivation was significantly different ($p<0.001$) when irradiated with 450 nm (-0.32±0.11) compared to 405 and 420 nm, where the inactivation was > 4.50 log. *P. fluorescens* inactivation kinetics where different for all the wavelengths. The microbial inactivation resulted from 405 nm-light irradiation showed a significant ($p < 0.05$) drop with 81 J cm^{-2}, which could represent a dose threshold for its inactivation, whereas by irradiating with 420 nm, a significant inactivation ($p < 0.05$) was obtained after 108 J cm^{-2}. The difficulty to inactivate *Pseudomonas* spp. at 450-460 nm was observed also in other studies (Hoenes et al., 2021b; Tomb et al., 2018), where the application of different doses, 91.9 or 500 J cm^{-2} determines the inactivation of 1 and 0.98 log, respectively, underlying a not linear response to the applied dose. As mentioned before, the differences between *E. coli* and *P. fluorescens* could be attributed to the different amounts of PS inside their cells. In fact, Dos Anjos et al. (2023)

evaluated that *E. coli* and *P. aeruginosa* have both a significant amount of intracellular porphyrins; however, the amount in *E. coli* was much lower and *P. aeruginosa* showed also the presence of hexaporphyrin and pentaporphyrin, which were not present in *E. coli* cells. In addition, it has been studied that this pathogen is able to produce various pigments (i.e., pyrocyanin, phenazine, and others) which conferee oxidative-stress resistance to the bacteria (Rapacka-Zdończyk et al., 2021).

Differently, *S. enterica* had an inactivation higher than 1 log only in the case of 405 nm, which was significantly different ($p=0.04$) compared to 420 and 450 nm (-0.92±0.60 and -0.34±0.02, respectively). Regarding its inactivation kinetic, only 162 J cm^{-2} by 405 nm irradiation determined a significantly different reduction ($p < 0.05$), whereas with 420 nm and 450 nm, not significant differences in the inactivation kinetics were observed since they probably required higher light dose. The microbial inactivation mechanism of BL against *Salmonella* spp. is not fully elucidated. However, Hu et al. (2021) studied a possible mechanism of sensitivity that could depend on the permeability of the outer membrane. The BL treatment could inactivate the *rfa*C gene, involved in lipopolysaccharides biosynthesis. A change in the fatty acid composition could increase the permeability of the outer membrane increasing the sensibility to BL.

In general, it was also evidenced that the lipid composition of bacterial cells can also be a form of protection. In fact, the segregated phases of the anionic lipids present in the cell wall are a cell defence mechanism and can determine the selectivity of bacteria to cationic PS. In the case of Gram (-) bacteria, cationic PS can remove bi-cationic ions and destabilize the cell wall organization with the lipopolysaccharides release (Alves et al., 2013).

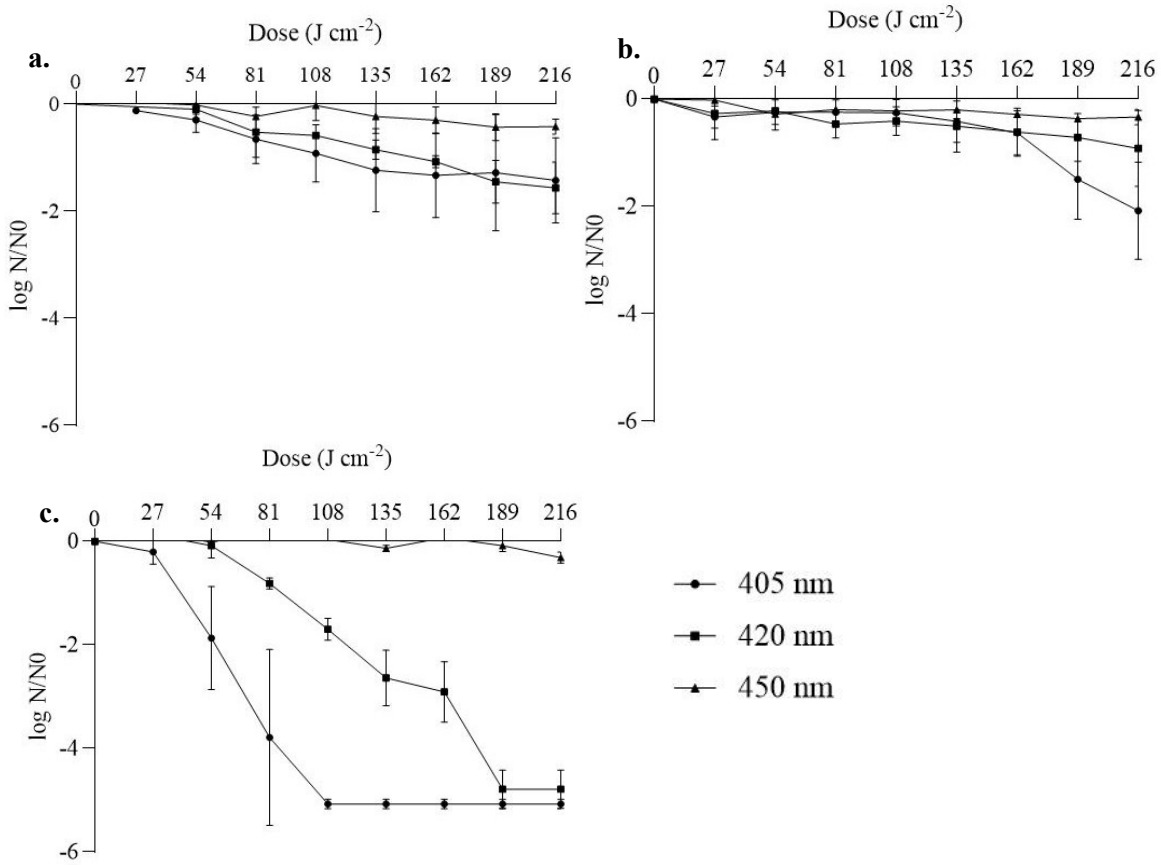


Figure 2.7. Inactivation kinetics of Gram (-) bacteria, (**a.**) *E. coli*, (**b.**) *S. enterica* and (**c.**) *P. fluorescens* after BL treatment with 405 nm, 420 nm and 450 nm. The results are the average of two biological replicates.

As in the agar assessment, the susceptibility among the tested Gram (-) bacterial species showed some differences: in particular, *P. fluorescens* seems to be the most susceptible, and *S. enterica* the most resistant, as observed before with the previous test. As already mentioned, the BL efficacy in inactivating microbes is strain-dependent. Therefore, the different microbial species respond differently when irradiated with BL. The different susceptibility among Gram (-) bacteria was also evidenced by Murdoch et al. (2012), who observed that the application of 288 J cm^{-2} (405 nm) determined the inactivation of 3.5 log of *S. enterica*, while the same dose inactivates 5 log of *E. coli*.

The application of BL treatment to a liquid media confirmed that Gram (-) bacteria seem to be more susceptible to 405 and 420 nm compared to 450 nm. As in the case of agar media, this

could be determined by the different types of PS present inside bacterial cells, the amount of PS, the intracellular location of the PS and also by the diffusion length of the generated ROS (Harris, 2023).

In the case of Gram (+) bacteria, all the tested wavelengths determined good microbial inactivation results, with 405 nm and 420 nm providing the highest inactivation results.

Going into the details, for *S. aureus* all the tested wavelengths provided significantly different results after 216 J cm^{-2} of irradiation ($p<0.001$), with 420 nm being the most efficient in terms of inactivation, followed by 405 nm. Light treatment with 405 nm and 420 nm determined similar inactivation kinetics, showing a significant reduction after 135 J cm^{-2} ($p<0.05$). Again, 450 nm was less effective against *S. aureus*, as mentioned by other authors (Hoenes et al., 2021; Maclean et al., 2008a). This result confirmed also what was observed in the agar assessment, where 405 nm and 420 nm provided the highest inactivation of *S. aureus*, and 450 nm was the least effective. The resistance of *S. aureus* to certain wavelengths can be also related to the presence of staohyloxanthin, a pigment that conferee resistance to BL (Rapacka-Zdończyk et al., 2021).

For *L. monocytogenes*, indeed, the inactivation kinetics were similar and seemed linear for all the wavelengths. However, after 216 J cm^{-2} irradiation with 405 nm and 450 nm, the microbial inactivation was significantly different ($p=0.05$). As in the previous test, 405 nm was the most effective wavelength, determining an inactivation of more than -3.00 log, while 450 nm consisted of approximately -1.08 log. These results are consistent with other studies (Endarko et al., 2012; Murdoch et al., 2012), which evaluated the inactivation of *L. monocytogenes* at several wavelengths between 400 and 450 nm, demonstrating that it was most sensitive with wavelengths between 400±5 and 410±5, with the peak of sensitivity at 405 nm and had similar microbial inactivation.

The inactivation kinetic of light treatment with 405 nm and 420 nm determined a significantly different reduction ($p<0.05$) after the application of 54 J cm^{-2}, allowing the identification of a possible light dose threshold for the inactivation of this bacteria. For 450 nm, a significant reduction was registered after 108 J cm^{-2} ($p<0.05$).

However, after 216 J cm^{-2} irradiation, the microbial inactivation of *B. subtilis* was significantly lower for 450 nm ($p<0.01$), where it accounted for -1.87 log, than from 405 and 420 nm where the inactivation was >5.00 log. The inactivation response of *B. subtilis* in these preliminary tests had different behaviour. Comparing what was observed in the agar assessment with the results on the liquid substrate, it is shown that 405 nm exhibited excellent microbial inactivation in

both substrates. Considering 420 nm, the effectiveness seems to be enhanced in liquid media, where it accounted for approximately -5.00 log. In the case of 450 nm, the inactivation rate was similar in liquid and agar media, approximately -2.00 and -3.00 log, respectively. The lower susceptibility of *Bacillus* spp. to higher wavelengths was observed also by Kumar et al. (2015), and it could be explained by the presence of Yvta, which regulates the BL absorption, as mentioned before (Gaidenko et al., 2006). However, research about the microbial inactivation of *Bacillus* spp. with BL at different wavelengths is still limited.

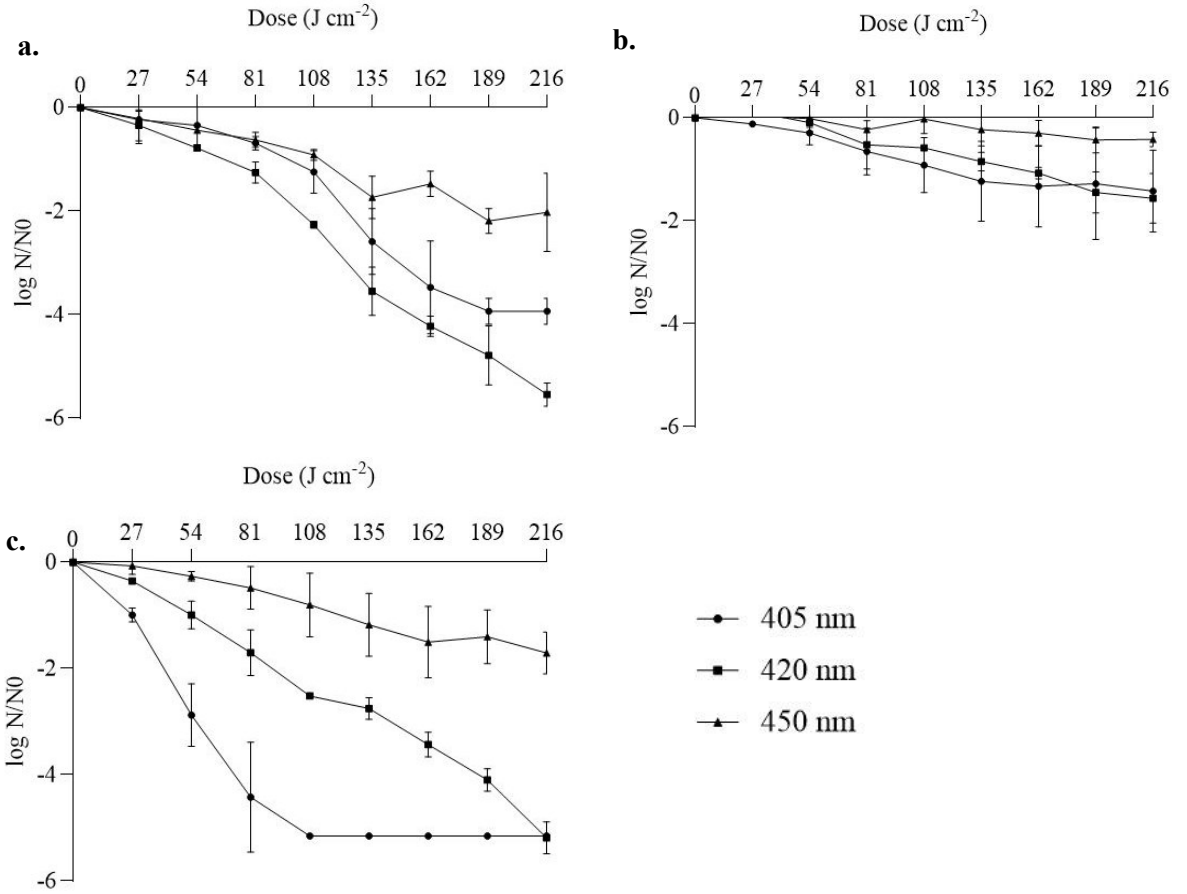


Figure 2.8. Inactivation kinetics of Gram (+) bacteria, (**a.**) *S. aureus*, (**b.**) *L. monocytogenes* and (**c.**) *B. subtilis* after BL treatment with 405 nm, 420 nm and 450 nm. The results are the average of two biological replicates.

When evaluating all the tested wavelengths, the choice of the optimal one should be guided by the specific application requirements. Thinking about the implementation of the sanitization procedures, all three wavelengths provided good results for the treatment of Gram (+) bacteria, with 405 nm and 420 nm being the most effective. Within the context of food processing and safety, the integration of BL technology could serve as a complementary sanitization step,

augmenting traditional cleaning practices by targeting residual microbial contamination. In this scenario, while the 450 nm wavelength exhibits comparatively lower antimicrobial efficacy against the tested microbes, it could result in compatibility with certain materials and food production, becoming a viable option for specific applications in food hygiene protocols. For Gram (-) bacteria, however, 405 nm and 420 nm are likely the preferred choices due to their ability to achieve microbial inactivation of <1 log in most cases. In the case of *P. fluorescens* exposed to 405 nm BL, a significant reduction in the microbial count was observed after 45 minutes (D = 81 J cm^{-2}), highlighting this as a potentially critical threshold for the inactivation process. However, a generalized threshold for microbial inactivation could not be determined for each wavelength or each microorganism. This variability underscores the necessity of tailoring BL treatment parameters to the specific application and microbial context, as no single wavelength can be universally recommended for all conditions. In addition, in the specific food sectors, these results open the possibility to select the best combination of wavelength and treatment time, to reduce the light irradiation and the application cost of this technology.

Among all the tests, the final temperature (Tf) reached after 120 min of BL treatment (**Table 2.6**) remained within their respective optimal growth ranges, with the highest value observed being 40.5°C for *S. enterica*. Conversely, the covered control samples maintained a stable condition across all microorganisms and wavelengths, exhibiting only minor physiological variations (<1 log). These findings confirm that the microbial inactivation observed was solely due to the BL treatment, with no contribution from temperature effects.

The results obtained on liquid media were coherent with what was observed in the tests on agar media, with Gram (+) bacteria being most susceptible to BL treatment compared to Gram (-) bacteria. In general, this higher susceptibility of Gram (+) bacteria can be a matter of type, quantity and location of the PS. Supporting this, Kumar et al. (2015) reported that Gram (+) bacteria possess higher coproporphyrin content per CFU. In particular, *B. cereus* 5.25 ag/CFU, *S. aureus* 3.38 ag/CFU and *L. monocytogenes* 2.03 ag/CFU. In contrast, Gram (-) were *S.* Thypimurium 0.21 ag/CFU, *E. coli* 0.14 ag/CFU and *P. aeruginosa* 0.67 ag/CFU. However, they did not find a linear correlation between microbial inactivation and the amount of coproporphyrin.

The quantitative assessment on agar and liquid media showed some differences in the inactivation rate, which could be attributable to the fact that in one case the BL treatment was done directly on microbes seeded in agar media, while in the second case, the treatment was done on a well-mixed bacterial suspension, that was going to be plated after the BL treatment (Murdoch et al., 2012). Additionally, the lower effectiveness in liquid media is also caused by

the higher thickness of the substrate (ca. 1 cm) and consequently less penetration of the BL to the liquid media.

Table 2.6. The final temperature (Tf) was reached for all the tested microbes with the three different wavelengths by using a light dose equal to 216 J cm^{-2}. The results are the average of two biological replicates.

Microbe	λ (nm)	Tf (°C)
E. coli	405	39.7
	420	34.5
	450	37.1
S. aureus	405	39.3
	420	33.9
	450	32.8
L. monocytogenes	405	31.6
	420	32.9
	450	31.5
S. enterica	405	43.3
	420	39.4
	450	40.5
P. fluorescens	405	31.1
	420	31.5
	450	29.6
B. subtilis	405	26.6
	420	28.1
	450	31.7

Overall, by fixing D = 216 J cm^{-2}, the microbial inactivation was dependent on two main factors, the BL wavelength and the type of tested microbe. In particular, the microbial inactivation was influenced significantly ($p < 0.001$) by the three used wavelengths (405 nm, 420 nm, and 450 nm), with 405 and 420 nm being the most effective in terms of inactivation (-3.47 and -3.29, respectively) while 450 nm accounting for -0.98 log, on average. Translating this result in terms of dose, it would be necessary to expose microbes to higher doses when irradiated with 450 nm BL compared to the doses required for 405 nm irradiation.

Also, the type of microbes influenced significantly ($p < 0.001$) the microbial inactivation, with *B. subtilis*, *S. aureus* and *P. fluorescens* being the most susceptible and statistically similar, followed by *L. monocytogenes* and, significantly different from *E. coli* and *S. enterica*, the most resistant. In addition, also the interaction between the type of microorganism and the used wavelength influenced significantly the microbial inactivation ($p= 0.002$). Similarly to the agar assessment results, microbial inactivation was determined for 66.3% by the BL wavelength, 28.8% by the type of microorganism, and 4.90% by the interaction of wavelengths and type of microbes (**Table 2.7**).

Table 2.7. Two -Way Analysis of variance (ANOVA) of the effect of two variables, the microorganism (M) and the wavelength (W).

Variables	SS%	$p \leq 0.05$
M	28.8	***
W	66.3	***
M x W	4.90	***

SS, sum of squares; p, significance; * $p \leq 0.05$; ** $p \leq 0.01$; *** $p \leq 0.001$.

2.5 Conclusions

This research was a preliminary study to understand the effectiveness of BL irradiation at 405 nm, 420 nm and 450 nm in the different substrates, that represent the different substrates that could be found in a food company, such as a surface or food in a solid or liquid state. The results evidenced that BL is effective against the tested pathogens and spoilage bacteria, with different grades of microbial inactivation due to the applied dose, the used wavelength and the type of microbes. This research confirmed the different susceptibility of Gram (+) and Gram (-) bacteria and, also, by monitoring the temperature, it was possible to attribute the microbial inactivation to blue light only.

For all the tested microbes, 405 nm was the most effective wavelength, followed by 420 nm and 450 nm. Unless 450 nm resulted in lower microbial inactivation, this wavelength has still produced good results for a sanitation application. In fact, considering an industrial implementation of the technology, as a food company, after the regular sanitation procedures, BL could be applied to eradicate the residual microbes (Luksiene, 2022). Therefore, all three wavelengths could be applied to sanitation processes.

Considering the specific application and the most probable strains that could be present (i.e., considering company critical control points, CCPs), BL technology could be easily implemented. Overall, this technology represents a green solution for microbial inactivation in food industries and the absence of residues confers a great advance to be used in the food sector, as well as the possibility to easily implement the lamps in facilities. However, to exploit its high potential is crucial to carefully evaluate the parameters to be applied.

Chapter 3

Reactive oxygen species formation by light technologies and microbial damages

3.1 Introduction

Light-based technologies, particularly those utilizing ultraviolet (UV) and blue light, have gained significant attention for their potential in microbial inactivation, especially for foodborne pathogens such as *L. monocytogenes*, *S. aureus*, and *E. coli*. These technologies operate on the fundamental principle that light irradiation excites endogenous PS within microbial cells, which, upon reacting with molecular oxygen, generate ROS. These ROS are highly reactive molecules that can damage cellular components such as proteins, lipids, and nucleic acids, ultimately leading to microbial cell death (Dos Anjos et al., 2023; Ghate et al., 2019; Luksiene & Zukauskas, 2009; Maclean et al., 2009).

While this mechanism of action is well established, the extent of ROS production and the tolerance of different bacterial species to these reactive molecules remain areas of scientific debate. Studies suggest that all bacterial species possess some form of oxidative stress defence mechanisms, yet their effectiveness in combating ROS is not fully understood. In addition, although cell death induced by light treatment is often attributed to damage to the cell membrane, the specific biochemical pathways involved in this process have not been thoroughly elucidated and also other types of cell damages could determine the cell death (Johnson & Hug, 2019; Zhao & Drlica, 2014).

Understanding the precise mechanisms regulating microbial inactivation via light technologies is crucial for optimizing their use. This knowledge could lead to more effective and targeted applications in various fields, such as food safety, healthcare, and environmental microbiology. Therefore, this study aims to investigate the relationship between ROS production, oxidative stress responses, and membrane damage in key foodborne pathogens, shedding light on the complexities of light-induced microbial inactivation.

3.2 Aim of the study

This study aimed to investigate how light irradiation influences the microbial inactivation of key foodborne pathogens, *L. monocytogenes* and *S. aureus* (Gram +) and *E. coli* (Gram -). The primary focus was on elucidating the role of intracellular ROS generation, as dictated by the principles of photobiology, in driving microbial inactivation.

Additionally, the study sought to explore the relationship between lipid peroxidation, membrane damage, and microbial cell death. By examining the correlation between ROS production, oxidative stress responses, and physical damage to the cell membrane, the research aimed to clarify the mechanisms behind microbial inactivation.

Using UVA (365 nm) and blue light (405 nm) at two distinct temperatures (4°C and 23°C), this study evaluated the influence of environmental and treatment variables on the effectiveness of photodynamic inactivation. This comprehensive approach aimed to provide critical insights into optimizing light-based technologies for pathogen control in food safety applications.

This work was carried out at MicroBio laboratory, at Electrolux Italia S.p.A (Porcia, Italy) in accordance with the guidelines set forth by the FSE REACT-EU PON funding program.

3.3 Material and methods

3.3.1 Microbial Strains and Culture Conditions

For this study, the strains used were part of the Electrolux Italia S.p.A. collection and were the following: *Staphylococcus aureus* ATCC_6538, *Escherichia coli* ATCC_8739 and *L. monocytogenes* ATCC_19115. Stock cultures of these strains were stored at −80◦C in Brain Heart Infusion (BHI, Oxoid, Basingstoke, United Kingdom) supplemented with 30% (v:v) glycerol. Stock cultures were subcultured overnight twice in BHI at 37◦C. Before each test, overnight cultures were prepared by growing the strains in their respective media under standardized conditions: *S. aureus* in Tryptone Soy Broth (TSB, Oxoid, Basingstoke, United Kingdom), *E. coli* in Nutrient Broth (NB, Oxoid, Basingstoke, United Kingdom), and *L. monocytogenes* in BHI, all at 37°C.

3.3.2 Light irradiation

For the light irradiation experiments, two customized LED lamps were employed. Each lamp consisted of an iron enclosure with adjustable height and a lid with eight LED connected in parallel (**Figure 3.1**). The lamps were designed to emit light at distinct wavelengths, with emission peaks at 405 nm and 365 nm. Irradiance on the surface of the experimental plates was quantified using an HD2302.2 radiometer (Delta Ohm, Caselle di Selvazzano, Italy) equipped with LP471 probes specific for blue light (BL) and ultraviolet-A (UVA) measurements (Delta Ohm, Caselle di Selvazzano, Italy). A light diffusor was added to emit a uniform irradiance. The final irradiation dose (D, expressed in J cm^{-2}) was calculated for each treatment.

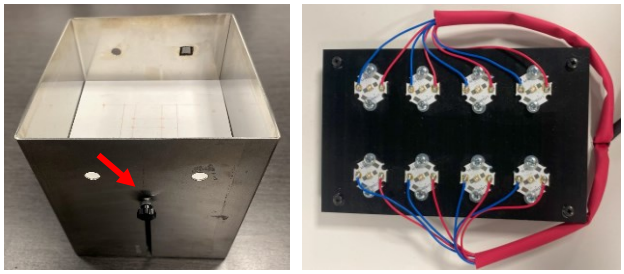


Figure 3.1. Bench set up for the illumination.

3.3.3 Bacterial cell culture preparation and light treatment

Overnight cultures were washed three times with PBS solution, centrifuged at 1700 *x g* for 15 min and diluted 1:100 in the culture broth. Cell suspensions were adjusted to an optical density

of 1, corresponding to a concentration of approximately 10^9 CFU/mL. The bacteria were treated during their logarithmic growth phase. After standardization, the cultures were further diluted to achieve a final concentration of 10^5–10^6 CFU/mL. The prepared bacterial suspensions were then dispensed into a 96-well plate as illustrated in **Figure 3.2**.

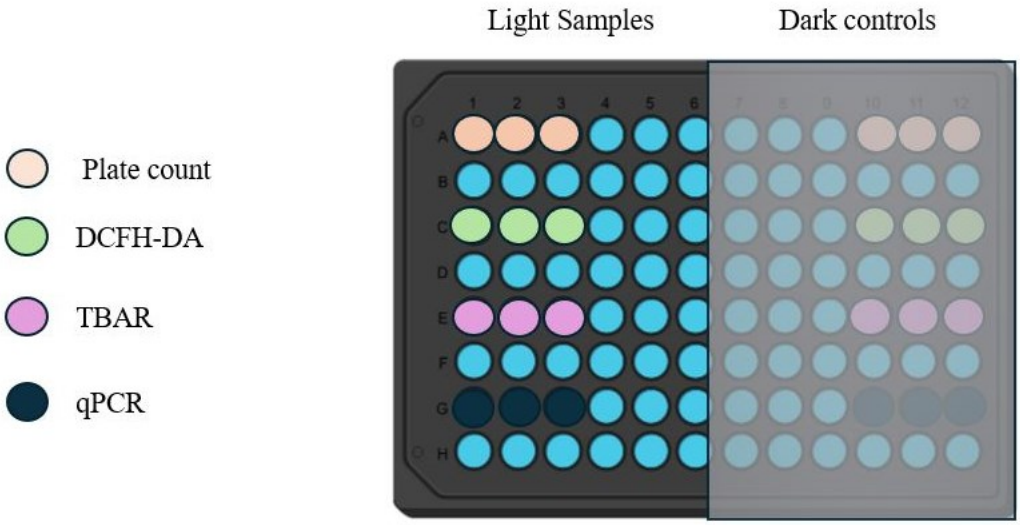


Figure 3.2. Experimental set-up of the light treatment. Irradiated samples and their respective dark controls were used for the plate count, the DCFH-DA assay for ROS quantification, the TBAR assay for the lipid peroxide quantification and for Real-Time PCR for the membrane integrity assessment.

The prepared multi-well plate was partially covered, with the samples under the covered section serving as the dark controls. All bacteria strains were exposed to light at 365 nm and 405 nm wavelengths, at both 4°C and 23°C, for 5h, receiving a light dose equal to 32.4 J cm^{-2}.

3.3.4 Cell Viability

The wells for the plate count were removed from the microwell-plate and serially diluted in PBS. After, to assess the cell viability, each sample was plated using the drop plate method in the respective culture media (NB for *E. coli*, BHI for *L. monocytogenes* and TSB for *S. aureus*). Results were finally expressed as CFU/mL and transformed in the logarithm CFU/mL. The Log (N/N0) were then calculated, where N is the log CFU/mL after the BL treatment and N0 is the log CFU/mL of the control.

3.3.5 Live/Dead PCR

Membrane integrity was assessed through a Live/Dead PCR, which relies on the addition of a propidium monoazide dye, PMAxx 25 µM (PMAxx 31075-X, Biotum, Shangai, China), following the manufacturer's instructions. PMAxx is a dye which intercalates between the DNA strands when a bacterium has a damaged membrane. After light treatment, 0.25 µM of PMAxx stock solution were added to 100 µL of bacterial suspension (10^5/10^6 CFU/mL). The samples were incubated at 37°C for 15 min, after which crosslinking was done for 15 min with PMA-Lite™ (PMA-Lite TM PT18A, Biotium, Shangai, China). After the second photoactivation step, the treated samples were stored at −20°C for further analysis.

3.3.5.1 DNA extraction

DNA extraction was carried out as follows: samples were defrosted for 10 minutes, and 250 µL of iQ-Check lysis buffer with glass beads (Bio-Rad, California, USA) was added to each sample. The mixtures were heated to 95°C for approximately 20 minutes in a thermoblock, followed by homogenization for 1 minute every 5 minutes. The samples were then centrifuged at 1700 × *g* for 5 minutes (810 R, Eppendorf, Milan, Italy). Subsequently, 100 µL of the supernatant was carefully transferred into a new tube and used as the template for Real-Time PCR analysis.

3.3.5.2 Real-Time PCR

The final volume of qPCR reaction in each well was 10 µL and the reaction mix was prepared by adding 5 µL of Master mix Luna® Universal Probe qPCR Master Mix 2x probe (New England Biolabs, Ipswich, MA, USA); 0.25 µM of forward primer, 0.25 µM of reverse primer, 0.125 µM of the probe, 3.375 µL of sterile water for PCR and 1 µL of DNA. The gene target for all the tested microbes was 16S. The specific primers are reported in **Table 3.1**.

Table 3.1. Primers and probes used for the Real-Time PCR reaction. Probes were designed based on the melting temperatures.

Microorganism	Target gene	Primer	Sequence (5'-3')
Listeria monocytogenes	16S	Forward	TTCCGCAATGGACGAAAGTC
		Reverse	ATACCGTCAAGGGACAAGCA
		Probe	ACACGCGGCGTTGCTCCGTC
Escherichia coli	16S	Forward	GAGAATGTGCCTTCGGGAAC
		Reverse	CCGCTGGCAACAAAGGATAA
		Probe	TCCCGCAACGAGCGCAACCC
Staphylococcus aureus	16S	Forward	ACTCGTTAAGGCTGAGCTGT
		Reverse	GACTACCTGTGTCGGTTTGC
		Probe	CGAGTCGTTGATTTCACACTGCCGA

Real-Time PCR reaction was performed with CFX96 TM Real-Time System (C1000 Touch TM Thermal Cycler, Bio-Rad, California) and iQ^{TM} 96-well PCR plates (Bio-Rad, Milan, Italy). The protocol consisted of 5 minutes of denaturation at 98°C, and 31 cycles of amplification of denaturation at 98°C for 5 sec, followed by annealing and extension at 60°C for 20 sec.

For each qPCR reaction, positive and negative controls were included. In particular, positive controls were genomic DNA extracted form *E. coli*, *S. aureus* and *L. monocytogenes* cells, while the negative control consisted of water only. For each sample, two technical replicates were done during all qPCR reactions, and three biological replicates were done.

3.3.5.3 Viable cell quantification through Live/Dead qPCR

After getting the amplification curves for each microorganism, the difference in Cycle threshold (dCt) was calculated by subtracting the Cycle threshold (Ct) of the Dark control from the Ct of the light sample. The dCt was then compared to the viable cell count. The Ct is the amplification cycle upon which the accumulated signal crosses the baseline threshold. Dead cells treated with PMAxx exhibit delayed amplification of DNA compared to untreated dead cells, which causes a large dCt.

3.3.6 DCFH-DA assay

ROS production was evaluated using the 2′,7′-Dichlorofluorescin Diacetate (DCFH-DA) assay (MAK143, Sigma-Aldrich, Milan, Italy). DCFH-DA is a non-fluorescent probe that becomes fluorescent upon oxidation, forming 2',7'-dichlorofluorescein (DCF). For this assay, bacterial cultures, after being centrifuged, were resuspended in 2X concentration of culture medium (TSB for *S. aureus*, NB for *E. coli* and BHI for *L. monocytogenes*) and 100 µL were used for the tests and the same volume of the DCFH-DA solution was added (100 µL).

The fluorescence spectrum of the solution was measured at an excitation wavelength of 485 nm and an emission wavelength equal to 520 nm with FLUOstar Omega 415-4475 (BMG Labech Gmbh, Ortenberg, Germany). Results were expressed as Relative Fluorescence Units (RFU).

3.3.7 TBAR assay

The lipid peroxidation was assessed through the Thiobarbituric Acid Reactive Substances (TBAR) assay (MAK085, Sigma-Aldrich, Milan, Italy), which relies on the production of end products such as malondialdehyde (MDA). The assay is based on the reaction between MDA and thiobarbituric acid (TBA), resulting in the formation of a colourimetric product whose intensity is proportional to the amount of MDA present. The assay was conducted according to the manufacturer's instructions, and the colourimetric product was quantified by measuring the absorbance at 532 nm with FLUOstar Omega 415-4475 (BMG Labech Gmbh, Ortenberg, Germany). Results were expressed as nmol/well.

3.3.8 Data Analysis

Results were expressed as CFU/mL and transformed in the logarithm CFU/mL. The Log (N/N0) were then calculated, where N is the log CFU/mL after the BL treatment and N0 is the log CFU/mL of the control. The data were elaborated with Microsoft Excel, represented as the mean of three biological replicates ± standard deviation (SD) with GraphPad Prism 9.0.0 and subjected to statistical analysis by IBM SPSS Statistics for Windows version 23.0 (IBM Corp., Armonk, N.Y., USA). The statistical methods used to determine the significant differences between the samples were the Paired T-Test, One-way ANOVA ($p \leq 0.05$), Three-way ANOVA ($p \leq 0.05$) and post-hoc Tuckey-B test.

3.4 Results and discussion

Figure 3.3 illustrates the microbial inactivation results of *L. monocytogenes* (**a.**), *S. aureus* (**b.**), and *E. coli* (**c.**) following exposure to 32.4 J cm^2 irradiation at 365 nm and 405 nm wavelengths under two temperature conditions, 23°C and 4°C. For all the tested microbes, the controls remained stable at 10^5–10^6 CFU/mL.

For *L. monocytogenes* (Gram +), the observed inactivation was approximately -2 log at both the wavelengths and temperatures, with no statistical difference ($p > 0.05$). *L. monocytogenes* employs specific mechanisms to counteract environmental stresses, such as low temperatures, including the production of superoxide dismutase and catalase to neutralize ROS generated via the respiratory pathway. Additional oxidative stress resistance mechanisms involve the metalloregulatory protein PerR and 2-Cys peroxiredoxin (Prx) (Mains et al., 2021), along with the sigma factor σ^B (Raengpradub et al., 2008). Furthermore, *L. monocytogenes* has been shown to contain saturated branched-chain fatty acids (BCFAs), which enhance survival under low pH and low-temperature conditions (Hong et al., 2024).

Considering *S. aureus* (Gram +), irradiation at 4°C achieved microbial inactivation levels of approximately -1.40 log for both wavelengths, while at 23°C, inactivation was approximately -0.98 log. Although these differences were not statistically different ($p > 0.05$), the findings align with prior research by Ghate et al., (2013), which reported enhanced inactivation of foodborne pathogens at lower temperatures (4°C and 10°C) when irradiated with 405 nm light, compared to higher temperatures (20°C). Furthermore, other studies (Bastock et al., 2021; Guan et al., 2024) have linked the temperature-dependent survival of *S. aureus* to variations in gene expression, transcriptomic, and proteomic profiles, facilitating environmental adaptation. Specific genes, including *rsbV*, *rsbW*, and *sigB*, were shown to exhibit differential expression in response to temperature shifts. These findings highlight variability in the stress response mechanisms among Gram (+) bacteria.

The Gram (-) *E. coli* exhibited the highest inactivation results, with reductions exceeding -4.60 log across both wavelengths and temperatures. Previous studies (i.e., Barth et al., 2009), have identified oxidative stress-related genes in *E. coli*, noting that reductions in cAMP levels can partially inactivate the global transcriptional regulator cAMP receptor protein (CRP). This reduction subsequently represses the *rpoS* gene, which encodes for the alternative sigma factor σ^B, essential for the general stress response in *E. coli*.

The influence of temperature on microbial inactivation has been the subject of varying findings. Some studies indicate that lower temperatures (10–15°C) enhance inactivation compared to

higher temperatures (20°C) (Ghate et al., 2013). Conversely, others have reported greater inactivation at higher temperatures (25°C) for specific microbes such as *S. aureus*, while observing minimal or no temperature effect for others, including *L. monocytogenes* (Kumar et al., 2015, 2016).

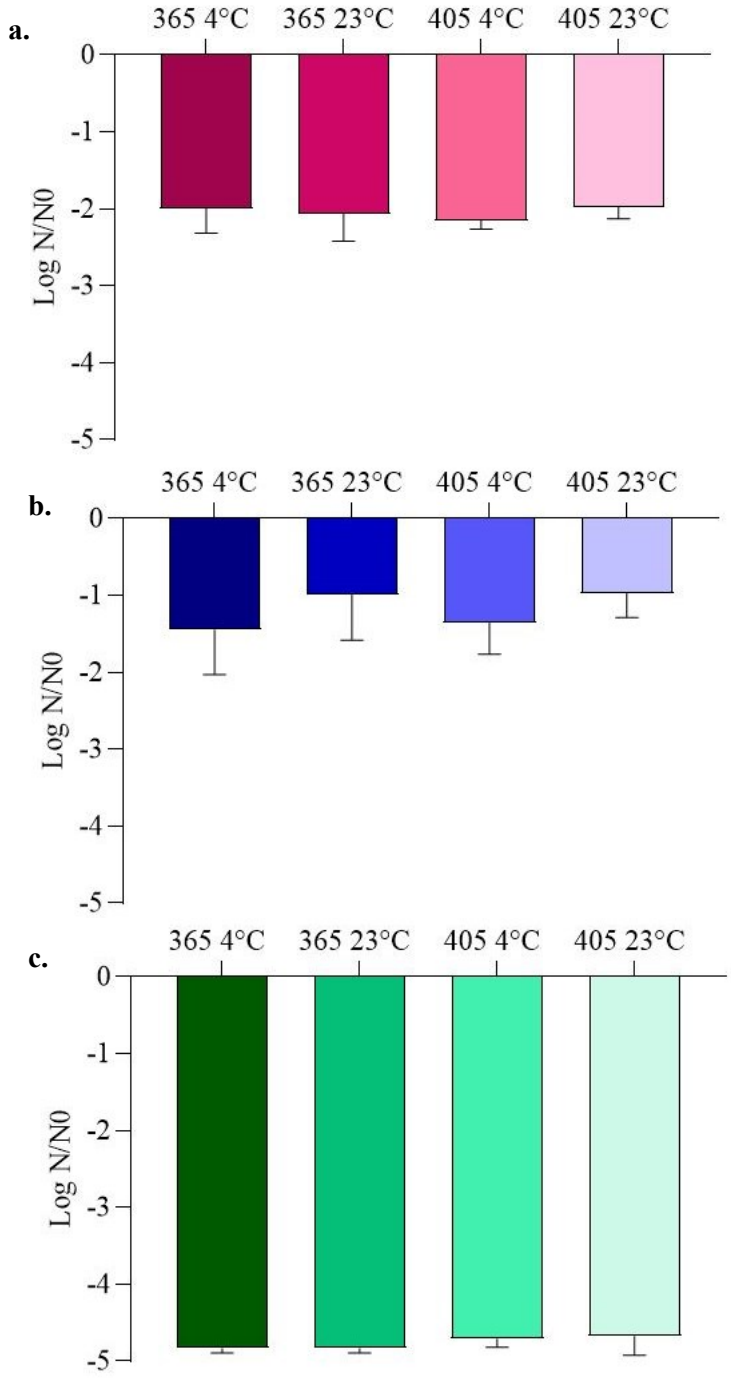


Figure 3.3. Microbial inactivation expressed as Log N/N0 of **a.** *L. monocytogenes*, **b.** *S. aureus*, and **c.** *E. coli*, after being irradiated for 5h with 365 nm and 405 nm wavelengths at 4°C and 23°C with a light dose of 32.4 J cm^{-2}. The results are the average of three biological replicates.

Controversy from what was observed in the literature and in the previous results (see Chapter 2), in this case, Gram (–) bacteria exhibit a higher susceptibility to BL compared to Gram +. However, the literature also presents some contradictions about this. For instance, Tomb et al. (2018) evaluated 80 articles and depicted that in some experimental conditions Gram (+) bacteria required higher doses to get 1 log of inactivation. Therefore, it could be pointed out that several parameters influence the inactivation results even in the same bacterial species. Factors like the temperature, the light sources, the bacterial strains and the culture media could be responsible for a non-homogeneity of the results. Furthermore, more studies are required to deeply investigate this feature.

ROS encountered by bacterial cells are generated both endogenously and exogenously, prompting microbes to develop diverse mechanisms for sensing oxidative stress and initiating detoxification processes. Typically, cells detect oxidative stress through transcription factors such as OxyR and PerR, which regulate the expression or repression of key enzymes, including catalase (Kat), alkyl hydroperoxide reductase (Ahp), and superoxide dismutase (SodA). Additionally, critical regulators of stress responses have been identified, such as Agr in *Staphylococcus aureus*, SarA in *staphylococci*, and σ^B (Rapacka-Zdończyk et al., 2021). The SOS system plays a central role in detoxification by activating various stress response pathways, primarily through the action of RecA and LexA (Baharoglu & Mazel, 2014). Despite the presence of these protective mechanisms, it remains unclear whether light treatments specifically enhance the expression of these genes in response to photodamage.

For all microorganisms studied, no significant differences were observed when comparing inactivation under different wavelengths or temperatures. However, as summarized in **Table 3.2**, when considering all variables (temperature, wavelength, and microorganism type), microbial inactivation was predominantly influenced by the microorganism type, accounting for 98.8%. Temperature contributed 0.82%, while the interaction between temperature and microorganism type explained only 0.29%.

Table 3.2. Three-Way Analysis of variance (ANOVA) of the effect of three variables: temperature (T), wavelength (W), microorganism (M).

Variables	SS%	$p \leq 0.05$
T	0.82	**
W	0.01	ns
M	98.8	***
T x W	0.00	ns
T x M	0.29	*
W x M	0.02	ns
T x W x M	0.08	ns

SS, sum of squares; p, significance; * $p \leq 0.05$; ** $p \leq 0.01$; *** $p \leq 0.001$; ns: not significant.

The production of ROS is depicted in **Figure 3.4**. All tested microorganisms exhibited substantial ROS production under light treatment, significantly exceeding levels observed in dark controls at both wavelengths and temperatures.

For all the tested microbes, the dark controls showed similar values which range from 59 to 475 RFU. On average, the ROS production of the controls was 304, 248 and 248 RFU for *L. monocytogenes*, *S. aureus* and *E. coli*. These values did not show any difference based on the applied wavelength or the temperature.

Among the microorganisms, *L. monocytogenes* (**Figure 3.4 a.**) displayed the highest ROS production, ranging between 12,000 and 14,000 RFU. This elevated ROS level may arise from intrinsic ROS generation by *L. monocytogenes*, which appears to be amplified by light exposure. This phenomenon aligns with findings from Guo et al. (2019), which documented endogenous ROS production by *L. monocytogenes* even in the absence of irradiation.

For *S. aureus* (**Figure 3.4 b.**), ROS production ranged from 9,400 to 11,000 RFU, slightly lower than that of *L. monocytogenes*. This corresponds with the slightly reduced microbial inactivation observed for *S. aureus*. However, the differences in microbial inactivation between 23°C and 4°C were not reflected in ROS production levels. Elevated ROS generation post-irradiation for *S. aureus* has been corroborated by previous studies (Jiang et al., 2013; Li et al., 2021).

In contrast, *E. coli* (**Figure 3.4 c.**) exhibited ROS levels ranging from 3,500 to 5,100 RFU, substantially lower than those of *L. monocytogenes* and *S. aureus* (approximately one-third to one-half). Despite this lower ROS production, *E. coli* achieved the highest microbial inactivation (approximately -4 log). These findings suggest that enhanced microbial inactivation for *E. coli* is not directly proportional to ROS levels. Zhang et al. (2018) similarly reported comparable ROS production in *E. coli* following light irradiation.

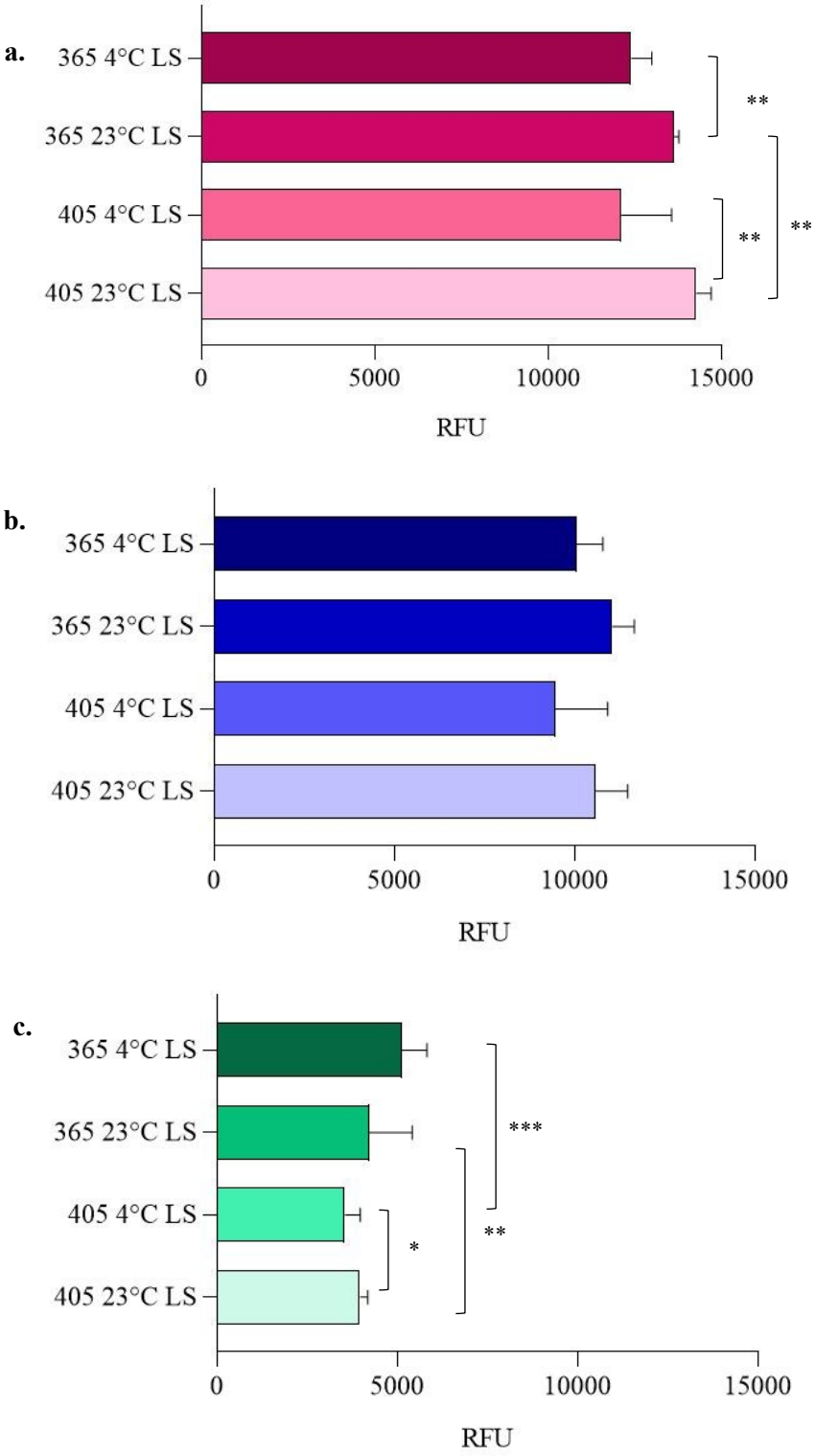


Figure 3.4. Amount of intracellular Reactive Oxygen Species (ROS) produced by **a.** *L. monocytogenes* **b.** *S. aureus* **c.** *E. coli* after 5h of light treatment at 32.4 J cm^{-2}. *$p<0.05$; **$p<0.005$; ***$p<0.001$. LS: samples treated with light. The results are the average of three biological replicates.

The observed ROS production is closely linked to the intracellular PS of each microorganism, which varies in type, quantity, and cellular localization. Even within the same species, these

factors can differ at the strain level, making microorganism type a critical determinant in the efficacy of light-based treatments. Dong et al. (2020) demonstrated variation in ROS production across three *Enterococcus* strains following light exposure.

These findings underscore the strain-dependency of light-based microbial inactivation technologies (Grinholc et al., 2008; Rapacka-Zdończyk et al., 2021). The production of ROS, the primary agents of inactivation, can vary significantly depending on the microbial species and strain irradiated. This conclusion is supported by the results of the Three-Way ANOVA (**Table 3.1**), which identified microorganism type as the primary factor influencing microbial inactivation.

Figure 3.5. presents MDA levels as an indicator of lipid peroxidation following light treatments across the selected microbial species. Unlike the trends observed for ROS production, MDA formation did not follow a consistent pattern. All light-irradiated samples (LS) exhibited higher MDA levels than their respective dark controls (DC), though these differences were not uniformly significant.

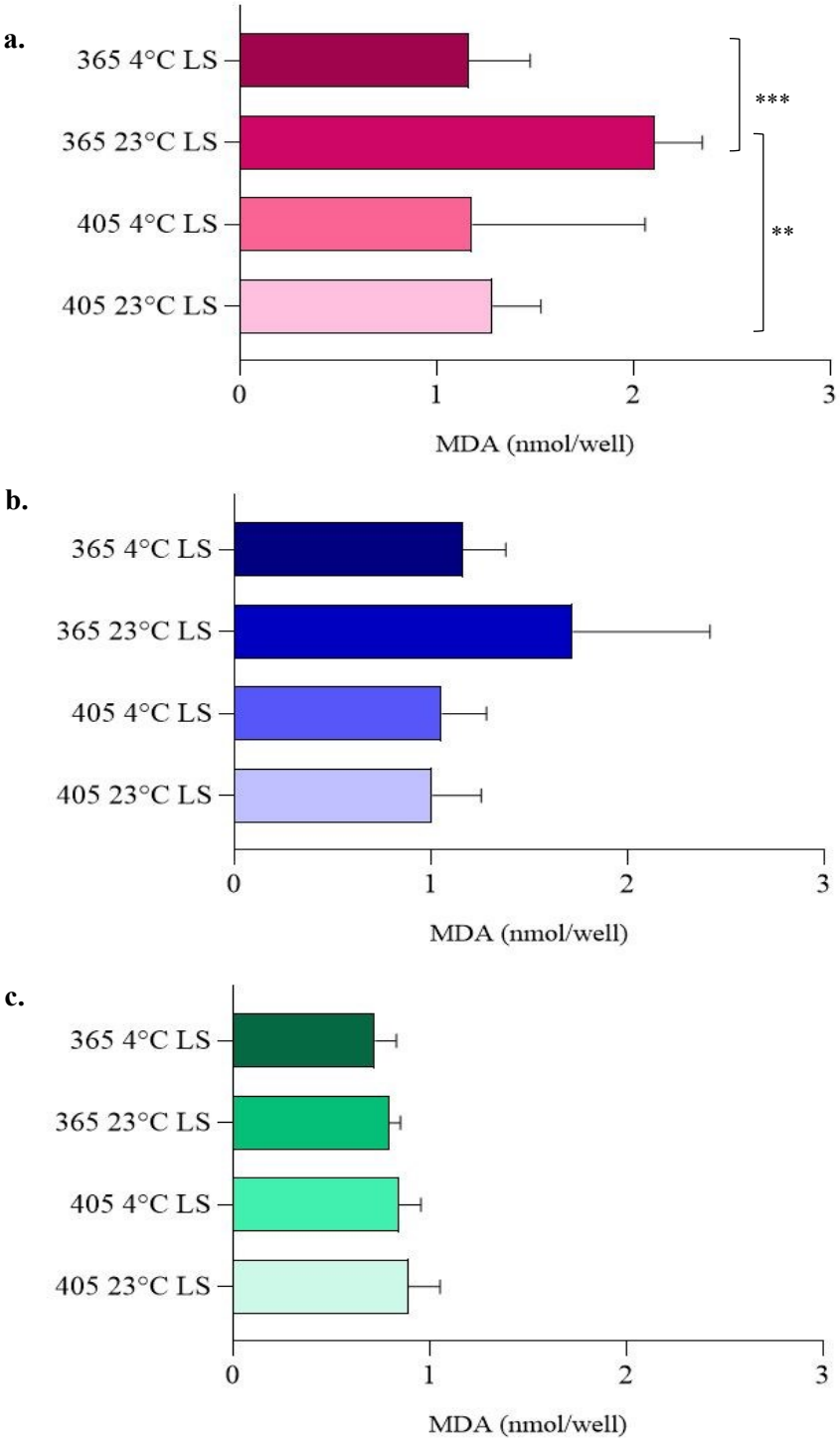


Figure 3.5. Malondialdehyde (MDA) levels detected in **a.** *L. monocytogenes* **b.** *S. aureus* **c.** *E. coli* after the cells were treated for 5h with 32.4 J cm^{-2}. *$p<0.05$; **$p<0.005$; ***$p<0.001$. LS: samples treated with light. The results are the average of three biological replicates.

For *L. monocytogenes* (**Figure 3.5 a.**), the highest MDA levels were observed under 365 nm irradiation at 23°C. Conversely, no significant difference was detected between light and dark conditions at 4°C for the same wavelength. *S. aureus* (**Figure 3.5 c.**) exhibited a similar pattern, with the highest MDA levels observed under 365 nm light at 23°C, though variations in MDA production across all light-irradiated samples were relatively minor.

In contrast, *E. coli* (**Figure 3.5 b.**) demonstrated relatively consistent MDA levels across all light-irradiated conditions. However, as observed with ROS production, MDA levels in *E. coli* were significantly lower than those recorded for the Gram (+) bacteria, *L. monocytogenes* and *S. aureus*.

These results indicate variability in lipid peroxidation among bacterial species, influenced by inherent differences in MDA production. Additionally, strain-level variations within the same species further contribute to the heterogeneity of lipid peroxidation. Dong et al. (2020) reported distinct MDA levels across three *Enterococcus* strains, emphasizing the role of strain-specific factors.

The membrane damage caused by lipid peroxidation can also be analysed using Real-Time PCR by using the PMAxx dye. PMAxx is a dye that intercalates between the DNA strands when a bacteria has a damaged membrane. After, it is cross-linked to DNA strands. **Figure 3.6** illustrates the amplification curves for (**a.**) *L. monocytogenes*, (**b.**) *E. coli*, and (**c.**) *S. aureus*, providing direct insights into membrane damage dynamics under the tested conditions.

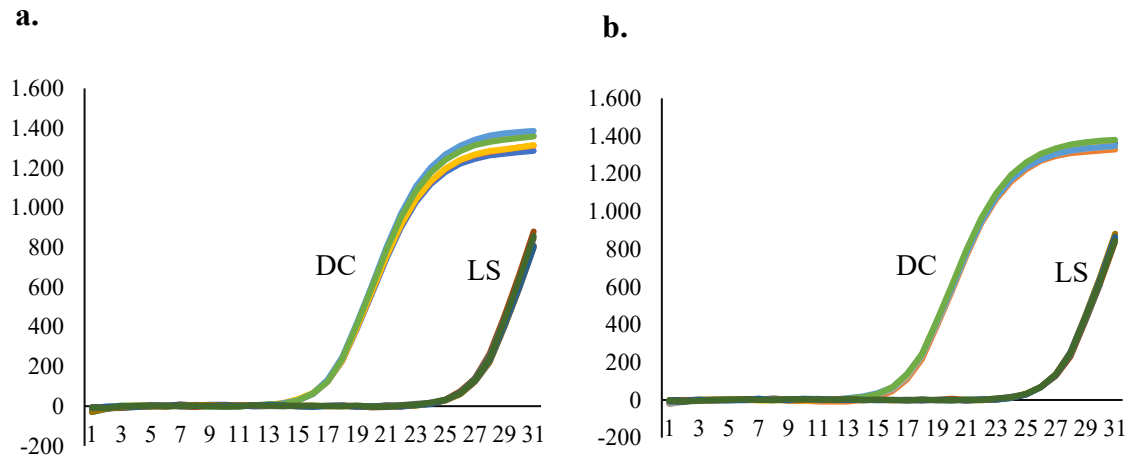


Figure 3.6. Example of amplification curves of *E. coli* treated at **a.** 4°C and **b.** 23°C with 365 nm. LS, Light Sample, are the samples treated under light irradiation, DC, Dark Controls.

The differences in Ct values for the tested microorganisms under all experimental conditions are summarized in **Table 3.3**. As reported by the manufacturer instructions, the expected result for the dead cell control is a dCt > 4, since Ct values are on a log2 scale, so a dCt of 4 represents approximately a 16-fold decrease or 94% of dead cell DNA removed. A dCt of 8 represents an approximately 250-fold decrease or 99.6%.

However, a comparison of qPCR-derived results with viable cell counts revealed that the dCt values do not align perfectly with microbial inactivation observed via plate counting.

For all tested microbes, qPCR underestimated the extent of microbial inactivation. Specifically, for *L. monocytogenes*, the dCt was approximately 3, corresponding to a theoretical 1 log reduction, while plate counts indicated a microbial inactivation of around -2.00 log under all tested conditions. This discrepancy was even more pronounced for *S. aureus*, where dCt values were minimal (approximately 0.50–0.60), suggesting negligible inactivation, in contrast to the observed reductions in viable counts. Similarly, *E. coli* exhibited the highest dCt values, but even in this case, the inferred microbial inactivation from qPCR was lower than that determined via plate counts.

It is essential to recognize that the correlation of 4 qPCR cycles to a 1 log reduction is not a fixed rule. Variations in reaction efficiency and other experimental factors can influence this relationship, highlighting the need for cautious interpretation of qPCR results in the context of microbial inactivation studies and underlining the existence of other factors inducing cell death in addition to membrane permeabilization.

Table 3.3. Difference of the average cycle threshold of samples added with PMAxx irradiated with light (LS) and the respective dark controls (DC) for all the tested microbes under all the treatment conditions. The results are the average of three biological replicates.

	365 4°C		**365 23°C**		**405 4°C**		**405 23°C**	
	dCt	**Log N/N0**	**dCt**	**Log N/N0**	**dCt**	**Log N/N0**	**dCt**	**Log N/N0**
L. monocytogenes	3.14	-2.00	3.25	-2.07	2.65	-2.15	3.23	-1.98
E. coli	9.94	-4.83	9.87	-4.66	9.85	-4.71	10.1	-4.68
S. aureus	0.53	-1.45	0.53	-0.99	0.54	-1.35	0.64	-0.97

The observed discrepancies between the dCt values obtained via qPCR and microbial inactivation determined by plate count may be attributed to two potential mechanisms.

The first hypothesis considers that Gram (+) and Gram (−) bacteria exhibit distinct responses to photodynamic inactivation, as previously reported (Luksiene 2005; Malik et al., 1992; Yin et al., 2013). In this study, *L. monocytogenes* and *S. aureus* (Gram +) displayed average inactivation levels of approximately -2.00 log and -1.10 log, respectively, while *E. coli* (Gram −) achieved significantly higher inactivation levels of approximately -4.70 log.

When comparing these inactivation levels with ROS production, a consistent trend was observed for Gram (+) bacteria. *L. monocytogenes* exhibited slightly higher microbial inactivation than *S. aureus*, which was mirrored in ROS production values. Specifically, the ROS levels for *S. aureus* were marginally lower than those for *L. monocytogenes*, correlating with the reduced cell viability observed.

For Gram (−) *E. coli*, the ROS levels following light irradiation were comparatively lower than those of the Gram (+) bacteria. Despite this, *E. coli* exhibited significantly higher microbial inactivation. This discrepancy suggests that different microbial species have varying thresholds for ROS-induced inactivation, influenced by their oxidative stress resistance mechanisms and intracellular PS activity. The presence of oxidative stress defences, such as catalase and superoxide dismutase, likely contributes to these differences in inactivation and ROS thresholds. Johnson & Hug (2019) emphasized that ROS detoxification systems are ubiquitous among bacteria, regardless of their environmental oxygen levels. However, assuming that superoxide dismutase, catalase, and peroxidase are the universal mechanisms for ROS detoxification across all bacterial phyla oversimplifies the complexity and diversity of bacterial ROS responses.

The levels of MDA, an indicator of lipid peroxidation, mirrored the trends observed for ROS production. Among Gram (+) bacteria, the light treatment led to higher MDA production, with *L. monocytogenes* showing slightly elevated levels compared to *S. aureus*. This finding aligns with the observed microbial inactivation trends. Conversely, Gram (−) *E. coli* produced lower MDA levels following irradiation.

When comparing MDA data with Real-Time PCR results, no direct linear correlation emerged between membrane damage-induced cell death and lipid peroxidation. This suggests the involvement of additional factors in membrane damage and subsequent microbial death (Anju et al., 2019; Choby & Skaar, 2016). Also, it should be considered that a BL treatment could produce a sub-lethal stress which could form viable but not countable cells (VBNC). VBNC are cells that do not grow in the culture media but are still alive, maintaining certain metabolic functions and, under favourable conditions, they can recover and reproduce again. Therefore,

their presence can favour an overestimation of the death cells by plate count, which is problematic in the possible context where the absence of specific pathogens is required (Truchado et al., 2020).

The second hypothesis posits that Gram (+) and Gram (−) bacteria differ in the expression of oxidative stress defence mechanisms. In Gram (−) bacteria, this likely results in lower tolerance to ROS and increased susceptibility to cell death, with substantial membrane damage as a secondary effect. Light irradiation in *E. coli* may generate ROS levels exceeding the microbe's tolerance threshold, leading to nucleic acid damage and subsequent cell death. Membrane damage, in this case, is a downstream effect of these primary oxidative injuries.

Hu et al. (2021) stated that the sensitivity to BL can be affected by the outer membrane permeability. *rfa*C gene, involved in lipopolysaccharides biosynthesis, could be suppressed by BL action, determining a modification of fatty acid composition and consequently on the outer membrane permeability, increasing the sensibility to BL.

In contrast, Gram (+) bacteria likely express more robust oxidative stress defences, enabling greater ROS tolerance and offering protection to critical intracellular components (i.e., nucleic acids) up to their tolerance threshold. Beyond this threshold, ROS accumulation leads to microbial death. This pattern aligns with findings from other studies (Anju et al., 2019; Nakamura et al., 2012), which highlighted ROS-induced oxidation of vital macromolecules and lipid peroxidation as mechanisms of microbial inactivation.

The natural habitats of these microbes may explain their differential ROS tolerance. *S. aureus* inhabits human skin and is routinely exposed to sunlight and oxidative stress, necessitating more robust defences. In contrast, *E. coli* resides in the human gut, where oxidative stress exposure is less pronounced. This ecological distinction supports differences in ROS handling and was corroborated by Johnson & Hug (2019), who noted that bacterial ROS defences vary widely and are shaped by environmental conditions.

Furthermore, extensive DNA damage from ROS can activate stress responses, such as the SOS response, characterized by the upregulation of genes like *uvrA* and *dinB*. Key genes such as *RecA*, *uvrA*, and *dinB* may be significantly overexpressed, indicating a strong SOS response. However, overexpression of such stress-related genes may ultimately suppress resistance mechanisms (Song et al., 2023).

3.5 Conclusion

This study highlights the complex interplay between ROS production, lipid peroxidation, and microbial inactivation under light irradiation conditions for both Gram (+) (*L. monocytogenes*, *S. aureus*) and Gram (-) (*E. coli*) bacteria by using UVA and BL wavelengths (365 and 405 nm) and two temperatures (4 °C and 23 °C). The results confirm that microbial type is the dominant factor influencing inactivation efficacy, with *E. coli* exhibiting the highest susceptibility despite producing lower ROS and MDA levels compared to Gram (+) species. This suggests that Gram (-) bacteria may have a lower tolerance to oxidative stress, leading to rapid cell death even at lower ROS levels, possibly due to nucleic acid damage preceding membrane compromise.

Conversely, Gram (+) bacteria, with more robust oxidative stress defences, demonstrated higher ROS and MDA levels before reaching their inactivation thresholds, implying that their resistance mechanisms allow for greater tolerance to oxidative stress until critical levels are reached. The observed discrepancies between viable plate counts, Real-Time PCR, and MDA levels indicate that microbial inactivation involves multifaceted mechanisms beyond lipid peroxidation, including oxidative damage to vital intracellular components and the induction of stress responses such as the SOS pathway. These differences could also be due to the presence of viable but not countable cells (VBNC), which may lead to an overestimation of the cell's death registered with place count due to their inability to grow in the culture media but their vitality. Their presence could be problematic in contexts where the absence of specific pathogens is a legal requirement for their possibility of restoration. The ecological adaptations of these microbes further underscore the role of environmental pressures in shaping their oxidative stress defences.

In conclusion, the findings reinforce the strain-specific and species-specific nature of light-induced microbial inactivation, emphasizing the importance of considering microbial physiology and environmental adaptation when optimizing light-based technologies for microbial control.

Future research should prioritize uncovering the precise molecular mechanisms underlying ROS production in treated microorganisms and the subsequent oxidative responses these processes trigger. This includes exploring how different microbial species and strains generate and tolerate ROS, the role of intracellular PS, and the activation of oxidative stress defence pathways.

Chapter 4

Inactivation of microbial Biofilm with Blue Light

4.1 Introduction

A biofilm is a structured, cooperative community of microorganisms that strongly adheres to a surface and is encased in a matrix, mainly composed of polysaccharides produced by the microorganisms themselves (Achinas et al., 2019; Costerton et al., 1987).

The formation of pathogenic biofilms on food contact surfaces is a primary source of cross-contamination within the food industry, posing a significant health risk to consumers as well as a huge economic loss (Kumar et al., 2017).

Most bacteria can form biofilms under favourable conditions, a capability that acts as an adaptive and resilient strategy for survival. Through biofilm formation, microbes enhance nutrient availability, improve water retention, and enable the exchange of genetic material. This adaptability is particularly concerning in the food industry, as biofilms can transfer antimicrobial resistance to other cells, increasing the risk of contamination and persistence of harmful bacteria (Cervantes-Huamán et al., 2022).

Traditional anti-biofilm methods primarily involve the use of chemical disinfectants, detergents, and antibiotics (Coughlan et al., 2016; Roy et al., 2018). Recently, light-based technologies have emerged as promising alternatives for biofilm eradication, as bacteria are less likely to develop resistance to these treatments (Argyraki et al., 2017; Gora et al., 2019). In the medical field, BL has gained attention for biofilm eradication due to its ability to target bacterial cells selectively, minimizing the harmful effects on mammalian cells. In the food sector, it could represent a good alternative to the classical disinfection method or in combination with other techniques (Ferrer-Espada et al., 2020; Yang et al., 2017).

Research on the effectiveness of BL against biofilms has predominantly focused on early-stage biofilms (Ferrer-Espada et al., 2019, 2020; McKenzie et al., 2013). However, testing on more mature biofilms is essential, as these conditions more closely represent the persistent biofilms encountered in food production environments.

4.2 Aim of the study

After the comprehensive studies on the effect of BL to inactivate planktonic cells in the forms which may be found in a food-related environment, this study takes a step forward to understand the BL could be a useful strategy to inactivate biofilms formed by a range of foodborne

pathogens and spoilage bacteria. Investigating biofilms in a food-related context is critical because biofilms can harbour microorganisms that contribute to food contamination, spoilage, and the transmission of foodborne illnesses. Moreover, biofilms are notoriously resistant to conventional cleaning and disinfection methods, posing significant challenges to food safety and quality. In addition to assessing inactivation, this study seeks to explore potential morphological changes in bacterial cells and modifications in biofilm architecture induced by BL treatment, which could provide insights into improving sanitation practices in the food industry.

4.3 Material and Methods

4.3.1 Microbial Strains and Culture Conditions

The microorganisms used for biofilm formation and inactivation were the same as described in **Chapter 2**, **paragraph 2.3.2**.

4.3.2 Blue Light source

BL sources were the same as described in **Chapter 2**, **paragraph 2.3.1**.

4.3.3 Biofilm formation

The overnight cultures were washed three times with 1 mL of PBS, followed by centrifugation at 13,000 *x g*. To prepare the inoculum, the microbial suspensions were diluted 1:1000 in Luria Bertani broth (LB, Oxoid, Milan), resulting in a final concentration of $10^5/10^6$ CFU/mL and a total volume of 80 mL.

4.3.3.1 5-days biofilm formation

Four 6-well microplates were prepared by adding 5 mL of the inoculum to four wells. The microplates were then incubated for 5-days at 30°C under orbital agitation. Every 48 hours, the biofilms were refreshed by removing 3 mL of exhausted broth and replacing it with 3 mL of fresh LB broth (**Figure 4.1**).

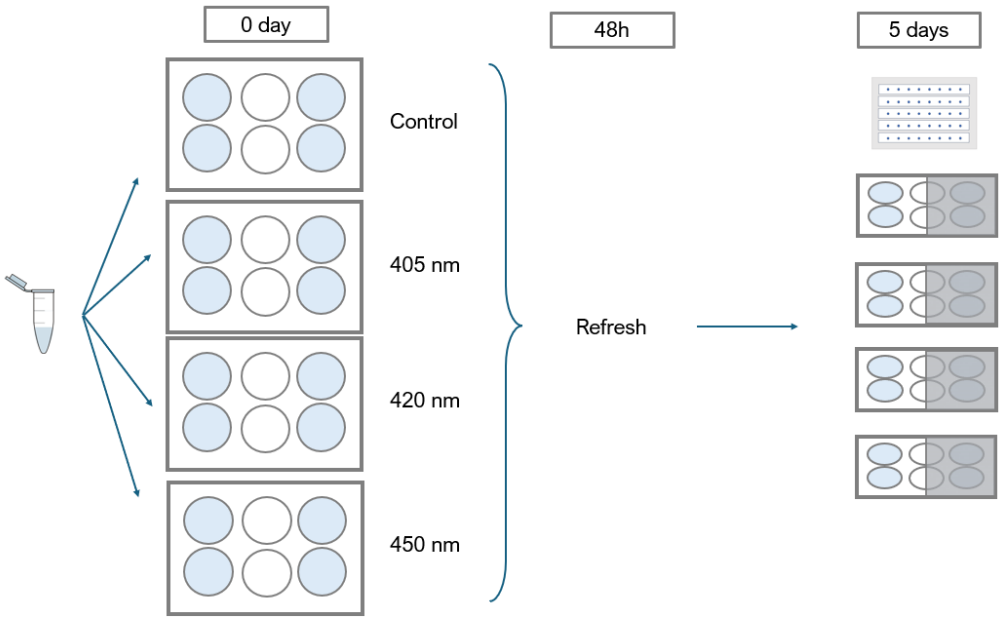


Figure 4.1. Experimental set-up of biofilm preparation. Bacterial cultures were added to four wells of the multi-well plates to let the biofilms growth; every 48h, the addition of fresh culture media was done (refresh) and, after 5-days, biofilms were treated with blue light.

4.3.3.2 Biofilm formation on glass surfaces

Sterile glass coverslips were placed into a sterile Petri dish, and 15 mL of the bacterial inoculum was added. The plates were then incubated for 13-days at 30°C under orbital agitation. Every 48 hours, the biofilms were refreshed by removing the exhausted broth and replacing it with fresh LB broth (**Figure 4.2**).

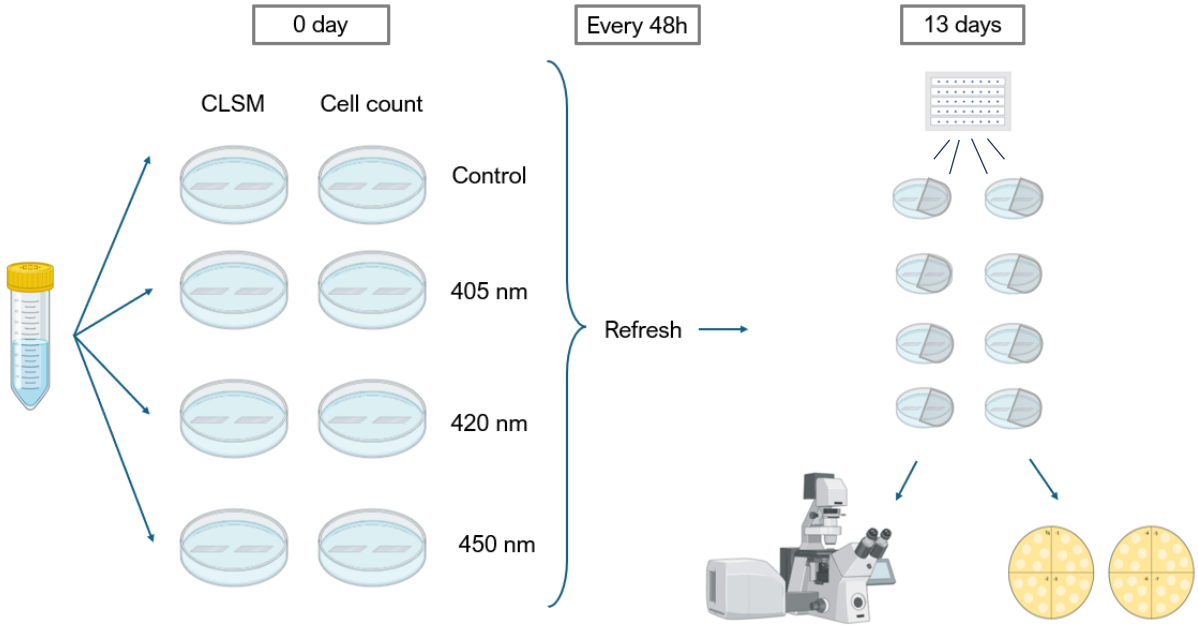


Figure 4.2. Experimental set-up of biofilm blue light treatment. Bacterial cultures were added to sterile Petri dishes with glass coverslips to let the growth of the biofilm (for the plate count and the confocal Laser Scanning Microscope (CLSM) visualization); every 48h, the refresh with fresh culture media was done and, finally, biofilms were treated with BL (the covered samples were considered the dark control while the samples exposed to light were the light samples). Treated biofilms were used to assess the cells' viability and or the visualization with CLSM.

4.3.4 5-days biofilm Blue Light treatment

After 5-days, biofilms were treated with BL. Before light exposure, 1 mL of the broth was removed to favour the BL penetration inside biofilms. Subsequently, half of the plate was covered and constituted the dark control, and the other part was exposed to BL. The experimental conditions are reported in **Table 4.1**.

After BL treatment, biofilms were detached with a cell scraper and mixed in order to obtain a homogeneous suspension. Then, an aliquot was taken and serially diluted in Maximum

Recovery Diluent (MRD, Oxoid, Basingstoke, United Kingdom) and cell viability was assessed by plating cells in BHI agar plates.

Table 4.1. Experimental parameters of BL treatment of 5-days and 13-days biofilms.

Wavelength (nm)	Voltage (V)	Irradiance (W cm^{-2})	Treatment time (h)	Final dose (J cm^{-2})
405 420 450	10	0.05	2	360

4.3.5 13-days biofilm Blue Light treatment

After 13 days, biofilms grown on glass surfaces were treated with BL. Before BL exposure, each glass coverslip was washed with some PBS drops and placed in a new sterile Petri dish.

For each wavelength, 2 glass coverslips were exposed to BL light and 2 glass coverslips were kept under the lamp but covered and used as dark controls, to be used for the viable cell count and for the CLSM visualization (**Figure 4.3**). The BL treatment parameters were the same as in the case of a 5-days biofilm (**Table 4.1**).

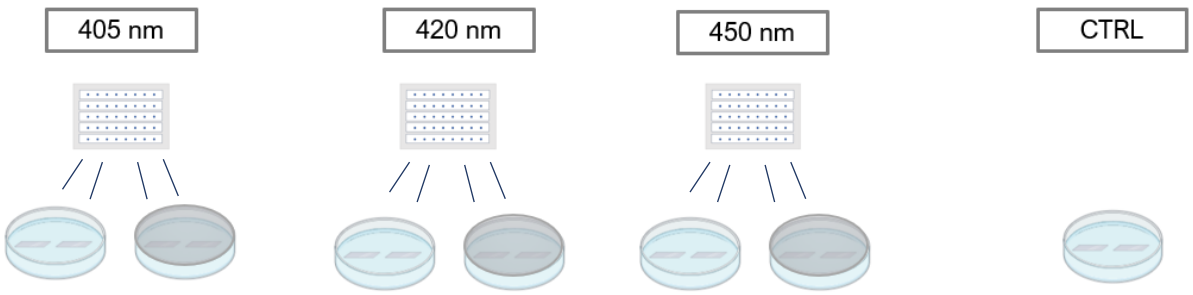


Figure 4.3. Blue Light treatment set-up for 13-days biofilms.

4.3.5.1 Confocal Laser Scanning Microscope (CLSM) Visualization

After BL treatment, each glass coverslip was washed twice in 0.9% NaCl by immersion. Then, biofilms were fixed by immersion in a glutaraldehyde 4% solution for 1h. Glutaraldehyde residues were removed by washing twice the glass coverslips with Milli-Q water. After, the glass coverslips were immersed in ethanol at growing concentrations (25%, 50%, 75%, 90% and 100%) for 10 min for each concentration. Samples were then dried in an oven at 50-60 °C for 10 min and kept immersed in PBS at 4°C.

Before CLSM visualization, glass coverslips were dried for 1h in an oven at 60 °C. Then, samples were immersed in a solution of acridine orange solution 0.1 mg/mL (Sigma, Milan, Italy) for 15 min in the dark. The dye residues were removed with PBS. Glass coverslips were then mounted in a glass slide by using a solution of glycerol 30%.

Stained biofilms were examined under an inverted Leica DMI6000RB epifluorescence microscope (Leica Microsystems GmbH, Wetzlar, Germany) and images were captured with a Micromax charge-coupled device camera (Roper Scientific). The image analysis was done with (Leica Application Suite X:3.5.7.23225, Wetzlar, Germany).

4.3.6 Sample quantification

The overnight culture, the inoculum, and 5-days and 13-days biofilms (both the samples treated with BL and the dark controls) were serially diluted and plated BHI agar plates in order to assess the cell viability. Plates were incubated at 30°C/37°C (depending on the microbe) for 24h. Microbial cells were then counted and expressed as log N/N0.

4.4 Statistical analysis

Results were expressed as CFU/cm^2 and transformed in the logarithm CFU/cm^2. The Log (N/N0) were then calculated, where N is the log CFU/cm^2 after the BL treatment and N0 is the log CFU/cm^2 of the control. The data were elaborated with Microsoft Excel, represented as the mean of three biological replicates ± standard deviation (SD) with GraphPad Prism 9.0.0 and subjected to statistical analysis by IBM SPSS Statistics for Windows version 23.0 (IBM Corp., Armonk, N.Y., USA). The statistical methods used to determine the significant differences between the samples were paired t-test ($p \leq 0.05$), One-way ANOVA ($p \leq 0.05$), Two-way ANOVA ($p \leq 0.05$) and post-hoc Tuckey-B test.

4.5 Results and Discussion

4.5.1 5-days biofilms

The data on microbial inactivation of bacterial biofilms by BL are presented in **Table 4.2**. For all the tested microbes the controls remained stable at 10^5-10^6 CFU/mL. Overall, the biofilm reductions observed after BL irradiation were consistent with the previous data on microbial inactivation of planktonic cells in agar and liquid substrates (**Chapter 2**), with some variations. In general, few studies evaluated the BL microbial inactivation of microbial biofilms of certain species, such as *E. coli*, *Salmonella* spp. and *Bacillus* spp.

Focusing on Gram (-) bacteria, *E. coli* showed greater susceptibility to shorter BL wavelengths, such as 405 nm and 420 nm, achieving inactivation levels exceeding -3 log. In contrast, exposure to higher BL wavelengths, such as 450 nm, resulted in significantly reduced inactivation (-1.77 log), with differences reaching statistical significance ($p \leq 0.05$) when compared to 405 and 420 nm.

These findings align with our prior research (**Chapter 2**) and with the work of Plavskii et al. (2018), who identified enhanced sensitivity of *E. coli* to shorter BL wavelengths (405 nm) due to the synergistic action of porphyrins and flavins as PS. They proposed that excitation of these PS occurs at different wavelengths and suggested that the relatively low intracellular flavin content in *E. coli* could account for reduced inactivation at higher BL wavelengths. Supporting this perspective, other studies have emphasized that the contribution of flavins to light-mediated inactivation is less pronounced compared to that of porphyrins (Bumah et al., 2020; Chen et al., 2021; Huang et al., 2023).

A similar response to BL treatment was observed for *P. fluorescens*, which exhibited behaviour akin to *E. coli*. Specifically, in the case of 5-days-old biofilms, inactivation levels at 405 nm and 420 nm were statistically similar ($p > 0.05$), with reductions of approximately -3.5 log for both wavelengths. In contrast, exposure to 450 nm resulted in significantly lower inactivation ($p \leq 0.05$), measuring less than -1 log. This differential response may be attributed to the greater intracellular presence of coproporphyrin III and/or uroporphyrin III, which likely influences the photosensitization process. Consistent with these findings, Ferrer-Espada et al. (2020) demonstrated that *Pseudomonas* spp. biofilms were more susceptible to 405 nm BL compared to other microbial species.

Unlike other Gram (-) species, *S. enterica* displayed a distinct inactivation pattern, with greater susceptibility to 405 nm BL but similar inactivation rates at 420 nm and 450 nm. At 405 nm,

the inactivation reached -2.1 log, whereas, at 420 nm and 450 nm, the inactivation was approximately -1 log. However, none of these differences was statistically significant ($p>0.05$).

This differential response may be attributed to variations in the quantity and localization of intracellular PS within the bacterial cells, as well as the expression of oxidative stress-resistant genes, including *OxyR*, *AhpC*, *GrxA*, *SulA*, *AtpC*, *groEL*, and *STM0225* (Buchovec et al., 2017; Hamblin & Hasan, 2004; Murdoch et al., 2012). Additionally, *S. enterica* may exhibit a reduced capability to synthesize endogenous PS. Buchovec et al. (2009), in fact, evaluated the bacterium's ability to produce porphyrins after incubation with 5-aminolevulinic acid (ALA), a precursor of porphyrins. Although *S. enterica* synthesized protoporphyrin IX, the overall production of porphyrins was markedly lower compared to Gram (+) *L. monocytogenes* (Buchovec et al., 2010).

Table 4.2. Microbial inactivation of 5-days-old biofilms following Blue Light (BL) treatment at 405 nm, 420 nm, and 450 nm are presented as log reductions in viable cell count (log N/N0, mean ± standard deviation). The final temperature (Tf) was measured after 120 minutes of BL exposure. Lowercase letters denote significant differences ($p \leq 0.05$) in inactivation levels for the same microbial species across different wavelengths. The results are the average of two biological replicates.

Microorganism	λ (nm)	Tf (°C)	log N/N0
S. aureus	405	34.8	-1.75±1.02[a]
	420	41.8	-2.52±0.64[a]
	450	36.3	-1.62±0.10[a]
E. coli	405	34.1	-3.10±0.28[a]
	420	32.9	-3.73±0.27[a]
	450	31.8	-1.77±0.91[b]
L. monocytogenes	405	29.4	-3.65±1.86[a]
	420	29.1	-2.95±1.23[a]
	450	30.1	-2.66±0.57[a]
S. enterica	405	34.8	-2.11±0.69[a]
	420	41.8	-1.07±0.41[a]
	450	36.3	-1.26±0.82[a]
B. subtilis	405	29.4	-2.64±0.91[a]
	420	29.1	-1.66±0.46[ab]
	450	30.1	-0.71±1.05[b]
P. fluorescens	405	29.4	-3.50±0.65[a]
	420	29.1	-3.27±0.65[a]
	450	30.1	-0.57±0.36[b]

The Gram (+) *L. monocytogenes* exhibit inactivation levels that were not statistically different ($p > 0.05$) across the three wavelengths, although slight variations were observed. The highest inactivation, reaching -3.65 log, was achieved with 405 nm BL. When 420 nm and 450 nm wavelengths were used, the inactivation levels were slightly lower (-2.95 log and -2.66 log, respectively), with marginally greater efficiency observed at 450 nm. These findings are in line with Olszewska et al. (2023), who reported that lower BL wavelengths are generally more effective for *L. monocytogenes* biofilm inactivation across various surfaces. Furthermore, Marino et al. (2018) highlighted the heightened susceptibility of *L. monocytogenes* biofilms compared to *S. aureus* and *P. fluorescens* when exposed to ROS-producing inactivation technologies.

Also in the case of biofilms, the most effective wavelength for *S. aureus* inactivation was 420 nm, achieving a reduction of -2.52 log. In contrast, irradiation at 405 nm and 450 nm resulted in similar inactivation levels, slightly exceeding -1.5 log. Yang et al. (2024) reported a more pronounced reduction of -4.11 log for *S. aureus* biofilms after 90 minutes of exposure to 270 J cm^{-2} using a broad-spectrum LED (410–510 nm). Their findings also highlighted the role of the *lrgAB* operon, which regulates autolysis and biofilm modulation, in light-based inactivation. The presence of this operon was associated with variations in survival rates, membrane damage, and biofilm formation for *S. aureus*. Furthermore, its overexpression was shown to amplify the damage induced by light treatment.

For *B. subtilis*, the highest microbial inactivation was achieved with 405 nm irradiation, consistent with previous findings. Inactivation following exposure to 420 nm and 450 nm was negligible (< -1 log). Significant differences ($p \leq 0.05$) were observed only between the inactivation levels at 405 nm and 450 nm, while the reduction provided by 420 nm was similar to both wavelengths. Compared to inactivation in liquid substrates, where reductions exceeded -5 log for 405 nm and 420 nm, the biofilm reductions were significantly lower. This outcome is expected due to the enhanced structural resistance and complexity of biofilms compared to planktonic cells. Additionally, the expression of *YvtA*, a protein implicated in biofilm resistance mechanisms, may differ when *B. subtilis* transitions into its biofilm form (Gaidenko et al., 2006).

In general, microbial inactivation achieved by BL irradiation was coherent between planktonic forms and 5-days biofilms, with trends varying across microbial species. In particular, for all tested microbes, lower BL wavelengths resulted in higher inactivation levels. These experiments further confirmed that none of the tested microorganisms were more susceptible to 450 nm light. This supports findings from previous studies suggesting that porphyrins, rather

than flavins, play a predominant role in light-mediated inactivation. Flavins contribute less significantly and are prone to degradation into lumichrome, another PS with reduced efficacy.

To provide an overall assessment of the influence of the tested factors on microbial reduction in 5-day biofilms, a Two-Way ANOVA was conducted (**Table 4.3**). The analysis revealed that the wavelength of light was the most influential factor, accounting for 58.1% of the observed variation in microbial inactivation. The type of microorganism was the second most significant factor, contributing 29.6% to the variation.

Table 4.3. Two -Way Analysis of variance (ANOVA) of the effect of two variables, the microorganism (M) and the wavelength (W).

Variables	SS%	$p \leq 0.05$
M	29.6	*
W	58.1	***
M x W	12.3	ns

SS, sum of squares; p, significance; * $p \leq 0.05$; ** $p \leq 0.01$; *** $p \leq 0.001$; ns: not significant.

4.5.2 13-days biofilm

L. monocytogenes, *E. coli* and *S. aureus* biofilms were grown on glass surfaces for 13-days (**Figure 4.4**) after BL irradiation at 405 nm, 420 nm and 450 nm. The microbial reduction trends observed after BL treatment were similar to previous experiments with planktonic cells and 5-days biofilms, with some minimal differences. For all the tested microbes the controls remained stable at 10^5-10^6 CFU/mL.

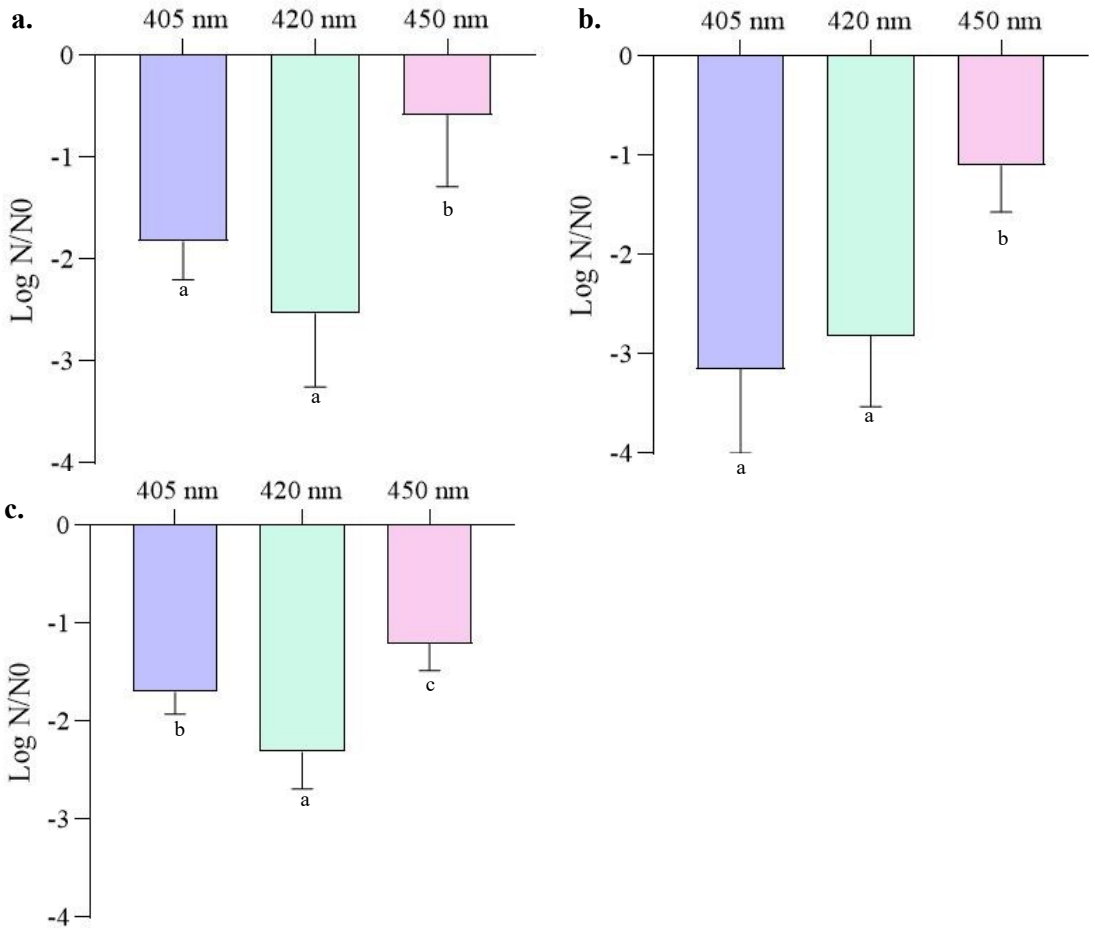


Figure 4.4. Microbial inactivation of **a.** *L. monocytogenes*, **b.** *S. aureus* and **c.** *E. coli* biofilms after Blue Light (BL) treatment (360 J cm^{-2}) with 405 nm, 420 nm and 450 nm wavelengths. Different lowercase letters indicate a significant difference ($p<0.05$) among the same bacteria treated with different wavelengths. The results are the average of two biological replicates.

L. monocytogenes (**Figure 4.4 a.**) showed the greatest reduction after 420 nm BL treatment, which accounted for -2.53 log, followed by 405 nm treatment (-1.82 log). A significantly lower reduction was observed for 450 nm (-0.59 log). Compared to the 5-days biofilm, the inactivation trend was similar, with lower BL wavelengths being the most effective compared to 450 nm.

The inactivation of *S. aureus* (**Figure 4.4 b.**) was the most efficient resulting in more than – 3 log after 405 nm irradiation, -2.80 log with 420 nm and -1.10 with 450 nm. Also in this case, the lower BL wavelengths resulted in a similar inactivation, which was significantly higher ($p \leq 0.05$) than 450 nm reduction.

In the case of the Gram (-) *E. coli* (**Figure 4.4 c.**), all the wavelengths provided a significantly different ($p \leq 0.05$) reduction of the 13-days biofilm. 420 nm provided the greatest reduction, which accounted for -2.31 log, and -1.20 log was determined by 450 nm. Differently from the 5-days biofilm, where the inactivation obtained with 405 and 420 nm were similar, in this case, 405 nm BL treatment provided a reduced microbial inactivation, which accounted for -1.70 log.

As in the case of 5-days biofilm, the Two-Way ANOVA evidenced that the factor that main influenced the 13-days biofilm inactivation was the BL wavelengths used, which accounted for 77%, followed by the type of microbes (16.2%) and their combination (6.78%) (**Table 4.4**).

Table 4.4. Two-Way ANOVA of the effect of two variables, the microorganism (M) and the wavelength (W).

Variables	SS%	$p \leq 0.05$
M	16.2	*
W	77	***
M x W	6.78	ns

SS, sum of squares; p, significance; * $p \leq 0.05$; ** $p \leq 0.01$; *** $p \leq 0.001$; ns: not significant.

The 13-days biofilms formed on glass surfaces had different conformations and heights, as shown in **Figure 4.5**. The different bacterial species were placed differently on the glass surfaces: some increased the biofilm thickness, such as *L. monocytogenes*, which reached 9 μm, while *S. aureus* and *E. coli* seemed to form multiple agglomerates that seemed to expand more in width than in thickness.

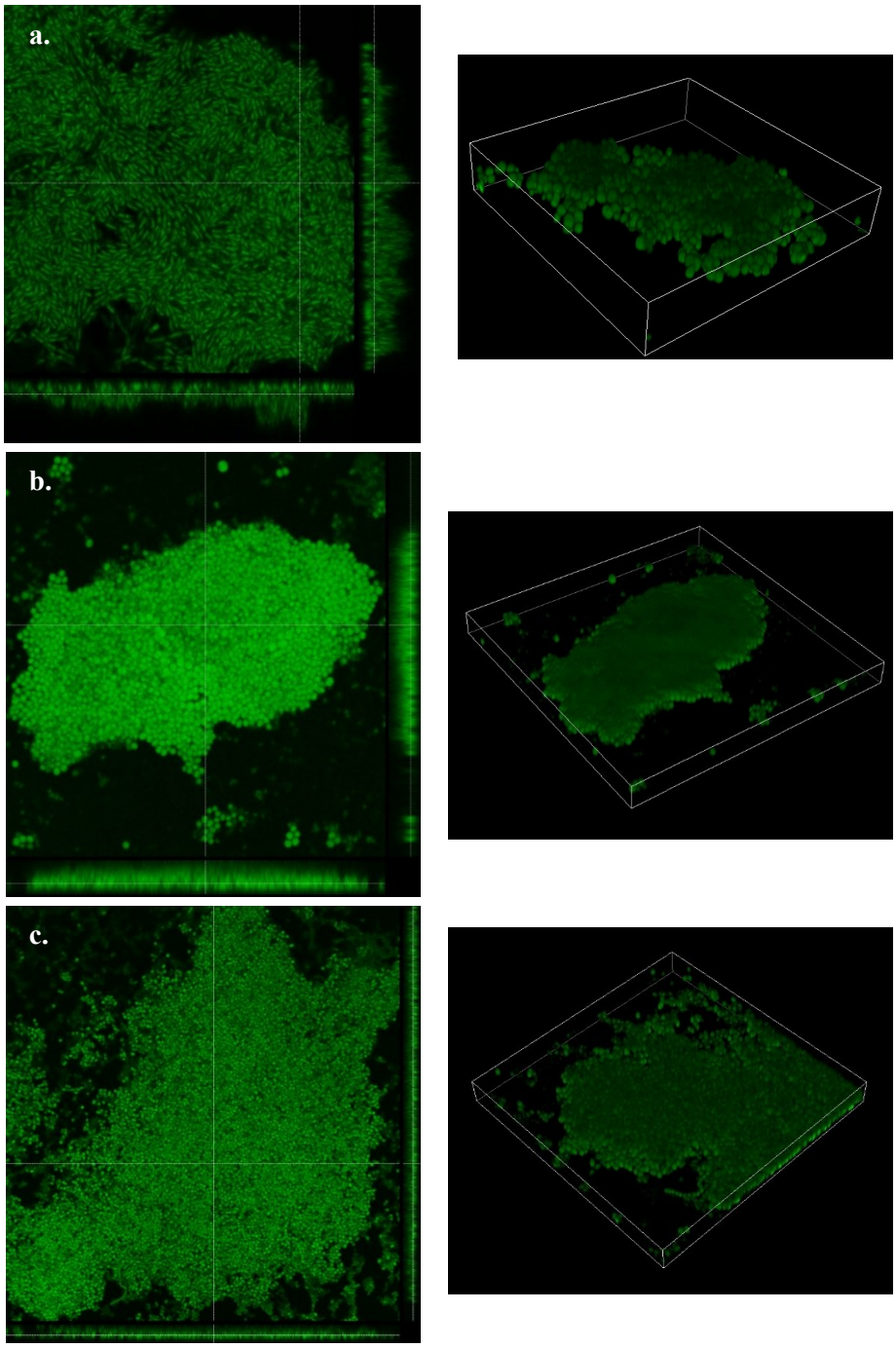


Figure 4.5. Confocal Laser Scanning Microscope (CLSM) images (100x, zoom 2.3) of (**a.**) *L. monocytogenes*, (**b.**) *S. aureus* and (**c.**) *E. coli* 13-days biofilm in two dimensions and in 3D.

This phenomenon may be attributed to the surface composition, which influences interactions between cells, as well as between cells and extracellular matrix components or the surface itself (Uruén et al., 2020). Glass is recognized as a challenging substrate for bacterial adhesion, as it does not promote microbial cell attachment and, consequently, hinders biofilm formation.

After the BL treatment with the application of a light dose of 360 J cm^{-2}, the overall microbial load of the biofilms decreased based on the used wavelength. This was also confirmed by the images taken with the CLSM (**Figure 4.6**). Each bacterium showed a different inactivation pattern; for instance, *L. monocytogenes* showed more agglomerates in the control compared to *E. coli*, confirming the major thickness of its biofilm (Bridier et al., 2010). The application of BL light seemed to shrink the agglomerates and reduce their thickness. CLSM pictures revealed also some elongation of the microbial cells into filamentous structures. The increased variability in the measurements suggests that this elongation was not uniform across all tested wavelengths. Even within the same sample, treated cells demonstrated significant heterogeneity in their morphological responses.

The elongation was appreciated particularly after the 450 nm light treatment, which was associated with lower microbial inactivation. The change in the bacterial cell morphology was also confirmed by the cell length measurements (**Table 4.5**), where the average of the measured cells varied from 2.20 μm of the control to 3.07 ± 3.75 in case of 405 nm BL treatment and 4.56 ± 8.04 in case of 450 nm light irradiation. Indeed, with 420 nm treatment, the cell lengths remained more similar to the controls.

This feature could represent a stress-response mechanism, as already underlined by other authors (Bereksi et al., 2002; Jones et al., 2013). The amount of modified cells was also seen to be dependent on the type and the severity of the stress, confirming the variability that was assessed between the different samples. Therefore, the higher incidence of long filaments after 450 nm BL treatment could be related to the lower inactivation efficiency of this wavelength to *L. monocytogenes*, which resulted in a higher stress condition. Also, filamentous formation has been related to some genetic factors, such as the alternate sigma factor σ^B (Giotis et al., 2007; Jones et al., 2013).

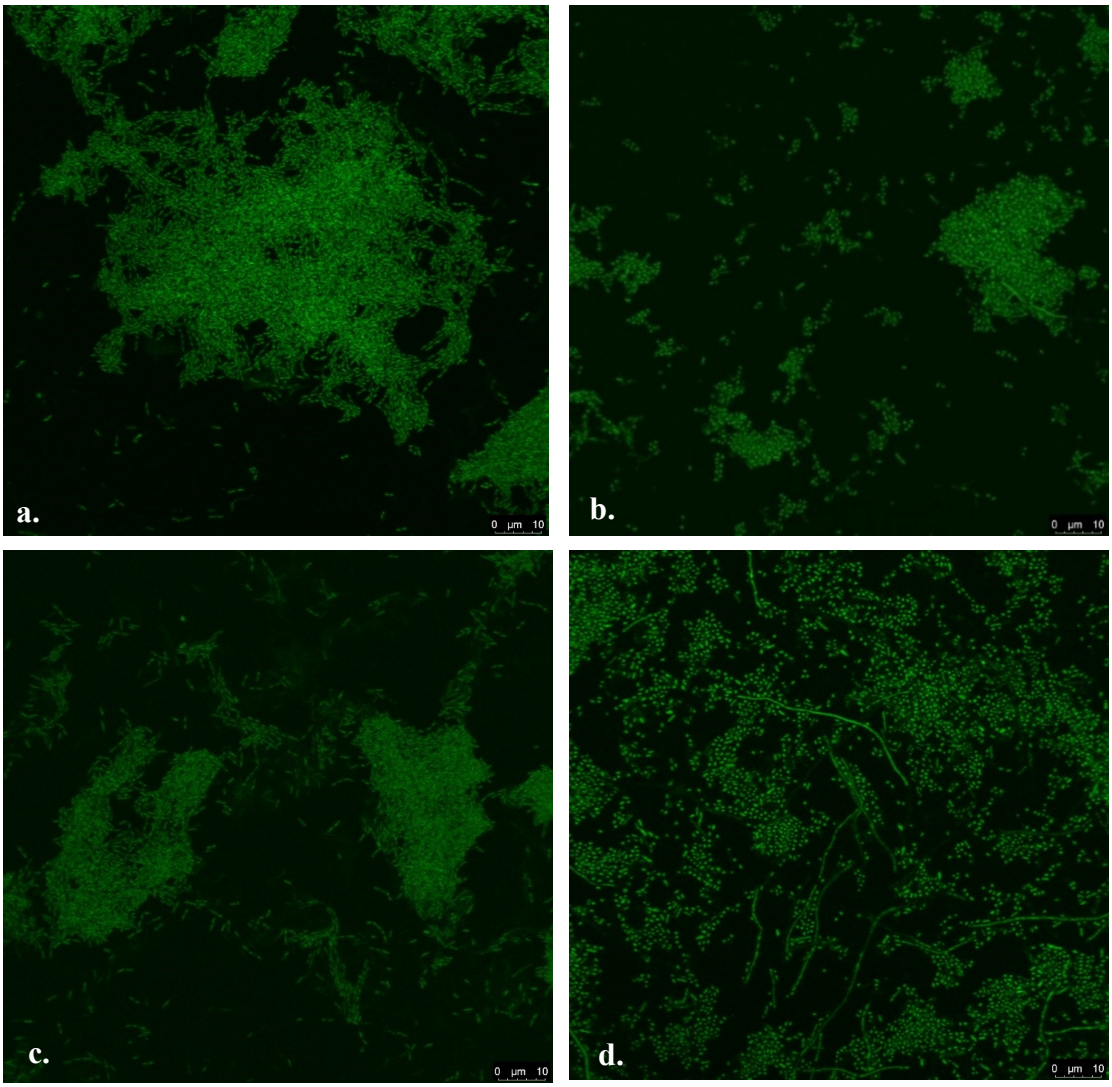


Figure 4.6. Confocal Laser Scanning Microscope (CLSM) images (100x, zoom 1) of *L. monocytogenes* 13-days biofilm (**a.** control) after being treated with **b.** 405 nm, **c.** 420 nm and **d.** 450 nm Blue Light (BL).

Table 4.5. Cell length (μm) of microbial biofilm cells (mean ± standard deviation).

	CTRL	**405 nm**	**420 nm**	**450 nm**
L. monocytogenes	2.20 ± 0.44	3.07 ± 3.75	2.19 ± 1.62	4.56 ± 8.04
S. aureus	0.98 ± 0.13	0.93 ± 0.26	0.88 ± 0.14*	0.98 ± 0.16
E. coli	1.28 ± 0.26	0.92 ± 0.17***	1.22 ± 0.32	1.07 ± 0.23**

Significant differences were made between the control and the sample at the different wavelengths. CTRL, control*; *$p \leq 0.05$; **$p \leq 0.01$; ***$p \leq 0.001$*

Regarding *E. coli* and *S. aureus* (**Figures 4.7 and 4.8**), the 13-days biofilm seemed to develop more across the surface rather than increasing in thickness, as observed in the CLSM images (Bridier et al., 2010). This peculiarity may be influenced by the water availability on the substrates, as suggested by Ziege et al. (2021), with a higher grade of homogeneity of the matrix in low water content growth situation. who reported that low water content growth conditions lead to a more homogeneous matrix structure.

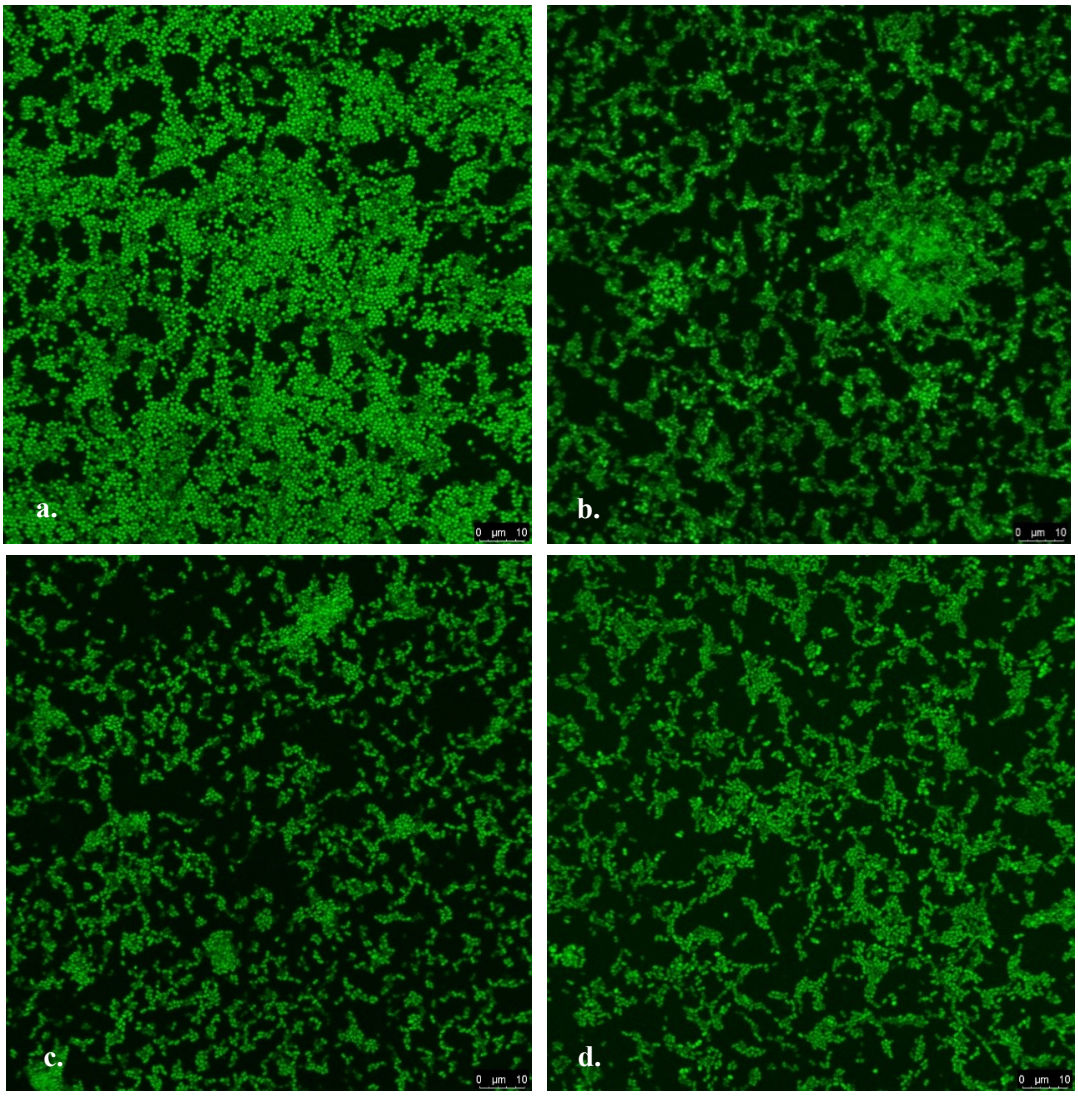


Figure 4.7. Confocal Laser Scanning Microscope (CLSM) images (100x, zoom 1) of *E. coli* 13-days biofilm (**a.** control) after being treated with **b.** 405 nm, **c.** 420 nm and **d.** 450 nm Blue Light (BL).

The results obtained from the cell counts were confirmed by the images for both microbes, where 405 nm BL provided the higher inactivation for *S. aureus* while 420 nm was the most efficient wavelength for *E. coli*. Differently from what was observed for *L. monocytogenes*, no

filaments were seen in the treated samples. However, a significant reduction in *E. coli* cell length was evidenced after 405 nm ($p \leq 0.001$) and 450 ($p \leq 0.01$) nm irradiation. The low cell dimension was assessed also by Jones et al. (2002), who saw a decrease in the cells' length after stress exposure. In contrast, some authors saw the formation of filaments also in the case of *E. coli*. However, this capability is not fully elucidated yet and seems to be dependent on some other factors, such as the growth phase of the microbes (Jones et al., 2002; Jones et al., 2013). The formation and the resistance of *E. coli* biofilms are regulated at a genetic level. In particular, *ariR* (*ymgB*) and *bhsA* (*ycfR*) genes contribute to the formation and in some form of resistance. Also, *bhsA* stimulates its formation and resistance under several stresses, such as hydrogen peroxide presence (Weber et al., 2010; Zhang et al., 2007).

Indeed, *S. aureus* biofilm cells appeared largely similar to the control, except under the 420 nm treatment, which resulted in a significantly reduced cell dimension. Notably, *S. aureus* exhibited the highest microbial inactivation. Baker et al. (2010) reported that activation of the oxidative stress response mechanism in *S. aureus*, involving the *ahpC*, *ahpF*, *sodA*, and *mrgA* genes, can suppress the expression of Agr and Sae, two key virulence regulators critical for biofilm formation. Additionally, the presence of the *ica* operon and the staphylococcal accessory regulator (*sarA*) is essential for the ability of *S. aureus* to form biofilms. Therefore, any potential repression of these pathways following BL treatment may have reduced the ability of *S. aureus* to regenerate the disrupted biofilm (Beenken et al., 2004).

Given the extensive involvement of genes in the SOS response mechanism—bacteria's primary system for addressing stress—and in biofilm formation and growth, the repression and/or overexpression of certain genes could contribute to increased biofilm susceptibility to BL treatment. Investigating the effects of both lethal and sub-lethal BL treatments on these specific genes for different classes of foodborne pathogens would provide valuable insights (Baharoglu & Mazel, 2014; Beenken et al., 2004).

Differences in microbial biofilm responses to BL treatment should also take into account the presence of *quorum sensing*, a cell-to-cell communication mechanism that plays a crucial role in biofilm formation, maintenance, and stress adaptation. QS is regulated by specific genes that control the production, detection, and response to signalling molecules, allowing microbial cells to coordinate collective behaviours based on population density (Barriuso et al., 2018). BL irradiation could influence the expression of genes involved in QS, i.e. *lasI*, *lasR*, *in Pseudomonas* spp. and *bla* and *mscL* in *E. coli*, either through repression or overexpression. Such changes may disrupt the regulation of biofilm-associated processes (Fekrirad et al., 2019; Hendiani et al., 2019; Jiang et al., 2024). Consequently, any alterations in QS signalling

pathways caused by BL irradiation may result in changes to biofilm structure, gene expression, and resistance, which are not typically observed in planktonic cells.

Also, Blasser (1999) demonstrated a different mechanism for QS in the different Gram-type bacteria. In particular, LuxI/LuxR system (two regulatory proteins) for Gram (-) and ABC transporter for Gram (+). However, several bacteria belonging to both the Gram classifications, like *E. coli*, *S. aureus*, *Salmonella* spp., have a hybrid QS system, which seems to be regulated by *luxS* gene. Its homologues have been identified in Gram (+) and Gram (-) bacteria, which stimulate bacterial communication via AI-1 and AI-2 signals. Thus, the author hypothesized that the bacterial species response regulated by the same autoinducer could have the same communication mechanism. Therefore, the presence of such communication mechanisms in the different species of biofilms could represent a possible factor that determines the differences in the biofilm inactivation with BL.

In general, comparing the microbial reduction in biofilms is challenging due to the variability associated with the available techniques. Specifically, mature biofilms are typically grown for 48–72 hours, whereas in this study, biofilms were cultivated for 5 days and 13 days. Additionally, to facilitate visualization with CLSM, the 13-day biofilms were developed on glass surfaces. Therefore, further research on the inactivation of mature biofilms is essential to address existing knowledge gaps and account for the significant variability observed in natural environments.

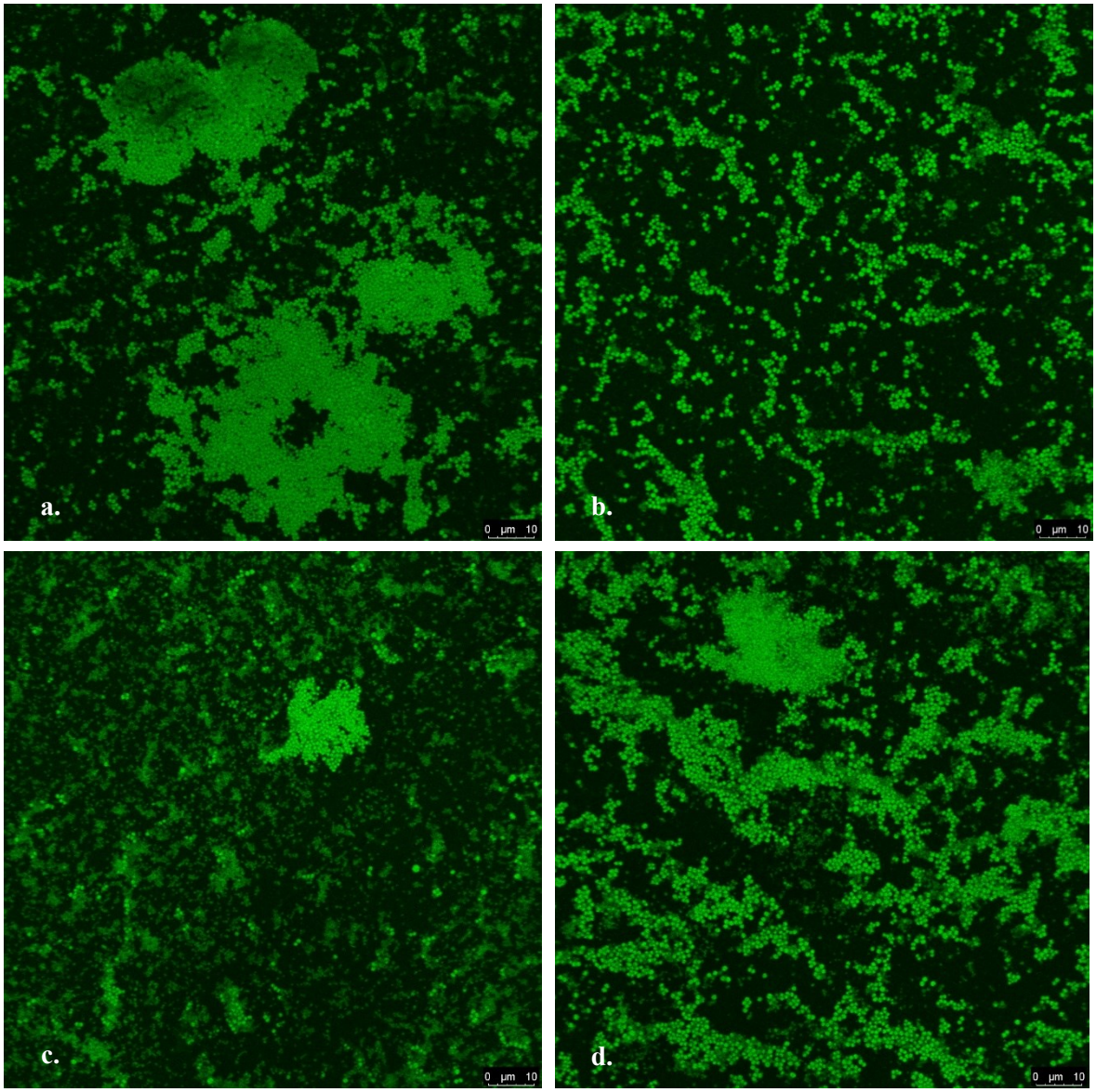


Figure 4.8. Confocal Laser Scanning Microscope (CLSM) images (100x, zoom 1) of *S. aureus* 13-days biofilm (**a.** control) after being treated with **b.** 405 nm, **c.** 420 nm and **d.** 450 nm Blue Light (BL).

4.6 Conclusions

Biofilms represent a significant hazard in the food environment, and their prevention and inactivation are the focus of numerous research efforts. This study aimed to evaluate the ability of BL treatment, utilizing endogenous PS only, to inactivate mature biofilms, which are commonly encountered in real-world environments.

For both 5-day and 13-day biofilms, the microbial inactivation trends were consistent with previous studies on planktonic cells across various substrates, where lower BL wavelengths demonstrated greater efficiency in microbial reduction compared to higher wavelengths. As previously discussed, this phenomenon may be attributed to differences in the quantity, type, and intracellular localization of PS, as well as variations in stress-related gene expression.

Analysis of biofilm images revealed distinct biofilm formation patterns among the tested species. *L. monocytogenes* produced the thickest biofilms, while *E. coli* and *S. aureus* were more likely to spread across the surface. Following BL irradiation, microbial species exhibited unique responses: *L. monocytogenes* developed elongated filamentous structures, whereas *E. coli* showed reduced cell length.

This study highlights the potential of BL treatment as an effective approach for inactivating mature biofilms in the food environment, leveraging the action of endogenous PS to generate oxidative stress. However, the observed variability in microbial responses underscores the need for further comprehensive analyses to optimize treatment parameters and better understand species-specific inactivation mechanisms. Nevertheless, further investigations into the inactivation of microbial biofilms by BL are necessary to generate more comprehensive data and to better elucidate the mechanisms of inactivation and/or stress response in different microbial species.

Chapter 5

Application of Light technologies to domestic furniture: Blue Light vs UVA

5.1 Introduction

Cross-contamination poses a significant threat to public health, particularly through contaminated surfaces that act as vectors for pathogenic transfer. In domestic settings, sanitization of food-contact surfaces and storage facilities is less frequent than in professional food-handling environments, where employees receive dedicated training on hygiene protocols which could result in the contamination of food products (Awuchi, 2023; Mazaheri et al., 2023; Schlegelová et al., 2010).

This gap in sanitation frequency and awareness suggests a need for household solutions that facilitate the control of the microbial load of food-related items, including utensils, storage containers, and food products themselves.

To address the need for safer and more effective sanitation methods, a novel approach could involve the development of household "sanitizing boxes" specifically designed to disinfect food utensils and sanitize food products. While UVC sterilizing boxes are currently available on the market, they come with notable drawbacks, primarily the potential hazards to operators due to UV radiation exposure and the risk of damaging the materials being irradiated (Lang et al., 2022; Yagi et al., 2007). Specifically, D.Lgs. Gov 81/2008 mandates a double control system to protect operators from UV radiation, adding complexity to the safe use of UVC technology in domestic settings. In contrast, the potential of using alternative light spectrums, such as UVA and BL, for microbial load control in food safety has not been fully explored (Lang et al., 2022; Yagi et al., 2007). BL, in particular, offers several advantages over UVC. First, it is safer for users, as it does not pose the same level of risk associated with UV radiation and is less likely to damage the materials it is applied to, making it a suitable option for disinfecting a wide range of food-related items without compromising their integrity. Another benefit is the lower cost of LED technology for blue light, which could make it more accessible and cost-effective for household use (Luksiene & Zukauskas, 2009). Furthermore, integrating BL technology into common kitchen appliances, such as refrigerators, could significantly enhance food safety practices within the home.

Implementing a sanitization system in storage environments could help minimize microbial growth on food items and utensils, potentially reducing the risk of foodborne illnesses and enhancing overall food hygiene. This novel approach could be a significant breakthrough in household food safety, offering a convenient, cost-effective solution with high efficacy, while avoiding the risks linked to conventional sterilization methods.

5.2 Aim of the study

The present study aimed to test a *mock-up* system for domestic sanitization based on UVA and BL, evaluating both room temperature and refrigerated conditions. The objective was to establish optimal operational parameters for effective microbial reduction in a domestic context, making it suitable for everyday household use from microbial load control and energy consumption. By exploring these two adjacent regions of the electromagnetic spectrum, this work seeks to identify effective light-based sanitization techniques that are compatible with food products and adaptable to common household appliances.

This work was carried out at MicroBio laboratory, at Electrolux Italia S.p.A (Porcia, Italy) in accordance with the guidelines set forth by the FSE REACT-EU PON funding program.

5.3 Material and Methods

5.3.1 Microbial Strains and Culture Conditions

In this study, *Escherichia coli* ATCC_8739 and *Staphylococcus aureus* ATCC_6538, sourced from the MicroBio Laboratory at Electrolux Italia S.p.A., were used as the microbial strains. Stock cultures of each strain were preserved at −80 °C in Brain Heart Infusion (BHI) broth (Oxoid, Basingstoke, United Kingdom), supplemented with 30% (v/v) glycerol as a cryoprotectant. Prior to experimentation, aliquots from these stock suspensions were streaked onto BHI agar plates (Technical Agar, Oxoid, Basingstoke, United Kingdom) and incubated at 37 °C to ensure viability. For each experimental assay, strains were revived by twice culturing in 15 mL of BHI broth at 37 °C overnight, thus establishing an active microbial culture (*overnight* culture).

5.3.2 Light Source

For the BL tests, a custom-designed stainless steel enclosure was constructed with dimensions of 40 x 30 x 40 cm (L x W x H) and an adjustable height feature (**Figure 5.1**). This modular height allowed for varying configurations depending on the selected vertical distance. For this study, two heights were employed: configuration A, providing a minimal lamp-to-sample distance of 17.8 cm, and configuration B, allowing a maximal distance of 38.8 cm.

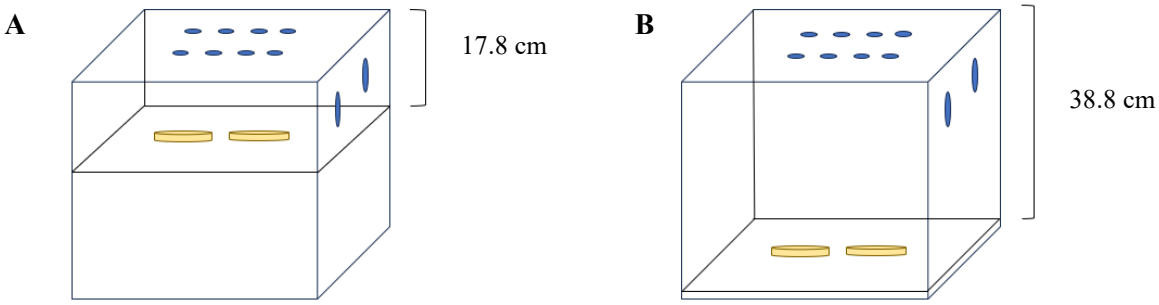


Figure 5.1. Box for light treatment created at Electrolux Italia S.p.A. **A**) Set-up for the experiments where the light-sample distance was the minimal (17.8 cm); **B**) Set-up for the experiments where the light-sample distance was the maximal (38.8 cm).

The enclosure was sealed with a removable lid, on which 8 LED (Electrolux Italia S.p.A., Porcia, Italy) were mounted. Two removable lids, each equipped with different LED, were prepared: one using 405 nm wavelength LED and another with 365 nm wavelength LED. For each wavelength and configuration (A or B), the average irradiance was determined using an

HD2302.0 radiometer (Delta Ohm, Caselle di Selvazzano, Italy) coupled with an LP471 probe (Delta Ohm, Caselle di Selvazzano, Italy). Measurements were taken within the LED-illuminated area, covering a grid of 24 points (**Figure 5.2),** with three measurements recorded at each point to ensure accuracy.

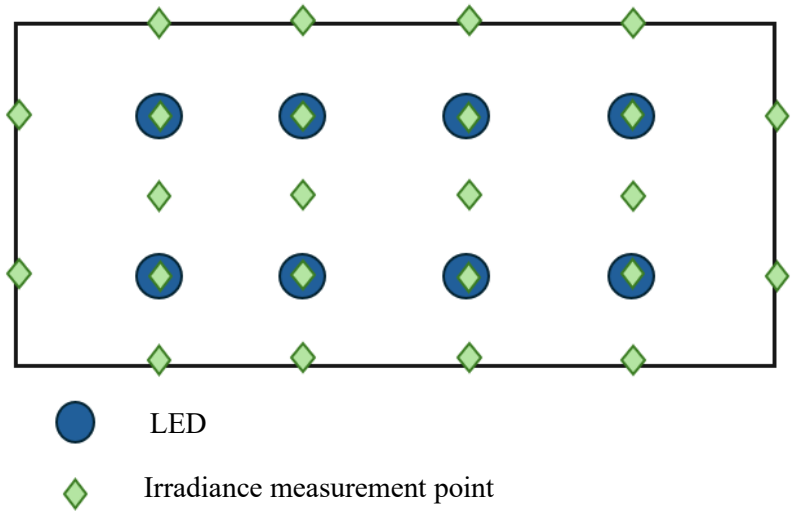


Figure 5.2. Irradiance measurement points. Blue points represent the LED position in the box lid while green rhombus indicates the point where the irradiance measurements have been taken.

5.3.3 Light treatment

Overnight bacterial cultures were washed three times with PBS, centrifuged at 13,000 *x g*, and subsequently serially diluted. Each plate was sectioned into six areas, within which the diluted bacterial suspensions were plated using the drop plate technique (Herigstad et al., 2001). Three replicate plates were prepared per condition: one incubated at 37 °C to serve as an untreated control (Non-treated Control, NC), a second exposed to light treatment (Light Sample, LS), and a third covered to shield from light exposure during treatment (Dark Control, DC).

DC and LS were then exposed to LED illumination at wavelengths of 405 nm and 365 nm, as detailed in **Table 5.1**.

Table 5.1. Experimental parameters used for light tests.

Wavelength	**405 nm**		**365 nm**	
Set-up	A	B	A	B
Treatment Time (h)	1 4	15	1 4	15
Dose (J cm^{-2})	6.95 27.8	29.3	8.21 32.8	33.1

Treatments were conducted at both room temperature (around 23°C) and refrigerated conditions (approximately 4 °C). The refrigerated condition was achieved by placing the stainless steel box inside a *built-in* refrigerator (Electrolux S.p.A., Porcia, Italy). Throughout the light exposure tests, the temperature was monitored at one-minute intervals using a probe from the EK-H4 Evaluation Kit (Sensirion, Gerlingen, Germany).

Following the light treatments, the plates designated as NC, LS, and DC were incubated at 37 °C for 24 hours to allow for bacterial growth. Viable cell counts were subsequently determined and expressed as CFU/mL and then, transformed in logarithmic values.

5.3.4 Data analysis

Results were expressed as CFU/mL and transformed in the logarithm CFU/mL. The Log (N/N0) were then calculated, where N is the log CFU/mL after the BL treatment and N0 is the log CFU/mL of the control. The data were elaborated with Microsoft Excel, represented as the mean of two biological replicates ± standard deviation (SD) and subjected to statistical analysis by IBM SPSS Statistics for Windows version 23.0 (IBM Corp., Armonk, N.Y., USA). The statistical method used to determine the significant differences between the samples was the Four-Way analysis of variance (ANOVA). The percentage of the total variability was calculated to quantify the variance attributed to each parameter, based on the sum of squares associated with the primary factors and their interactions. Additionally, a post-hoc Tukey-B test ($p \leq 0.05$) was employed to identify statistically significant differences among the sample groups.

5.4 Result and Discussion

5.4.1 Irradiance measurements

Figure 5.3 presents the irradiance values for two lamps at two wavelengths, 365 nm (**a.** and **b.**) and 405 nm (**c.** and **d.**), across two experimental setups. The data in **Figure 5.3**, represented visually through colour maps, reveal notable differences in irradiance intensity and distribution patterns for each setup and wavelength, highlighting important considerations in optimizing light delivery for applications requiring precise irradiance control. Setup A (lower light-sample distance) exhibited the highest irradiance values for both 365 nm and 405 nm wavelengths (**a.** and **c.**), indicating that it delivered a stronger intensity of light across the surface of the sample. However, the irradiance distribution in Setup A was non-uniform, with hotspots and areas of increased irradiance due to the specific spatial arrangement and intensity profile of the LEDs. This non-uniformity suggests that while Setup A achieves a high peak irradiance, it may produce uneven energy delivery across the sample surface. In contrast, Setup B (higher light-sample distance) demonstrated lower irradiance values across the entire surface for both wavelengths (**b.** and **d.**). However, this setup produced a more uniform distribution of light intensity, with less variability in irradiance across different measurement points. The uniformity in Setup B is advantageous for applications requiring consistent light exposure across the entire surface, despite its lower peak irradiance.

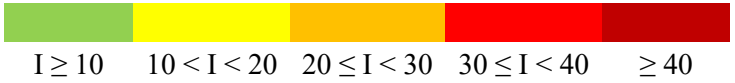
The 365 nm wavelength (**a.** and **b.**) showed a higher degree of variability in irradiance across the sample surface, as observed by the fluctuations in intensity across different measurement points. In contrast, the 405 nm wavelength (**c.** and **d.**) displayed relatively more stable irradiance distributions, which may be due to differences in how visible light at this wavelength interacts with surfaces and diffuses across the sample area (Lu et al., 2021).

The observed irradiance patterns are influenced by the 120° emission angle characteristic of LED, which causes light to propagate in a cone-shaped distribution (Lang et al., 2022). The conical nature of LED light emission results in an uneven spread of irradiance across the sample, especially when the sample is positioned near the light source. At shorter sample-to-light distances, the conical overlap of adjacent LED intensifies irradiance in certain regions, leading to hotspots. This phenomenon occurs because LED arrays, when placed close together, produce overlapping cones of light at specific points on the surface, creating localized regions of heightened irradiance (Beauchamp & Kitai, 2019). Therefore, when a sample is positioned closer to the light source, non-uniformity increases, complicating efforts to achieve homogeneous irradiance. Also Cheng et al. (2020) and Chua et al. (2021) documented similar

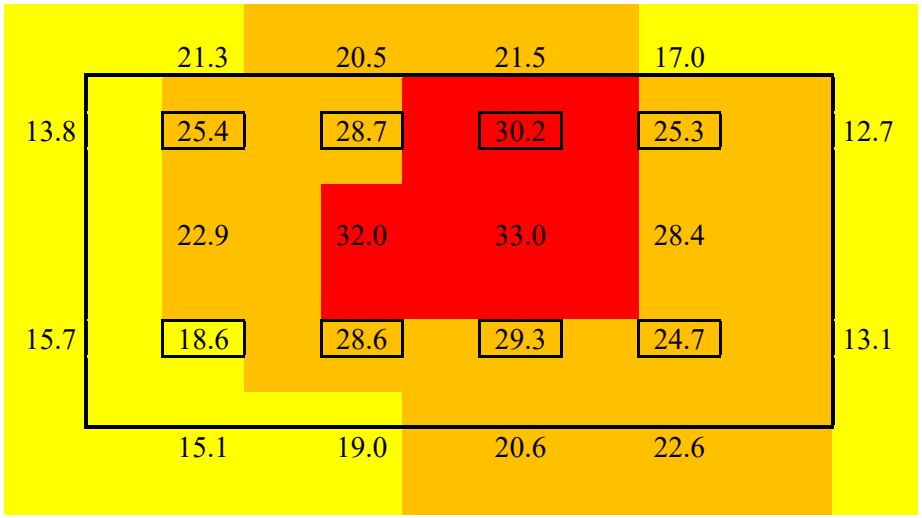
difficulties in achieving uniform irradiance with LED due to their inherent directional emission properties.

According to Jung & Yoon (2023), the distance between the light source and sample is a critical determinant of irradiance distribution uniformity. Increasing this distance helps to mitigate the effects of conical light emission by allowing the light cones from each LED to spread more evenly before reaching the sample surface. This increased separation can reduce hotspots and achieve a more even distribution of irradiance across the surface. However, this adjustment also reduces the overall irradiance intensity on the sample, which, in turn, may require prolonged exposure times to achieve the desired energy dose, particularly for applications like microbial inactivation where sufficient energy delivery is essential (Jung et al., 2019). The trade-off between irradiance uniformity and intensity at different distances represents a key design consideration when optimizing LED-based illumination systems. Wang et al. (2017) also explored strategies for mitigating these inconsistencies, emphasizing the importance of LED arrangement, emission angle, and light source-sample distance in producing a desired light distribution.

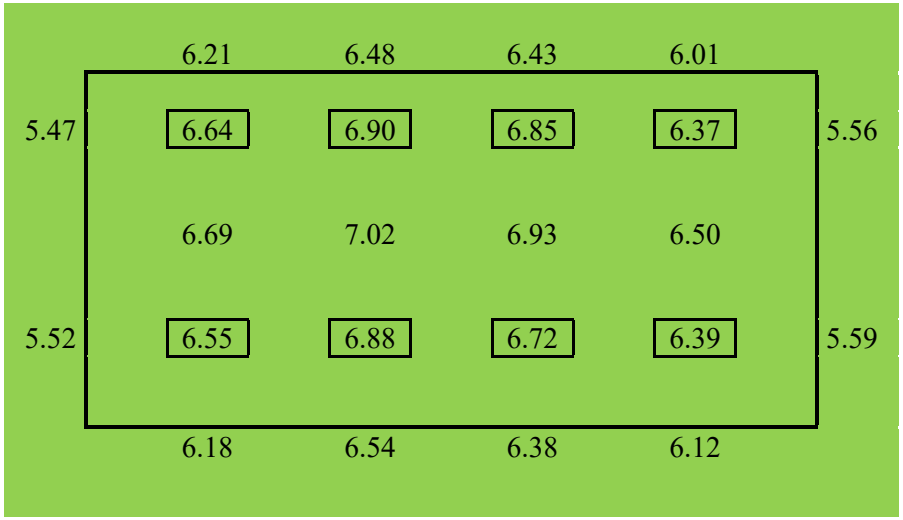
Legend


I ≥ 10
10 < I < 20
20 ≤ I < 30
30 ≤ I < 40
≥ 40

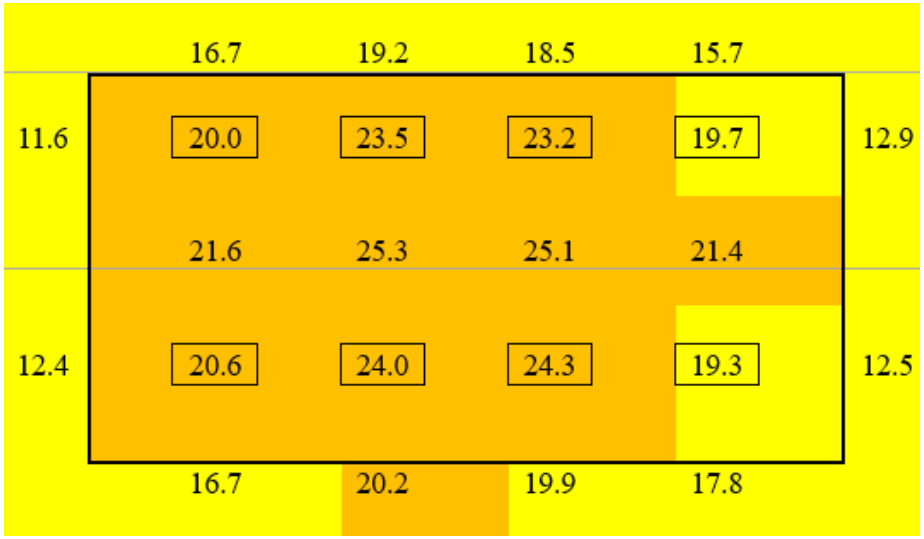
a.


21.3
20.5
21.5
17.0
13.8
25.4
28.7
30.2
25.3
12.7
22.9
32.0
33.0
28.4
15.7
18.6
28.6
29.3
24.7
13.1
15.1
19.0
20.6
22.6

b.


6.21
6.48
6.43
6.01
5.47
6.64
6.90
6.85
6.37
5.56
6.69
7.02
6.93
6.50
5.52
6.55
6.88
6.72
6.39
5.59
6.18
6.54
6.38
6.12

c.



d.

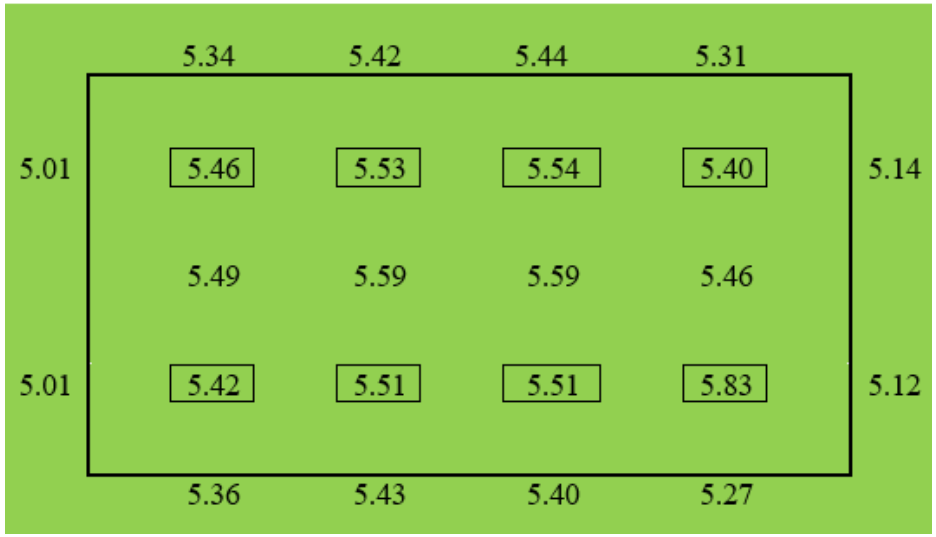


Figure 5.3. Mean of irradiance values (W m^{-2}) measured for **a.** set-up A (height: 17.8 cm) at 365 nm; **b.** set-up B (height: 38.8 cm) at 365 nm; **c.** set-up A (height: 17.8 cm) at 405 nm, **d.** set-up B (height: 38.8 cm) at 405 nm. *I* indicate the irradiance. The results are the average of three replicates.

5.4.2 Effectiveness of light treatment at different wavelengths (UVA and Blue Light)

The present study evaluated the effectiveness of light treatment at wavelengths of 365 nm and 405 nm for microbial inactivation, utilizing two distinct experimental setups (Setup A and Setup B) with varying temperatures and emitted doses. For Setup A, two treatment times were tested: 1 hour and 4 hours, while Setup B involved a single treatment duration of 15 hours (**Table 5.1**). The light dose delivered at each exposure time was directly correlated with the observed microbial inactivation, as shown in **Figure 5.4**.

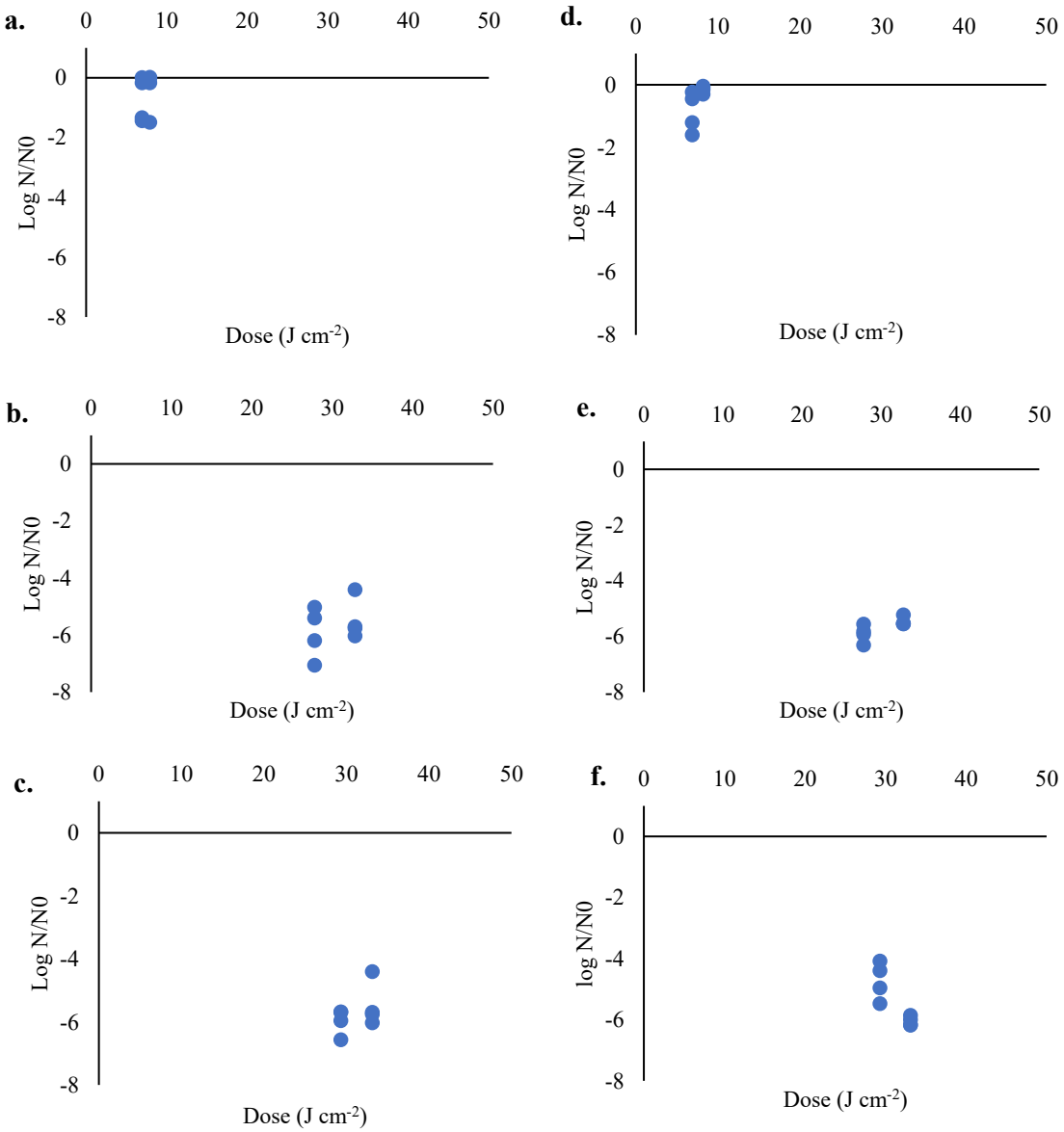


Figure 5.4. Microbial inactivation results versus applied light dose for *E. coli* after 1h (**a.**), 4h (**b.**) and 15h (**c.**) of light treatment and *S. aureus* after 1h (**d.**), 4h (**e.**) and 15h (**f.**) of light treatment. The results are the average of two biological replicates.

The microbial inactivation experiments demonstrated that the degree of inactivation clustered based on the applied light dose, with minor variability among samples subjected to identical conditions. For both tested wavelengths, the 1-hour exposure (Setup A) corresponded to a lower light dose (mean: 7.58 J cm^{-2}) and generally resulted in less than 1 log reduction in microbial viability, although some samples showed slightly higher reductions (**Figure 5.4 a.** and **b.**). In contrast, longer treatment durations of 4 hours (Setup A) and 15 hours (Setup B) achieved comparable levels of microbial inactivation, as the applied light doses were similar (mean: 30.3 J cm^{-2} and 31.1 J cm^{-2}, respectively). For all the tested conditions, the controls remained stable at 10^5–10^6 CFU/mL.

Interestingly, for both Gram (+) and Gram (-) bacteria, when the light dose was held constant, microbial inactivation reached the detection limit, regardless of the wavelength (UVA, 365 nm; or BL, 405 nm) or temperature. While UV light is conventionally deemed more effective for microbial inactivation than visible light (Kebbi et al., 2020; Soro et al., 2023; Yin et al., 2013), this study highlighted the equivalent efficacy of these specific wavelengths, possibly due to the broad emission spectrum of the LED, which could reduce wavelength-specific differences due to the proximity in the light spectrum. Also, changing the temperature did not affect the microbial inactivation for both conditions. The inactivation capacity of 405 nm against the tested microbes was confirmed by other studies (Plavskii et al., 2018; Wu et al., 2021). Therefore, it was possible to state that the light dose was the crucial factor for microbial inactivation, independently from the temperature and the wavelength.

Temperature variations did not influence microbial inactivation, corroborating prior findings on the effectiveness of 405 nm light against tested microbes (Plavskii et al., 2018; Wu et al., 2021). Thus, the study identifies light dose as the primary determinant of microbial inactivation, independent of wavelength, which in this case were near in the light spectrum, or temperature. This conclusion aligns with other reports, such as Yagi et al. (2007), who achieved complete inactivation of *E. coli* with a 54 J cm^{-2} dose using 365 nm LED, and Zhao et al. (2023), who achieved nearly 4-log *S. aureus* inactivation by applying the same light dose. However, contrary to this study, Mori et al. (2007) observed reduced efficiency of 405 nm light against *E. coli* compared to 365 nm.

Temperature data (**Table 5.4**) indicate that *E. coli* and *S. aureus* displayed similar responses across conditions. Experiments conducted at room temperature (20–23°C) showed fluctuations

of 1–3°C while, under standard operational conditions, the average air temperature inside the refrigerator was recorded at 4.14 ± 0.39°C. This small variation is a result of the refrigerator's compressor cycling mechanism, where the compressor activates to lower the internal temperature after it surpasses a predetermined threshold and deactivates once the target temperature is achieved, allowing gradual warming before the cycle resumes. These air temperature fluctuations do not affect the temperature of stored food, as food items act as a thermal mass that maintains a stable temperature (Almenta et al., 2014; Bonanno et al., 2024; James et al., 2017).

The refrigerator used in these experiments was a *built-in* model typically integrated into kitchen cabinetry, which generally has reduced insulation compared to *stand-alone* models. Consequently, this design feature may amplify air temperature fluctuations within the fridge.

Introducing a stainless steel box into the refrigerator chamber altered the thermal dynamics of the system. The average internal temperature rose to 5.95 ± 0.95°C, likely due to heat generated by the LED's heat dissipator transferring to the surrounding air. This localized heating, facilitated by the high thermal conductivity of stainless steel, increased the chamber's temperature by approximately 2°C compared to standard conditions.

The stainless steel efficiently transfers heat from the LED, leading to localized temperature elevation, which in turn imposes a higher thermal load on the refrigerator. This additional load may cause the cooling system to activate more frequently in an effort to restore the desired temperature, highlighting the interaction between heat dissipation processes and the refrigeration cycle.

As discussed in previous chapters, microbial inactivation using light technologies is influenced by several factors, including the type of microorganism, wavelength, and light dose. In this study, the light dose—determined solely by the treatment duration—emerged as the most critical parameter, explaining 95.7% of the observed variation in microbial inactivation. These findings underscore the predominant role of light dose in achieving microbial inactivation.

Specifically, adjustments to the light dose through variations in treatment duration (i.e., 1 hour, 4 hours, or 15 hours) resulted in significant changes in inactivation rates. In contrast, other factors, contributed minimally to the observed variation, with each accounting for less than 1%. This highlights the importance of optimizing treatment duration to deliver the appropriate light dose for effective microbial control.

Table 5.3. Mean temperature ± SD (standard deviation) of light treatments. The results are the average of two biological replicates.

Microbes	λ (nm)	T (°C)	Time (h)	Temperature (°C)
E. coli	405	Room T	1	24.1±0.99
			4	25.3±1.85
			15	23.2±0.52
		4	1	6.95±0.67
			4	5.36±0.75
			15	7.70±0.74
	365	Room T	1	24.7±0.81
			4	26.8±0.11
			15	21.5±1.28
		4	1	6.16±0.86
			4	6.90±0.80
			15	6.87±0.33
S. aureus	405	Room T	1	24.8±0.15
			4	24.4±2.47
			15	22.5±0.99
		4	1	5.41±0.36
			4	6.39±0.23
			15	7.31±0.76
	365	Room T	1	24.6±0.44
			4	26.5±0.49
			15	21.5±1.28
		4	1	7.77±0.48
			4	6.67±0.80
			15	5.42±1.39

In light of these results, the most effective microbial inactivation was achieved with a light dose of 30 J cm^{-2}, corresponding to 4 hours of irradiation in Setup A or 15 hours in Setup B. However, from an energy efficiency perspective, a 1-hour irradiation is preferable to a 15-hour treatment, as energy consumption increases with prolonged exposure due to constant energy output per unit of time. Additionally, longer durations may impose greater strain on the refrigerator compressor, leading to higher operational demands.

The primary limitation of the 1-hour treatment is its lower emitted dose (7 J cm^{-2}), which falls short of the required 30 J cm^{-2} for effective microbial inactivation. A potential solution involves incorporating systems to enhance light irradiance and ensure uniform light distribution at shorter lamp-sample distances, as in Setup A, to adapt this technology for applications such as fridge drawers. Optimizing these parameters would enable microbial inactivation to be achieved more efficiently.

Therefore, after identifying the necessary dose to have a microbial inactivation at a short distance (as in a fridge drawer), it would be necessary to uniformly distribute the incident light and to add a system to enhance the power of the LED per unit of time.

Table 5.4. Four Way Analysis of Variance (ANOVA) of the effect of four variables: microorganism (M), wavelength (W), temperature (T) and treatment time (t).

Variables	SS%	$p \leq 0.05$
M	0.43	*
W	0.13	ns
T	0.03	ns
t	95.7	***
M * W	0.31	ns
M * T	0.02	ns
M * t	0.22	ns
W * T	0.08	ns
W * t	0.89	ns
T * t	0.94	**
M * W * T	0.01	ns
M * W * t	0.26	ns
M * T * t	0.04	ns
W * T * t	0.54	*
M * W * T * t	0.55	*

SS, sum of squares, *p*, significance; *$p \leq 0.05$; **$p \leq 0.01$; *** $p \leq 0.001$; ns: not significant.

5.5 Conclusions

This study aimed to develop a *mock-up* for applying light technology in domestic and industrial settings to achieve microbial inactivation. The findings emphasized the critical role of designing an effective prototype and thoroughly assessing experimental parameters. Specifically, the results highlighted that the final dose could vary depending on the experimental configuration. After determining a fixed irradiance value, treatment time emerged as the most pivotal factor in optimizing the setup. Moreover, factors such as microbial species and temperature were identified as significant variables that could interact with other parameters to influence outcomes.

The study's comprehensive approach to evaluating multiple parameters—irradiance, treatment time, microbial type, and temperature—demonstrates its potential for real-world application. By prioritizing the optimization of treatment time and considering synergistic effects between variables, the research paves the way for practical and adaptable applications of light technology. Additionally, the focus on integrating these factors into the prototype design ensures a versatile and scalable solution for microbial inactivation in diverse environments, reinforcing the study's innovative and applied significance.

Section 2

Exploitation of Exogenous Photosensitizers for Photodynamic Inactivation

Photodynamic inactivation (PDI) is a process that relies on three primary components: light, molecular oxygen, and a photosensitizer (PS). As previously discussed, PS can either be endogenous (naturally present within bacterial cells) or exogenous (externally added). Exogenous PS can be either natural or synthetic. In recent years, many new molecules with PS properties have been discovered, and several synthetic PS have been developed for use in PDI (Martins Antunes De Melo et al., 2021; Mesquita et al., 2018; Vieira et al., 2018). Among the most common synthetic PS identified in the literature are Rose Bengal, toluidine blue (TBO), porphyrins, methylene blue, and eosin Y (Alhenaki et al., 2021; Bonin et al., 2018; Castro et al., 2019; He et al., 2022; Thandu et al., 2014). However, given the growing interest in applications within the food sector, research has also focused on natural PS, including curcumin, riboflavin, organic acids, and quercetin (Aurum & Nguyen, 2019; Ghate et al., 2015; Josewin et al., 2018a; Lee, 2023). Few studies have assessed the effectiveness of exogenous PS in food products, primarily due to the novelty of this technology and the complexity of the variables involved in such experiments.

The inclusion of exogenous PS in PDT can enhance the antimicrobial effect of light, thus improving microbial inactivation. Moreover, the use of PS enables a reduction in light irradiance or treatment duration, resulting in energy savings and cost reductions (Cossu et al., 2021). This makes the technology more feasible for practical, large-scale applications, especially in food safety, where cost-effectiveness is critical.

Consequently, this section explores the use of both natural and synthetic exogenous PS to optimize microbial inactivation through light treatment.

Chapter 6

Exploitation of a synthetic photosensitizer: Methylene Blue

6.1 Introduction

Methylene blue (MB) (**Figure 6.1**) is a positively charged, heterocyclic aromatic compound that has found extensive applications in the medical field. Classified as a phenothiazinium dye, MB functions as an alternative electron carrier involved in ROS regulation (Tariq et al., 2021). Recently, MB has gained recognition as a PS capable of absorbing light in the 500–700 nm range, with a peak excitation wavelength at 664 nm. This absorption triggers the production of various ROS, including H_2O_2, $OH\cdot$ and $O_2^{\cdot -}$.

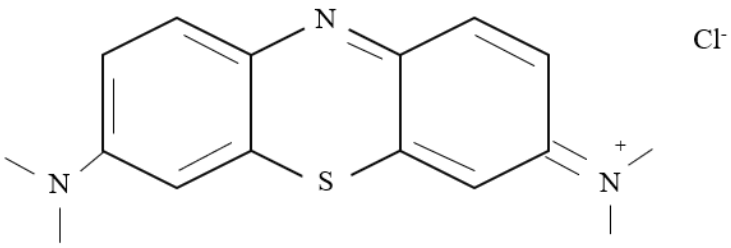


Figure 6.1. Methylene Blue structure.

White light, a segment of the electromagnetic spectrum visible to the human eye, spans 400–700 nm. Transitioning from UV light to white light for disinfection has become popular due to white light's safety for humans, eco-friendly nature, cost-effectiveness, and higher penetrative ability. Additionally, its emission through LED ensures a contamination-free process (Lena et al., 2024).

Between 2000 and 2022, MB was predominantly studied against *S. aureus* and *E. coli*, the latter being the second most targeted microorganism due to its clinical significance (Piksa et al., 2023). While MB has primarily been utilized in PDT in the medical field, its applications in the food industry remain underexplored (Galstyan & Dobrindt, 2019; Khan et al., 2022). One notable advantage of MB is its photodegradation into water and carbon dioxide, which supports its safe use in food-related contexts (Khan et al., 2022). When combined with visible light, MB shows potential as a surface sanitization agent for food contact areas.

6.2 Aim of the study

After evaluating the potentiality of BL by exploiting endogenous PS-only in various conditions, the present study aims to evaluate the feasibility of PDT using MB as an exogenous PS in various conditions, including liquid substrates of differing opacity and organic content, as well as in biofilms formed on stainless steel. These experiments simulate common scenarios where biofilms develop due to inadequate cleaning practices.

This work was carried out at the Laboratory of Applied Microbiology (LMA) of the University of Aveiro (Aveiro, Portugal) under the supervision of Professor Adelaide Almeida.

6.3 Material and methods

6.3.1 Microbial culture

In the present study, *E. coli* ATCC_23922 and *L. monocytogenes* ATCC_20600, part of the collection of the Laboratory of Applied Microbiology (LMA) of the University of Aveiro were used for the experimentation. Stock cultures of the tested microbes were stored at −80 °C in BHI or TSB in the case of *L. monocytogenes* and *E. coli*, respectively, supplemented with 30% (v:v) glycerol. Before each test, stock cultures were subcultured overnight twice in the relative culture media and grew in BHI agar and Tryptone Soy Agar (TSA, Oxoid, Basingstoke, United Kingdom) plates. The microbial suspensions were incubated overnight twice at 37°C resulting in a final concentration of 10^9 CFU/mL.

6.3.2 Photosensitizer

A stock solution of Methylene Blue (MB, CAS 122965–43–9, Sigma-Aldrich/Merck KGaA, Darmstadt, Germany) was prepared at 500 μM in PBS and stored in the dark and at room temperature until their usage. Before each test, MB solution was sonicated for homogenization for 5 min at room temperature (Ultrasonic Bath, Nahita 0.6 L, 40 kHz). The MB absorption spectra (**Figure 6.2**) were obtained by measuring the absorbance of 30 μM of MB from 400 nm to 700 nm.

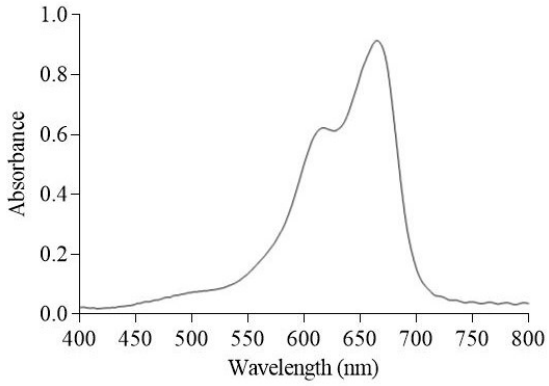


Figure 6.2. Methylene Blue (MB) absorption spectra in the visible light spectra.

6.3.3 Lamp characterisation

The PDI experiments were performed under white light irradiation (400-700 nm) setting the irradiance at 50 mW cm^{-2} delivered by a LED system (LUMECO light®, 30 W, 4000 K, 2000 lm). The irradiance of the light sources was measured using a power meter Coherent® FieldMaxII-Top combined with a thermopile power sensor Coherent® PS19Q. The LED emission spectra (**Figure 6.3**) were provided by the lamp manufacturer.

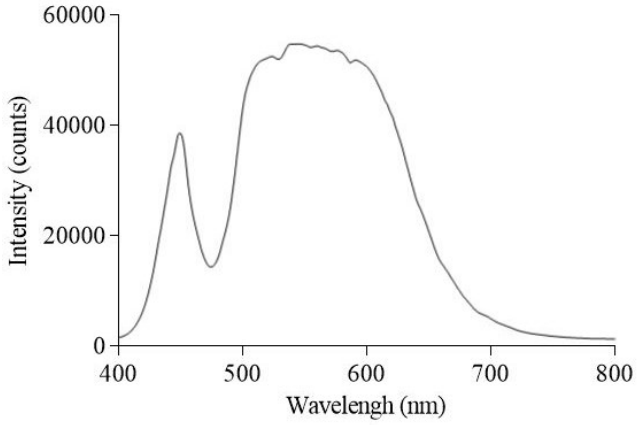


Figure 6.3. LED emission spectra.

6.3.4 Photodynamic inactivation tests in transparent liquid substrate

The capability of white light to inactivate the tested microbes was evaluated on PBS. Three experimental conditions were tested: samples with methylene blue (SMB), light controls (LC), and dark controls (DC). The experiments were conducted using two 24-well microplates: one containing SMB and LC, and the other reserved for DC. Each well contained a final volume of 2 mL, a bacterial concentration of $10^7/10^8$ CFU/mL and MB at concentrations of 1 μM or 5 μM. While SMB and DC were prepared identically, MB was excluded in LC wells.

Inactivation kinetics were assessed at six time points: 0, 5, 10, 15, 30, and 60 minutes. Throughout the tests, the samples were agitated in a room maintained at approximately 16°C. At each time point, SMB, LC, and DC samples were plated on TSA or BHI agar using the drop plate method. The plates were then incubated at 37°C for 24 hours, and viable cell counts were

recorded as log CFU/mL. PDI tests in PBS were performed in three independent biological replicates.

6.3.5 Photodynamic inactivation test in an organic substrate

To evaluate the PDI in a complex liquid substrate, ultra-high-temperature (UHT) milk was chosen due to its opacity and high organic matter content. The milk was sourced from a local store. As with previous tests, two 24-well microplates were used: one for the SMB and LC, and the other for DC. Each well contained a total volume of 2 mL, a bacterial concentration of $10^7/10^8$ CFU/mL, and MB at concentrations of 20 µM or 50 µM. SMB and DC were prepared similarly by combining milk, the microbial suspension, and MB, whereas MB was excluded in the LC wells.

The microplates were incubated in dark conditions for 15 minutes under agitation before collecting the initial samples (t0) for serial dilution. SMB, LC, and DC were then exposed to light treatment for 60 and 120 minutes at an intensity of 50 mW cm^{-2} in a room maintained at 16°C. A fan was positioned near the microplates to prevent temperature increases during the treatment (**Figure 6.4**). All samples were agitated continuously throughout the experiment.

After 60 and 120 minutes of light exposure, SMB, LC, and DC samples were collected, serially diluted, and plated on BHI agar (for *L. monocytogenes*) or TSA (for *E. coli*) using the drop plate method. Agar plates were incubated at 37°C for 24 hours, after which the colonies were counted to quantify microbial inactivation induced by the light treatment. Results were expressed in log CFU/mL. PDI tests in milk were performed in triplicate, with three biological replicates and three technical replicates for each condition.

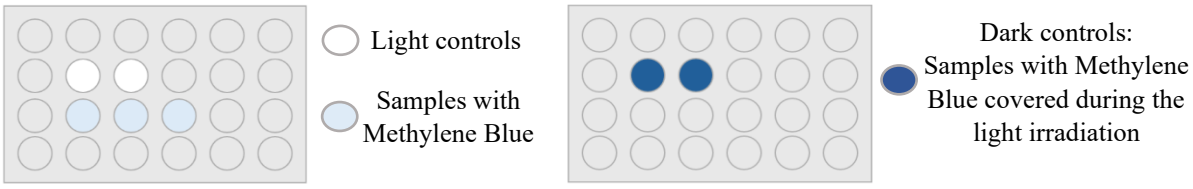


Figure 6.4. Schematical representation of experimental set-up for PDI test using milk and methylene blue.

6.3.6 Biofilm preparation on culture media and milk

Overnight microbial cultures were diluted 1:1000 in TSA or BHI broth. Stainless steel coupons were sterilized by exposure to UV light for 120 seconds on each side and placed in sterile Petri dishes. A 200 µL aliquot of the microbial culture was then deposited at the centre of each coupon, in an area of 1 cm^2 (**Figure 6.5**). The coupons were incubated at 37°C for 48 hours to allow biofilm formation. To maintain viability, the medium was refreshed every 24 hours by removing the 200 µL inoculum and replacing it with 200 µL of fresh broth.

The same procedure was done also by using UHT milk instead of culture media.

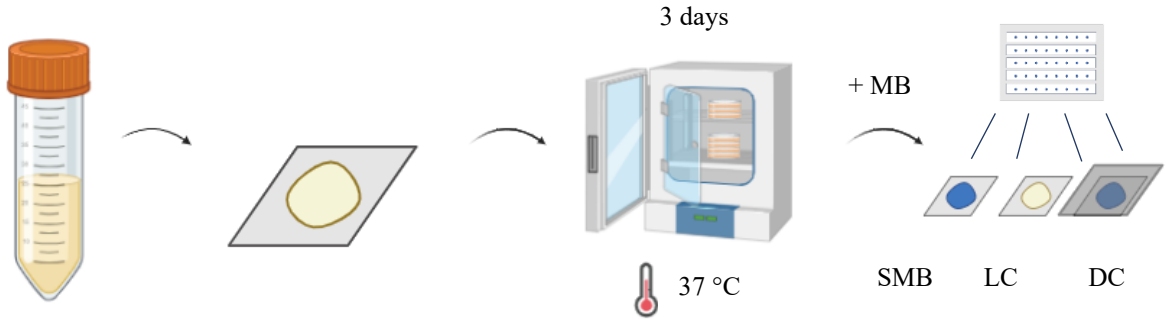


Figure 6.5. Experimental phases for biofilm growth: microbial culture growth, seeding on a stainless steel coupon, incubation for 3 days at 37°C (refresh every day), addition of Methylene Blue (MB) and light treatment.

6.3.7 Biofilm treatment

After 48 hours of incubation, the biofilms were washed three times with PBS to remove non-adherent cells. For SMB and DC samples, 200 µL of MB solution in PBS (at concentrations of 5 µM for *L. monocytogenes* and 20 µM for *E. coli*) was added. In contrast, LC samples received 200 µL of PBS alone. The biofilms were then exposed to white light (wavelength range 400-700 nm) at an irradiance of 50 mW cm^{-2} for durations of 30 and 60 minutes.

Following light treatment, the biofilms were detached from the stainless steel coupons using sterile swabs. Each coupon was swabbed 30 times across its surface, and the detached biofilms were released into 1 mL of PBS. The SMB, LC, and DC samples were subsequently serially diluted and plated on TSA or BHI agar plates using the drop plate method (**Figure 6.6**). The plates were incubated for 24 hours at 37°C, after which colony-forming units (CFU) were enumerated. The results were expressed as log N/N0, where N represents the final microbial concentration and N0 is the initial microbial concentration at time zero. Biofilm experiments,

conducted both in culture media and milk, included three biological replicates, with each experiment comprising three technical replicates.

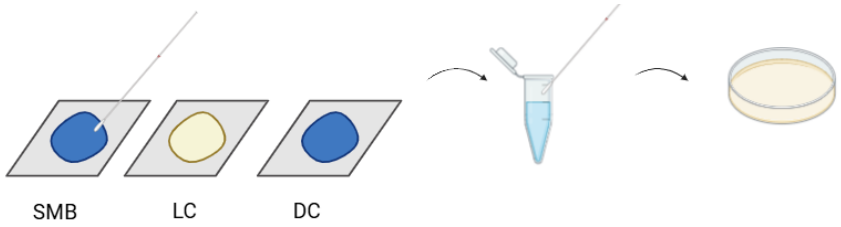


Figure 6.6. Experimental steps for biofilm enumeration.

6.3.8 Statistical Analysis

Results were expressed as CFU/mL or CFU/cm^2 (planktonic cells or biofilms, respectively) and transformed in the logarithm CFU/mL or logarithm CFU/cm^2. The Log (N/N0) were then calculated, where N is the log CFU/mL or log CFU/cm^2 after the BL treatment and N0 is the log CFU/mL or log CFU/cm^2 of the control. The data were elaborated with Microsoft Excel and GraphPad Prism software (9.0.0) and represented as the mean of two biological replicates ± standard deviation (SD) and subjected to statistical analysis by IBM SPSS Statistics for Windows version 23.0 (IBM Corp., Armonk, N.Y., USA). The statistical methods used to determine the significant differences between the samples were One-way ANOVA ($p < 0.05$), and post-hoc Tuckey's test.

6.4 Results and Discussion

This study investigates the PDI of two foodborne pathogens, the Gram (+) *L. monocytogenes* and the Gram (-) *E. coli*, both of which are key targets for sanitization in the food industry. Microbial inactivation was achieved using MB as an exogenous PS, activated by low doses of light (Lin et al., 2012). MB has been extensively studied as a PS in PDI for the inactivation of various pathogens, particularly in medical applications (Demidova & Hamblin, 2005; Sabino et al., 2019; Yuan et al., 2020; Vecchio et al., 2015).

6.4.1 Photodynamic Inactivation (PDI) in a liquid substrate

The results of PDI tests conducted in PBS for planktonic *E. coli* and *L. monocytogenes* are summarized in **Figure 6.7**. Both bacterial strains had an initial concentration of 10^7 CFU/mL and the LC and the DC remained constant at 10^7 CFU/mL for the test duration. These PDI tests were designed to evaluate the PDI efficiency in a transparent liquid medium devoid of organic matter and to determine the optimal MB concentration required. The irradiance was set at 50 mW cm^{-2}, based on preliminary experiments (Bartolomeu et al., 2024).

For *E. coli* (**Figure 6.7 a.**), a concentration of 1 µM MB resulted in a -3.53 log reduction after 60 minutes of light exposure (180 J cm^{-2}). When the MB concentration was increased to 5 µM, the bacterial load fell below the detection limit within 15 minutes (45 J cm^{-2}). A significant microbial reduction was observed after 10 minutes with 5 µM MB, whereas with 1 µM, a similar effect was achieved only after 60 minutes.

In the case of *L. monocytogenes* (**Figure 6.7 b.**), 1 µM MB was sufficient to completely inactivate the bacterial population below the detection limit within 15 minutes (45 J cm^{-2}). A significant reduction in microbial load was already apparent after just 5 minutes of treatment.

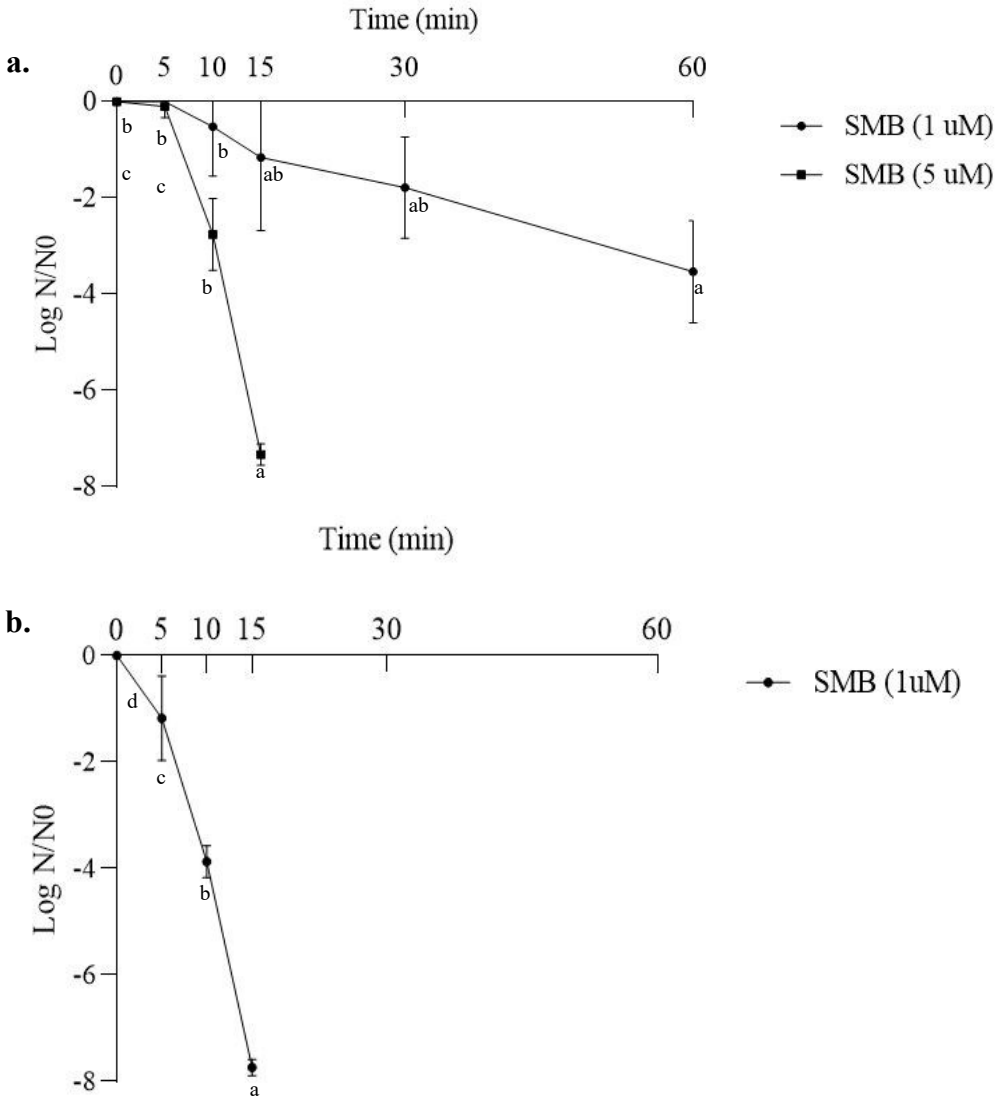


Figure 6.7. Mean ± standard deviations of PDI test of *E. coli* (**a.**) and *L. monocytogenes* (**b.**) in PBS media. SMB (light-irradiated samples) represent the sample which consisted of the microbial suspension in PBS added with Methylene Blue (MB) at specific concentrations (1 μM or 5 μM). Different lower case letter in the same line indicates a significant difference among the same MB concentration at different treatment times ($p<0.05$). The results are the average of three biological replicates.

These results highlight two critical factors influencing bacterial inactivation: the bacterial type (Gram + vs. Gram -) and the PS concentration, which affects inactivation in a dose-dependent manner. The Gram (+) *L. monocytogenes* required only 1 μM MB and 45 J cm^{-2} of light to

completely inactivate 10^7 CFU/mL, whereas the same conditions achieved only a -3.53 log reduction for *E. coli*.

To get the same result of *L. monocytogenes*, the MB concentration was increased 5 times.

These findings align with the previous test results without exogenous PS (**Chapters 2** and **4**), where Gram (+) bacteria were characterised by a higher susceptibility to BL than Gram (-), and by the results reported by Vecchio et al. (2015), who demonstrated that 10 μM MB combined with 5 J cm^{-2} of 660 nm light reduced *S. aureus* (Gram +) and *E. coli* concentrations by approximately 4 log and 2 log, respectively, within 20 minutes. The higher effectiveness of PDI against Gram (+) bacteria is attributed to their permeable cell wall, which facilitates the diffusion of PS of various charges (cationic, neutral, or anionic) into the cells. In contrast, the cell wall of Gram (-) bacteria restricts entry to cationic PS only (Minnock et al., 1996).

As MB is a cationic dye, it exhibits affinity for both Gram (+) and Gram (-) bacteria (Liang et al., 2022). However, its effectiveness is greater in Gram (+) bacteria due to better penetration. Within Gram (-) species, susceptibility may vary. Yang et al. (2019) observed only a -1 log reduction in *P. aeruginosa* using 250 μM MB combined with 20 J cm^{-2} of light.

6.4.2 Photodynamic Inactivation (PDI) treatment on milk

In the PDI tests conducted on a complex liquid substrate such as milk, MB concentrations were increased to 20 μM and 50 μM to account for the matrix's opacity and complexity, which includes fats, proteins, and lipids.

The PDI results for *E. coli* and *L. monocytogenes* in milk with MB are summarized in **Figure 6.8**. Both bacterial strains had an initial concentration of 10^7 CFU/mL and the LC and the DC remained constant at 10^7 CFU/mL for the test duration. For *E. coli*, using 20 μM MB did not result in significant inactivation within 120 minutes (< 1 log reduction). However, with 50 μM MB, *E. coli* showed a reduction of -1.35 log over 120 minutes (D = 360 J cm^{-2}). For *L. monocytogenes*, 20 μM MB achieved a reduction of approximately -1.00 log after 60 minutes (180 J cm^{-2}) and -2.26 ± 0.37 log after 120 minutes (360 J cm^{-2}). When the MB concentration was increased to 50 μM, the treatment achieved more than a -2 log reduction within 60 minutes, and the microbial load fell below the detection limit after 120 minutes. The inactivation levels achieved with 50 μM MB at 60 and 120 minutes were statistically significant ($p = 0.023$).

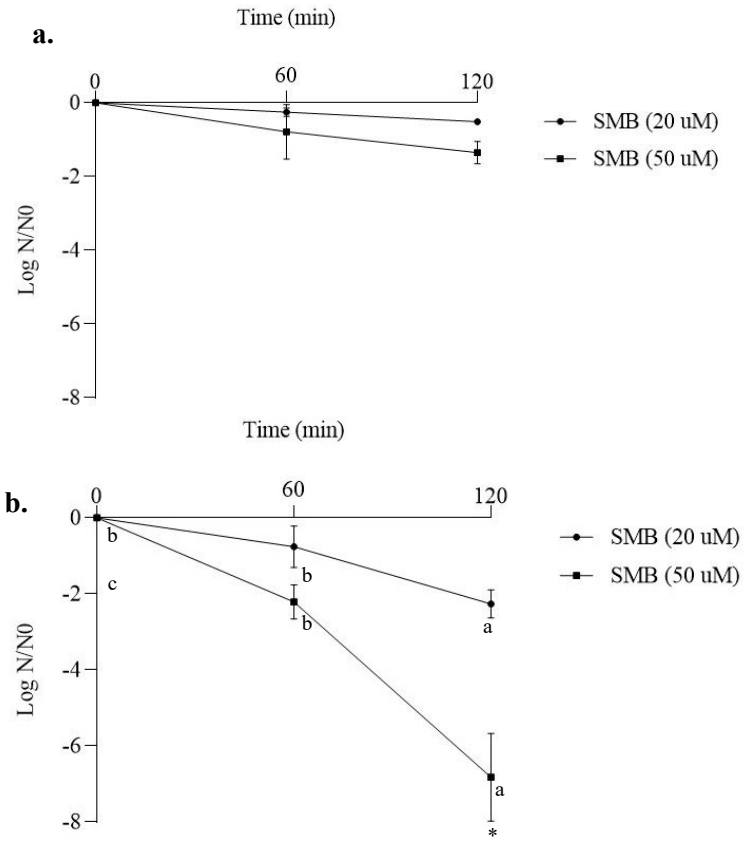


Figure 6.8. Mean ± standard deviations of test of PDI test of *E. coli* (**a.**) and *L. monocytogenes* (**b.**) in milk. SMB (light-irradiated samples) represent the sample which consisted of the microbial suspension in milk, an opaque suspension with organic matter added with Methylene Blue (MB) at specific concentrations (20 μM or 50 μM). Different lowercase letters indicate in the same line a significant difference among the same MB concentration at the different time points ($p<0.05$), no letters indicate that there are no significant differences; * Indicate a significant difference in the microbial inactivation produced at the same time with different MB concentrations ($p<0.05$). The results are the average of three technical replicates and three biological replicates.

These findings align with the trends observed in PDI tests conducted in PBS, confirming that Gram (+) *L. monocytogenes* is more susceptible to MB treatment than Gram (-) *E. coli*. Specifically, a light dose of 360 J cm^{-2} combined with 20 μM MB reduced *L. monocytogenes* by approximately -2 log, and increasing MB concentration to 50 μM resulted in complete

inactivation. Conversely, for *E. coli*, even 50 μM MB achieved only modest inactivation, with no significant reductions ($p > 0.05$).

These results are in agreement with findings by Galstyan & Dobrindt (2019), who observed greater reductions in Gram (+) bacteria (*S. aureus*, *Staphylococcus hominis*, and *Staphylococcus warneri*) compared to Gram (-) *E. coli* when treated with 10 μM MB in milk. The higher resistance of Gram (-) bacteria is associated with the integrity of their outer membrane, which is stabilized by lipopolysaccharides. Divalent cations like Ca^{2+} and Mg^{2+}, abundant in milk, stabilize the negative charge of the lipopolysaccharide structure and mitigate the membrane disruption caused by MB, reducing the photodynamic effect (George et al., 2009).

Comparing results between a transparent and "simple" substrate, like PBS, and a complex and opaque substrate as milk revealed a significantly lower microbial inactivation in the second one. This discrepancy is attributed to factors such as milk's opacity and its complex components. Unlike PBS, which is transparent, milk's white-yellowish colour creates higher optical density and absorbs more light, reducing the penetration of the light treatment. Additionally, milk's fat globules and casein micelles scatter light, further limiting MB activation and decreasing quantum yield (Saraiva et al., 2024). Milk proteins, particularly caseins, also promote MB aggregation, reducing the availability of non-aggregated MB for microbial inactivation and altering its absorption spectra. As demonstrated by Chen et al. (2014), the antimicrobial effectiveness of PS can vary significantly depending on the protein content in the surrounding medium.

The use of MB in the milk and dairy sector could be questioned by the modification of the colour that could occur in milk after MB addition. This dye is known to be photodegraded after light irradiation into H_2O and CO_2 making its usage suitable (Khan et al., 2022). This peculiarity was clear also visually, as shown in **Figure 6.9**, where independently of the MB concentration (20 μM or 50 μM), after 120 min of light treatment and 360 J cm^{-2}, it was degraded almost completely.

However, two possible solutions could be applied to remove it. The first method could be the immobilization of MB in a polymeric support that does not release the dye in order to exploit its efficacy without being dispersed in the liquid matrix. Secondly, ultrasound treatment or thistle seeds are techniques known to possibly remove the MB (Çiftçi, 2022; Djelloul & Hasseine, 2013).

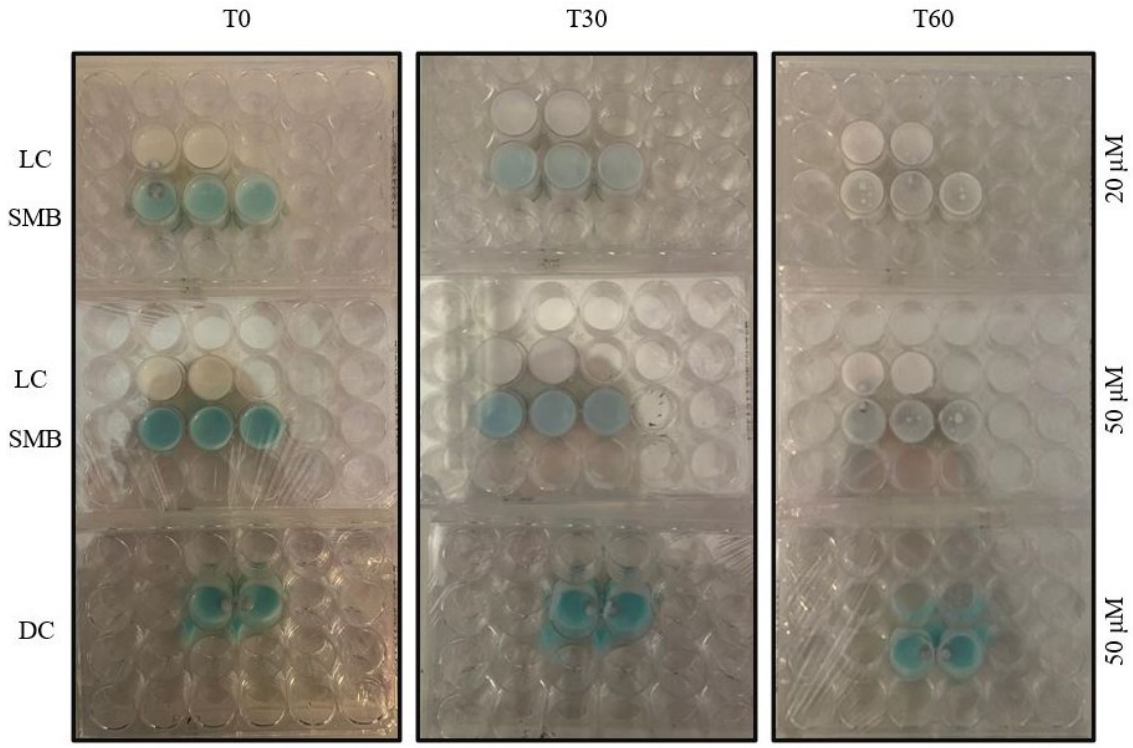


Figure 6.9. Change in the colour of milk added with Methylene Bue (MB) as a photosensitizer. At time 0 (T0), the samples displayed a blue colour, with intensity directly proportional to the MB concentration. After 60 minutes (T60), the blue colour in the light-irradiated samples (SMB) significantly faded. In contrast, the samples containing MB but not exposed to light (DC) retained their original colour throughout the experiment.

6.4.3 Photodynamic Inactivation (PDI) treatment on microbial biofilm formed in culture media

E. coli and *L. monocytogenes* biofilms were grown on stainless steel coupons using TSA and BHI, respectively, and treated in PBS. Results are reported in **Figure 6.10 a.** and **b.** The biofilm concentration was 10^7 CFU cm^{-2} for both microbes and the light treatment was performed by emitting a light dose of 180 J cm^{-2}. For the treatment of biofilm, the MB concentrations were selected based on previous tests using the same MB concentration used for the treatment of planktonic cells on PBS media. Therefore, the used MB concentrations were 20 µM for *E. coli* and 5 µM for *L. monocytogenes*. For both tested microbes, the LC and the DC remained constant at 10^7 CFU/cm^2 for the test duration.

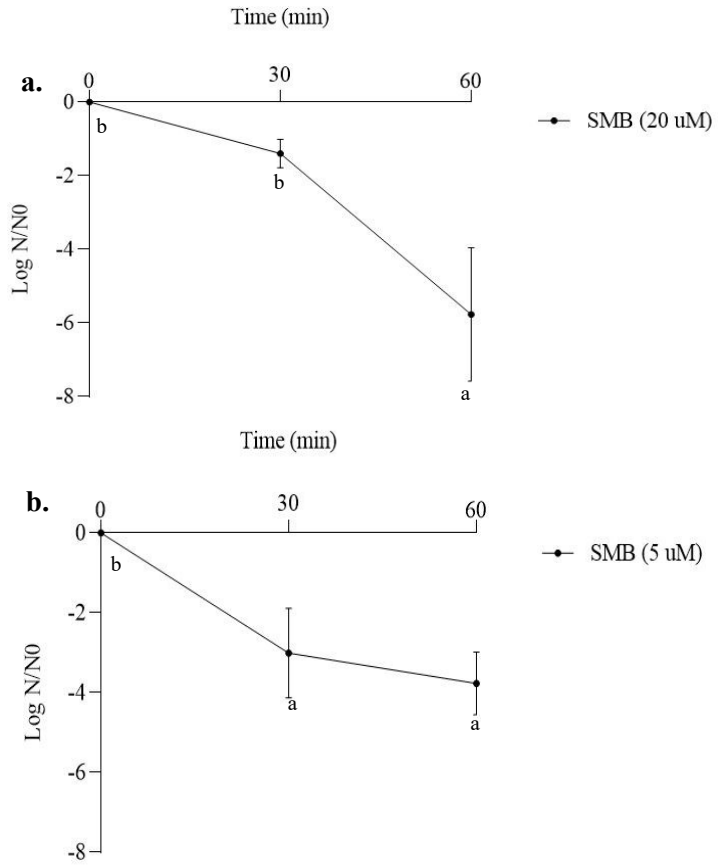


Figure 6.10. Mean ± standard deviations of biofilms of *E. coli* (**a.**) and *L. monocytogenes* (**b.**) growth in stainless steel surface in TSA and BHI, respectively. SMB (light-irradiated samples) represent the sample which consisted of the microbial biofilm suspension in PBS added with methylene blue at specific concentrations (5 μM or 20 μM). Different lowercase letters indicate a significant difference among the same Methylene Blue (MB) concentration at different time points ($p<0.05$). The results are the average of three technical replicates and three biological replicates.

Considering *E. coli* (**Figure 6.10 a.**), 20 μM of MB was able to provide -1.20 log in 30 min and -6.00 log in 60 min. After 60 min there was a significant inactivation, which could be due to the fact that the PS needed some time to be activated. Differently, for *L. monocytogenes* (**Figure 6.10 b.**), 5 μM of MB provided a significant inactivation of -3.00 log in 30 min and – 3.80 log in 60 min. In this case seemed that the MB was activated earlier than in the case of *E. coli*. These trends were evidenced also in another study, where *E. coli* and *L. innocua* treated with a PS and light reached the same inactivation but the inactivation of *L. innocua* was faster. Also, the different inactivation results could be due to the differences in the bacteria structure, as

mentioned in **Chapters 2**, **3** and **5**, and also to the different biofilm structures that these bacteria are able to form (Bridier et al., 2010). In fact, as underlined in **Chapter 4**, *E. coli* seemed to develop more across the surface while *L. monocytogenes* increased was observed to form more thick aggregates. These divergencies may determine a different water and nutrient content inside the matrix and, also, a different amount of persister cells – which through their dormant state can resist some treatments – may be present, resulting in a dissimilar response to BL treatment (Ziege et al., 2021).

Notwithstanding that the concentration of MB was four times higher for *E. coli* than for *L. monocytogenes*, the application of 90 J cm^{-2} (after 30 min) provided a significant reduction of *L. monocytogenes.* By applying a light dose of 180 J cm^{-2}, the reduction was significant for both the microbial species in a PS-concentration-dependent manner.

Again, the higher susceptibility of Gram (+) bacteria was demonstrated since with the use of 5 μM, ca. 3.80 log were inactivated while using 4 times higher MB concentration, *E. coli* was reduced to approximately 6 log. The different susceptibility of bacterial species to the PS was demonstrated also by Shi et al. (2022a, 2022b), where the tested Gram (-) bacteria required a higher concentration of the PS compared to the Gram (-) bacteria and the same inactivation occurred at different treatment times.

6.4.4 Photodynamic Inactivation (PDI) treatment on microbial biofilms formed in milk

The PDI of biofilms formed in milk was tested using the same concentrations of MB as in previous experiments: 5 μM for *L. monocytogenes* and 20 μM for *E. coli*. The light treatment consisted of a light dose of 180 J cm^{-2} over 60 minutes. To simulate a realistic food industry scenario, biofilms were grown on stainless steel coupons, a common surface material in food processing environments. The microbial inactivation results are reported in **Figure 6.11**. For both tested microbes, the LC and the DC remained constant at 10^7 CFU cm^{-2} for the test duration.

After being irradiated for 30 min, *E. coli* was reduced of -1.74 ± 0.29 log after 30 min and ca. -2.00 log after 60 min (**Figure 6.11 a.**). Differently from what was observed before, the

inactivation trend was more accentuated in the first 30 min of treatment. Furthermore, compared to the PDI treatments in PBS, the microbial reduction was appreciably lower.

Considering *L. monocytogenes* (**Figure 6.11 b.**), the light treatment combined with MB determined -1.31 ± 0.57 log after 30 min and ca. -2.30 log after 60 min, in a linear decreasing trend.

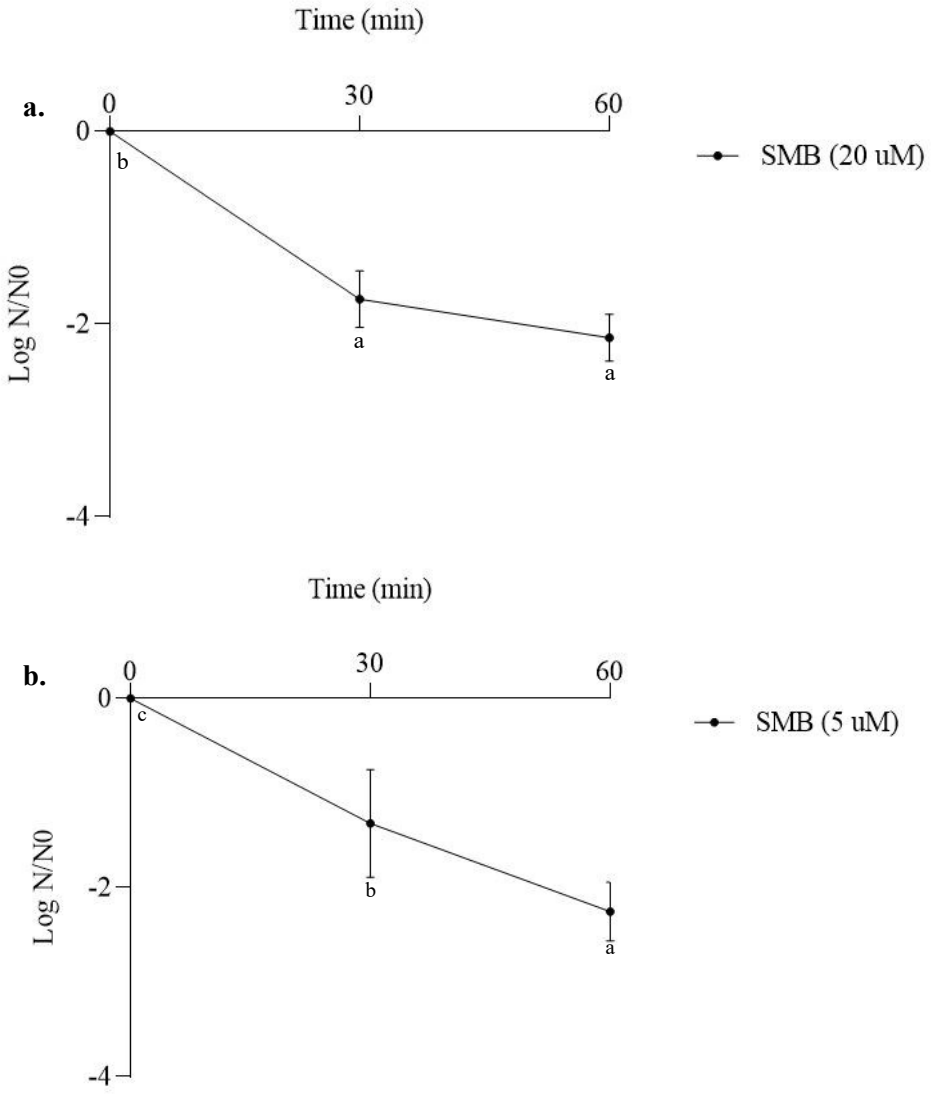


Figure 6.11. Mean ± standard deviations of biofilms of *E. coli* (**a.**) and *L. monocytogenes* (**b.**) growth in milk above a stainless steel surface. SMB (light-irradiated samples) represents the sample which consisted of the microbial biofilm suspension in PBS added with methylene blue (MB) at specific concentrations (5 μM or 20 μM). Different lowercase letters indicate a significant difference among the same MB concentration at different time points ($p<0.05$). The results are the average of three technical replicates and three biological replicates.

As anticipated, the results confirmed that Gram (+) bacteria (*L. monocytogenes*) were more susceptible to PDI treatment than Gram (-) bacteria (*E. coli*), as evidenced by the higher inactivation achieved with only one-quarter of the MB concentration (George et al., 2009).

However, when comparing the results to biofilms grown in culture media, the inactivation of biofilms formed in milk was lower for both bacterial species. This observation can be attributed to the binding of MB to milk components (fats, lipids, and proteins), which diminishes its availability as a PS for PDI. Furthermore, the higher concentration of divalent cations in milk, compared to PBS, likely reduced microbial inactivation by competing for surface adsorption sites, which is known to affect PDI efficacy.

As Galstyan & Dobrindt (2019) evidenced, PDT efficacy is affected by the fat content as well as the milk dilution. Also, the interactions between milk proteins and MB can affect the aggregation equilibrium and alter photophysical and photochemical pathways.

This study provides a useful exploration of PDI effectiveness in reducing biofilm contamination, specifically in food-related environments where biofilms are a significant concern. The choice of stainless steel coupons is particularly relevant for simulating the surfaces commonly found in food processing facilities.

An interesting result of the study is the examination of biofilm inactivation, which mimics the real-world challenge of eradicating bacterial biofilms in food production systems. Biofilms are notoriously difficult to treat, and the study's findings are valuable for understanding how PDI can be optimized in complex substrates like milk. Although the results show that biofilm inactivation in milk is less efficient than in simpler media, this opens avenues for future research to focus on improving the biofilm penetration and interaction of PS, potentially through new formulations or enhanced light delivery methods.

On the other hand, the observed reduced efficacy of PDI in milk compared to PBS underscores the complexity of applying this technique in food industries. The binding of MB to milk components, along with the interference of divalent cations, limits the PS availability and highlights a significant challenge for the practical application of PDI in food safety. Future research could explore strategies to mitigate these challenges, such as optimizing MB concentrations or enhancing its stability and availability in complex matrices. Additionally, understanding the specific interactions between milk proteins and MB could lead to more

effective PDI treatments for foodborne pathogens, ultimately making this technology more applicable for sanitization in food production environments.

6.5 Conclusions

The findings from this study highlight the effectiveness of MB as a PS for the PDI of *L. monocytogenes* and *E. coli* in both poor and rich nutrient substrates. The results demonstrate that Gram (+) bacteria, in both planktonic and biofilm forms, are more susceptible to PDI. However, the study also emphasizes the challenges posed by complex matrices like milk, where the presence of fats, proteins, and other components significantly impacts the effectiveness of PDI.

While the results are promising, a few points merit further exploration. First, while the study presents a clear comparison of MB concentrations and light doses, the impact of the specific milk components on the inactivation process could be more thoroughly investigated. The role of milk's fat content, proteins, and specific minerals (like calcium and magnesium) on MB aggregation and PS availability could be better understood. Additionally, the light penetration issue in opaque matrices, such as milk, was identified as a major limiting factor.

Moreover, although the study provides valuable data on the effects of MB in a food-related context, further research should assess the potential toxicity and safety implications of using MB in food environments, particularly when considering its aggregation or degradation in complex liquids. Investigating the interaction of MB with various types of food matrices (such as dairy, meat, or products) and how these interactions affect microbial inactivation could help optimize its application in real-world scenarios.

In conclusion, while the study provides valuable insights into the use of MB for PDI in food safety, more research into optimizing light delivery and understanding the interactions between PS and complex food matrices is essential for improving the practical application of this technology in food industry sanitization.

Chapter 7

Exploitation of a natural photosensitizer: Curcumin

7.1 Introduction

Curcumin (1,7-bis-4-hydroxy-3-methoxyphenyl-1,6-heptadiene-3,5-dione, **Figure 7.1**) is a natural compound extracted from the rhizomes of *Curcuma longa*, which has recently gained attention due to its photodynamic properties. Known for its anti-cancer effects and its ability to manage pathogen infections (Dias et al., 2020), curcumin has also been investigated for its potential as a photosensitizer (PS) in various studies (Aurum & Nguyen, 2019; Dias et al., 2020; Joshi et al., 2024; Xu et al., 2024).

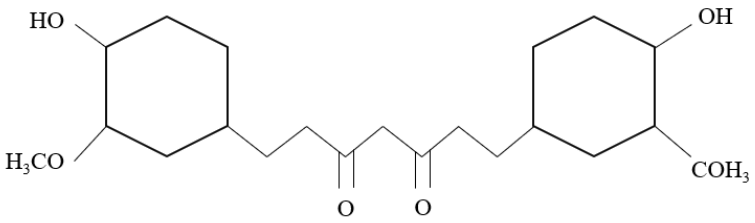


Figure 7.1. Structure of curcumin.

As a PS, curcumin is capable of absorbing light in the 350-450 nm range, becoming excited and generating reactive oxygen species (ROS). In the food industry, curcumin is used both as a colourant and a flavouring agent, and it is approved as a food additive (E100), ensuring its safety for consumption (Geralde et al., 2021; Glueck et al., 2017). A key advantage of curcumin is its Generally Recognized as Safe (GRAS) status, which, in combination with its photodynamic properties, makes it an attractive alternative to conventional sanitisers. The fact that curcumin is already widely used in food as a colourant and flavouring agent makes it a promising candidate for sanitization purposes, particularly as an alternative to more conventional and potentially harmful sanitisers. The use of a natural compound with both photodynamic properties and inherent safety is a significant advantage, especially in addressing the increasing consumer demand for "green" or sustainable food safety technologies.

This could address limitations related to food quality, operator safety, and the environmental impact of chemical disinfectants (De Oliveira et al., 2018). However, some challenges remain, such as its rapid metabolism and elimination, which may affect its effectiveness over time (Munir et al., 2022).

7.2 Aim of the study

This study seeks to evaluate the effectiveness of curcumin as a natural PS in a liquid substrate against two major foodborne pathogens, *L. monocytogenes* and *E. coli*, by testing its action under three different wavelengths within the BL spectrum (405nm, 420 nm and 450 nm).

7.3 Material and Methods

7.3.1 Microbial Strains and Culture Conditions

The strains used were *E. coli* DSMZ_8739 and *L. monocytogenes* DSMZ_7644, part of the University of Udine collection. The cell culture and the overnight preparation were done as described in **Chapter 2**, **paragraph 2.3.2**.

7.3.2 Blue Light Source

The BL light sources were described in **Chapter 2**, **paragraph 2.2.2**.

7.3.3 Curcumin solution preparation

The absorbance spectra of curcumin (Sigma-Aldrich, Milan, Italy) were done at 5 µM, 10 µM, and 20 µM in MeCN (**Figure 7.2**). It was weighted and, due to its poor solubility in aqueous solutions (Munir et al., 2022), it was dissolved in 1mL of Dimethyl sulfoxide (DMSO) to dissolve it. The final concentration was 500 µM.

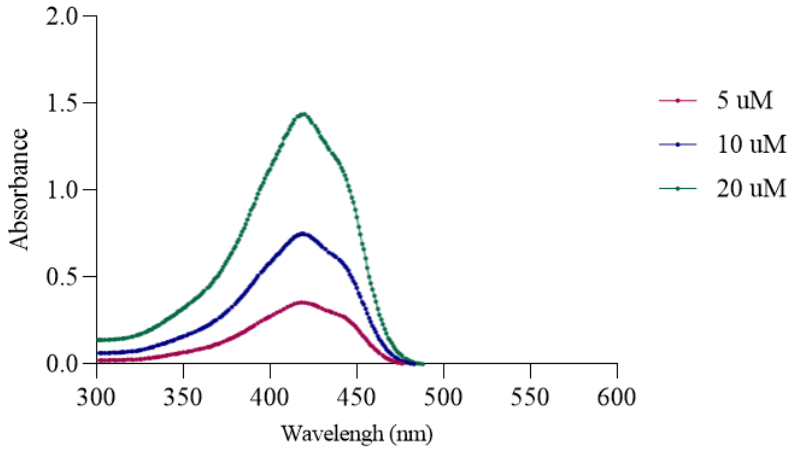


Figure 7.2. Absorbance spectra of Curcumin at different concentrations (5 µM, 10 µM and 20 µM) in methyl cyanide **(**MeCN).

7.3.4 Blue Light treatment

The bacterial strains, previously cultured on agar plates, were transferred to BHI broth and incubated overnight. Afterwards, they were washed three times with PBS, centrifuged at 13,000 *x g*, and serially diluted.

For the light treatment, a 48-well microtiter plate was used. Specifically, 4 wells were filled as follows: two wells contained the curcumin solution (0.5 µM) along with the microbial cell culture, adjusted to a concentration of $10^6/10^7$ CFU/mL, and PBS to reach a final volume of 2 mL. The other two wells contained only the cell culture solution, without curcumin (**Figure 7.3**). Of the four wells, two were exposed to blue light (BL): one containing curcumin (sample control, SC) and the other without curcumin (light control, LC). The remaining two wells were kept in the dark to serve as dark controls (with and without curcumin, DC). After the addition of curcumin, the microtiter plate was kept in the dark for 15 minutes with continuous agitation.

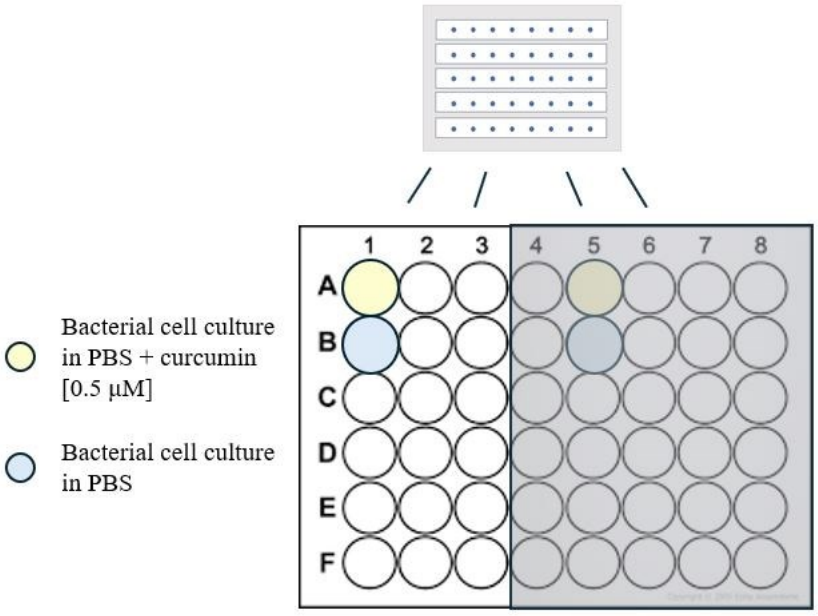


Figure 7.3. Experimental set-up of photodynamic inactivation treatment with curcumin: A1 and B1 wells were used as sample (SC) and light control (LC), respectively; A5 and B5 wells were used as dark controls (with and without curcumin, DC).

The microplate was then exposed with BL (405 nm, 420 nm and 450 nm) at 50 mW cm^{-2} for 5, 10, 15 and 30 min. During the experiment, the samples were kept in movement to guarantee a homogenous irradiation and oxygenation of all the samples (SC, LC and DC). Every time, samples were taken from each well, serially diluted and plated with the drop plate method.

During BL treatment, the temperature was monitored with a probe Checktemp 1 (HI98509, Hanna, Ronchi di Villafranca Padovana, Italy).

7.3.5 Data analysis

Results were expressed as CFU/mL and transformed in the logarithm CFU/mL. The Log (N/N0) were then calculated, where N is the log CFU/mL after the BL treatment and N0 is the log CFU/mL at time 0. The data were elaborated with Microsoft Excel and GraphPad Prism software (9.0.0) and represented as the mean of two biological replicates ± standard deviation (SD) and subjected to statistical analysis by IBM SPSS Statistics for Windows version 23.0 (IBM Corp., Armonk, N.Y., USA). The statistical methods used to determine the significant differences between the samples were One-way ANOVA ($p < 0.05$), Two-way ANOVA ($p < 0.05$) and post-hoc Tuckey-B test.

7.4 Results and Discussion

The microbial inactivation effect of BL, in combination with curcumin, emitted at a light dose of 0.90 J cm^{-2}, was assessed against *L. monocytogenes* (Gram +) and *E. coli* (Gram -) using wavelengths of 405 nm, 420 nm, and 450 nm. The results are shown in **Figure 7.4**.

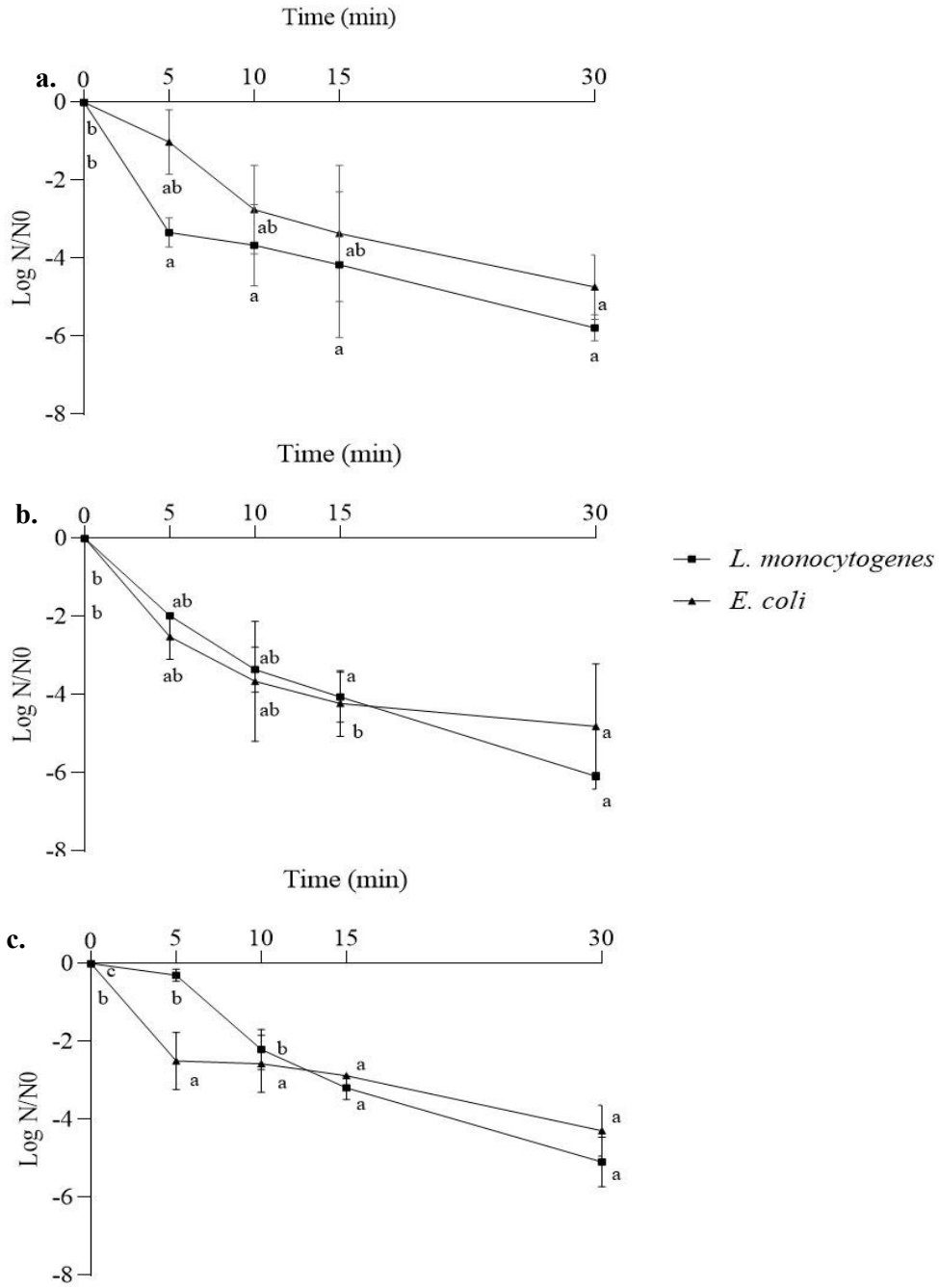


Figure 7.4. Microbial inactivation operated by BL emitted at **a.** 405 nm, **b.** 420 nm and **c.** 450 nm by using curcumin (0.5 μM) of *L. monocytogenes* (square) and *E. coli* (triangle). Lowercase letters in the same line indicate a significant difference by using the same wavelength at different times ($p < 0.05$). The results are the average of two technical replicates.

For both the microbes, the LC and the DC remained constant at 10^6-10^7 CFU/mL. For *E. coli*, the treatment with BL for 30 minutes and 0.5 μM curcumin resulted in a reduction of approximately -4 log with all three wavelengths. When comparing different treatment times, a significant reduction in the microbial count was observed in 30 minutes for all wavelengths, with 450 nm showing a significant reduction just after 5 min ($p < 0.05$). As shown in the graphs, 5 min of PDI determined a fast microbial reduction at all the wavelengths. Indeed, the different wavelengths did not show differences after 30 min ($p > 0.05$).

Considering *L. monocytogenes*, the same treatment conditions (30 minutes of BL and 0.5 μM curcumin) led to a reduction of approximately -5.50 log for 405 nm and 420 nm and -3.30 log for 450 nm. This result is coherent with curcumin absorption spectra (**Figure 7.2**), which exhibit a peak of absorption at 420 nm. Differently from what was observed for *E. coli*, the reduction was significantly different after 5 minutes of light treatment for 405 nm and 450 nm ($p < 0.05$), while in the case of 420 nm, it took 15 minutes. The low BL wavelengths determined a faster reduction in 5 minutes, while at 450 nm the inactivation became more accentuated between 5 and 15 minutes. After 30 minutes, the microbial reductions obtained at 405 and 420 nm were similar and were significantly different from the inactivation at 450 nm ($p < 0.05$).

Interestingly, despite the known higher susceptibility of Gram (+) bacteria to BL, the microbial responses to treatment observed in this study were comparable for both *L. monocytogenes* and *E. coli*. Comparing these results with the ones obtained by inactivating bacteria by exploiting endogenous PS-only (Chapter 2), the inactivation rate and trend are different. Specifically, the addition of curcumin in a low concentration allowed a drastic reduction of the required light dose to obtain similar or even more enhanced reductions. For both the tested pathogens, after 30 minutes the reductions by BL only were lower than -1 log, independently of the used wavelength. Therefore, the use of exogenous PS results in higher and faster microbial inactivation. Also, these observations may reflect the strain-dependent nature of curcumin's effectiveness, as noted in previous studies.

In both cases, the temperature increase was minimal (about 3-4°C on average, reaching a maximum of 23°C for *E. coli*), suggesting that temperature did not significantly influence the microbial inactivation.

Overall, the study found no significant factor - whether bacterial strain, wavelength, or their combination - that strongly influenced microbial inactivation ($p > 0.05$). These results align

with findings from other studies (De Oliveira et al., 2018; Stura et al., 2023), which reported slightly less efficacy of BL and curcumin against *E. coli* compared to Gram (+) bacteria like *S. aureus* or *L. innocua*. This minimal difference in efficacy was attributed to factors like inoculum size, curcumin formulation, and experimental conditions. Other studies (i.e., Tyagi and Malik, 2012) have suggested that both Gram (+) and Gram (-) bacteria experience damage to their cell membranes when treated with BL and curcumin. Additionally, previous research has highlighted the different susceptibilities of Gram (+) and Gram (-) bacteria to curcumin and BL due to differences in cell wall composition and the presence of a lipopolysaccharide layer (Penha et al., 2017; Xu et al., 2024). A recent study by Laneri et al. (2023) underlined the photo behaviour of curcumin when encapsulated in different host media. Interestingly, they observed that curcumin predominantly exists in the diketo tautomeric form due to favourable intermolecular hydrogen bonding with water molecules in the hosts. This form promotes the formation of curcumin-derived ketyl radicals, which, upon exposure to oxygen, undergo oxidation, leading to the generation of peroxyl radical species. Consequently, curcumin is inefficiently quenched by molecular oxygen, preventing the production of singlet oxygen $^1O_2$. As a result, the photoinactivation of bacterial cells may not be attributed to the action of $^1O_2$.

One potential factor influencing the results of this study is the use of monochromatic LED, which emits light at specific wavelengths. It is hypothesized that using a broad-spectrum LED might not excite the PS (curcumin) as effectively, which could alter the results. Further investigation into the type of LED used and the mechanisms underlying curcumin's photodynamic action would be beneficial.

7.5 Conclusions

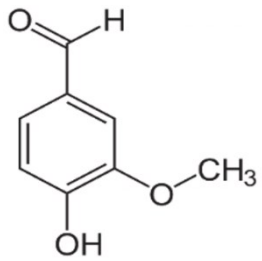
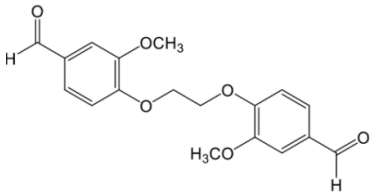
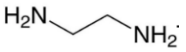
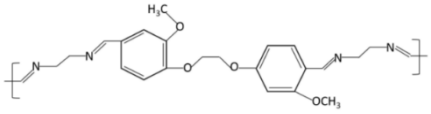
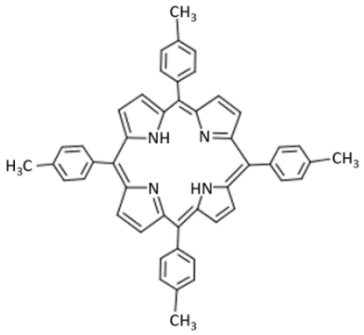
This study provides a preliminary evaluation of the efficacy of curcumin and BL in inactivating two foodborne pathogens, *L. monocytogenes* and *E. coli*, across different wavelengths. The results are generally consistent with poor existing literature, which suggests that Gram (+) bacteria are more susceptible to BL, but the similar inactivation rates observed for both bacteria in this study raise interesting questions about the strain-dependent activity of curcumin as well as the $^1O_2$ independent photoinactivation.

A notable strength of the study is the inclusion of multiple wavelengths, which helps elucidate the potential impact of light exposure on curcumin's photodynamic effects. The methodology is also well-controlled, with careful monitoring of temperature increases and the use of both light and dark controls to rule out non-specific effects. The study would benefit from a comparison with broad-spectrum light sources to better understand the full potential of curcumin in photodynamic treatments.

Another valuable aspect is the acknowledgement of various factors that could influence microbial inactivation, such as the inoculum, curcumin formulation, and experimental conditions. This reflects a holistic approach, although future studies could further refine these factors to better isolate the contributions of each. Additionally, the results highlight that while Gram (+) bacteria are generally more susceptible to BL, there are still variances in inactivation efficacy that suggest other underlying factors (possibly the bacterial strain, the precise formulation of curcumin, or even the method of light application) that deserve further exploration.

Chapter 8

Microbial inactivation by Photoactive Materials

Number	Chemical structure	Name
1		4-idrossi-3-metossibenzaldehide
2	**$BrCH_2CH_2Br$**	1,2-dibromoetano
3		4-4'-(Etan-1,2-dibis(ossi))bis(3-metossibenzaldeide)
4		Etan-1,2-diammina (Ethylenediamine, EDA)
5		Valpol
6	 **6**	Meso-Tetra (4-methylphenyl) porphyrin (4MeP)

Corresponding numbers, chemical structure and nomenclature of the chemical compounds present in the text.

8.1 Introduction

In recent years, there has been a growing interest in eco-sustainable and green technologies for decontaminating and sanitizing surfaces, particularly in the food industry. This has led to the development of antimicrobial surfaces and coatings, commonly referred to as antimicrobial materials or coatings (AMC) (Coma, 2008). These innovative solutions are designed to prevent and control microbial contamination along the food production chain, reducing the need for chemical disinfectants and the associated costs of both the chemicals and labour required for traditional cleaning methods (Van Dijk et al., 2022).

Such antimicrobial surfaces are particularly beneficial in food production environments, where they can be applied to machinery and equipment that automatically clean themselves after each cycle (Gnanasekar et al., 2023). These materials are designed to be active against a broad range of pathogens, including bacteria, viruses, moulds, and yeasts. They are classified based on their functional properties or the mechanisms through which they exert antimicrobial effects (Mesquita et al., 2018).

Various materials can serve as support for these antimicrobial agents, such as metal nanoparticles (e.g., gold, silver, platinum), silicon, hydrogels, and biopolymers. Previous studies have focused on immobilizing antimicrobial agents in both natural supports, such as bacterial cellulose or chitosan, and synthetic ones, such as polystyrene, dipyrromethane, or polyethylamine (Comuzzi et al., 2020; Henke et al., 2020; Jia et al., 2019; Li et al., 2020; Ning et al., 2019).

The growing demand for green, eco-sustainable solutions, which may also involve the use of waste products, has driven the focus toward natural supports. These materials are particularly appealing for the food industry, where non-toxicity and biodegradability are essential. Natural supports offer a sustainable alternative while maintaining the necessary functional properties for effective microbial inactivation (Mesquita et al., 2018; Wang et al., 2022). This research into sustainable materials aligns with the increasing need to balance technological innovation with environmental responsibility.

4-Hydroxy-3-methoxybenzaldehyde ($C_8H_8O_3$), commonly known as Vanillin (**Figure 8.1**), is a phenolic compound that contains three functional groups: an aldehyde, an ester, and a phenol. It is widely used in various industries, including pharmaceuticals, chemicals, food, and

cosmetics (Liu et al., 2023). In addition to its aromatic properties, Vanillin has demonstrated antibacterial and antioxidant activities, which make it a potential candidate for use as a biological preservative (Converti et al., 2010). Its ability to inhibit microbial growth and its oxidative stability have prompted research into its application in preserving food and extending the shelf life of products. This makes Vanillin a versatile compound with a broad range of uses, from flavouring agents to potential solutions for microbial control.

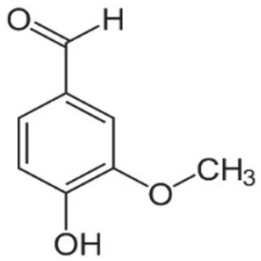


Figure 8.1. Vanillin molecule structure.

Vanillin is found in several plant species, including *Vanilla tahitensis*, *Vanilla pompona*, and most abundantly in *Vanilla planifolia* (Xu et al., 2023). However, the natural production of vanillin is expensive, with prices ranging from $1,200 to $4,000 per kilogram. As a result, natural vanillin production meets less than 1% of global demand (Calva-Estrada et al., 2018). To meet the high demand, about 85% of the worldwide vanillin supply is derived from petrochemical sources, while the remaining 15% is produced through the depolymerization of lignin (Fitzgerald et al., 2005). Lignin, the second most abundant biopolymer in nature after cellulose, is found in the cell walls of plants and can be extracted from lignocellulosic biomass (Taher et al., 2023; Tao et al., 2020). To obtain vanillin from lignin, a chemical process involving oxidants at high temperatures and pressures in an alkaline environment is used to break down the lignin structure, followed by extraction and purification of the resulting compounds (Liu et al., 2023; Martău et al., 2021). This method not only offers a renewable source of vanillin but also contributes to the concept of "waste-to-value," utilizing by-products from the pulp and paper industry and other lignocellulosic materials.

The development of polymeric vanillin-based materials is a promising approach for creating high-performance materials derived from biological waste matrices, contributing to sustainability goals (Qiang et al., 2023). To enable activation by light, a PS must be incorporated, which absorbs light and generates reactive species upon irradiation. Porphyrins

are naturally occurring molecules in bacterial cells, or they can be synthetically produced. Meso-Tetra (4-methylphenyl) porphyrin (4MeP), known for its strong π–π interactions, is especially suitable for conjugating with nanomaterials or biopolymers, enhancing stability and photodynamic efficiency (Managa et al., 2019).

8.2 Aim of the study

The aim of this study was to evaluate the microbial inactivation capacity of BL treatment against *Escherichia coli* and *Listeria monocytogenes* using 4MeP porphyrin at various concentrations (0%, 5%, and 10%) immobilized within a biopolymer, Valpol, synthesized from vanillin under solid-state conditions by Dr. C. Comuzzi's research group at the University of Udine. The biopolymer was irradiated with different BL wavelengths (405 nm, 420 nm, and 450 nm), and its inactivation efficacy was assessed on both the planktonic and biofilm forms of the target microorganisms.

8.3 Material and Methods

8.3.1 Experimental set-up

The activities of this chapter were done as represented in **Figure 8.2**.

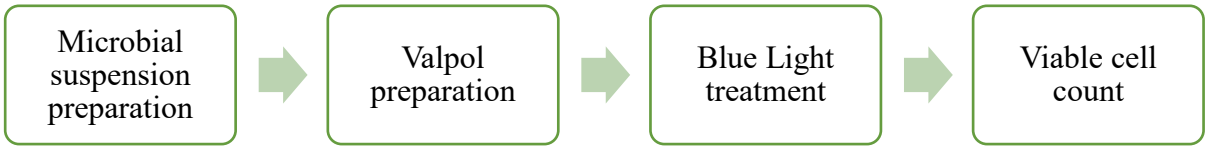


Figure 8.2. Scheme of the experimental activities.

8.3.2 Microbial Strains and bacterial cell culture preparation

For this study, *Escherichia coli* DSMZ_8739 and *Listeria monocytogenes* DSMZ_7644, both strains from the collection of the Department of AgriFood Science, Animal, and Environmental Department at the University of Udine, were used. The cell culture and the overnight preparation were done as described in Chapter 2, paragraph 2.3.2.

8.3.3 Material preparation

The preparation of the vanillin polymer, to which later the PS (4MeP) was added, is reported in the following sections.

8.3.3.1 Preparation of the vanillin dimer

10.0 g (65.7 mmol) of vanillin (**1**) was added to a flask under magnetic agitation, at which 40 mL (37.92 g, 518.8 mmol) of *N,N*-dimetilformammide anhydrous (DMF) were added. Subsequently, 5.68 mL (12.38 g, 65.8 mmol) of 1,2-dibromoetano (**2**) and 18.16 g (131.4 mmol) of potassium carbonate of anhydrous potassium (K_2CO_3) were added. The system was then hermetically closed with a silica cap and the blend was left to react at 80°C for 24h (**Figure 8.3**). After 24h, 400 mL of deionized water was added to the flask, which was then kept in refrigerated conditions for 24h to let the crystallization. The result was the 4-4'-(Etan-1,2-dibis(ossi))bis(3-metossibenzaldeide), the vanillin dimer (**3**).

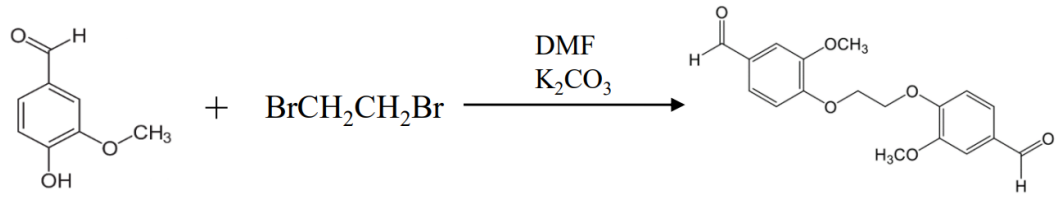


Figure 8.3. Dimer of anillin formation.

The precipitate was filtered, washed with deionized water and dried in a Fisher gun (Büchi TO-50, Cornaredo, Italy) in the presence of phosphoric anhydride (P_2O_5) at 60°C for 1h. The sample was then re-crystalized in acetonitrile (MeCN). For this reason, for every gram of **3** to re-crystalized, 5.9 mL of MeCN were added. The final suspension was heated to 100°C for 20 min to dissolve **3**. Later, the solution was cooled down to room temperature and the final product was filtered by several washed with MeCN and dried in a Fisher gun with the presence of P_2O_5 at 60°C for 1h. The yield was ca. 85-90%.

8.3.3.2 Preparation of Valpol material

In a flask under magnetic agitation, 6.19g (15 mmol) of **3** and 468.75 (617.81 g, 7.3 mmol) of dichloromethane (CH_2Cl_2) were added. 1.25 (15 mmol) of ethylenediamine (**4**) (EDA) was added to the flask and the solution was let react for 3 days at room temperature. The precipitate was then filtered and washed with dichloromethane. Then, the sample was dried in a Fisher gun with the presence of P_2O_5 at 60°C for 1h. The polymer, Valpol (**5**), was obtained with a yield of ca. 65-70% (**Figure 8.4**).

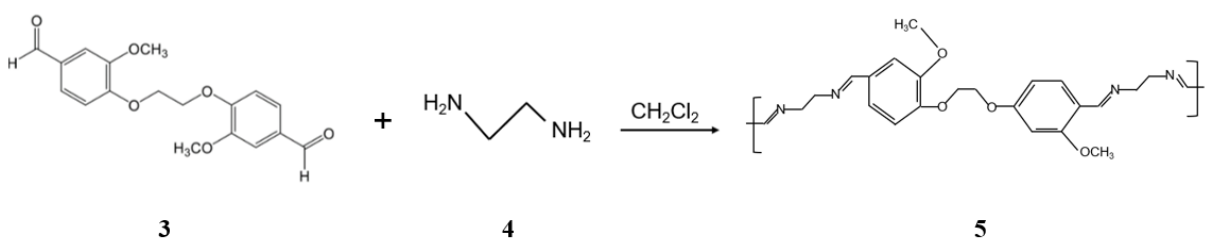


Figure 8.4. Reaction of Valpol preparation.

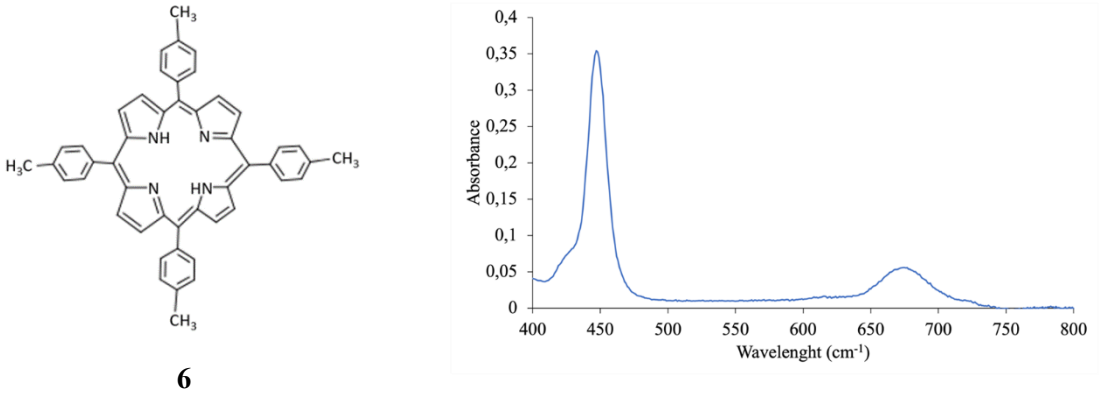
8.3.4 Synthesis of the photoactive material

8.3.4.1 Pretreatment of Valpol for the preparation of composite blends

1 g of **5** was ground, put in a crystalliser, suspended in 10 mL of dimethyl sulfoxide (11 g, 140.8 mmol) (DMSO) and kept under magnetic stirring at 100°C for 10 min. Then, the obtained suspension was transferred in a Falcon, added with 10 mL of deionized water and centrifuged (Centrifuge 5804 R, Eppendorf, Milan, Italy) at 24°C and 4000 *x g* for 10 min. The pellet was washed with 2x 10 mL of deionized water, separated and died at 70°C for 3-4 days. The result was approximately 11 g of Valpol MeP 0% (0% of porphyrin). The yield was > 99%.

8.3.4.2 Preparation of composite blends to obtain active materials

The active material preparation was done by adding the photosensitizer meso-Tetra (4-methylphenyl) porphyrin (4MeP) (**6**) (**Figure 8.5**) to every 1 g of **5**. Two powder blends were prepared by adding 0.05 g (5%) and 0.1 g (10%) of **6** to every 1g of **5**. After being ground, the blends undergo the same procedure previously described obtaining, at the end, 1 g of each active Valpol powder (yield > 99%), named Valpol 4MeP 5%, the one with the 5% of porphyrin, and 4MeP 10%, the one with 10% of porphyrin.



6

Figure 8.5. Meso-Tetra (4-methylphenyl) porphyrin (4MeP) structure and its UV-Vis spectra.

8.3.4.3 Preparation of polymeric material tablets

0.03 g of each 0%, 5% and 10% blend were placed in a circular die (Ø= 10 mm) of a hydraulic press (Specac, Orpington, UK) and pressed with 10 tons weight for 2 min, obtaining circular tablets of ca. 1 mm of diameter and 0.2 mm of thickness. The tablets were then placed in the anti-adherent paper and heated in an oven (Memmert, Venice, Italy) at 210 °C for 4 min,

obtaining polymeric material sheets with a glassy aspect. Finally, materials were kept at -18°C until their usage.

8.3.5 Blue Light source

The BL light sources used are described in **Chapter 2**, **paragraph 2.2.2**.

8.3.6 Blue Light Treatment

Before starting each test, the voltage of the lamps and the irradiance were set up (**Table 8.1**): irradiance was measured using a photo radiometer HD2302.0 coupled with a radiometric probe LP 471 RAD (Delta OHM, Padua, Italy).

Preliminary tests were done to establish the voltage and irradiance conditions at which the microbial concentration of the samples posed on the Valpol 4MeP 0% remained constant (about 10^6 CFU/mL) after 30 and 60 min. Considering this, Valpol 4MeP 0% was used as a control.

Table 8.1. Parameters for blue light treatment (voltage, irradiance, dose) applied to the tested bacteria.

Microbe	Voltage (V)	Irradiance (W/cm^2)	Dose (D) (J/cm^2)	
			30 min	60 min
E. coli	2.5	0.01	18	36
L. monocytogenes	1.0	0.003	5.4	10.8

8.3.7 Photodynamic Inactivation of microorganisms on Valpol material at different 4MeP concentrations

Valpol with different 4MeP concentrations (0%, 5% and 10%) were defrosted at room temperature in the dark for 20 min and washed with deionized water before being used. For each microbe, Valpol with all the 4MeP concentrations and all the wavelengths (405 nm, 420 nm and 450 nm), were used (**Figure 8.6**).

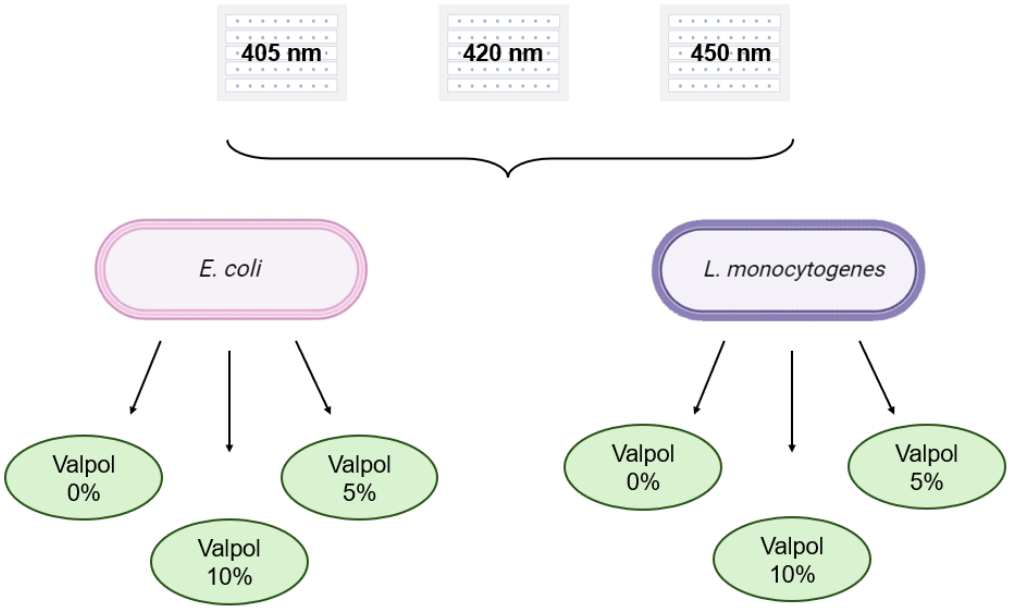


Figure 8.6. Test conditions of the photodynamic treatment. *E. coli* and *L. monocytogenes* were seeded on the Valpol 4MeP at three different concentrations (0%, 5% and 10%) and treated with Blue Light at 405 nm, 420 nm and 450 nm.

From the bacterial suspension, 50 µL of bacterial suspension was placed above each Valpol tablet. One sample (**Figure 8.7. A**) was used to confirm the microbial concentration for the experiment. The procedure involved placing the material in a sterile Falcon tube containing 3 mL of MRD and 5/6 sterile glass beads to detach the biofilm from the material (Sigma-Aldrich, Milan, Italy). The sample was then homogenized and serially diluted. Quantification was performed by plating serial dilutions onto Plate Count Agar (PCA, Oxoid, Basingstoke, United Kingdom) and incubating the agar plates at 37°C for 24 hours. The final cell concentration for all samples was determined to be 10^6 CFU/mL.

The remaining three Valpol tablets with microbial samples were left to dry, allowing for the adhesion of the material and microbes (**Figure 8.7. B**). The average drying time for the *E. coli* samples was 54.2 ± 6.49 minutes, while for the *L. monocytogenes* specimens, it was 69.9 ± 7.09 minutes.

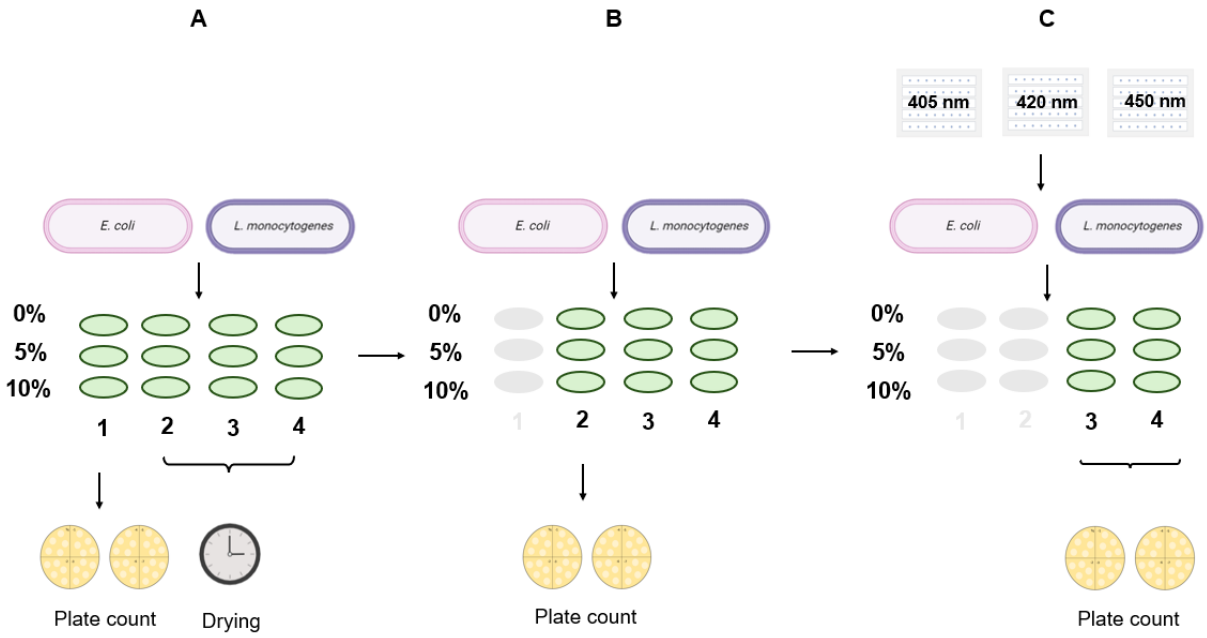


Figure 8.7. Experimental set-up of samples of *E. coli* and *L. monocytogenes* on Valpol 4MeP (0%, 5%, 10%) with 405 nm, 420 nm and 450 nm.

The cell viability of the second sample (**Figure 8.7. B**) was assessed after drying to determine if the microbial concentration remained unchanged following the drying process. The results indicated that the final cell concentration remained stable at approximately 10^6 CFU/mL.

The two remaining samples underwent BL treatment for 30 and 60 min, respectively, at 405 nm, 420 nm and 450 nm, for both microbes (**Figure 8.7. C**). After BL treatment, the viability of the samples was assessed through cell viable count on PCA plates. Dark controls were included by placing the samples under the BL lamp but covering them with foil to ensure they remained in the dark. This helped assess any possible changes in microbial concentration not attributed to the BL treatment.

To determine whether the efficacy of Valpol with 5% and 10% 4MeP was due to the BL action, an additional control test was conducted. Microbial samples were added to Valpol materials containing all 4MeP concentrations and kept in dark conditions for the same treatment times (30 min and 60 min, respectively). This allowed for the assessment of whether the microbial concentration remained stable at room temperature in the absence of BL exposure.

Throughout the BL treatment, the temperature was monitored for all wavelengths using a probe (Hanna, Romania).

8.3.8 Photodynamic Inactivation of microorganisms on glass

Glass tests were done on glass coverslips, 20 x 20 mm (Menzel-Gläser, Germany), previously sterilized. The procedure for specimens' preparation and treatment was the same as described in **paragraphs 2.2** and **2.6**.

8.3.9 Microbial Biofilm

8.3.10 Biofilm formation

For biofilm formation, an overnight culture was prepared as described in **paragraph 2.2**. The microbial culture was then resuspended in Luria Bertani Broth (LB Broth, VWR International, Belgium) to achieve a concentration of approximately 10^6 CFU/mL, as determined through viable cell count.

In sterile Petri dishes, four glass coverslips and four Valpol tablets at varying concentrations (0%, 5%, and 10%) were placed (**Figure 8.8**). Following this, 10 mL of the bacterial suspension was added to each dish, and the plates were incubated for 5 days at 30°C under orbital agitation. To maintain the biofilm growth, the medium was refreshed every 3 days by removing 6 mL of the spent broth and replacing it with 6 mL of fresh broth.

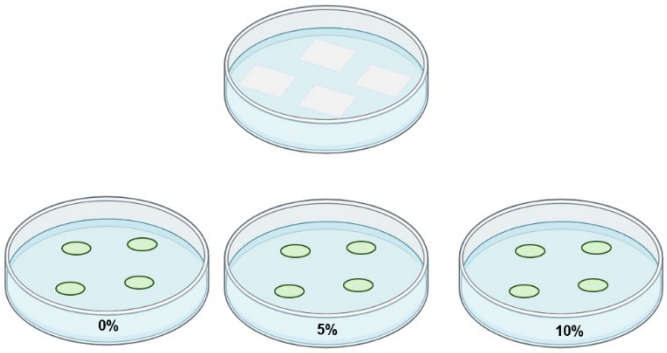


Figure 8.8. Biofilm preparation. Biofilms were formed in glass coverslip and Valpol 4MeP (0%, 5% and 10%).

8.3.11 Biofilm Blue Light treatment

After 5 days of incubation, the glass coverslips and Valpol samples were washed twice with 0.9% NaCl solution to remove non-adherent cells. The initial biofilm concentration on glass and Valpol was established by microbial cell count immediately after the washing step, which resulted in approximately 10^7 CFU/mL for *E. coli* and 10^6 CFU/mL for *L. monocytogenes*. To quantify the biofilm, the samples (glass, Valpol 4MeP 0%, Valpol 4MeP 5%, and Valpol 4MeP 10%) were placed in sterile Falcon tubes containing 3 mL of MRD and 5/6 glass beads. The samples were then homogenized to detach the biofilm, followed by quantification using plate count methods.

The biofilms were treated with BL at wavelengths of 405 nm, 420 nm, and 450 nm. One glass coverslip and one Valpol sample for each 4MeP concentration were placed in sterile Petri dishes and exposed to BL under the specified voltage and irradiance conditions (described in **paragraph 8.5**) for 2 hours. The final BL doses were 72 J cm^{-2} for *E. coli* and 21.6 J cm^{-2} for *L. monocytogenes* (Figure 8.9). The efficacy of the BL treatment was assessed by determining the cell viability through plate count.

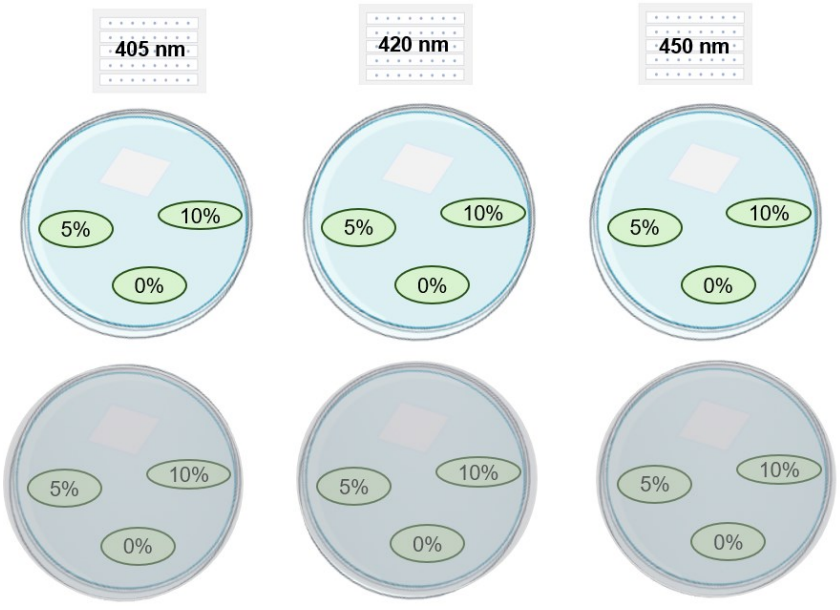


Figure 8.9. Treatment of biofilms formed in glass coverslip and Valpol 4MeP (0%, 5% and 10%).

8.3.12 Reutilisation of the Valpol material

For planktonic cells, following the recovery of the specimens, all the Valpol tablets were washed as follows: each tablet was immersed in alcohol for 10 minutes, followed by immersion in deionized water for 20 minutes. After washing, the tablets were dried and stored at -18°C. In the case of biofilms, the washing procedure was similar, but the exposure times were longer: 20 minutes in alcohol and 40 minutes in deionized water.

For planktonic cells, after the washing step, the material was used a second time following the same procedure described in paragraphs 8.3.6 and 8.3.7.

To evaluate whether any residual microbes remained on the tablets after the washing process, washed Valpol tablets, which were then stored at -18°C, were thawed and placed in a sterile Falcon tube containing 3 mL of MRD and 5/6 glass beads. The tablets were subsequently homogenized, and the microbial concentration was determined through viable cell count.

8.3.13 Data analysis

Results were expressed as CFU/cm^2 and transformed in the logarithm CFU/cm^2. The Log (N/N0) were then calculated, where N is the log CFU/cm^2 after the BL treatment and log CFU/cm^2 is the initial microbial concentration. The data were elaborated with Microsoft Excel and represented as the mean of two biological replicates ± standard deviation (SD) and subjected to statistical analysis by IBM SPSS Statistics for Windows version 23.0 (IBM Corp., Armonk, N.Y., USA). The statistical methods used to determine the significant differences between the samples were One-way ANOVA ($p \leq 0.05$), Two-way ANOVA ($p \leq 0.05$) and post-hoc Tuckey's test.

8.4 Results and Discussion

In this study, the capability of a polymer synthesized from vanillin and added with the 4MeP porphyrin at different concentrations (0%, 5% and 10%) to inactivate microbes was assessed when activated by BL at different wavelengths (405 nm, 420 nm and 450 nm). The tested microbial species were *E. coli* and *L. monocytogenes*, in their planktonic and biofilm form.

8.4.1 Characteristics of the Valpol material

After the heating phase during the preparation, Valpol 4MeP 0% diameter was reduced by 20%, from 10.0 mm to 8.00 mm, due to the shrinking phenomena (**Figure 8.10**). Differently, in the case of Valpol 4MeP 5% and Valpol 4MeP 10%, the shrinking phenomena was not observed, probably due to the presence of the porphyrin, which interferes with the assembly of the Valpol chains. The shrinking phenomena occur as a consequence of the incrementation of the internal energy of the oriented system, possibly caused by an increase of the temperature or by a decrease of intermolecular interactions (Trznadel & Kryszewski, 1992).

Also, the thickness was modified after the cooking step. Starting from 0.20 mm, the thickness was 0.74 mm, 0.48 mm and 0.29 mm, for Valpol 4MeP 0%, Valpol 4MeP 5% and Valpol 4MeP 10%, respectively. These results are in accordance with the diameter's data since the material by reducing its surface increases its thickness. Other changes in the materials that could be noticed are the darker colour and the glassy appearance, both due to the heat treatment.

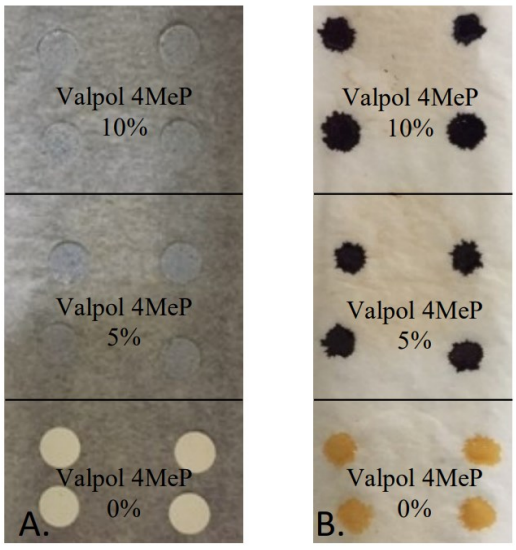


Figure 8.10. Before (A.) and after (B.) heating treatment Valpol's tablets.

The use of DMSO was essential for the Valpol tablets, as it served as the solvent in this study to mix the powders (Valpol and 4MeP), given their low solubility in water. It's noteworthy that a 2% concentration of DMSO is toxic to microorganisms and reduces cell vitality in other cell types (Lee & Park, 2017; Verheijen et al., 2019). To ensure safety for human use, including food applications, the final concentration must be below 0.01% (v/v) (Gallardo-Villagrán et al., 2022). In this study, a washing step with deionized water followed DMSO addition for two purposes: first, to fully remove the solvent, as it dissolves in water; and second, to promote the formation of porosities and channels within the material. These structures, formed during cooking as water evaporates, are essential for porphyrin activation. The material was heat-treated at 210 °C, which could make the evaporation of any remaining DMSO, given its boiling point of 189 °C.

For all these reasons, it is possible to state that the final concentration of DMSO inside the Valpol material is lower than 0.01% (v/v) and it could be used for food applications, i.e. packaging or food contact surfaces. In addition, it was possible to exclude any possible antimicrobial activity operated by the DMSO, and the results could be attributed to the activation of 4MeP inside the material operated by BL.

8.4.2 Photodynamic inactivation of *E. coli* with Valpol at different porphyrin (4MeP) concentrations

The antimicrobial efficacy of Valpol at 0% concentration, both new and reused after one application, was evaluated following BL treatment at intervals of 30 and 60 minutes using three wavelengths (405 nm, 420 nm, and 450 nm). Results indicated a minimal and statistically non-significant microbial reduction ($p > 0.05$) across all wavelengths, achieving inactivation levels below 1 log unit, likely attributable to physiological adaptations in the microbial cells.

For all the 4MeP concentrations tested (0%, 5%, 10%) inside the Valpol, new or reused, the controls remained constant at 10^6 CFU/mL. In the case of new Valpol4MeP 5%, BL treatment at 405 nm proved the most effective wavelength after 30 minutes, yielding a microbial reduction of -1.79 ± 0.64 log. Extending the treatment to 60 minutes led to *E. coli* inactivation exceeding 2.00 log for all wavelengths tested, with 420 nm producing the highest reduction of -3.30 ± 0.13 log (**Table 5.2.a**). Upon reusing the Valpol 4MeP5% material post-washing (see **Paragraph 2.8**), the microbial inactivation across all three wavelengths improved further; specifically, 420

nm yielded reductions surpassing -3 log and -4 log at 30 and 60 minutes, respectively (**Table 5.2.b**). The inactivation performance of reused materials differed significantly from new materials across all wavelengths (405 nm; $p= 0.036$; 420 nm; $p= 0.041$; 450 nm; $p= 0.001$).

A similar pattern was observed with Valpol 4MeP10%, where 405 nm produced the highest microbial reduction after 30 and 60 minutes. However, when combined with 450 nm, Valpol 4MeP10% demonstrated less than 1 log reduction after 60 minutes. Reuse of Valpol 4MeP10% resulted in 420 nm providing optimal microbial inactivation, achieving over -4 log reduction within 60 minutes. Statistically significant differences were also noted in microbial inactivation between new and reused materials for 420 nm ($p= 0.002$) and 450 nm ($p= 0.026$). These results can be explained by the fact that 4MeP exhibits an absorption peak at 418 nm, indicating that its photosensitizing (PS) efficacy is maximized when excited by wavelengths near this value, specifically 405 nm and 420 nm, which facilitate interaction with molecular oxygen to generate reactive oxygen species (ROS) as described by Long et al. (2008).

Under the applied dose conditions, *E. coli* samples irradiated with 36 J cm^{-2} across all three wavelengths exhibited reductions below 3.5 log with new Valpol 4MeP (5% and 10%) and below 5 log when the material was reused. Comparatively, Bhavya and Umesh Hebbar (2019) demonstrated that irradiation of *E. coli* at 462 nm with 12.96 J/cm^2 in the presence of varying curcumin concentrations achieved higher microbial reductions, ranging from 2.75 log CFU/mL to 5.65 log CFU/mL. These findings suggest that microbial inactivation is influenced by variables such as PS type, wavelength, dose, and lamp characteristics, which differed from those used in this study.

The reuse of Valpol materials generally enhanced microbial reduction probably due to the formation of pores and canals in the material which favour the exposure of the PS to the light. For instance, Valpol 4MeP10% treated with 420 nm achieved a reduction of -1.78 log in its first use and -4.18 log upon reuse. Comuzzi et al. (2022) also explored the reusability of similar PS materials (4PyP5-OA20 and 4NH2P5-OA20) across four cycles, finding a decline in antimicrobial activity with repeated uses, contrary to the current study's findings. However, since the material in this study was only reused once, further investigation is warranted to determine the potential longevity of PS activity through multiple uses and whether PS reloading, as demonstrated by Comuzzi et al. (2020), could sustain antimicrobial effectiveness over extended applications.

Table 8.2. Microbial inactivation results (log N/N0) of *E. coli* by irradiating at 405 nm, 420 nm and 450 nm Valpol 4MeP (0%, 5%, 10%) after 30 and 60 min. **a.** new material and **b.** reused material a second time. Different lowercase letters indicate significant differences ($p < 0.05$) between the same Valpol 4MeP% at the same time irradiated with the different wavelengths. The results are the average of two biological replicates. *Indicate a significant difference between the same sample Valpol 4MeP%, the same wavelength at different times (30 min, 60 min).

a.	**New Valpol**					
	Valpol 4MeP 0%		**Valpol 4MeP 5%**		**Valpol 4MeP 10%**	
	30 min	60 min	30 min	60 min	30 min	60 min
405 nm	-0.56±0.29a	-0.90±0.11a	-1.79±0.64a	-2.50±0.61b*	-2.19±0.99a	-2.59±0.94a*
420 nm	-0.58±0.16a	-0.58±0.16a	-0.73±0.26b	-3.38±0.13a*	-1.30±0.87a	-1.78±1.00a*
450 nm	-0.39±0.52a	-0.80±0.14a	-1.23±0.87ab	-2.44±0.45b	-0.43±0.07b	-0.66±0.17b
b.	**Reused Valpol**					
	Valpol 4MeP 0%		**Valpol 4MeP 5%**		**Valpol 4MeP 10%**	
	30 min	60 min	30 min	60 min	30 min	60 min
405 nm	-0.42±0.00a	-0.67±0.31a	-2.23±0.54b	-3.08±0.09b*	-1.80±0.56a	-2.94±0.56b*
420 nm	-0.42±0.00a	-0.67±0.31a	-3.23±0.24a	-4.10±0.26a*	-2.18±0.90a	-4.18±0.32a*
450 nm	-0.37±0.15a	-0.67±0.43a	-2.60±0.52ab	-3.90±0.11a	-1.77±0.33a	-2.98±0.25b*

Legend: average log N/N0 ± standard deviation

It is noteworthy that microbial inactivation did not increase linearly with higher concentrations of 4MeP in Valpol. Instead, extended exposure (60 minutes) consistently enhanced microbial reduction. Specifically, doubling the porphyrin concentration did not result in a proportional increase in E. coli inactivation across all three wavelengths. Castro et al. (2019) reported similar findings using a photoactive material (PHEMA-co-Porph) containing varying concentrations of

5,10,15,20-tetrakis(pentafluorophenyl)porphyrin (10, 20, and 40 μM), which showed no significant differences in microbial inactivation across concentrations.

Conversely, other studies have identified a linear relationship between PS concentration and microbial inactivation (Gerba et al., 1977; Rossi et al., 2012). Rincón and Pulgarin (2003) observed that increasing TiO_2 concentration from 0.025 g/L to 1 g/L proportionally increased microbial inactivation rates, while concentrations above 1 g/L did not yield further enhancement. These findings suggest a threshold concentration beyond which additional PS does not improve the inactivation rate (Thandu et al., 2015). Castro et al. (2019) also noted that excessive PS concentrations might impede light penetration, reducing singlet oxygen formation and, consequently, antimicrobial efficacy.

Furthermore, the substrate supporting the porphyrin affects PS bioavailability. Wang et al. (2022) incorporated PS within a film, demonstrating increased E. coli inactivation with higher PS concentrations; however, variations in substrate chemical composition influenced inactivation effectiveness.

In this experiment, slight temperature increases (3°C) were observed in dark controls exposed to BL for 60 minutes. This temperature rise did not impact microbial counts, which remained steady at approximately 10^6 CFU cm^{-2}, confirming that changes in microbial concentration were attributable solely to BL exposure. Additionally, Valpol tablets with various 4MeP concentrations in dark conditions showed no changes in microbial concentration over 30 and 60 minutes, remaining around 10^6 CFU cm^{-2}, indicating that Valpol alone exhibited no inherent bactericidal effect.

For comparative purposes, the study also evaluated microbial inactivation on a glass surface, known for its limited support of microbial growth (Li & Logan, 2004). As reported in **Table 8.3**, BL treatment on the glass surface produced no significant change in microbial concentration after both 30 and 60 minutes of exposure.

In this study, BL treatment alone on bacteria placed on glass surfaces showed no microbial inactivation. Similarly, no reduction in microbial concentration was observed with Valpol 4MeP at 0% concentration. Conversely, exposure of Valpol 4MeP at 5% and 10% concentrations to BL effectively reduced *E. coli* populations, demonstrating that higher 4MeP concentrations enhanced microbial inactivation under BL treatment.

Table 8.3. Reduction of *E. coli* concentration on glass surface after 30 and 60 min of BL treatment at 405 nm, 420 nm and 450 nm. Results are reported as log N/N0. The results are the average of two biological replicates.

	405 nm	**420 nm**	**450 nm**
30 min	-0.32 ± 0.05	-0.37 ± 0.16	-0.29 ± 0.46
60 min	-0.68 ± 0.26	-0.56 ± 0.38	-0.40 ± 0.21

Legend: average ± standard deviation

8.4.3 Photodynamic inactivation of *L. monocytogenes* with Valpol at different porphyrin (4MeP) concentrations

Table 8.4 presents the microbial reduction of *L. monocytogenes* following the combined treatment of BL and Valpol over 30 and 60 minutes. Similar to the observations for *E. coli*, treatment of samples with Valpol 4MeP at 0% concentration resulted in a reduction of less than 1 log, which likely reflects physiological changes rather than true microbial inactivation.

All the 4MeP concentrations tested (0%, 5%, 10%) inside the Valpol, new or reused, the controls remained constant at 10^6 CFU/mL. For Valpol 4MeP 5%, 60 minutes of BL exposure across all three wavelengths (405 nm, 420 nm, and 450 nm) yielded comparable microbial reductions, around -1.50 to -1.80 log, with no statistically significant differences among wavelengths ($p > 0.05$). Reuse of the material yielded similar results to the new Valpol, with inactivation levels for 405 and 450 nm remaining consistent. However, for 420 nm, microbial inactivation increased significantly upon reuse, rising from approximately -1.50 to -2.25 log after 60 minutes of BL exposure ($p = 0.047$).

With new Valpol 4MeP 10%, inactivation exceeded -1 log for both 405 nm and 450 nm wavelengths after 30 minutes of treatment, with slight increases in microbial reduction after 60 minutes. At 420 nm, bacterial inactivation was significantly different between the 30- and 60-minute time points ($p = 0.002$), with the highest reduction achieved after 60 minutes (> -2 log). Reusing Valpol 4MeP at 10% further enhanced inactivation across all wavelengths, with reductions exceeding -1 log at 30 minutes and reaching more than -1.95 log after 60 minutes. As observed previously, the 420 nm wavelength produced the highest inactivation level,

reaching -2.74 ± 0.22 log, which was significantly different from the inactivation achieved by other wavelengths.

When comparing results across all wavelengths, Valpol 4MeP 10%, whether new or reused, demonstrated significant differences in microbial inactivation at 30 minutes for 420 nm and 450 nm (420 nm, $p = 0.023$; 450 nm, $p = 0.012$), and at 60 minutes for 405 nm and 420 nm (405 nm, $p = 0.015$; 420 nm, $p = 0.022$).

The microbial inactivation results (log N/N$_0$) for *L. monocytogenes* upon irradiation at 405 nm, 420 nm, and 450 nm using Valpol 4MeP at concentrations of 0%, 5%, and 10%, after 30 and 60 minutes are reported in **Table 8.4**.

Table 8.4. Microbial inactivation results (log N/N0) of *L. monocytogenes* by irradiating at 405 nm, 420 nm and 450 nm Valpol 4MeP (0%, 5%, 10%) after 30 and 60 min. **a.** new material and **b.** reused material a second time. The results are the average of two biological replicates. *Indicate a significant difference between the same sample Valpol 4MeP%, the same wavelength at different times (30 min, 60 min).

a.	**New material**					
	Valpol 4MeP 0%		**Valpol 4MeP 5%**		**Valpol 4MeP 10%**	
	30 min	60 min	30 min	60 min	30 min	60 min
405	-0.16±0.07$_a$	-0.65±0.01$_a$	-1.09±0.68$_a$	-1.78±0.20$_{a*}$	-1.00±0.62$_a$	-1.53±0.20$_{a*}$
420	0.01±0.02$_a$	-0.02±0.00$_c$	-0.42±0.43$_a$	-1.57±0.74$_{a*}$	-0.33±0.08$_a$	-2.03±0.66$_{a*}$
450	-0.10±0.32$_a$	-0.39±0.07$_b$	-1.44±0.63$_a$	-1.85±0.54$_{a*}$	-1.44±0.60$_a$	-1.66±0.35$_{a*}$
b.	**Reused material**					
	Valpol 4MeP 0%		**Valpol 4MeP 5%**		**Valpol 4MeP 10%**	
	30 min	60 min	30 min	60 min	30 min	60 min
405	-0.11±0.17$_a$	-0.30±0.13$_a$	-1.22±0.37$_a$	-1.79±0.06$_{a*}$	-1.83±0.15$_a$	-2.02±0.08$_{b*}$
420	-0.05±0.03$_a$	-0.26±0.29$_a$	-0.47±0.09$_a$	-2.25±0.58$_{a*}$	-1.38±0.76$_a$	-2.74±0.22$_{a*}$
450	-0.10±0.12$_a$	-0.25±0.07$_a$	-1.26±0.81$_a$	-1.86±0.80$_{a*}$	-1.15±0.80$_a$	-1.95±0.52$_{b*}$

Legend: average log N/N0 ± standard deviation

As observed with *E. coli*, microbial inactivation of *L. monocytogenes* was attributable solely to the photodynamic effect, with no contribution from the material itself or any photothermal effect. Control samples, both within the irradiation chamber and dark controls, maintained microbial counts at approximately 10^6 CFU cm^{-2}, confirming that Valpol 4MeP (0%, 5%, and 10%) alone had no bactericidal effect in the absence of irradiation. Additionally, the slight temperature increase (1.5 °C over 60 minutes) did not contribute to microbial reduction.

The dose used for *L. monocytogenes* treatment was 10.8 J cm^{-2}. Rossi et al. (2012) applied a similar dose (14.4 J/cm^2) to irradiate *S. aureus* on polycarbonate surfaces, achieving a 99.997% reduction within one hour. Buchovec et al. (2010) also applied comparable doses, irradiating *L. monocytogenes* suspensions with 5-aminolevulinic acid (ALA) at 400 nm and achieving a 4-log reduction with a 24 J cm^{-2} dose over 20 minutes. However, these findings highlight that photodynamic treatment efficacy depends on numerous factors beyond dose alone.

Regarding porphyrin concentration, as with *E. coli*, a linear relationship between porphyrin percentage in Valpol and microbial inactivation was not observed. This aligns with findings from some previous studies, although none specifically investigated *L. monocytogenes*. Certain studies, such as those by Kim et al. (2021) and Wang et al. (2022), have reported a linear relationship between porphyrin concentration and inactivation. Further investigation is required to clarify this relationship in different contexts and with various microbial species.

Finally, irradiation of microbial samples on a glass surface showed no inactivation after 60 minutes of treatment, as was also observed with *E. coli*. This may be attributed to the known resistance of glass surfaces to microbial attachment and growth, as presented in **Table 8.5**.

Table 8.5. Reduction of *L. monocytogenes* concentration on glass surface after 30 and 60 min of BL treatment at 405 nm, 420 nm and 450 nm. Results are reported as log N/N0. The results are the average of two biological replicates.

	405 nm	**420 nm**	**450 nm**
30 min	-0.14±0.04	-0.16±0.43	-0.21±0.20
60 min	-0.70±0.09	-0.42±0.43	-0.59±013

Legend: average log N/N0 ± standard deviation

The literature indicates that Gram (+) bacteria are generally more susceptible to BL than Gram (-) bacteria. In line with this, *E. coli* required a higher dose for effective inactivation compared to *L. monocytogenes* in this study. Pereira et al. (2014) similarly observed that *E. coli*, among

various Gram (-) bacteria tested, showed relatively high susceptibility to combined 4MeP and visible light treatment, achieving complete inactivation with a 5 μM concentration of 4MeP in solution over 180 minutes. They further highlighted that Gram (+) bacteria, in contrast, reached inactivation levels below the detection limit within 60 minutes, illustrating a greater inherent sensitivity to this photodynamic approach.

The results from **Tables 8.2** and **8.4** in this study reveal that a higher BL dose does not always correlate with increased microbial inactivation, and no single wavelength emerged as definitively optimal for treating both *E. coli* and *L. monocytogenes*. Given the observed differences in microbial inactivation across wavelengths, which were not statistically significant, the choice of wavelength and 4MeP concentration may be adapted based on specific applications. Also, this study underlined how the reuse of the material increased the inactivation rate for all the tested conditions probably due to the formation of pores and canals which favour the exposure of the PS to the light.

As a food-contact surface, Valpol 4MeP films at 5% or 10% concentrations could be activated post-cleaning as an additional sanitization step. This approach enables customization of wavelength to maximize microbial inactivation based on the specific application requirements, thereby enhancing the potential utility of these films in food safety and hygiene settings.

8.4.4 Photodynamic inactivation of *E. coli* and *L. monocytogenes* biofilms grown in Valpol and glass surfaces

In experiments with microbial biofilms, only new Valpol 4MeP was tested, with results illustrated in **Figures 8.11** and **8.12**. These figures depict the microbial inactivation of *E. coli* and *L. monocytogenes* biofilms following BL treatment. Biofilms were grown on various substrates: glass coverslips (**a.**), Valpol 4MeP0% (**b.**), Valpol 4MeP5% (**c.**), and Valpol 4MeP10% (**d.**). Across all wavelengths tested, microbial inactivation for both *E. coli* and *L. monocytogenes* remained below 1 log on all substrate types.

In all cases, treated samples demonstrated statistically significant differences compared to untreated controls for each substrate. Within the same substrate, Valpol 4MeP0% and Valpol 4MeP10% showed significant variations in microbial inactivation when treated with 450 nm and 420 nm compared to 405 nm ($p = 0.02$). This is in contrast to the results observed for planktonic cells, where BL treatment effectively reduced microbial counts. Here, however,

microbial biofilms of both species demonstrated greater resistance to BL, resulting in only minimal inactivation. Reynoso et al. (2021), by contrast, reported a PEDOT-fullerene C60 film achieving comparable inactivation (>99.9%) of *S. aureus* in both planktonic and biofilm states under light irradiation.

Notably, in the case of *E. coli*, the combination of varying 4MeP concentrations in Valpol and different wavelengths contributed significantly to microbial inactivation, accounting for an influence of 8.61%. This suggests that while biofilm form generally confers increased resistance to BL, the specific 4MeP concentration and BL wavelength can slightly impact the inactivation rate within these constraints.

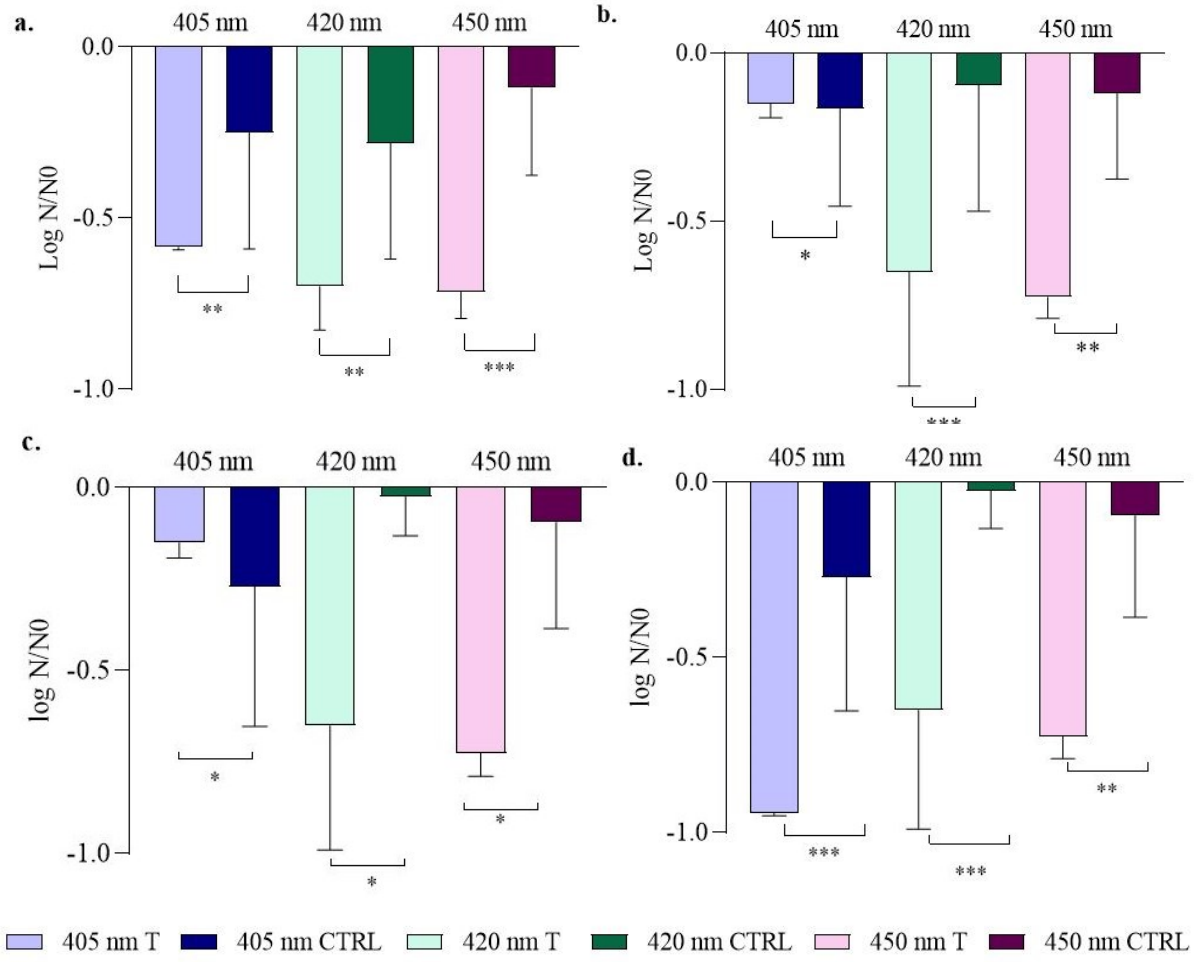


Figure 8.11. Microbial inactivation of *E. coli* in **a.** Glass **b.** Valpol 4MeP0% **c.** Valpol 4MeP5%, **d.** Valpol 4MeP10%. The results are the average of two biological replicates. *$p \leq 0.05$, **$p \leq 0.01$, ***$p \leq 0.001$.

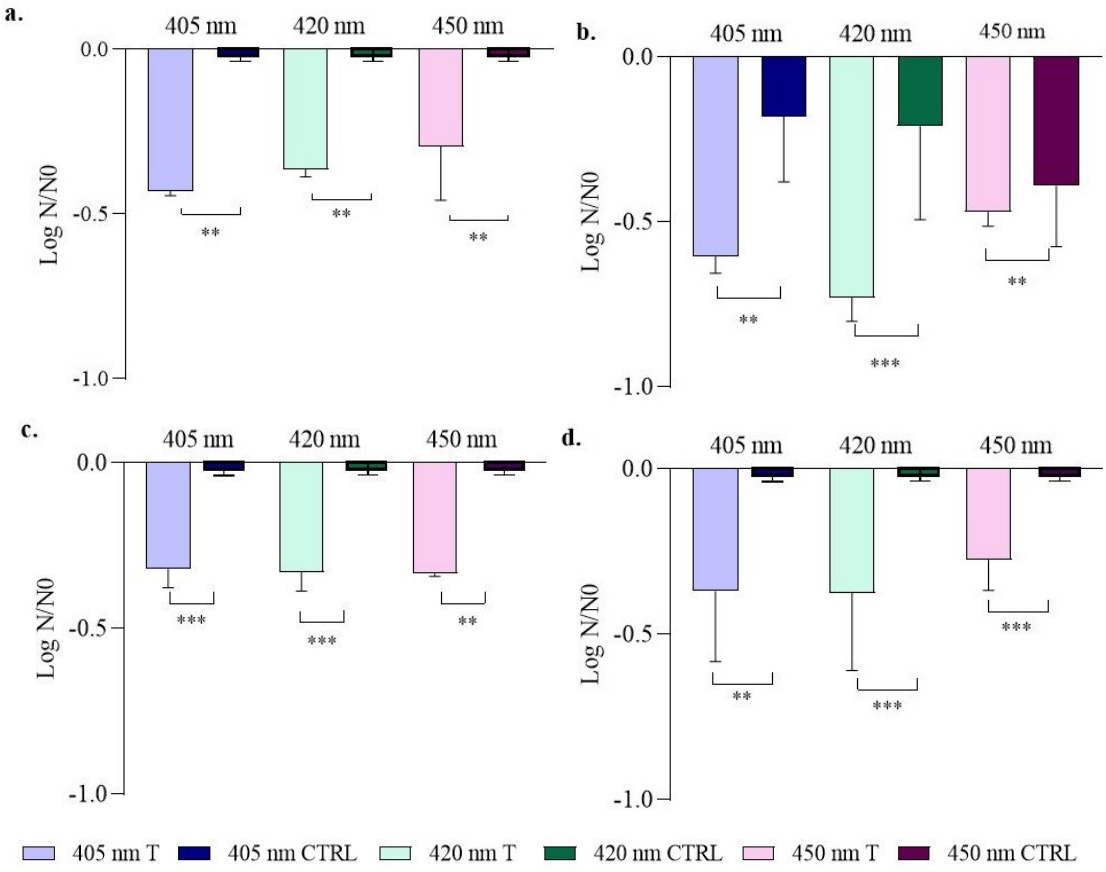


Figure 8.12. Microbial inactivation of *L. monocytogenes* on **a.** Glass **b.** Valpol 4MeP0% **c.** Valpol 4MeP5%, **d.** Valpol 4MeP10%. The results are the average of two biological replicates. *$p \leq 0.05$, **$p \leq 0.01$, ***$p \leq 0.001$.

For *L. monocytogenes*, microbial inactivation on glass and Valpol substrates with various 4MeP concentrations also displayed a statistically significant difference between treated samples and their respective controls. Within the same substrate type, however, only Valpol 4MeP0% showed a significant variation in microbial inactivation across different wavelengths (450 nm, 420 nm, and 405 nm), with a significance ($p < 0.001$).

In contrast to the results obtained for *E. coli*, the microbial inactivation of *L. monocytogenes* was substantially influenced by the percentage of 4MeP in Valpol when considering all experimental variables. Specifically, the concentration of 4MeP accounted for 83.6% of the variation in microbial inactivation, suggesting that for *L. monocytogenes*, the porphyrin concentration within the Valpol material played a crucial role in achieving effective microbial

reduction. This highlights a marked difference in response to BL treatment between the two species, with *L. monocytogenes* showing a far greater dependency on 4MeP concentration for inactivation efficacy.

Comparing these results with the ones obtained on the glass coverslip presented in Chapter 4, the overall reduction is lower in this case. The glass, an inert material, required considerably higher doses compared to the Valpol, a photoactive material (36 and 10.8 J cm^{-2} vs 360 J cm^{-2}).

8.5 Conclusion

This study investigated the potential application of a vanillin-based photoactive material (Valpol) with varying concentrations of 4MeP porphyrin (0%, 5%, and 10%) to inactivate microbial populations under BL irradiation. Two target microorganisms, *E. coli* and *L. monocytogenes*, were tested in both planktonic and biofilm forms to assess the efficacy of Valpol across different microbial states.

Valpol possesses several advantageous properties, including the ease of obtaining vanillin, derived from lignin, which is abundant and renewable. The synthesis process of Valpol is straightforward and yields high production efficiency with minimal losses. Additionally, when porphyrin efficacy declines after repeated uses, the material itself can be recycled or biodegraded, enhancing its environmental sustainability.

The results indicate that Valpol formulations with 5% and 10% 4MeP concentrations effectively inactivated the tested microbes, with *E. coli* requiring a higher BL dose due to its inherent resistance as a Gram (-) bacterium. Notably, the material demonstrated an improved microbial reduction upon reuse, which not only enhances microbial inactivation but also aligns with eco-sustainable practices.

However, for microbial biofilms, both *E. coli* and *L. monocytogenes* exhibited negligible inactivation. This is likely due to the protective extracellular matrix characteristic of biofilms, which may hinder oxygen diffusion and compromise the formation of reactive oxygen species (ROS), thus reducing the effectiveness of photodynamic inactivation. This limitation underscores the complexity of biofilm eradication and suggests that additional strategies may be needed to enhance Valpol's efficacy against biofilm-embedded cells.

Chapter 9

General Discussion

9.1 Brief Introduction

Light-based technologies have garnered considerable interest over the past year as non-thermal approaches for applications in the food industry. Among these, visible light—particularly Blue Light (BL)—has emerged as a highly promising alternative. This technology is considered safe for both operators and treated materials, does not generate harmful residues, is environmentally sustainable, and has shown no evidence of inducing bacterial resistance.

BL is typically emitted by light-emitting diodes (LED), which offer several advantages, including low cost, long lifespan, and high versatility. In fact, LED can be configured in various ways to provide either broad-spectrum or monochromatic light emission, further enhancing their applicability in microbial inactivation processes (Josewin et al., 2018; MartÍn-Sómer et al., 2017; Singh et al., 2021).

Until now, light technology has found its application in the medical field, where it is used for instance for treating superficial and deep-seed infections. Indeed, in the food sector, there remains a considerable gap in knowledge regarding the potential applications of these technologies, the operational parameters, and the possible combination with exogenous photosensitizers (PS) molecules.

To clarify this, the present study focuses on conducting a comprehensive investigation into the applicability of BL in various common food-related contexts, by exploiting endogenous and exogenous photosensitizers (PS) and testing different light wavelengths to understand the best conditions to apply this technology. An overall summary of the main findings of this thesis is presented in **Table 9.1**.

Table 9.1. Summary of the aims and the main results of the projects developed in the thesis.

	Aim	Main results
Section 1	• Investigation of BL at different wavelengths (405 nm, 420 nm, 450 nm) capacity to inactivate foodborne pathogens and spoilage bacteria in planktonic form (**Chapter 2**).	• BL is effective against the tested pathogens and spoilage bacteria, with the outcome being influenced by the applied dose, the used wavelength and the type of microbes. Additionally, it is also necessary to consider the mode of light emission of the source and the lamp design.

Section 1		*L. monocytogenes*, *E. coli*, *S. aureus*, *S. enterica*, *P. fluorescens*, and *B. subtilis* exhibit different susceptibilities to light treatments. • Lower BL wavelengths showed greater efficiency in microbial reduction compared to higher wavelengths, likely due to differences in the quantity, type, and intracellular localization of photosensitizers (PS), as well as variations in stress-related gene expression.
	• Evaluation of mature biofilm inactivation by BL irradiation, identification of the optimal treatment conditions and investigation of the structural modification of biofilms (**Chapter 4**).	• Plate count analysis and CLSM images confirmed the microbial inactivation operated by BL. Also, distinct formation patterns among the tested species were underlined. BL irradiation induced different biofilm responses, including the modification in cell morphology.
	• Elucidation of the role of intracellular ROS and exploration of the relationship between lipid peroxidation, membrane damage, and microbial cell death by using UVA (365 nm) and blue light (405 nm) at two distinct temperatures (4°C and 23°C) (**Chapter 3**).	• ROS are the primary agents responsible for microbial inactivation, with the required ROS levels varying depending on the bacterial species. The amount of ROS required may depend on the bacterial species. • Membrane damage is partially attributed to lipid peroxidation induced by ROS, leading to structural and functional disruptions. Light treatment may also induce sublethal stress in microbial cells, rendering them Viable but Non-Cultivable (VBNC), which could impact their detectability and potential for regrowth.
	• Elucidation of the role of intracellular ROS and exploration of the relationship between lipid peroxidation, membrane damage,	• The design of the system to be implemented in domestic furniture is crucial and several parameters need to be considered, such as the power

	and microbial cell death by using UVA (365 nm) and blue light (405 nm) at two distinct temperatures (4°C and 23°C) (**Chapter 3**).	of the lamp, the irradiance distribution, the light emission (broad-spectrum or monochromatic), the possibility to modulate the height and the voltage. • However, other parameters such as treatment time, light dose, microbial type, and temperature can vary the antimicrobial efficacy of BL treatment.
Section 2	• Exploitation of free exogenous photosensitizers (PS), methylene blue (MB, synthetic) and curcumin (natural), for the inactivation of key pathogens (**Chapters 6** and **7**).	• Both MB and curcumin were effective in inactivating *L. monocytogenes* and *E. coli*. Gram (+) bacteria were more susceptible to PDI compared to Gram (-). The nature of the PS, the type of light used for its activation and the substrate characteristics (nutrient-rich or nutrient-poor) required different concentrations of the PS for effective microbial inactivation.
	• The exploitation of an immobilized PS, 4MeP porphyrin, at different concentrations in a vanillin-based material for the inactivation of key pathogens in planktonic and biofilm forms (**Chapter 8**).	• The material's different 4MeP concentrations (5% and 10%) effectively inactivated the tested microbes. *E. coli* required a higher BL dose due to its inherent resistance as a Gram (-) bacterium. However, the microbial inactivation of biofilms was negligible • The preparation of the material from biological waste matrices, as well as, the improved microbial reduction upon reuse renders this a sustainable material.

9.2 Discussion

9.2.1 Section 1

This section started with the investigation of the effects of different blue light (BL) wavelengths (405 nm, 420 nm, and 450 nm), visible light and UVA (365 nm) on foodborne pathogens and spoilage bacteria by exploiting endogenous PS, revealing key differences in microbial susceptibility.

The light was delivered using three monochromatic LED lamps with emission peaks at 405, 420, and 450 nm. These selected wavelengths enabled the evaluation of different regions of the spectrum. Additionally, the dimmerability of the lamps allowed for precise modulation of irradiance, which could also be adjusted by varying the distance between the light source and the sample.

The initial screening of BL wavelengths (**Chapter 2**) under a fixed light dose range demonstrated the effective inactivation of all tested microorganisms. The preliminary tests evidenced a high heat dissipation by the lamps when providing elevated light doses (300–700 J cm^{-2}), which determined an increase of the temperature to (60–80°C). Such temperatures may have contributed to cellular stress, which could have made the bacterial cells more sensible to photoinactivation.

Indeed, a minimal increase of the temperature was reached by emitting lower light doses (below 300 J cm^{-2}) through the modulation of lamp parameters (light-sample distance and voltage). The microbial inactivation in this case exhibited more variability in the results, which were dependent on the specific wavelength and microbial species, yielding results consistent with those obtained in agar media. As previously observed, Gram (+) bacteria demonstrated greater susceptibility to BL treatment compared to Gram (-) bacteria, with some exceptions, such as *Pseudomonas fluorescens*, which together with *Listeria monocytogenes*, exhibited the highest susceptibility at 405 nm and 420 nm.

The distinct Gram (+) and (-) sensibility could be related to differences in the cell wall, variations in the type of PS present, their quantity, and their activation wavelengths.

405 nm and 420 nm led to greater inactivation than at 450 nm, suggesting that probably the PS present is mainly excited at lower BL wavelengths. These findings align with previous studies (Maclean et al., 2008b; Murdoch et al., 2012; Plavskii et al., 2018), which also reported

variability in BL treatment efficacy among microbial species. This work was crucial for the determination and evaluation of the main parameters that influence the photodynamic inactivation, such as the light dose, the wavelength and the microbial species and allowed to set up the best operational conditions to perform the light treatments.

Considering the microbial susceptibility, a contradictory result emerged in **Chapter 3**, where an opposite inactivation response was observed when considering the different Gram classification, with Gram (-) bacteria being more sensible than Gram (+). The inclusion of a UVA wavelength (365 nm) facilitated a comparison between distinct regions of the light spectrum, yielding results consistent with BL treatment. The similarity of the results obtained across different parts of the spectrum highlights the potential to select a visible wavelength instead of a UV one. This choice offers several advantages, including improved operator safety, lower costs, and enhanced practicality.
Although Gram (+) bacteria are generally considered more sensitive to light-based inactivation, similar discrepancies have been documented in the literature. Tomb et al. (2018), for instance, reported that certain Gram (+) bacteria required a higher light dose to achieve a 1 log reduction. Additionally, variability was noted even within the same Gram classification and among the same species, influenced by factors such as the type, quantity, and intracellular localization of PS compounds. In particular, it is known that the majority of the PS inside bacterial cells are porphyrins, which have a peak of absorbance between 400 and 420 nm. Flavins, indeed, are excited with higher BL wavelengths, around 450 nm (Zenichowski et al., 2007).
This further supports the notion that microbial inactivation is dependent on both the specific BL wavelengths applied and the intrinsic characteristics of each microorganism.

Furthermore, consistent with previous studies (Plavskii et al., 2018; Wu et al., 2021), altering the temperature during light exposure (23°C vs. 4°C) did not significantly affect inactivation outcomes. However, for *S. aureus*, a slight variation was detected, in agreement with other findings (Bastock et al., 2021; Guan et al., 2024), which demonstrated that the differential expression of specific genes (*rsbV, rsbW,* and *sigB*) was influenced by temperature fluctuations. These findings further highlight the variability in bacterial responses to BL treatment, emphasizing the role of species-specific characteristics in determining susceptibility. The role of specific stress genes and their implication in bacteria's light-sensibility is needed to clarify the different inactivation responses among the same bacterial classes.

Despite the observed discrepancy in susceptibility between Gram (-) *E. coli* and the Gram (+) *S. aureus* and *L. monocytogenes*, the production of Reactive Oxygen Species (ROS) was lower in Gram (-) bacteria, ranging from 3500 to 5100 RFU, compared to the higher ROS levels observed in Gram (+) species (9400 to 11,000 RFU) (**Chapter 3**). The lower ROS production in *E. coli*, despite its higher susceptibility to inactivation, suggests that microbial species may have distinct thresholds for ROS-induced lethality. This variation is likely influenced by differences in oxidative stress resistance mechanisms and intracellular PS activity. Additionally, ROS production was not significantly affected by variations in wavelength or temperature. However, testing different BL wavelengths could be useful to establish which are the best parts of the spectra to be used for a specific purpose.

The levels of malondialdehyde (MDA), an indicator of lipid peroxidation, followed a similar pattern to ROS production. Among Gram (+) bacteria, light treatment induced higher MDA levels, with *L. monocytogenes* exhibiting slightly greater lipid peroxidation than *S. aureus*, consistent with the observed microbial inactivation trends. In contrast, Gram (-) *E. coli* produced lower MDA levels following irradiation.
Overall, no clear trend was identified in lipid peroxidation across the tested species. Moreover, a comparison of MDA levels with Real-Time PCR data revealed no direct linear correlation between membrane damage-induced cell death and lipid peroxidation, suggesting the involvement of additional factors in membrane disruption and subsequent microbial inactivation.

Furthermore, the comparison between viable count and Real-Time PCR results suggested the potential presence of viable but non-countable (VBNC) cells. This could lead to an overestimation of microbial inactivation when relying solely on plate counting. These findings indicate that light treatment may induce sublethal stress in microbial cells, which, although non-countable, may retain metabolic activity and the potential for regrowth. Therefore, the impact of VBNC formation should be carefully considered when assessing the efficacy of light-based microbial inactivation strategies.

Similar to the observations made with planktonic bacterial cells, the treatment of microbial biofilms yielded results consistent with previous findings. Specifically, lower BL wavelengths (405 nm and 420 nm) resulted in more effective than 450 nm in reducing microbial populations in both 5-day and 13-day biofilms, with variations in inactivation trends depending on the

microbial species (**Chapter 4**). The differences in inactivation across wavelengths may be attributed to the PS, as in the case of planktonic cells, and to additional factors such as *quorum sensing*, the presence of persister cells, and the expression of oxidative stress-resistant genes (*OxyR, AhpC, GrxA*). Furthermore, BL exposure may lead to the suppression or overexpression of genes involved in stress responses (Buchovec et al., 2017; Murdoch et al., 2012). Therefore, in this study, by maintaining a fixed light dose, inactivation was primarily dependent on the selected wavelength, whether it was able to activate or not the endogenous PS, and microbial species, for their PS presence as well as their stress-response mechanisms.

Confocal Laser Scanning Microscopy (CLSM) images revealed structural differences in 13-day biofilms among bacterial species, corroborating reductions observed via plate count. Notably, CLSM imaging confirmed the distinct biofilm architecture of each microorganism before and after BL treatment. For instance, untreated *L. monocytogenes* biofilms exhibited increased thickness, while post-treatment images displayed long filamentous formations. In contrast, *E. coli* biofilms before treatment developed laterally across the surface rather than in thickness, and, after BL exposure, resulted in a decrease in cell size. These findings highlight the differential impact of light treatment on biofilm integrity and cell morphology, emphasizing the importance of tailoring BL treatment strategies based on microbial biofilm characteristics and maturation.

A further investigation, conducted in collaboration with Electrolux Italia S.p.A, examined the effects of UVA (365 nm) and BL (405 nm) in a controlled system designed for potential integration into household appliances (**Chapter 5**). This study initially focused on evaluating a *mock-up* system from a technical perspective to determine the optimal operational setup and conditions for practical application.

The findings underscored the crucial role of system design in optimizing the efficacy of light-based microbial inactivation. Notably, the distance between the light source and the sample significantly affected irradiance distribution. A more uniform light distribution was achieved at a greater distance (38.8 cm), whereas a closer positioning (17.8 cm) resulted in non-uniform irradiance, potentially compromising treatment effectiveness.

Additionally, the study emphasized the necessity of defining an effective inactivation dose on the base of the used lamp and the treatment purpose and adjusting the treatment duration accordingly. In this case, to achieve the target dose (30 J cm^{-2}), samples required irradiation for

4 hours when the lamp-sample distance was 17.8 cm and 15 hours when it was 38.8 cm. A lower dose, applied through 1 hour of light treatment, was insufficient to reduce microbial counts of 1 log, unlike higher doses (approximately 30 J cm^{-2}) achieved the microbial reduction under the detection limit through extended irradiation (4h and 15h). Although increasing treatment time is a straightforward approach to reaching a specific dose, from an energy efficiency perspective, a more effective strategy would involve increasing LED power and optimizing surface light distribution. This would allow for the required dose to be delivered in a shorter treatment duration, improving both efficacy and energy efficiency.

9.2.2 Section 2

This section focused on the application of exogenous PS, either in free form or supported within a material, to enhance microbial inactivation.

Using methylene blue (MB), a synthetic PS, light irradiation experiments confirmed the greater susceptibility of the Gram (+) *L. monocytogenes* compared to the Gram (-) *E. coli*, which necessitated distinct MB concentrations (1 μM and 5 μM, respectively) to achieve similar reductions in 15 minutes (D = 45 J cm^{-2}).

When MB was tested in a turbid matrix rich in organic matter, both the MB concentration and the required light dose increased for effective microbial inactivation in both Gram (+) and Gram (-) bacteria. However, Gram (-) bacteria consistently required higher MB concentrations (50 μM) to reach inactivation levels comparable to Gram (+) ones (20 μM). This trend was also observed in biofilm formation within both standard culture media and the opaque matrix.

The difference in inactivation efficiency between transparent media and the turbid matrix was attributed to variations in light absorption and the interaction of PS with organic matter. Considering the matrix composition is crucial when developing PS-based decontamination strategies, particularly for potential applications in food systems.

In contrast, curcumin, a natural PS, achieved comparable microbial reductions in both the bacteria Gram classifications when applied at the same concentration. Additionally, while variations in the applied wavelengths (405 nm, 420 nm, and 450 nm) influenced the inactivation kinetics, the overall microbial reduction remained similar. This consistency may be attributed to the lamp power, the ability of all tested wavelengths to effectively activate the PS, also to the chemical state of curcumin in the substrate to which is applied, which could determine different radical formations.

The use of exogenous PS at low concentrations, regardless of its type (natural or synthetic), significantly accelerated microbial inactivation and enhanced the overall inactivation rate, aligning with previous research findings. However, for practical implementation in the food industry, several critical factors must be addressed. These include ensuring that the PS is food-grade, selecting an appropriate excitation wavelength for optimal PS activation, and mitigating potential substrate modification. In cases where the PS is not fully photodegraded, strategies for removing residual PS must be developed to ensure product safety and quality.

A further step was conducted by testing the inactivation efficiency of a PS when immobilized in a support (**Chapter 8**). In this case, 4MeP, a porphyrin, was immobilized in different concentrations within Valpol, a vanillin-based material, obtained through waste materials.
As in the case of free PS, also after its immobilisation, the results evidenced that Gram (-) bacteria, *E. coli* in this case, required more than three times the light doses needed by *L. moncytogenes* (Gram +) for effective inactivation in planktonic form. The structural differences of the bacteria are crucial for the interaction with the PS and the absorption of the generated ROS.
The photoactive material Valpol, containing 5% and 10% of 4MeP, exhibited significant inactivation efficacy against planktonic cells of *L. monocytogenes* and *E. coli*. Interestingly, the material's effectiveness improved with reuse. This enhancement could be attributed to the formation of pores, which increased the exposure of the PS to light.

However, no linear relationship was observed between the concentration of porphyrin and microbial inactivation, as Valpol materials with 5% and 10% 4MeP achieved similar results. As was observed in **Chapter 3**, it may be that to effectively inactivate bacteria, it is required a ROS threshold and maybe at 5 and 10 % the amount of ROS produced is similar. Further studies would be necessary to elucidate the correlation between the ROS amount and the related microbial inactivation.

In contrast to planktonic cells, when microbial biofilms formed on the Valpol surface were treated, the reductions in microbial populations were less than 1 log for both *L. monocytogenes* and *E. coli*, regardless of the 4MeP concentration or wavelength used. This lower efficiency could be related to a possible difficulty in activating the PS inside the material (used for the

first time), which is also covered by the biofilm matrix that could cover the light absorption by the PS.
These findings highlight the specific challenges associated with biofilm inactivation and suggest that further optimization of the photoactive material may be necessary to enhance its effectiveness against biofilms.

Overall, this work emphasized the potential application of visible light, particularly BL, in the food-related sector. A notable strength of this study lies in the use of endogenous PS for light treatment across various forms (solid, liquid, and biofilm), which are commonly found in food-related environments. These PS were excited using different wavelengths spanning the BL spectrum. Furthermore, the use of broad-spectrum lamps or UVA wavelengths in certain cases allowed for a comparison of the effectiveness of different emission lamps and the effects of near wavelengths from different parts of the electromagnetic spectrum in order to possibly choose the one which responds better to the expected results.

The findings underscore several critical factors that must be considered depending on the intended application. Specifically, the light dose, wavelength, and type of microbes are the most influential parameters. Additionally, careful selection of the PS characteristics and concentrations is essential for optimizing effectiveness based on the specific application.

The synthesis of this material, its high yield, its reusability, the stable incorporation of the PS and the effectiveness with a lower porphyrin percentage position this technology as an environmentally friendly, green solution. Also, the low cost of the raw material made this technology interesting for a food company. The use of photoactive material in the food context is still preliminary but it could be hypnotized as a food contact surface, for water sanitation or even food packaging. More studies should be done in order to understand the feasibility of their application in the food context, which requires several features, such as being food-grade and the capability to not lose the PS in the matrix.

Future Prospective

Despite the comprehensive analysis provided in this study, several aspects regarding the use of visible light for microbial inactivation remain unclear. Specifically, the exact mechanisms responsible for cell death and the genetic factors involved in microbial inactivation are not fully

elucidated for all microorganisms, particularly when considering both planktonic cells and microbial biofilms. While it is known that light exposure triggers the generation of ROS that damage cellular structures, the specific pathways leading to inactivation may vary between species and under different conditions, making it a complex process that requires further exploration. Also, the precise mechanism of action of the various exogenous PS is still unclear.

From a food industry perspective, there is still a lack of studies focused on the direct application of light to food products, especially in terms of understanding the potential biochemical, structural, and sensory changes that may occur. While light treatment offers a promising method for microbial control, it is essential to explore how different wavelengths, light doses, and treatment durations might affect the quality and safety of food products. Furthermore, the potential for beneficial effects, such as preservation of nutritional value or enhancement of certain food characteristics, warrants investigation. Therefore, conducting a broader screening of various food products exposed to different light wavelengths would provide valuable insights into the effects of this technique, helping to understand both the risks and possible improvements it could bring to specific food categories.

References

Abana, C. M., Brannon, J. R., Ebbott, R. A., Dunigan, T. L., Guckes, K. R., Fuseini, H., Powers, J., Rogers, B. R., & Hadjifrangiskou, M. (2017). Characterization of blue light irradiation effects on pathogenic and nonpathogenic *Escherichia coli*. *MicrobiologyOpen*, *6*(4), 1–10. https://doi.org/10.1002/mbo3.466

Achinas, S., Charalampogiannis, N., & Euverink, G. J. W. (2019). A Brief Recap of Microbial Adhesion and Biofilms. *Applied Sciences*, *9*(14), 2801. https://doi.org/10.3390/app9142801

Akram, F. E., El-Tayeb, T., Abou-Aisha, K., & El-Azizi, M. (2016). A combination of silver nanoparticles and visible blue light enhances the antibacterial efficacy of ineffective antibiotics against methicillin-resistant *Staphylococcus aureus* (MRSA). *Annals of Clinical Microbiology and Antimicrobials*, *15*(48), 1–13. https://doi.org/10.1186/s12941-016-0164-y

Alberto, M. E., Comuzzi, C., Thandu, M., Adamo, C., & Russo, N. (2016). 22π-Electrons [1.1.1.1.1] pentaphyrin as a new photosensitizing agent for water disinfection: Experimental and theoretical characterization. *Theoretical Chemistry Accounts*, *135*(2), 1–10. https://doi.org/10.1007/s00214-015-1794-4

Alhenaki, A. M., Alqarawi, F. K., Tanveer, S. A., Alshahrani, F. A., Alshahrani, A., AlHamdan, E. M., Alzahrani, K. M., Aldahiyan, N., Naseem, M., Vohra, F., & Abduljabbar, T. (2021). Disinfection of acrylic denture resin polymer with Rose Bengal, Methylene blue and Porphyrin derivative in photodynamic therapy. *Photodiagnosis and Photodynamic Therapy*, *35*(May), 102362. https://doi.org/10.1016/j.pdpdt.2021.102362

Almenta, M. M., Morrow, J., Best, R., Fox, B., & Foley, A. (2014). A smart load appliance application using a single compressor fridge-freezer to support grid operations. *2014 49th International Universities Power Engineering Conference (UPEC)*, 1–5. https://doi.org/10.1109/UPEC.2014.6934662

Alves, E., Costa, L., Carvalho, C. M., Tomé, J. P., Faustino, M. A., Neves, M. G., Tomé, A. C., Cavaleiro, J. A., Cunh, A., & Almeida, A. (2009). Charge effect on the photoinactivation of gram-negative and gram-positive bacteria by cationic meso-substituted porphyrins. *BMC Microbiology*, *9*, 1–13. https://doi.org/10.1186/1471-2180-9-70

Alves, E., Santos, N., Melo, T., Maciel, E., Dõria, M. L., Faustino, M. A. F., Tomé, J. P. C., Neves, M. G. P. M. S., Cavaleiro, J. A. S., Cunha, Â., Helguero, L. A., Domingues, P., Almeida, A., & Domingues, M. R. M. (2013). Photodynamic oxidation of *Escherichia coli* membrane phospholipids: New insights based on lipidomics. *Rapid Communications in Mass Spectrometry*, *27*(23), 2717–2728. https://doi.org/10.1002/rcm.6739

Alves, F., Gomes Guimarães, G., Mayumi Inada, N., Pratavieira, S., Salvador Bagnato, V., & Kurachi, C. (2021). Strategies to Improve the Antimicrobial Efficacy of Photodynamic, Sonodynamic, and Sonophotodynamic Therapies. *Lasers in Surgery and Medicine*, *53*(8), 1113–1121. https://doi.org/10.1002/lsm.23383

Amin, R. M., Bhayana, B., Hamblin, M. R., & Dai, T. (2016). Antimicrobial blue light inactivation of *Pseudomonas aeruginosa* by photo-excitation of endogenous porphyrins: In vitro and in vivo studies. *Lasers in Surgery and Medicine*, *48*(5), 562–568. https://doi.org/10.1002/lsm.22474

Andino, A., & Hanning, I. (2015). *Salmonella enterica*: Survival, Colonization, and Virulence Differences among Serovars. *The Scientific World Journal*, *2015*, 1–16. https://doi.org/10.1155/2015/520179

Angarano, V., Akkermans, S., Smet, C., Chieffi, A., & Van Impe, J. F. M. (2020). The potential of violet, blue, green and red light for the inactivation of *P. fluorescens* as planktonic cells, individual cells on a surface and biofilms. *Food and Bioproducts Processing*, *124*, 184–195. https://doi.org/10.1016/j.fbp.2020.07.019

Anju, V. T., Paramanantham, P., Sruthil, S. L. S. B., Sharan, A., Syed, A., Bahkali, N. A., Alsaedi, M. H., K., K., & Busi, S. (2019). Antimicrobial photodynamic activity of toluidine blue-carbon nanotube conjugate against *Pseudomonas aeruginosa* and *Staphylococcus aureus*—Understanding the mechanism of action. *Photodiagnosis and Photodynamic Therapy*, *27*(5), 305–316. https://doi.org/10.1016/j.pdpdt.2019.06.014

Argyraki, A., Markvart, M., Bjørndal, L., Bjarnsholt, T., & Petersen, P. M. (2017). Inactivation of *Pseudomonas aeruginosa* biofilm after ultraviolet light-emitting diode treatment: A comparative study between ultraviolet C and ultraviolet B. *Journal of Biomedical Optics*, *22*(6), 065004. https://doi.org/10.1117/1.jbo.22.6.065004

Ash, C., Dubec, M., Donne, K., & Bashford, T. (2017). Effect of wavelength and beam width on penetration in light-tissue interaction using computational methods. *Lasers in Medical Science*, *32*(8), 1909–1918. https://doi.org/10.1007/s10103-017-2317-4

Astuti, S. D., Wibowo, R. A., Abdurachman, N. 0011096602, & Triyana, K. (2017). Antimicrobial Photodynamic Effects of Polychromatic Light Activated by Magnetic Fields to Bacterial Viability. *Journal of International Dental and Medical Research*, *10*(1), 111–117.

Aurum, F. S., & Nguyen, L. T. (2019). Efficacy of photoactivated curcumin to decontaminate food surfaces under blue light emitting diode. *Journal of Food Process Engineering*, *42*(3), 1–9. https://doi.org/10.1111/jfpe.12988

Awuchi, C. G. (2023). HACCP, quality, and food safety management in food and agricultural systems. *Cogent Food & Agriculture*, *9*(1), 2176280. https://doi.org/10.1080/23311932.2023.2176280

Bache, S. E., Maclean, M., Gettinby, G., Anderson, J. G., MacGregor, S. J., & Taggart, I. (2018). Universal decontamination of hospital surfaces in an occupied inpatient room with a continuous 405 nm light source. *Journal of Hospital Infection*, *98*(1), 67–73. https://doi.org/10.1016/j.jhin.2017.07.010

Baharoglu, Z., & Mazel, D. (2014). SOS, the formidable strategy of bacteria against aggressions. *FEMS Microbiology Reviews*, *38*(6), 1126–1145. https://doi.org/10.1111/1574-6976.12077

Baigorria, E., Durantini, J. E., Martínez, S. R., Milanesio, M. E., Palacios, Y. B., & Durantini, A. M. (2021). Potentiation Effect of Iodine Species on the Antimicrobial Capability of Surfaces Coated with Electroactive Phthalocyanines. *ACS Applied Bio Materials*, *4*(12), 8559–8570. https://doi.org/10.1021/acsabm.1c01029

Baker, J., Sitthisak, S., Sengupta, M., Johnson, M., Jayaswal, R. K., & Morrissey, J. A. (2010). Copper Stress Induces a Global Stress Response in *Staphylococcus aureus* and Represses *sae* and *agr* Expression and Biofilm Formation. *Applied and Environmental Microbiology*, *76*(1), 150–160. https://doi.org/10.1128/AEM.02268-09

Barneck, M. D., Rhodes, N. L. R., de la Presa, M., Allen, J. P., Poursaid, A. E., Nourian, M. M., Firpo, M. A., & Langell, J. T. (2016). Violet 405-nm light: A novel therapeutic agent against common pathogenic bacteria. *Journal of Surgical Research*, *206*(2), 316–324. https://doi.org/10.1016/j.jss.2016.08.006

Barriuso, J., Hogan, D. A., Keshavarz, T., & Martínez, M. J. (2018). Role of quorum sensing and chemical communication in fungal biotechnology and pathogenesis. *FEMS Microbiology Reviews*, *42*(5), 627–638. https://doi.org/10.1093/femsre/fuy022

Barth, E., Gora, K. V., Gebendorfer, K. M., Settele, F., Jakob, U., & Winter, J. (2009). Interplay of cellular cAMP levels, σ S activity and oxidative stress resistance in *Escherichia coli*. *Microbiology*, *155*(5), 1680–1689. https://doi.org/10.1099/mic.0.026021-0

Bartolomeu, M., Gomes, T. J., Campos, F., Vieira, C., Loureiro, S., Neves, M. G. P. M. S., Faustino, M. A. F., Gomes, A. T. P. C., & Almeida, A. (2024). Wastewater disinfection with photodynamic treatment and evaluation of its ecotoxicological effects. *Chemosphere*, *361*, 142421. https://doi.org/10.1016/j.chemosphere.2024.142421

Bastock, R. A., Marino, E. C., Wiemels, R. E., Holzschu, D. L., Keogh, R. A., Zapf, R. L., Murphy, E. R., & Carroll, R. K. (2021). *Staphylococcus aureus* Responds to Physiologically Relevant Temperature Changes by Altering Its Global Transcript and Protein Profile. *mSphere*, *6*(2), e01303-20. https://doi.org/10.1128/mSphere.01303-20

Beales, N. (2004). Adaptation of Microorganisms to Cold Temperatures, Weak Acid Preservatives, Low pH, and Osmotic Stress: A Review. *Comprehensive Reviews in Food Science and Food Safety*, *3*(1), 1–20. https://doi.org/10.1111/j.1541-4337.2004.tb00057.x

Beauchamp, A., & Kitai, A. (2019). Fourier series-based optimization of LED angular intensity profiles for displays and backlighting. *OSA Continuum*, *2*(9), 2539. https://doi.org/10.1364/OSAC.2.002539

Beenken, K. E., Dunman, P. M., McAleese, F., Macapagal, D., Murphy, E., Projan, S. J., Blevins, J. S., & Smeltzer, M. S. (2004). Global Gene Expression in *Staphylococcus aureus* Biofilms. *Journal of Bacteriology*, *186*(14), 4665–4684. https://doi.org/10.1128/JB.186.14.4665-4684.2004

Belozerskaya, T. A., & Gessler, N. N. (2007). Reactive oxygen species and the strategy of antioxidant defense in fungi: A review. *Applied Biochemistry and Microbiology*, *43*(5), 506–515. https://doi.org/10.1134/S0003683807050031

Bereksi, N., Gavini, F., Bénézech, T., & Faille, C. (2002). Growth, morphology and surface properties of *Listeria monocytogenes* Scott A and LO28 under saline and acid environments. *Journal of Applied Microbiology*, *92*, 556–565. https://doi.org/10.1046/j.1365-2672.2002.01564.x

Bhardwaj, S. K., Singh, H., Deep, A., Khatri, M., Bhaumik, J., Kim, K. H., & Bhardwaj, N. (2021). UVC-based photoinactivation as an efficient tool to control the transmission of coronaviruses. *Science of the Total Environment*, *792*, 148548. https://doi.org/10.1016/j.scitotenv.2021.148548

Bhavya, M. L., & Umesh Hebbar, H. (2019). Efficacy of blue LED in microbial inactivation: Effect of photosensitization and process parameters. *International Journal of Food Microbiology*, *290*(March 2018), 296–304. https://doi.org/10.1016/j.ijfoodmicro.2018.10.021

Bishai, W. R., Howard, N. S., Winkelstein, J. A., & Smith, H. O. (1994). Characterization and virulence analysis of catalase mutants of *Haemophilus influenzae*. *Infection and Immunity*, *62*(11), 4855–4860. https://doi.org/10.1128/iai.62.11.4855-4860.1994

Bassler, B. L. (1999). How bacteria talk to each other: regulation of gene expression by quorum sensing. *Current Opinion in Microbiology*, 2(6), 582-587. https://doi.org/10.1016/S1369-5274(99)00025-9.

Bolton, J. R., & Linden, K. G. (2003). Standardization of Methods for Fluence (UV Dose) Determination in Bench-Scale UV Experiments. *Journal of Environmental Engineering*, *129*(3), 209–215. https://doi.org/10.1061/(asce)0733-9372(2003)129:3(209)

Bolton, J. R., Mayor-Smith, I., & Linden, K. G. (2015). Rethinking the Concepts of Fluence (UV Dose) and Fluence Rate: The Importance of Photon-based Units—A Systemic Review. *Photochemistry and Photobiology*, *91*(6), 1252–1262. https://doi.org/10.1111/php.12512

Bonanno, L., Bergis, H., Gnanou-Besse, N., Asséré, A., & Danan, C. (2024). Which domestic refrigerator temperatures in Europe? - Focus on shelf-life studies regarding *Listeria monocytogenes* (Lm) in ready-to-eat (RTE) foods. *Food Microbiology*, *123*, 104595. https://doi.org/10.1016/j.fm.2024.104595

Bonin, E., dos Santos, A. R., Fiori da Silva, A., Ribeiro, L. H., Favero, M. E., Campanerut-Sá, P. A. Z., de Freitas, C. F., Caetano, W., Hioka, N., & Mikcha, J. M. G. (2018). Photodynamic inactivation of foodborne bacteria by eosin Y. *Journal of Applied Microbiology*, *124*(6), 1617–1628. https://doi.org/10.1111/jam.13727

Bridier, A., Dubois-Brissonnet, F., Boubetra, A., Thomas, V., & Briandet, R. (2010). The biofilm architecture of sixty opportunistic pathogens deciphered using a high throughput CLSM

method. *Journal of Microbiological Methods*, *82*(1), 64–70. https://doi.org/10.1016/j.mimet.2010.04.006

Buchovec, I., Lukseviciūtė, V., Kokstaite, R., Labeikyte, D., Kaziukonyte, L., & Luksiene, Z. (2017). Inactivation of Gram (−) bacteria Salmonella enterica by chlorophyllin-based photosensitization: Mechanism of action and new strategies to enhance the inactivation efficiency. *Journal of Photochemistry and Photobiology B: Biology*, *172*, 1–10. https://doi.org/10.1016/j.jphotobiol.2017.05.008

Buchovec, I., Paskeviciute, E., & Luksiene, Z. (2010). Photosensitization-based inactivation of food pathogen *Listeria monocytogenes* in vitro and on the surface of packaging material. *Journal of Photochemistry and Photobiology B: Biology*, *99*(1), 9–14. https://doi.org/10.1016/j.jphotobiol.2010.01.007

Buchovec, I., Vaitonis, Z., & Luksiene, Z. (2009). Novel approach to control *Salmonella enterica* by modern biophotonic technology: Photosensitization. *Journal of Applied Microbiology*, *106*(3), 748–754. https://doi.org/10.1111/j.1365-2672.2008.03993.x

Buchovec I, Vyčaitė E, Badokas K, Sužiedelienė E, Bagdonas S. (2022). Application of Antimicrobial Photodynamic Therapy for Inactivation of *Acinetobacter baumannii* Biofilms. *Int J Mol Sci*., 24(1),722. https://doi.org/10.3390/ijms24010722

Bumah, V. V., Masson-Meyers, D. S., Tong, W., Castel, C., & Enwemeka, C. S. (2020). Optimizing the bactericidal effect of pulsed blue light on *Propionibacterium acnes*—A correlative fluorescence spectroscopy study. *Journal of Photochemistry and Photobiology B: Biology*, *202*, 111701. https://doi.org/10.1016/j.jphotobiol.2019.111701

Cabral, J., & Rodrigues, A. (2019). Blue Light Disinfection in Hospital Infection Control: Advantages, Drawbacks, and Pitfalls. *Antibiotics*, *58*(8), 1–21. https://doi.org/10.3390/antibiotics8020058

Caires, C. S. A., Farias, L. A. S., Gomes, L. E., Pinto, B. P., Gonçalves, D. A., Zagonel, L. F., Nascimento, V. A., Alves, D. C. B., Colbeck, I., Whitby, C., Caires, A. R. L., & Wender, H. (2020). Effective killing of bacteria under blue-light irradiation promoted by green synthesized silver nanoparticles loaded on reduced graphene oxide sheets. *Materials Science and Engineering: C*, *113*, 110984. https://doi.org/10.1016/j.msec.2020.110984

Calva-Estrada, S. J., Mendoza, M. R., García, O., Jiménez-Fernández, V. M., & Jiménez, M. (2018). Microencapsulation of vanilla (Vanilla planifolia Andrews) and powder characterization. *Powder Technology*, *323*, 416–423. https://doi.org/10.1016/j.powtec.2017.10.035

Carpenter, B. L., Feese, E., Sadeghifar, H., Argyropoulos, D. S., & Ghiladi, R. A. (2012). Porphyrin-cellulose nanocrystals: A photobactericidal material that exhibits broad spectrum antimicrobial activity. *Photochemistry and Photobiology*, *88*(3), 527–536. https://doi.org/10.1111/j.1751-1097.2012.01117.x

Castro, K. A. D. F., Moura, N. M. M., Simões, M. M. Q., Cavaleiro, J. A. S., Faustino, M. do A. F., Cunha, Â., Almeida Paz, F. A., Mendes, R. F., Almeida, A., Freire, C. S. R., Vilela, C., Silvestre, A. J. D., Nakagaki, S., & Neves, M. da G. P. M. S. (2019). Synthesis and characterization of photoactive porphyrin and poly(2-hydroxyethyl methacrylate) based materials with bactericidal properties. *Applied Materials Today*, *16*, 332–341. https://doi.org/10.1016/j.apmt.2019.06.010

Cervantes-Huamán, B. R. H., Ripolles-Avila, C., Mazaheri, T., & Rodríguez-Jerez, J. J. (2022). Pathogenic mono-species biofilm formation on stainless steel surfaces: Quantitative, qualitative, and compositional study. *LWT*, *159*, 113211. https://doi.org/10.1016/j.lwt.2022.113211

Chen, B., Huang, J., Li, H., Zeng, Q. H., Wang, J. J., Liu, H., Pan, Y., & Zhao, Y. (2020). Eradication of planktonic *Vibrio parahaemolyticus* and its sessile biofilm by curcumin-mediated photodynamic inactivation. *Food Control*, *113*, 107181. https://doi.org/10.1016/j.foodcont.2020.107181

Chen, H. W., & Yeh, S. L. (2019). Effects of blue light on dynamic vision. *Frontiers in Psychology*, *10*(3). https://doi.org/10.3389/fpsyg.2019.00497

Chen, J., Cesario, T. C., & Rentzepis, P. M. (2014). Rationale and mechanism for the low photoinactivation rate of bacteria in plasma. *Proceedings of the National Academy of Sciences*, *111*(1), 33–38. https://doi.org/10.1073/pnas.1315053111

Chen, Z., Qin, H., Lin, S., Lu, Z., Fan, X., Liu, X., & Liu, M. (2021). Comparative transcriptome analysis of gene expression patterns on B16F10 melanoma cells under Photobiomodulation of different light modes. *Journal of Photochemistry and Photobiology B: Biology*, *216*, 112127. https://doi.org/10.1016/j.jphotobiol.2021.112127

Cheng, Y., Chen, H., Sánchez Basurto, L. A., Protasenko, V. V., Bharadwaj, S., Islam, M., & Moraru, C. I. (2020). Inactivation of *Listeria* and *E. coli* by Deep-UV LED: effect of substrate conditions on inactivation kinetics. *Scientific Reports*, *10*(1), 3411. https://doi.org/10.1038/s41598-020-60459-8

Choby, J. E., & Skaar, E. P. (2016). Heme Synthesis and Acquisition in Bacterial Pathogens. *Journal of Molecular Biology*, *428*(17), 3408–3428. https://doi.org/10.1016/j.jmb.2016.03.018

Chua, A., Chong, L., Ghate, V., Yuk, H.-G., & Zhou, W. (2021). Antifungal action of 405 nm light emitting diodes on tomatoes in a meso-scale system and their effect on the physicochemical properties. *Postharvest Biology and Technology*, *172*, 111366. https://doi.org/10.1016/j.postharvbio.2020.111366

Çiftçi, H. (2022). Removal of methylene blue from water by ultrasound-assisted adsorption using low-cost bentonites. *Chemical Physics Letters*, *802*, 139758. https://doi.org/10.1016/j.cplett.2022.139758

Ciofu, O., Moser, C., Jensen, P. Ø., & Høiby, N. (2022). Tolerance and resistance of microbial biofilms. *Nature Reviews Microbiology*, *0123456789*. https://doi.org/10.1038/s41579-022-00682-4

Coma, V. (2008). Bioactive packaging technologies for extended shelf life of meat-based products. *Meat Science*, *78*(1–2), 90–103. https://doi.org/10.1016/j.meatsci.2007.07.035

Comuzzi, C., Fiorot, A., Baggio, A., Maifreni, M., Strazzolini, P., Marino, M., & Susmel, S. (2020). Imprinting Pentaphyrin on Conductive Electropolymerized Dipyrromethane Films: A New Strategy towards the Synthesis of Photokilling Materials. *ChemPlusChem*, *85*(4), 776–782. https://doi.org/10.1002/cplu.202000137

Comuzzi, C., Marino, M., Poletti, D., Boaro, M., & Strazzolini, P. (2022). New antimicrobial PVC composites. Porphyrins self-aggregation in tuning surface morphologies and photodynamic inactivation towards sustainable water disinfection. *Journal of Photochemistry and Photobiology A: Chemistry*, *430*(March), 113967. https://doi.org/10.1016/j.jphotochem.2022.113967

Converti, A., Aliakbarian, B., Domínguez, J. M., Vázquez, G. B., & Perego, P. (2010). Microbial production of biovanillin. *Brazilian Journal of Microbiology*, *41*(3), 519–530. https://doi.org/10.1590/S1517-83822010000300001

Cossu, M., Ledda, L., & Cossu, A. (2021). Emerging trends in the photodynamic inactivation (PDI) applied to the food decontamination. *Food Research International*, *144*(November 2020), 110358. https://doi.org/10.1016/j.foodres.2021.110358

Costerton, J. W., Cheng, K.-J., Greesy, G. G., Timothy, I. L., Nickel, J. C., Mrinal, D., & Thomas, J. M. (1987). Bacterial biofilms in nature and disease. *Ann. Rev. Microbiol.*, *41*, 435–464.

Coughlan, L. M., Cotter, P. D., Hill, C., & Alvarez-Ordóñez, A. (2016). New weapons to fight old enemies: Novel strategies for the (bio)control of bacterial biofilms in the food industry. *Frontiers in Microbiology*, *7*(OCT), 1–21. https://doi.org/10.3389/fmicb.2016.01641

Crawford, M. H., Banas, M. a, Ross, M. P., Ruby, D. S., Nelson, J. S., Boucher, R., & Allerman, A. a. (2005). *Final LDRD Report: Ultraviolet Water Purification Systems for Rural Environments and Mobile Applications*. 1–37.

Daglia, M. (2012). Polyphenols as antimicrobial agents. *Current Opinion in Biotechnology*, *23*(2), 174–181. https://doi.org/10.1016/j.copbio.2011.08.007

Dai, T., Gupta, A., Huang, Y.-Y., Yin, R., Murray, C. K., Vrahas, M. S., Sherwood, M. E., Tegos, G. P., & Hamblin, M. R. (2013). Blue Light Rescues Mice from Potentially Fatal *Pseudomonas aeruginosa* Burn Infection: Efficacy, Safety, and Mechanism of Action. *Antimicrobial Agents and Chemotherapy*, *57*(3), 1238–1245. https://doi.org/10.1128/AAC.01652-12

Dai, T., Gupta, A., Murray, C. K., Vrahas, M. S., Tegos, G. P., & Hamblin, M. R. (2012). Blue light for infectious diseases: *Propionibacterium acnes*, *Helicobacter pylori*, and beyond? *Drug Resistance Updates*, *15*(4), 223–236. https://doi.org/10.1016/j.drup.2012.07.001

Dai, T., Huang, Y. Y., & Hamblin, M. R. (2009). Photodynamic therapy for localized infections-State of the art. *Photodiagnosis and Photodynamic Therapy*, *6*(3–4), 170–188. https://doi.org/10.1016/j.pdpdt.2009.10.008

De Oliveira, E. F., Tosati, J. V., Tikekar, R. V., Monteiro, A. R., & Nitin, N. (2018). Antimicrobial activity of curcumin in combination with light against *Escherichia coli* O157:H7 and *Listeria innocua*: Applications for fresh produce sanitation. *Postharvest Biology and Technology*, *137*, 86–94. https://doi.org/10.1016/j.postharvbio.2017.11.014

Demidova, T. N., & Hamblin, M. R. (2005). Photodynamic Inactivation of *Bacillus* Spores, Mediated by Phenothiazinium Dyes. *Applied and Environmental Microbiology*, *71*(11), 6918–6925. https://doi.org/10.1128/AEM.71.11.6918-6925.2005

Diao, W. R., Hu, Q. P., Feng, S. S., Li, W. Q., & Xu, J. G. (2013). Chemical composition and antibacterial activity of the essential oil from green huajiao (Zanthoxylum schinifolium) against selected foodborne pathogens. *Journal of Agricultural and Food Chemistry*, *61*(25), 6044–6049. https://doi.org/10.1021/jf4007856

Dias, L. D., Blanco, K. C., Mfouo-Tynga, I. S., Inada, N. M., & Bagnato, V. S. (2020). Curcumin as a photosensitizer: From molecular structure to recent advances in antimicrobial photodynamic therapy. *Journal of Photochemistry and Photobiology C: Photochemistry Reviews*, *45*, 100384. https://doi.org/10.1016/j.jphotochemrev.2020.100384

Djelloul, C., & Hasseine, A. (2013). Ultrasound-assisted removal of methylene blue from aqueous solution by milk thistle seed. *Desalination and Water Treatment*, *51*(28–30), 5805–5812. https://doi.org/10.1080/19443994.2012.760113

do Prado-Silva, L., Brancini, G. T. P., Braga, G. Ú. L., Liao, X., Ding, T., & Sant'Ana, A. S. (2022). Antimicrobial photodynamic treatment (aPDT) as an innovative technology to control spoilage and pathogenic microorganisms in agri-food products: An updated review. *Food Control*, *132*(June 2021), 108527. https://doi.org/10.1016/j.foodcont.2021.108527

Dong, X., Ge, L., Abu Rabe, D. I., Mohammed, O. O., Wang, P., Tang, Y., Kathariou, S., Yang, L., & Sun, Y. P. (2020). Photoexcited state properties and antibacterial activities of carbon dots relevant to mechanistic features and implications. *Carbon*, *170*, 137–145. https://doi.org/10.1016/j.carbon.2020.08.025

Donlan, R. M. (2002). Biofilms: Microbial Life on Surfaces. *Emerging Infectious Diseases*, *8*(9), 881–890. https://doi.org/10.3201/eid0809.020063

Donnelly, R. F., McCarron, P. A., & Tunney, M. M. (2008). Antifungal photodynamic therapy. *Microbiological Research*, *163*(1), 1–12. https://doi.org/10.1016/j.micres.2007.08.001

Dorman, H. J. D., & Deans, S. G. (2000). Antimicrobial agents from plants: Antibacterial activity of plant volatile oils. *Journal of Applied Microbiology*, *88*(2), 308–316. https://doi.org/10.1046/j.1365-2672.2000.00969.x

Dos Anjos, C., Leanse, L. G., Ribeiro, M. S., Sellera, F. P., Dropa, M., Arana-Chavez, V. E., Lincopan, N., Baptista, M. S., Pogliani, F. C., Dai, T., & Sabino, C. P. (2023). New Insights into the Bacterial Targets of Antimicrobial Blue Light. *Microbiology Spectrum*, *11*(2), e02833-22. https://doi.org/10.1128/spectrum.02833-22

dos Anjos, C., Sellera, F. P., de Freitas, L. M., Gargano, R. G., Telles, E. O., Freitas, R. O., Baptista, M. S., Ribeiro, M. S., Lincopan, N., Pogliani, F. C., & Sabino, C. P. (2020). Inactivation of milk-borne pathogens by blue light exposure. *Journal of Dairy Science*, *103*(2), 1261–1268. https://doi.org/10.3168/jds.2019-16758

Dutta Gupta, S., & Jatothu, B. (2013). Fundamentals and applications of light-emitting diodes (LEDs) in in vitro plant growth and morphogenesis. *Plant Biotechnology Reports*, *7*(3), 211–220. https://doi.org/10.1007/s11816-013-0277-0

Endarko, E., Maclean, M., Timoshkin, I. V., MacGregor, S. J., & Anderson, J. G. (2012). High-intensity 405 nm light inactivation of *Listeria monocytogenes*. *Photochemistry and Photobiology*, *88*(5), 1280–1286. https://doi.org/10.1111/j.1751-1097.2012.01173.x

Eng, S.-K., Pusparajah, P., Ab Mutalib, N.-S., Ser, H.-L., Chan, K.-G., & Lee, L.-H. (2015). *Salmonella*: A review on pathogenesis, epidemiology and antibiotic resistance. *Frontiers in Life Science*, *8*(3), 284–293. https://doi.org/10.1080/21553769.2015.1051243

European Food Safety Authority (EFSA). (2009). Assessment of the Public Health significance of meticillin resistant *Staphylococcus aureus* (MRSA) in animals and foods. *EFSA Journal*, *7*(3). https://doi.org/10.2903/j.efsa.2009.993

European Food Safety Authority (EFSA) & European Centre for Disease Prevention and Control (ECDC). (2023). The European Union One Health 2022 Zoonoses Report. *EFSA Journal*, *21*(12). https://doi.org/10.2903/j.efsa.2023.8442

Fang, F. C. (2004). Antimicrobial reactive oxygen and nitrogen species: Concepts and controversies. *Nature Reviews Microbiology*, *2*(10), 820–832. https://doi.org/10.1038/nrmicro1004

Fang, F. C., Degroote, M. A., Foster, J. W., Bäumler, A. J., Ochsner, U., Testerman, T., Bearson, S., Giárd, J. C., Xu, Y., Campbell, G., & Laessig, T. (1999). Virulent *Salmonella typhimurium* has two periplasmic Cu, Zn-superoxide dismutases. *Proceedings of the National Academy of Sciences of the United States of America*, *96*(13), 7502–7507. https://doi.org/10.1073/pnas.96.13.7502

Feese, E., Sadeghifar, H., Gracz, H. S., & Argyropoulos, Dimitris S. Ghiladi, R. A. (2011). Photobactericidal Porphyrin-Cellulose Nanocrystals: Synthesis, Characterization, and Antimicrobial Properties. *Biomacromolecules*, *12*, 3528–3539.

Fekrirad, Z., Kashef, N., & Arefian, E. (2019). Photodynamic inactivation diminishes *quorum sensing*-mediated virulence factor production and biofilm formation of *Serratia marcescens*. *World*

Journal of Microbiology and Biotechnology, *35*(12), 1–9. https://doi.org/10.1007/s11274-019-2768-9

Ferrer-Espada, R., Liu, X., Goh, X. S., & Dai, T. (2019). Antimicrobial blue light inactivation of polymicrobial biofilms. *Frontiers in Microbiology*, *10*(4), 1–10. https://doi.org/10.3389/fmicb.2019.00721

Ferrer-Espada, R., Wang, Y., Goh, X. S., & Dai, T. (2020). Antimicrobial Blue Light Inactivation of Microbial Isolates in Biofilms. *Lasers in Surgery and Medicine*, *52*(5), 472–478. https://doi.org/10.1002/lsm.23159

Fetsch, A., & Johler, S. (2018). *Staphylococcus aureus* as a Foodborne Pathogen. *Current Clinical Microbiology Reports*, *5*(2), 88–96. https://doi.org/10.1007/s40588-018-0094-x

Feuerstein, O., Moreinos, D., & Steinberg, D. (2006). Synergic antibacterial effect between visible light and hydrogen peroxide on *Streptococcus mutans*. *Journal of Antimicrobial Chemotherapy*, *57*(5), 872–876. https://doi.org/10.1093/jac/dkl070

Fitzgerald, D. J., Stratford, M., Gasson, M. J., & Narbad, A. (2005). Structure−Function Analysis of the Vanillin Molecule and Its Antifungal Properties. *Journal of Agricultural and Food Chemistry*, *53*(5), 1769–1775. https://doi.org/10.1021/jf048575t

Fraikin, G. Y., Strakhovskaya, M. G., & Rubin, A. B. (1996). The role of membrane-bound porphyrin-type compound as endogenous sensitizer in photodynamic damage to yeast plasma membranes. *Journal of Photochemistry and Photobiology B: Biology*, *34*(2–3), 129–135. https://doi.org/10.1016/1011-1344(96)07287-9

Funes, M. D., Caminos, D. A., Alvarez, M. G., Fungo, F., Otero, L. A., & Durantini, E. N. (2009). Photodynamic properties and photoantimicrobial action of electrochemically generated porphyrin polymeric films. *Environmental Science and Technology*, *43*(3), 902–908. https://doi.org/10.1021/es802450b

Gábor, F., Szocs, K., Maillard, P., & Csík, G. (2001). Photobiological activity of exogenous and endogenous porphyrin derivatives in *Escherichia coli* and *Enterococcus hirae* cells. *Radiation and Environmental Biophysics*, *40*(2), 145–151. https://doi.org/10.1007/s004110100092

Gaidenko, T. A., Kim, T.-J., Weigel, A. L., Brody, M. S., & Price, C. W. (2006). The Blue-Light Receptor YtvA Acts in the Environmental Stress Signaling Pathway of *Bacillus subtilis*. *Journal of Bacteriology*, *188*(17), 6387–6395. https://doi.org/10.1128/JB.00691-06

Gallardo-Villagrán, M., Paulus, L., Leger, D. Y., Therrien, B., & Liagre, B. (2022). Dimethyl Sulfoxide: A Bio-Friendly or Bio-Hazard Chemical? The Effect of DMSO in Human Fibroblast-like Synoviocytes. *Molecules*, *27*(14), 4472. https://doi.org/10.3390/molecules27144472

Galstyan, A., & Dobrindt, U. (2019). Determining and unravelling origins of reduced photoinactivation efficacy of bacteria in milk. *Journal of Photochemistry and Photobiology B: Biology*, *197*, 111554. https://doi.org/10.1016/j.jphotobiol.2019.111554

Gao, J., & Matthews, K. R. (2020). Effects of the photosensitizer curcumin in inactivating foodborne pathogens on chicken skin. *Food Control*, *109*(October 2019), 106959. https://doi.org/10.1016/j.foodcont.2019.106959

George, S., Hamblin, M. R., & Kishen, A. (2009). Uptake pathways of anionic and cationic photosensitizers into bacteria. *Photochemical & Photobiological Sciences*, *8*(6), 788–795. https://doi.org/10.1039/b809624d

Geralde, M. C., Correa, T. Q., Vollet-Filho, J. D., Kurachi, C., Bagnato, V. S., Pratavieira, S., & De Souza, C. W. O. (2021). Evaluation of curcumin incubation time in *Staphylococcus aureus* and *Pseudomonas aeruginosa* Photodynamic Inactivation. *2021 SBFoton International Optics and Photonics Conference (SBFoton IOPC)*, 1–4. https://doi.org/10.1109/SBFotonIOPC50774.2021.9461951

Gerba, C. P., Wallis, C., & Melnick, J. L. (1977). Application of photodynamic oxidation to the disinfection o tap water, seawater, and sewage contaminated with poiliovirus. *Photochemistry and Photobiology*, *26*(5), 499–504. https://doi.org/10.1111/j.1751-1097.1977.tb07521.x

Ghate, V. S., Leong, A. L., Kumar, A., Bang, W. S., Zhou, W., & Yuk, H. G. (2015). Enhancing the antibacterial effect of 461 and 521 nm light emitting diodes on selected foodborne pathogens in trypticase soy broth by acidic and alkaline pH conditions. *Food Microbiology*, *48*, 49–57. https://doi.org/10.1016/j.fm.2014.10.014

Ghate, V. S., Ng, K. S., Zhou, W., Yang, H., Khoo, G. H., Yoon, W. B., & Yuk, H. G. (2013). Antibacterial effect of light emitting diodes of visible wavelengths on selected foodborne pathogens at different illumination temperatures. *International Journal of Food Microbiology*, *166*(3), 399–406. https://doi.org/10.1016/J.IJFOODMICRO.2013.07.018

Ghate, V. S., Zhou, W., & Yuk, H. G. (2019). Perspectives and Trends in the Application of Photodynamic Inactivation for Microbiological Food Safety. *Comprehensive Reviews in Food Science and Food Safety*, *18*(2), 402–424. https://doi.org/10.1111/1541-4337.12418

Giotis, E. S., Blair, I. S., & McDowell, D. A. (2007). Morphological changes in *Listeria monocytogenes* subjected to sublethal alkaline stress. *International Journal of Food Microbiology*, *120*(3), 250–258. https://doi.org/10.1016/j.ijfoodmicro.2007.08.036

Glueck, M., Schamberger, B., Eckl, P., & Plaetzer, K. (2017). New horizons in microbiological food safety: Photodynamic Decontamination based on a curcumin derivative. *Photochemical and Photobiological Sciences*, *16*(12), 1784–1791. https://doi.org/10.1039/c7pp00165g

Gnanasekar, S., Kasi, G., He, X., Zhang, K., Xu, L., & Kang, E. T. (2023). Recent advances in engineered polymeric materials for efficient photodynamic inactivation of bacterial pathogens. *Bioactive Materials*, *21*(May 2022), 157–174. https://doi.org/10.1016/j.bioactmat.2022.08.011

Gora, S. L., Rauch, K. D., Ontiveros, C. C., Stoddart, A. K., & Gagnon, G. A. (2019). Inactivation of biofilm-bound *Pseudomonas aeruginosa* bacteria using UVC light emitting diodes (UVC LEDs). *Water Research*, *151*, 193–202. https://doi.org/10.1016/j.watres.2018.12.021

Grinholc, M., Szramka, B., Kurlenda, J., Graczyk, A., & Bielawski, K. P. (2008). Bactericidal effect of photodynamic inactivation against methicillin-resistant and methicillin-susceptible *Staphylococcus aureus* is strain-dependent. *Journal of Photochemistry and Photobiology B: Biology*, *90*(1), 57–63. https://doi.org/10.1016/j.jphotobiol.2007.11.002

Guan, P., Fan, S., Dong, W., Wang, X., Li, Z., Song, M., & Suo, B. (2024). Comparative genomic analysis and multilocus sequence typing of *Staphylococcus aureus* reveals candidate genes for low-temperature tolerance. *Science of The Total Environment*, *923*, 171331. https://doi.org/10.1016/j.scitotenv.2024.171331

Guerrero-Beltrán, J. A., & Barbosa-Cánovas, G. V. (2004). Review: Advantages and limitations on processing foods by UV light. *Food Science and Technology International*, *10*(3), 137–147. https://doi.org/10.1177/1082013204044359

Guffey, J. S., Payne, W. C., Motts, S. D., Towery, P., Hobson, T., Harrell, G., Meurer, L., & Lancaster, K. (2016). Inactivation of *Salmonella* on tainted foods: Using blue light to disinfect cucumbers and processed meat products. *Food Science and Nutrition*, *4*(6), 878–887. https://doi.org/10.1002/fsn3.354

Guffey, J. S., Payne, W., Jones, T., & Martin, K. (2013). Evidence of resistance development by *Staphylococcus aureus* to an in vitro, multiple stage application of 405 nm light from a supraluminous diode array. *Photomedicine and Laser Surgery*, *31*(4), 179–182. https://doi.org/10.1089/pho.2012.3450

Guffey, J. S., & Wilborn, J. (2006). In vitro bactericidal effects of 405-nm and 470-nm blue light. *Photomedicine and Laser Surgery*, *24*(6), 684–688. https://doi.org/10.1089/pho.2006.24.684

Guillou, C., & Guespin-Michel, J. F. (1996). Evidence for two domains of growth temperature for the psychrotrophic bacterium *Pseudomonas fluorescens* MF0. *Applied and Environmental Microbiology*, *62*(9), 3319–3324. https://doi.org/10.1128/aem.62.9.3319-3324.1996

Gunther, N. W., Phillips, J. G., & Sommers, C. (2016). The Effects of 405-nm Visible Light on the Survival of *Campylobacter* on Chicken Skin and Stainless Steel. *Foodborne Pathogens and Disease*, *13*(5), 245–250. https://doi.org/10.1089/fpd.2015.2084

Guo, L., Zhang, C., Chen, G., Wu, M., Liu, W., Ding, C., Dong, Q., Fan, E., & Liu, Q. (2019). Reactive oxygen species inhibit biofilm formation of *Listeria monocytogenes*. *Microbial Pathogenesis*, *127*, 183–189. https://doi.org/10.1016/j.micpath.2018.11.023

Gusev, I., Ferreira, M., Versace, D. L., Abbad-Andaloussi, S., Pluczyk-Małek, S., Erfurt, K., Duda, A., Data, P., & Blacha-Grzechnik, A. (2022). Electrochemically Deposited Zinc

(Tetraamino)phthalocyanine as a Light-activated Antimicrobial Coating Effective against *S. aureus*. *Materials*, *15*(3). https://doi.org/10.3390/ma15030975

Gwynne, P. J., & Gallagher, M. P. (2018). Light as a broad-spectrum antimicrobial. *Frontiers in Microbiology*, *9*(FEB), 1–9. https://doi.org/10.3389/fmicb.2018.00119

Halstead, F. D., Thwaite, J. E., Burt, R., Laws, T. R., Raguse, M., Moeller, R., Webber, M. A., & Oppenheim, B. A. (2016). Antibacterial activity of blue light against nosocomial wound pathogens growing planktonically and as mature biofilms. *Applied and Environmental Microbiology*, *82*(13), 4006–4016. https://doi.org/10.1128/AEM.00756-16

Hamblin, M. R., & Abrahamse, H. (2020). Oxygen-independent antimicrobial photoinactivation: Type III photochemical mechanism? *Antibiotics*, *9*(2), 1–17. https://doi.org/10.3390/antibiotics9020053

Hamblin, M. R., & Hasan, T. (2004). Photodynamic therapy: A new antimicrobial approach to infectious disease? *Photochemical & Photobiological Sciences*, *3*(5), 436–450. https://doi.org/10.1039/b311900a

Harris, D. M. (2023). Spectra of pathogens predict lethality of blue light photo-inactivation. *Laser Therapy*, *30*(1). https://doi.org/10.4081/ltj.2023.314

He, Y., Pang, J., Yang, Z., Zheng, M., Yu, Y., Liu, Z., Zhao, B., Hu, G., & Yin, R. (2022). Toluidine blue O-induced photoinactivation inhibit the biofilm formation of methicillin-resistant *Staphylococcus aureus*. *Photodiagnosis and Photodynamic Therapy*, *39*(May), 102902. https://doi.org/10.1016/j.pdpdt.2022.102902

Hendiani, H., Pornour, M., Kashef, N. (2019). *Quorum-sensing*-regulated virulence factors in *Pseudomonas aeruginosa* are affected by sub-lethal photodynamic inactivation. *Photodiagnosis and Photodynamic Therapy*, 26, 8-12. https://doi.org/10.1016/j.pdpdt.2019.02.010.

Henke, P., Dolanský, J., Kubát, P., & Mosinger, J. (2020). Multifunctional Photosensitizing and Biotinylated Polystyrene Nanofiber Membranes/Composites for Binding of Biologically Active Compounds. *ACS Applied Materials & Interfaces*, *12*(16), 18792–18802. https://doi.org/10.1021/acsami.9b23104

Heredia, D. A., Martínez, S. R., Durantini, A. M., Pérez, M. E., Mangione, M. I., Durantini, J. E., Gervaldo, M. A., Otero, L. A., & Durantini, E. N. (2019). Antimicrobial Photodynamic Polymeric Films Bearing Biscarbazol Triphenylamine End-Capped Dendrimeric Zn(II) Porphyrin. *ACS Applied Materials and Interfaces*, *11*(31), 27574–27587. https://doi.org/10.1021/acsami.9b09119

Herigstad, B., Hamilton, M., & Heersink, J. (2001). How to optimize the drop plate method for enumerating bacteria. *Journal of Microbiological Methods*, *44*(2), 121–129. https://doi.org/10.1016/S0167-7012(00)00241-4

Hessling, M., Spellerberg, B., & Hoenes, K. (2017). Photoinactivation of bacteria by endogenous photosensitizers and exposure to visible light of different wavelengths—A review on existing data. *FEMS Microbiology Letters*, *364*(2), 1–12. https://doi.org/10.1093/femsle/fnw270

Hessling, M., Wenzel, U., Meurle, T., Spellerberg, B., & Hönes, K. (2020). Photoinactivation results of *Enterococcus moraviensis* with blue and violet light suggest the involvement of an unconsidered photosensitizer. *Biochemical and Biophysical Research Communications*, *533*(4), 813–817. https://doi.org/10.1016/j.bbrc.2020.09.091

Hinds, L. M., O'Donnell, C. P., Akhter, M., & Tiwari, B. K. (2019). Principles and mechanisms of ultraviolet light emitting diode technology for food industry applications. *Innovative Food Science and Emerging Technologies*, *56*(October 2018), 102153. https://doi.org/10.1016/j.ifset.2019.04.006

Hoenes, K., Bauer, R., Meurle, T., Spellerberg, B., & Hessling, M. (2021a). Inactivation Effect of Violet and Blue Light on ESKAPE Pathogens and Closely Related Non-pathogenic Bacterial Species – A Promising Tool Against Antibiotic-Sensitive and Antibiotic-Resistant Microorganisms. *Frontiers in Microbiology*, *11*, 612367. https://doi.org/10.3389/fmicb.2020.612367

Hoenes, K., Bauer, R., Spellerberg, B., & Hessling, M. (2021b). Microbial photoinactivation by visible light results in limited loss of membrane integrity. *Antibiotics*, *10*(3), 1–15. https://doi.org/10.3390/antibiotics10030341

Hoenes, K., Hess, M., Vatter, P., Spellerberg, B., & Hessling, M. (2018). 405 nm and 450 nm photoinactivation of *Saccharomyces cerevisiae*. *European Journal of Microbiology and Immunology*, *8*(4), 142–148. https://doi.org/10.1556/1886.2018.00023

Hong, H., Choi, J., Kim, H. J., & Park, S. H. (2024). Stress resistance insights of 65 *Listeria* strains: Acidic, low temperature, and high salt environments. *Microbial Pathogenesis*, *194*, 106793. https://doi.org/10.1016/j.micpath.2024.106793

Hu, X., Zhang, X., Luo, S., Wu, J., Sun, X., Liu, M., Wang, X., & Wang, X. (2021). Enhanced Sensitivity of *Salmonella* to Antimicrobial Blue Light Caused by Inactivating rfaC Gene Involved in Lipopolysaccharide Biosynthesis. *Foodborne Pathogens and Disease*, *18*(8), 599–606. https://doi.org/10.1089/fpd.2020.2888

Huang, L., Yong, K. W. L., Fernando, W. C., Carpinelli de Jesus, M., De Voss, J. J., Sultanbawa, Y., & Fletcher, M. T. (2021). The Inactivation by Curcumin-Mediated Photosensitization of *Botrytis cinerea* Spores Isolated from Strawberry Fruits. *Toxins*, *13*(3), 196. https://doi.org/10.3390/toxins13030196

Huang, S., Qin, H., & Liu, M. (2023). Photoinactivation of Escherichia coli by 405 nm and 450 nm light-emitting diodes: Comparison of continuous wave and pulsed light. *Journal of Photochemistry and Photobiology B: Biology*, *248*, 112799. https://doi.org/10.1016/j.jphotobiol.2023.112799

Huang, Y., Pei, Q., Deng, R., Zheng, X., Guo, J., Guo, D., Yang, Y., Liang, S., & Shi, C. (2020). Inactivation Efficacy of 405 nm LED Against *Cronobacter sakazakii* Biofilm. *Frontiers in Microbiology*, *11*(November), 1–12. https://doi.org/10.3389/fmicb.2020.610077

Hyun, J. E., & Lee, S. Y. (2020a). Antibacterial effect and mechanisms of action of 460–470 nm light-emitting diode against *Listeria monocytogenes* and *Pseudomonas fluorescens* on the surface of packaged sliced cheese. *Food Microbiology*, *86*(August 2019), 103314. https://doi.org/10.1016/j.fm.2019.103314

Hyun, J. E., & Lee, S. Y. (2020b). Blue light-emitting diodes as eco-friendly non-thermal technology in food preservation. *Trends in Food Science and Technology*, *105*(April), 284–295. https://doi.org/10.1016/j.tifs.2020.09.008

International Commission for Non-Ionizing Radiation Protection ICNIRP. (2013). ICNIRP Guidelines on Limits of Exposure to Incoherent Visible and Infrared Radiation. *Health Physics*, *105*(1), 74–96. https://doi.org/10.1097/hp.0000000000000119

Italian Government. (2008). D. Lgs. Gov. 81/2008. Consolidated law on health and safety at work—Testo unico in materia di salute e sicurezza sul lavoro. *Gazzetta Ufficiale*.

Izzo, A. D., & Walsh, J. T. (2004). Light-induced modulation of *Porphyromonas gingivalis* growth. *Journal of Photochemistry and Photobiology B: Biology*, *77*(1–3), 63–69. https://doi.org/10.1016/j.jphotobiol.2004.05.015

James, C., Onarinde, B. A., & James, S. J. (2017). The Use and Performance of Household Refrigerators: A Review. *Comprehensive Reviews in Food Science and Food Safety*, *16*(1), 160–179. https://doi.org/10.1111/1541-4337.12242

Jia, R., Tian, W., Bai, H., Zhang, J., Wang, S., & Zhang, J. (2019). Sunlight-Driven Wearable and Robust Antibacterial Coatings with Water-Soluble Cellulose-Based Photosensitizers. *Advanced Healthcare Materials*, *8*(5), 1801591. https://doi.org/10.1002/adhm.201801591

Jiang, Q., Geng, F., Shen, J., Zhu, P., Lu, Z., Lu, F., & Zhou, L. (2024). Blue light-mediated gene expression as a promising strategy to reduce antibiotic resistance in *Escherichia coli*. *Biotechnology Journal*, 19, e2400023. https://doi.org/10.1002/biot.202400023

Jiang, Y., Leung, A. W., Wang, X., Zhang, H., & Xu, C. (2013). Inactivation of *Staphylococcus aureus* by photodynamic action of hypocrellin B. *Photodiagnosis and Photodynamic Therapy*, *10*(4), 600–606. https://doi.org/10.1016/j.pdpdt.2013.06.004

Jo, W. K., & Tayade, R. J. (2014). New generation energy-efficient light source for photocatalysis: LEDs for environmental applications. *Industrial and Engineering Chemistry Research*, *53*(6), 2073–2084. https://doi.org/10.1021/ie404176g

Johnson, L. A., & Hug, L. A. (2019). Distribution of reactive oxygen species defense mechanisms across domain bacteria. *Free Radical Biology and Medicine*, *140*, 93–102. https://doi.org/10.1016/j.freeradbiomed.2019.03.032

Jones, T., Gill, C. O., & McMullen, L. (2002). The behaviour of log phase *Escherichia coli* at temperatures below the minimum for sustained growth. *Food Microbiology*, *19*(1), 83–90. https://doi.org/10.1006/fmic.2001.0465

Jones, T. H., Vail, K. M., & McMullen, L. M. (2013). Filament formation by foodborne bacteria under sublethal stress. *International Journal of Food Microbiology*, *165*(2), 97–110. https://doi.org/10.1016/j.ijfoodmicro.2013.05.001

Josewin, S. W., Ghate, V., Kim, M. J., & Yuk, H. G. (2018a). Antibacterial effect of 460 nm light-emitting diode in combination with riboflavin against *Listeria monocytogenes* on smoked salmon. *Food Control*, *84*, 354–361. https://doi.org/10.1016/j.foodcont.2017.08.017

Josewin, S. W., Kim, M. J., & Yuk, H. G. (2018b). Inactivation of *Listeria monocytogenes* and *Salmonella* spp. On cantaloupe rinds by blue light emitting diodes (LEDs). *Food Microbiology*, *76*(June 2017), 219–225. https://doi.org/10.1016/j.fm.2018.05.012

Joshi, P., Soares, J. M., Martins, G. M., Zucolotto Cocca, L. H., De Boni, L., De Oliveira, K. T., Bagnato, V. S., & Blanco, K. C. (2024). Enhancing the efficacy of antimicrobial photodynamic therapy through curcumin modifications. *Photochemistry and Photobiology*, php.14000. https://doi.org/10.1111/php.14000

Jung, H., & Yoon, W. B. (2023). Effect of 450 nm Visible Blue Light from Light-Emitting Diode on *Escherichia coli* O157:H7 in Agar Gels: Optimizing the Lighting Array and Quantitative Microbial Exposure Assessment. *Processes*, *11*(5), 1331. https://doi.org/10.3390/pr11051331

Jung, H., Yuk, H.-G., & Yoon, W. B. (2019). Effect of LED light on the inactivation of *Bacillus cereus* for extending shelf-life of extruded rice cake and simulation of the patterns of LED irradiation by various arrays of LEDs. *Journal of Applied Biological Chemistry*, *62*(2), 181–186. https://doi.org/10.3839/jabc.2019.025

Kadariya, J., Smith, T. C., & Dipendra. (2014). *Staphylococcus aureus* and *Staphylococcal* Food-Borne Disease: An Ongoing Challenge in Public Health. *BioMed Research International*, *827965*. https://doi.org/10.1155/2014/827965

Kebbi, Y., Muhammad, A. I., Sant'Ana, A. S., do Prado-Silva, L., Liu, D., & Ding, T. (2020). Recent advances on the application of UV-LED technology for microbial inactivation: Progress and mechanism. *Comprehensive Reviews in Food Science and Food Safety*, *19*(6), 3501–3527. https://doi.org/10.1111/1541-4337.12645

Keshishyan, E. S., Zaporozhtseva, Z. V., Zenina, O. M., & Zrodnikov, V. S. (2015). Photodynamic Inactivation of Bacteria In Vitro Under the Effect of Blue Light. *Bulletin of Experimental Biology and Medicine*, *158*(4), 475–477. https://doi.org/10.1007/s10517-015-2788-x

Keyvan, E., Kahraman, H. A., Tutun, H., Donmez, S., Sen, E., Denirtas, A., & Akyuz, A. O. (2022). Inactivation efficacy of 405 nm light emitting diodes (LEDs) on *Salmonella Enteritidis* at different illumination temperatures. *Food Science and Technology*, *42*, 1–7. https://doi.org/10.1590/fst.08721

Khan, I., Saeed, K., Zekker, I., Zhang, B., Hendi, A. H., Ahmad, A., Ahmad, S., Zada, N., Ahmad, H., Shah, L. A., Shah, T., & Khan, I. (2022). Review on Methylene Blue: Its Properties, Uses, Toxicity and Photodegradation. *Water*, *14*(2), 242. https://doi.org/10.3390/w14020242

Kim, D., & Kang, D. (2018). UVC LED Irradiation Effectively Inactivates Aerosolized Viruses, Bacteria, and Fungi in a Chamber-Type Air Disinfection System. *Environmental Microbiology*, *84*(17), 1–11.

Kim, M. J., Adeline Ng, B. X., Zwe, Y. H., & Yuk, H. G. (2017a). Photodynamic inactivation of *Salmonella enterica* Enteritidis by 405 ± 5-nm light-emitting diode and its application to control salmonellosis on cooked chicken. *Food Control*, *82*, 305–315. https://doi.org/10.1016/j.foodcont.2017.06.040

Kim, M. J., Bang, W. S., & Yuk, H. G. (2017b). 405 ± 5 nm light emitting diode illumination causes photodynamic inactivation of *Salmonella* spp. on fresh-cut papaya without deterioration. *Food Microbiology*, *62*, 124–132. https://doi.org/10.1016/j.fm.2016.10.002

Kim, M. J., Mikš-Krajnik, M., Kumar, A., Ghate, V., & Yuk, H. G. (2015). Antibacterial effect and mechanism of high-intensity 405 ± 5 nm light emitting diode on *Bacillus cereus*, *Listeria monocytogenes*, and *Staphylococcus aureus* under refrigerated condition. *Journal of Photochemistry and Photobiology B: Biology*, *153*, 33–39. https://doi.org/10.1016/j.jphotobiol.2015.08.032

Kim, M. J., Tang, C. H., Bang, W. S., & Yuk, H. G. (2017c). Antibacterial effect of 405 ± 5 nm light emitting diode illumination against *Escherichia coli* O157:H7, *Listeria monocytogenes*, and *Salmonella* on the surface of fresh-cut mango and its influence on fruit quality. *International Journal of Food Microbiology*, *244*, 82–89. https://doi.org/10.1016/j.ijfoodmicro.2016.12.023

Kim, M. J., & Yuk, H. G. (2017d). Antibacterial mechanism of 405-nanometer light-emitting diode against *Salmonella* at refrigeration temperature. *Applied and Environmental Microbiology*, *83*(5). https://doi.org/10.1128/AEM.02582-16

Kim, M.-J., Lianto, D. K., Koo, G. H., & Yuk, H.-G. (2021). Antibacterial mechanism of riboflavin-mediated 460 nm light emitting diode illumination against *Listeria monocytogenes* in phosphate-buffered saline and on smoked salmon. *Food Control*, *124*, 107930. https://doi.org/10.1016/j.foodcont.2021.107930

Kleinpenning, M. M., Smits, T., Frunt, M. H. A., van Erp, P. E. J., van de Kerkhof, P. C. M., & Gerritsen, R. M. J. P. (2010). Clinical and histological effects of blue light on normal skin.

Photodermatology Photoimmunology and Photomedicine, *26*(1), 16–21. https://doi.org/10.1111/j.1600-0781.2009.00474.x

Knodler, L. A., & Elfenbein, J. R. (2019). *Salmonella enterica*. *Trends in Microbiology*, *27*(11), 964–965. https://doi.org/10.1016/j.tim.2019.05.002

Kokare, C. R., Chakraborty, S., Khopade, A. N., & Mahadik, K. R. (2009). Biofilm: Importance and applications. *Indian Journal of Biotechnology*, *8*(2), 159–168.

Kumar, A., Alam, A., Rani, M., Ehtesham, N. Z., & Hasnain, S. E. (2017). Biofilms: Survival and defense strategy for pathogens. *International Journal of Medical Microbiology*, *307*(8), 481–489. https://doi.org/10.1016/j.ijmm.2017.09.016

Kumar, A., Ghate, V., Kim, M. J., Zhou, W., Khoo, G. H., & Yuk, H. G. (2015). Kinetics of bacterial inactivation by 405 nm and 520 nm light emitting diodes and the role of endogenous coproporphyrin on bacterial susceptibility. *Journal of Photochemistry and Photobiology B: Biology*, *149*, 37–44. https://doi.org/10.1016/j.jphotobiol.2015.05.005

Kumar, A., Ghate, V., Kim, M. J., Zhou, W., Khoo, G. H., & Yuk, H. G. (2016). Antibacterial efficacy of 405, 460 and 520 nm light emitting diodes on *Lactobacillus plantarum*, *Staphylococcus aureus* and *Vibrio parahaemolyticus*. *Journal of Applied Microbiology*, *120*(1), 49–56. https://doi.org/10.1111/jam.12975

Kumar, C. G., & Anand, S. K. (1998). Significance of microbial biofilms in food industry: A review. *International Journal of Food Microbiology*, *42*(1–2), 9–27. https://doi.org/10.1016/S0168-1605(98)00060-9

Kumar, H., Franzetti, L., Kaushal, A., & Kumar, D. (2019). Pseudomonas fluorescens: A potential food spoiler and challenges and advances in its detection. *Annals of Microbiology*, *69*(9), 873–883. https://doi.org/10.1007/s13213-019-01501-7

Lai, P., & Roy, J. (2012). Antimicrobial and Chemopreventive Properties of Herbs and Spices. *Current Medicinal Chemistry*, *11*(11), 1451–1460. https://doi.org/10.2174/0929867043365107

Lanieri, F., Conte, C., Parisi, C., Catanzano, O., Fraix, A., Quaglia, F., & Sortino, S. (2023). On the photobehaviour of curcumin in biocompatible hosts: The role of H-abstraction in the photodegradation and photosensitization. *Journal of Photochemistry & Photobiology, B: Biology*, 245, 1-10. https://doi.org/10.1016/j.jphotobiol.2023.112756

Lang, E., Thery, T., Peltier, C., Colliau, F., Adamuz, J., Grangeteau, C., Dupont, S., & Beney, L. (2022). Ultra-high irradiance (UHI) blue light: Highlighting the potential of a novel LED-based device for short antifungal treatments of food contact surfaces. *Applied Microbiology and Biotechnology*, *106*(1), 415–424. https://doi.org/10.1007/s00253-021-11718-9

Leccese, F., Vandelanotte, V., Salvadori, G., & Rocca, M. (2015). Blue light hazard and risk group classification of 8 W LED tubes, replacing fluorescent tubes, through optical radiation measurements. *Sustainability*, *7*(10), 13454–13468. https://doi.org/10.3390/su71013454

Lee, H., & Park, J.-B. (2017). Evaluation of the effects of dimethylsulphoxide on morphology, cellular viability, mRNA, and protein expression of stem cells culture in growth media. *Biomedical Reports*, *7*(4), 291–296. https://doi.org/10.3892/br.2017.961

Lee, I.-H. (2023). Quercetin mediated antimicrobial photodynamic treatment using blue light on *Escherichia coli* O157:H7 and *Listeria monocytogenes*. *Current Research in Food Science*.

Lena, A., Marino, M., Manzano, M., Comuzzi, C., & Maifreni, M. (2024). An Overview of the Application of Blue Light-Emitting Diodes as a Non-Thermic Green Technology for Microbial Inactivation in the Food Sector. *Food Engineering Reviews*. https://doi.org/10.1007/s12393-023-09355-1

Li, Q., Wang, X., Wang, P., Zhang, K., Wang, H., Feng, X., & Liu, Q. (2014). Efficacy of Chlorin e6-Mediated Sono-Photodynamic Therapy on 4T1 Cells. *Cancer Biotherapy and Radiopharmaceuticals*, *29*(1), 42–52. https://doi.org/10.1089/cbr.2013.1526

Li, T., Zhao, Y., Matthews, K., Gao, J., Hao, J., Wang, S., Han, J., & Jia, Y. (2020). Antibacterial activity against *Staphylococcus aureus* of curcumin-loaded chitosan spray coupled with photodynamic treatment. *LWT*, *134*, 110073. https://doi.org/10.1016/j.lwt.2020.110073

Li, X., Kim, M. J., Bang, W. S., & Yuk, H. G. (2018). Anti-biofilm effect of 405-nm LEDs against *Listeria monocytogenes* in simulated ready-to-eat fresh salmon storage conditions. *Food Control*, *84*, 513–521. https://doi.org/10.1016/j.foodcont.2017.09.006

Li, Y., Xu, Y., Liao, Q., Xie, M., Tao, H., & Wang, H. (2021). Synergistic effect of hypocrellin B and curcumin on photodynamic inactivation of *Staphylococcus aureus*. *Microbial Biotechnology*, *14*(2), 692–707. https://doi.org/10.1111/1751-7915.13734

Liang, C., Shi, Q., Feng, J., Yao, J., Huang, H., & Xie, X. (2022). Adsorption Behaviors of Cationic Methylene Blue and Anionic Reactive Blue 19 Dyes onto Nano-Carbon Adsorbent Carbonized from Small Precursors. *Nanomaterials*, *12*(11), 1814. https://doi.org/10.3390/nano12111814

Lin, S.-L., Hu, J., Tang, Shu-shu, Wu, Xi-yang, Chen, Zhen-qiang, & Tang, Shu-ze. (2012). Photodynamic Inactivation of Methylene Blue and Tungsten-Halogen Lamp Light against Food Pathogen *Listeria monocytogenes*. *Photochemistry and Photobiology*, *88*, 985–991. https://doi.org/10.1111/j.1751-1097.2012.01154.x

Liu, X., Chang, Q., Ferrer-Espada, R., Leanse, L. G., Goh, X. S., Wang, X., Gelfand, J. A., & Dai, T. (2020). Photoinactivation of Moraxella catarrhalis Using 405-nm Blue Light: Implications for the Treatment of Otitis Media. *Photochemistry and Photobiology*, *96*(3), 611–617. https://doi.org/10.1111/php.13241

Liu, Y., Sun, L., Huo, Y.-X., & Guo, S. (2023). Strategies for improving the production of bio-based vanillin. *Microbial Cell Factories*, *22*(1), 147. https://doi.org/10.1186/s12934-023-02144-9

Long, B., Bakr, O., & Stellacci, F. (2008). Reversible aggregation of porphyrins in the solid state. *Journal of Experimental Nanoscience*, *3*(1), 53–60. https://doi.org/10.1080/17458080802073091

Lopez, E. J. G., Rodriguez, M. R., Santamarina, S. C., Macor, L., Otero, L. A., Gervaldo, M. A., Durantini, M., Durantini, E. N., Durantini, J. E., & Heredia, D. A. (2022). Light-Activated Antibacterial Polymeric Surface Based on Porphycene. *ACS Applied Polymer Materials*, 5(1). https://doi.org/10.1021/acsapm.2c01890

Lu, P., Ahn, D., Yunis, R., Delafresnaye, L., Corrigan, N., Boyer, C., Barner-Kowollik, C., & Page, Z. A. (2021). Wavelength-selective light-matter interactions in polymer science. *Matter*, *4*(7), 2172–2229. https://doi.org/10.1016/j.matt.2021.03.021

Luksiene. (2022). A Prospect for Visible Light-Driven Nonthermal Fresh Produce Sanitation. In *Nonthermal Processing in Agri-Food-Bio Sciences*. Springer Nature.

Luksiene, Z. (2005). New approach to inactivation of harmful and pathogenic microorganisms by photosensitization. *Food Technology and Biotechnology*, *43*(4), 411–418.

Luksiene, Z., & Paskeviciute, E. (2011). Novel approach to the microbial decontamination of strawberries: Chlorophyllin-based photosensitization. *Journal of Applied Microbiology*, *110*(5), 1274–1283. https://doi.org/10.1111/j.1365-2672.2011.04986.x

Luksiene, Z., & Paskeviciute, E. (2012). Reprint of: Novel approach to decontaminate food-packaging from pathogens in non-Thermal and not chemical way: Chlorophyllin-based photosensitization q. *Journal of Food Engineering*, *110*(2), 317–323. https://doi.org/10.1016/j.jfoodeng.2011.12.028

Luksiene, Z., & Zukauskas, A. (2009). Prospects of photosensitization in control of pathogenic and harmful micro-organisms. *Journal of Applied Microbiology*, *107*(5), 1415–1424. https://doi.org/10.1111/j.1365-2672.2009.04341.x

Luo, S., Yang, X., Hu, S. W., Liu, M., Zhang, X., Sun, X., Li, Y., & Wang, X. (2021). Role of blue light in bactericidal effect against meat-borne pathogens and freshness maintaining of beef. *Journal of Food Protection*.

Maclean, M., MacGregor, S. J., Anderson, J. G., & Woolsey, G. (2008a). High-intensity narrow-spectrum light inactivation and wavelength sensitivity of *Staphylococcus aureus*. *FEMS Microbiology Letters*, *285*(2), 227–232. https://doi.org/10.1111/j.1574-6968.2008.01233.x

Maclean, M., MacGregor, S. J., Anderson, J. G., & Woolsey, G. (2009). Inactivation of bacterial pathogens following exposure to light from a 405-nanometer light-emitting diode array. *Applied and Environmental Microbiology*, *75*(7), 1932–1937. https://doi.org/10.1128/AEM.01892-08

Maclean, M., MacGregor, S. J., Anderson, J. G., & Woolsey, G. A. (2008b). The role of oxygen in the visible-light inactivation of *Staphylococcus aureus*. *Journal of Photochemistry and Photobiology B: Biology*, *92*(3), 180–184. https://doi.org/10.1016/j.jphotobiol.2008.06.006

Mains, D. R., Eallonardo, S. J., & Freitag, N. E. (2021). Identification of *Listeria monocytogenes* Genes Contributing to Oxidative Stress Resistance under Conditions Relevant to Host Infection. *Infection and Immunity*, *89*(4), e00700-20. https://doi.org/10.1128/IAI.00700-20

Makdoumi, K., Goodrich, R., & Bäckman, A. (2017). Photochemical eradication of methicillin-resistant *Staphylococcus aureus* by blue light activation of riboflavin. *Acta Ophthalmologica*, *95*(5), 498–502. https://doi.org/10.1111/aos.13409

Malik, Z., Ladan, H., & Nitzan, Y. (1992). Photodynamic inactivation of Gram-negative bacteria: Problems and possible solutions. *Journal of Photochemistry and Photobiology, B: Biology*, *14*(3), 262–266. https://doi.org/10.1016/1011-1344(92)85104-3

Managa, M., Ngoy, B. P., & Nyokong, T. (2019). Photophysical properties and photodynamic therapy activity of a *meso* -tetra(4-carboxyphenyl)porphyrin tetramethyl ester–graphene quantum dot conjugate. *New Journal of Chemistry*, *43*(11), 4518–4524. https://doi.org/10.1039/C8NJ06175K

Manzocco, L., Da Pieve, S., & Maifreni, M. (2011). Impact of UV-C light on safety and quality of fresh-cut melon. *Innovative Food Science and Emerging Technologies*, *12*(1), 13–17. https://doi.org/10.1016/j.ifset.2010.11.006

Marek, V., Mélik-Parsadaniantz, S., Villette, T., Montoya, F., Baudouin, C., Brignole-Baudouin, F., & Denoyer, A. (2018). Blue light phototoxicity toward human corneal and conjunctival epithelial cells in basal and hyperosmolar conditions. *Free Radical Biology and Medicine*, *126*(April), 27–40. https://doi.org/10.1016/j.freeradbiomed.2018.07.012

Marino, M., Maifreni, M., Baggio, A., & Innocente, N. (2018). Inactivation of foodborne bacteria biofilms by aqueous and gaseous ozone. *Frontiers in Microbiology*, *9*(AUG), 1–12. https://doi.org/10.3389/fmicb.2018.02024

Marqués-Calvo, M. S., Codony, F., Agustí, G., & Lahera, C. (2017). Visible light enhances the antimicrobial effect of some essential oils. *Photodiagnosis and Photodynamic Therapy*, *17*, 180–184. https://doi.org/10.1016/j.pdpdt.2016.12.002

Martău, G. A., Călinoiu, L.-F., & Vodnar, D. C. (2021). Bio-vanillin: Towards a sustainable industrial production. *Trends in Food Science & Technology*, *109*, 579–592. https://doi.org/10.1016/j.tifs.2021.01.059

Martegani, E., Bolognese, F., Trivellin, N., & Orlandi, V. T. (2020). Effect of blue light at 410 and 455 nm on *Pseudomonas aeruginosa* biofilm. *Journal of Photochemistry and Photobiology B: Biology*, *204*, 111790. https://doi.org/10.1016/j.jphotobiol.2020.111790

Martins Antunes De Melo, W. D. C., Celiešiūtė-Germanienė, R., Šimonis, P., & Stirkė, A. (2021). Antimicrobial photodynamic therapy (aPDT) for biofilm treatments. Possible synergy between aPDT and pulsed electric fields. *Virulence*, *12*(1), 2247–2272. https://doi.org/10.1080/21505594.2021.1960105

Martín-Sómer, M., Pablos, C., van Grieken, R., & Marugán, J. (2017). Influence of light distribution on the performance of photocatalytic reactors: LED vs mercury lamps. *Applied Catalysis B: Environmental*, *215*, 1–7. https://doi.org/10.1016/j.apcatb.2017.05.048

Mazaheri, T., Ripolles-Avila, C., & Rodríguez-Jerez, J. J. (2023). Cross-contamination of mature *Listeria monocytogenes* biofilms from stainless steel surfaces to chicken broth before and after the application of chlorinated alkaline and enzymatic detergents. *Food Microbiology*, *112*, 104236. https://doi.org/10.1016/j.fm.2023.104236

McKenzie, K., Maclean, M., Timoshkin, I. V., Endarko, E., Macgregor, S. J., & Anderson, J. G. (2013). Photoinactivation of bacteria attached to glass and acrylic surfaces by 405 nm light: Potential application for biofilm decontamination. *Photochemistry and Photobiology*, *89*(4), 927–935. https://doi.org/10.1111/php.12077

Mesquita, M. Q., Dias, C. J., Neves, M. G. P. M. S., Almeida, A., & Faustino, M. A. F. (2018). Revisiting current photoactive materials for antimicrobial photodynamic therapy. *Molecules*, *23*(10). https://doi.org/10.3390/molecules23102424

Minhaco, V. M. T. R., Maquera Huacho, P. M., Mancim Imbriani, M. J., Tonon, C. C., Chorilli, M., Rastelli, A. N. D. S., & Spolidorio, D. M. P. (2023). Improving antimicrobial activity against endodontic biofilm after exposure to blue light-activated novel curcumin nanoparticle. *Photodiagnosis and Photodynamic Therapy*, *42*, 103322. https://doi.org/10.1016/j.pdpdt.2023.103322

Minnock, A., Vernon, D. I., Schofield, J., Griffiths, J., Parish, J. H., & Brown, S. B. (1996). Photoinactivation of bacteria. Use of a cationic water-soluble zinc phthalocyanine to photoinactivate both gram-negative and gram-positive bacteria. *Journal of Photochemistry and Photobiology B: Biology*, *32*(3), 159–164. https://doi.org/10.1016/1011-1344(95)07148-2

Minor, M., & Sabillón, L. (2023). Effectiveness of Ultra-High Irradiance Blue Light-Emitting Diodes in Inactivating *Escherichia coli* O157:H7 on Dry Stainless Steel and Cast-Iron Surfaces. *Foods*, *12*(16), 3072. https://doi.org/10.3390/foods12163072

Mori, M., Hamamoto, A., Takahashi, A., Nakano, M., Wakikawa, N., Tachibana, S., Ikehara, T., Nakaya, Y., Akutagawa, M., & Kinouchi, Y. (2007). Development of a new water sterilization device with a 365 nm UV-LED. *Medical and Biological Engineering and Computing*, *45*(12), 1237–1241. https://doi.org/10.1007/s11517-007-0263-1

Muhib, M. I., Uddin, M. K., Rahman, M. M., & Malafaia, G. (2023). Occurrence of microplastics in tap and bottled water, and food packaging: A narrative review on current knowledge. *Science of the Total Environment*, *865*(11). https://doi.org/10.1016/j.scitotenv.2022.161274

Munir, Z., Banche, G., Cavallo, L., Mandras, N., Roana, J., Pertusio, R., Ficiarà, E., Cavalli, R., & Guiot, C. (2022). Exploitation of the Antibacterial Properties of Photoactivated Curcumin as 'Green'

Tool for Food Preservation. *International Journal of Molecular Sciences*, *23*(5). https://doi.org/10.3390/ijms23052600

Murdoch, L. E., MacLean, M., Endarko, E., MacGregor, S. J., & Anderson, J. G. (2012). Bactericidal effects of 405nm light exposure demonstrated by inactivation of *Escherichia*, *Salmonella*, *Shigella*, *Listeria*, and *mycobacterium* species in liquid suspensions and on exposed surfaces. *The Scientific World Journal*, *2012*. https://doi.org/10.1100/2012/137805

Murdoch, L. E., McKenzie, K., Maclean, M., MacGregor, S. J., & Anderson, J. G. (2013). Lethal effects of high-intensity violet 405-nm light on *Saccharomyces cerevisiae*, *Candida albicans*, and on dormant and germinating spores of Aspergillus niger. *Fungal Biology*, *117*(7–8), 519–527. https://doi.org/10.1016/j.funbio.2013.05.004

Nakamura, K., Ishiyama, K., Sheng, H., Ikai, H., Kanno, T., & Niwano, Y. (2015). Bactericidal Activity and Mechanism of Photoirradiated Polyphenols against Gram-Positive and -Negative Bacteria. *Journal of Agricultural and Food Chemistry*, *63*(35), 7707–7713. https://doi.org/10.1021/jf5058588

Nakamura, K., Yamada, Y., Ikai, H., Kanno, T., Sasaki, K., & Niwano, Y. (2012). Bactericidal Action of Photoirradiated Gallic Acid via Reactive Oxygen Species Formation. *Journal of Agricultural and Food Chemistry*, *60*(40), 10048–10054. https://doi.org/10.1021/jf303177p

Negri, L. B., Mannaa, Y., Korupolu, S., Farinelli, W. A., Anderson, R. R., & Gelfand, J. A. (2023). Vitamin K3 (Menadione) is a multifunctional microbicide acting as a photosensitizer and synergizing with blue light to kill drug-resistant bacteria in biofilms. *Journal of Photochemistry and Photobiology B: Biology*, *244*, 112720. https://doi.org/10.1016/j.jphotobiol.2023.112720

Nie, M., e Silva, R. C., de Oliveira, K. T., Bagnato, V. S., de Souza Rastelli, A. N., Crielaard, W., Yang, J., & Deng, D. M. (2021). Synergetic antimicrobial effect of chlorin e6 and hydrogen peroxide on multi-species biofilms. *Biofouling*, *37*(6), 656–665. https://doi.org/10.1080/08927014.2021.1954169

Ning, L. G., Liu, P., Wang, B., Li, C. M., Kang, E.-T., Lu, Z. S., Hu, X. F., & Xu, L. Q. (2019). Hydrothermal derived protoporphyrin IX nanoparticles for inactivation and imaging of bacteria strains. *Journal of Colloid and Interface Science*, *549*, 72–79. https://doi.org/10.1016/j.jcis.2019.04.050

Nitzan, Y., Salmon-Divon, M., Shporen, E., & Malik, Z. (2004). ALA induced photodynamic effects on Gram positive and negative bacteria. *Photochemical & Photobiological Sciences*, *3*(5), 430–435. https://doi.org/10.1039/b315633h

Olsson, U., Billberg, A., Sjövall, S., Al-Karadaghi, S., & Hansson, M. (2002). In Vivo and In Vitro Studies of *Bacillus subtilis* Ferrochelatase Mutants Suggest Substrate Channeling in the Heme Biosynthesis Pathway. *Journal of Bacteriology*, *184*(14), 4018–4024. https://doi.org/10.1128/JB.184.14.4018-4024.2002

Olszewska, M. A., Dev Kumar, G., Hur, M., & Diez-Gonzalez, F. (2023). Inactivation of dried cells and biofilms of *Listeria monocytogenes* by exposure to blue light at different wavelengths and the influence of surface materials. *Applied and Environmental Microbiology*, *89*(10), e01147-23. https://doi.org/10.1128/aem.01147-23

Olszewska, M. A., Zimińska, A., Draszanowska, A., & Sawicki, T. (2024). Blackthorn fruit peel polyphenol extracts and photodynamic effect under blue light against *Listeria monocytogenes*. *Food Microbiology*, *124*, 104608. https://doi.org/10.1016/j.fm.2024.104608

Oriel, S., & Nitzan, Y. (2010). Photoinactivation of candida albicans by its own endogenous porphyrins. *Current Microbiology*, *60*(2), 117–123. https://doi.org/10.1007/s00284-009-9514-8

Orlandi, V. T., Bolognese, F., Trivellin, N., Cipriano, G., Ricci, P., & Carlucci, R. (2024). Antimicrobial Blue Light (aBL) as a potential tool to reduce bacterial spoilage in the fishery chain. *Food Control*, *158*, 110254. https://doi.org/10.1016/j.foodcont.2023.110254

Page, K., Correia, A., Wilson, M., Allan, E., & Parkin, I. P. (2015). Light-activated antibacterial screen protectors for mobile telephones and tablet computers. *Journal of Photochemistry and Photobiology A: Chemistry*, *296*, 19–24. https://doi.org/10.1016/j.jphotochem.2014.08.011

Penha, C. B., Bonin, E., Da Silva, A. F., Hioka, N., Zanqueta, É. B., Nakamura, T. U., De Abreu Filho, B. A., Campanerut-Sá, P. A. Z., & Mikcha, J. M. G. (2017). Photodynamic inactivation of foodborne and food spoilage bacteria by curcumin. *LWT - Food Science and Technology*, *76*, 198–202. https://doi.org/10.1016/j.lwt.2016.07.037

Pereira, M. A., Faustino, M. A. F., Tomé, J. P. C., Neves, M. G. P. M. S., Tomé, A. C., Cavaleiro, J. A. S., Cunha, Â., & Almeida, A. (2014). Influence of external bacterial structures on the efficiency of photodynamic inactivation by a cationic porphyrin. *Photochemical & Photobiological Sciences*, *13*(4), 680–690. https://doi.org/10.1039/c3pp50408e

Peters, B. M., Jabra-Rizk, M. A., O'May, G. A., Costerton, J. W., & Shirtliff, M. E. (2012). Polymicrobial Interactions: Impact on Pathogenesis and Human Disease. *Clinical Microbiology Reviews*, *25*(1), 193–213. https://doi.org/10.1128/CMR.00013-11

Piksa, M., Lian, C., Samuel, I. C., Pawlik, K. J., Samuel, I. D. W., & Matczyszyn, K. (2023). The role of the light source in antimicrobial photodynamic therapy. *Chemical Society Reviews*, *52*(5), 1697–1722. https://doi.org/10.1039/D0CS01051K

Pileggi, G., Wataha, J. C., Girard, M., Grad, I., Schrenzel, J., Lange, N., & Bouillaguet, S. (2013). Blue light-mediated inactivation of *Enterococcus faecalis* in vitro. *Photodiagnosis and Photodynamic Therapy*, *10*(2), 134–140. https://doi.org/10.1016/j.pdpdt.2012.11.002

Plavskii, V. Y., Mikulich, A. V., Tretyakova, A. I., Leusenka, I. A., Plavskaya, L. G., Kazyuchits, O. A., Dobysh, I. I., & Krasnenkova, T. P. (2018). Porphyrins and flavins as endogenous acceptors of optical radiation of blue spectral region determining photoinactivation of microbial cells.

Journal of Photochemistry and Photobiology B: Biology, *183*(March), 172–183. https://doi.org/10.1016/j.jphotobiol.2018.04.021

Pourhajibagher, M., Ghafari, H.-A., Bahrami, R., & Bahador. (2024). Photoinactivation of *Enterococcus faecalis* Biofilm: In Vitro Antimicrobial Effect of Photoexcited Rutin-Gallium(III) Complex via Visible Blue Light. *Journal of Endodontics*, *50*(5), 602–611.

Prasad, A., Du, L., Zubair, M., Subedi, S., Ullah, A., & Roopesh, M. S. (2020). Applications of Light-Emitting Diodes (LEDs) in Food Processing and Water Treatment. *Food Engineering Reviews*, *12*(3), 268–289. https://doi.org/10.1007/s12393-020-09221-4

Prasad, A., Gänzle, M., & Roopesh, M. S. (2021). Antimicrobial activity and drying potential of high intensity blue light pulses (455 nm) emitted from LEDs. *Food Research International*, *148*, 110601. https://doi.org/10.1016/j.foodres.2021.110601

Qiang, H., Wang, J., Liu, H., & Zhu, Y. (2023). From vanillin to biobased aromatic polymers. *Polymer Chemistry*, *14*(37), 4255–4274. https://doi.org/10.1039/D3PY00767G

Rajmohan, S., Dodd, C. E. R., & Waites, W. M. (2002). Enzymes from isolates of *Pseudomonas fluorescens* involved in food spoilage. *Journal of Applied Microbiology*, *93*(2), 205–213. https://doi.org/10.1046/j.1365-2672.2002.01674.x

Rapacka-Zdończyk, A., Woźniak, A., Michalska, K., Pierański, M., Ogonowska, P., Grinholc, M., & Nakonieczna, J. (2021). Factors Determining the Susceptibility of Bacteria to Antibacterial Photodynamic Inactivation. *Frontiers in Medicine*, *8*, 642609. https://doi.org/10.3389/fmed.2021.642609

Rapacka-Zdonczyk, A., Wozniak, A., Pieranski, M., Woziwodzka, A., Bielawski, K. P., & Grinholc, M. (2019). Development of *Staphylococcus aureus* tolerance to antimicrobial photodynamic inactivation and antimicrobial blue light upon sub-lethal treatment. *Scientific Reports*, *9*(1), 1–18. https://doi.org/10.1038/s41598-019-45962-x

Ray, P. D., Huang, B. W., & Tsuji, Y. (2012). Reactive oxygen species (ROS) homeostasis and redox regulation in cellular signaling. *Cellular Signalling*, *24*(5), 981–990. https://doi.org/10.1016/j.cellsig.2012.01.008

Reynoso, E., Durantini, A. M., Solis, C. A., Macor, L. P., Otero, L. A., Gervaldo, M. A., Durantini, E. N., & Heredia, D. A. (2021). Photoactive antimicrobial coating based on a PEDOT-fullerene C60polymeric dyad. *RSC Advances*, *11*(38), 23519–23532. https://doi.org/10.1039/d1ra03417k

Ricciardi, E. F., Pedros-Garrido, S., Papoutsis, K., Lyng, J. G., Conte, A., & Del Nobile, M. A. (2020). Novel technologies for preserving ricotta cheese: Effects of ultraviolet and near-ultraviolet–visible light. *Foods*, *9*(5). https://doi.org/10.3390/foods9050580

Rincón, A. G., & Pulgarin, C. (2003). Photocatalytical inactivation of *E. coli*: Effect of (continuous–intermittent) light intensity and of (suspended–fixed) TiO2 concentration. *Applied Catalysis B: Environmental*, *44*(3), 263–284. https://doi.org/10.1016/S0926-3373(03)00076-6

Rossi, G., Goi, D., & Comuzzi, C. (2012). The photodynamic inactivation of *Staphylococcus aureus* in water using visible light with a new expanded porphyrin. *Journal of Water and Health*, *10*(3), 390–399. https://doi.org/10.2166/wh.2012.034

Roy, R., Tiwari, M., Donelli, G., & Tiwari, V. (2018). Strategies for combating bacterial biofilms: A focus on anti-biofilm agents and their mechanisms of action. *Virulence*, *9*(1), 522–554. https://doi.org/10.1080/21505594.2017.1313372

Sabino, C. P., Wainwright, M., dos Anjos, C., Sellera, F. P., Baptista, M. S., Lincopan, N., & Ribeiro, M. S. (2019). Inactivation kinetics and lethal dose analysis of antimicrobial blue light and photodynamic therapy. *Photodiagnosis and Photodynamic Therapy*, *28*(July), 186–191. https://doi.org/10.1016/j.pdpdt.2019.08.022

Saltos, J. A., Shi, W., Mancuso, A., Sun, C., Park, T., Averick, N., Punia, K., Fata, J., & Raja, K. (2014). Curcumin-derived green plasticizers for poly(vinyl) chloride. *RSC Advances*, *4*(97), 54725–54728. https://doi.org/10.1039/c4ra10581h

Santamarina, S. C., Heredia, D. A., Durantini, A. M., & Durantini, E. N. (2022). Antimicrobial Photosensitizing Material Based on Conjugated Zn(II) Porphyrins. *Antibiotics*, *11*(1). https://doi.org/10.3390/antibiotics11010091

Saraiva, B. B., Sestito, J. M. B., Bezerra, R. A. D., De Oliveira, G. L. M., Da Silva Júnior, R. C., Machado, R. R. B., Nakamura, C. V., Alfieri, A. A., & Pozza, M. S. D. S. (2024). Reduction of *Staphylococcus aureus* in vitro and in milk by photodynamic inactivation using riboflavin and curcumin as photosensitizers: Cell damage and effects on product quality. *Journal of Photochemistry and Photobiology A: Chemistry*, *446*, 115120. https://doi.org/10.1016/j.jphotochem.2023.115120

SCCS, S. C. on C. S. (2010). Opinion on triclosan—Antimicrobial resistance. In *Scientific Committee on Consumer Safety SCCS*. https://doi.org/10.2772/11162

Schlegelová, J., Babák, V., Holasová, M., Konstantinová, L., Necidová, L., Šišák, F., Vlková, H., Roubal, P., & Jaglic, Z. (2010). Microbial contamination after sanitation of food contact surfaces in dairy and meat processing plants. *Czech Journal of Food Sciences*, *28*(5), 450–461. https://doi.org/10.17221/65/2009-CJFS

Seyler, J., Olson, J. W., & Maier, R. J. (2001). Superoxide dismutase-deficient mutants of *Helicobacter pylori* are hypersensitive to oxidative stress and defective in host colonization. *Infection and Immunity*, *69*(6), 4034–4040. https://doi.org/10.1128/IAI.69.6.4034-4040.2001

Shapiro, R. S., & Cowen, L. E. (2012). Thermal Control of Microbial Development and Virulence: Molecular Mechanisms of Microbial Temperature Sensing. *mBio*, *3*(5), e00238-12. https://doi.org/10.1128/mBio.00238-12

Sheng, L., Li, X., & Wang, L. (2022). Photodynamic inactivation in food systems: A review of its application, mechanisms, and future perspective. *Trends in Food Science and Technology*, *124*(10), 167–181. https://doi.org/10.1016/j.tifs.2022.04.001

Shi, Y. gang, Jiang, L., Lin, S., Jin, W. gang, Gu, Q., Chen, Y. wen, Zhang, K., & Ettelaie, R. (2022a). Ultra-efficient antimicrobial photodynamic inactivation system based on blue light and octyl gallate for ablation of planktonic bacteria and biofilms of *Pseudomonas fluorescens*. *Food Chemistry*, *374*(August 2021), 131585. https://doi.org/10.1016/j.foodchem.2021.131585

Shi, Y., Lin, S., Chen, W., Jiang, L., Gu, Q., Li, D., & Chen, Y. (2022b). Dual-Stage Blue-Light-Guided Membrane and DNA-Targeted Photodynamic Inactivation Using Octyl Gallate for Ultraefficient Eradication of Planktonic Bacteria and Sessile Biofilms. *Journal of Agricultural and Food Chemistry*, *70*(24), 7547–7565. https://doi.org/10.1021/acs.jafc.2c01667

Shirai, A., Yasutomo, Y., & Kanno, Y. (2022). Effects of Violet-Blue Light-Emitting Diode on Controlling Bacterial Contamination in Boiled Young Sardine. *Biocontrol Science*, *27*(1), 9–19.

Singh, H., Bhardwaj, S. K., Khatri, M., Kim, K. H., & Bhardwaj, N. (2021). UVC radiation for food safety: An emerging technology for the microbial disinfection of food products. *Chemical Engineering Journal*, *417*, 128084. https://doi.org/10.1016/j.cej.2020.128084

Soares, C. J., de Paula Rodrigues, M., Vilela, A. B. F., Rizo, E. R. C., Ferreira, L. B., Giannini, M., & Price, R. B. (2017). Evaluation of eye protection filters used with broad-spectrum and conventional LED curing lights. *Brazilian Dental Journal*, *28*(1), 9–15. https://doi.org/10.1590/0103-6440201701380

Song, J., Wang, M., Tao, H., Yang, A., Zhu, Z., Bai, S., Luo, M., Xu, J., Liu, X., Sun, Y., Hu, P., Wong, W.-L., Li, F., Chen, Y., Cai, Q., Liu, H., Huang, S.-Y., Su, Z., & Feng, X. (2023). Manipulation of Bacterial ROS Production Leads to Self-escalating DNA Damage and Resistance-resistant Lethality for Intracellular Mycobacteria. *BioRxiv,* https://doi.org/10.1101/2023.07.07.548098

Song, L., Zhang, F., Yu, J., Wei, C., Han, Q., & Meng, X. (2020). Antifungal effect and possible mechanism of curcumin mediated photodynamic technology against *Penicillium expansum*. *Postharvest Biology and Technology*, *167*(May), 111234. https://doi.org/10.1016/j.postharvbio.2020.111234

Soro, A. B., Shokri, S., Nicolau-Lapeña, I., Ekhlas, D., Burgess, C. M., Whyte, P., Bolton, D. J., Bourke, P., & Tiwari, B. K. (2023). Current challenges in the application of the UV-LED technology for food decontamination. *Trends in Food Science & Technology*, *131*, 264–276. https://doi.org/10.1016/j.tifs.2022.12.003

Srimagal, A., Ramesh, T., & Sahu, J. K. (2016). Effect of light emitting diode treatment on inactivation of *Escherichia coli* in milk. *LWT - Food Science and Technology*, *71*, 378–385. https://doi.org/10.1016/j.lwt.2016.04.028

Stura, I., Munir, Z., Cavallo, L., Torri, L., Mandras, N., Banche, G., Spagnolo, R., Pertusio, R., Cavalli, R., & Guiot, C. (2023). Combining Blue Light and Yellow Curcumin to Obtain a “Green” Tool for Berry Preservation against Bacterial Contamination: A Preliminary Investigation. *Foods*, *12*(10), 2038. https://doi.org/10.3390/foods12102038

Taher, M. A., Wang, X., Faridul Hasan, K. M., Miah, M. R., Zhu, J., & Chen, J. (2023). Lignin Modification for Enhanced Performance of Polymer Composites. *ACS Applied Bio Materials*, *6*(12), 5169–5192. https://doi.org/10.1021/acsabm.3c00783

Tao, J., Li, S., Ye, F., Zhou, Y., Lei, L., & Zhao, G. (2020). Lignin – An underutilized, renewable and valuable material for food industry. *Critical Reviews in Food Science and Nutrition*, *60*(12), 2011–2033. https://doi.org/10.1080/10408398.2019.1625025

Tariq, B., Simon, S. R., Pilz, W., Maxim, A., Kremer, B., & Baijens, L. W. J. (2021). Evaluating the safety of oral methylene blue during swallowing assessment: A systematic review. *European Archives of Oto-Rhino-Laryngology*, *278*(9), 3155–3169. https://doi.org/10.1007/s00405-020-06509-3

Thakur, M., Asrani, R. K., & Patial, V. (2018). Chapter 6—*Listeria monocytogenes*: A Food-Borne Pathogen. In A. M. Holban & A. M. Grumezescu (Eds.), *Foodborne Diseases* (pp. 157–192). Academic Press. https://doi.org/10.1016/B978-0-12-811444-5.00006-3

Thandu, M. M., Cavalli, S., Rossi, G., Rizzardini, C. B., Goi, D., & Comuzzi, C. (2017). Biological evaluation of a Porphyrin-SPION nanoconjugate as an antimicrobial magnetic photosensitizer. *Journal of Porphyrins and Phthalocyanines*, *21*(9), 581–588. https://doi.org/10.1142/S1088424617500560

Thandu, M. M., Rossi, G., Goi, D., Guerriero, P., Poletti, D., Strazzolini, P., & Comuzzi, C. (2021). Synthesis, characterization, and photodynamic activity of new antimicrobial PVC based composite materials. *European Polymer Journal*, *160*, 110805. https://doi.org/10.1016/j.eurpolymj.2021.110805

Thandu, M., Rapozzi, V., Xodo, L., Albericio, F., Comuzzi, C., & Cavalli, S. (2014). Clicking porphyrins to magnetic nanoparticles for photodynamic therapy. *ChemPlusChem*, *79*(1), 90–98. https://doi.org/10.1002/cplu.201300276

Tomb, R. M., White, T. A., Coia, J. E., Anderson, J. G., MacGregor, S. J., & Maclean, M. (2018). Review of the Comparative Susceptibility of Microbial Species to Photoinactivation Using 380–480 nm Violet-Blue Light. *Photochemistry and Photobiology*, *94*(3), 445–458. https://doi.org/10.1111/php.12883

Tortik, N., Spaeth, A., & Plaetzer, K. (2014). Photodynamic decontamination of foodstuff from *Staphylococcus aureus* based on novel formulations of curcumin. *Photochemical and Photobiological Sciences*, *13*(10), 1402–1409. https://doi.org/10.1039/c4pp00123k

Trevisan, A., Piovesan, S., Leonardi, A., Bertocco, M., Nicolosi, P., Pelizzo, M. G., & Angelini, A. (2006). Unusual High Exposure to Ultraviolet-C Radiation. *Photochemistry and Photobiology*, *82*(4), 1077. https://doi.org/10.1562/2005-10-27-ra-728

Trinetta, V., Vaidya, N., Linton, R., & Morgan, M. (2011). Evaluation of Chlorine Dioxide Gas Residues on Selected Food Produce. *Journal of Food Science*, *76*(1). https://doi.org/10.1111/j.1750-3841.2010.01911.x

Truchado, P., Gil, M. I., Larrosa M., & Allende A. (2020). Detection and Quantification Methods for Viable but Non-culturable (VBNC) Cells in Process Wash Water of Fresh-Cut Produce: Industrial Validation. *Frontiers in Microbiology*, 11. 10.3389/fmicb.2020.00673

Trzaska, W. J., Wrigley, H. E., Thwaite, J. E., & May, R. C. (2017). Species-specific antifungal activity of blue light. *Scientific Reports*, *7*(1), 1–7. https://doi.org/10.1038/s41598-017-05000-0

Trznadel, M., & Kryszewski, M. (1992). Thermal Shrinkage of Oriented Polymers. *Journal of Macromolecular Science, Part C: Polymer Reviews*, *32*(3–4), 259–300. https://doi.org/10.1080/15321799208021428

Tsutsumi-Arai, C., Arai, Y., Terada-Ito, C., Imamura, T., Tatehara, S., Ide, S., Wakabayashi, N., & Satomura, K. (2022). Microbicidal effect of 405-nm blue LED light on *Candida albicans* and *Streptococcus mutans* dual-species biofilms on denture base resin. *Lasers in Medical Science*, *37*(2), 857–866. https://doi.org/10.1007/s10103-021-03323-z

Tyagi, A. K., & Malik, A. (2012). Bactericidal action of lemon grass oil vapors and negative air ions. *Innovative Food Science & Emerging Technologies*, *13*, 169–177. https://doi.org/10.1016/j.ifset.2011.09.007

Uruén, C., Chopo-Escuin, G., Tommassen, J., Mainar-Jaime, R. C., & Arenas, J. (2020). Biofilms as Promoters of Bacterial Antibiotic Resistance and Tolerance. *Antibiotics*, *10*(1), 3. https://doi.org/10.3390/antibiotics10010003

Utsunomiya, T., Yamane, Y. I., Watanabe, M., & Sasaki, K. (2003). Stimulation of porphyrin production by application of an external magnetic field to a photosynthetic bacterium, *Rhodobacter sphaeroides*. *Journal of Bioscience and Bioengineering*, *95*(4), 401–404. https://doi.org/10.1263/jbb.95.401

Van Dijk, H. F. G., Verbrugh, H. A., Ad hoc advisory committee on disinfectants of the Health Council of the Netherlands, Abee, T., Andriessen, J. W., Van Dijk, H. F. G., Ter Kuile, B. H., Mevius, D. J., Montforts, M. H. M. M., Van Schaik, W., Schmitt, H., Smidt, H., Veening, J.-W., & Voss, A. (2022). Resisting disinfectants. *Communications Medicine*, *2*(1), 6. https://doi.org/10.1038/s43856-021-00070-8

Vecchio, D., Gupta, A., Huang, L., Landi, G., Avci, P., Rodas, A., & Hamblin, M. R. (2015). Bacterial Photodynamic Inactivation Mediated by Methylene Blue and Red Light Is Enhanced by

Synergistic Effect of Potassium Iodide. *Antimicrobial Agents and Chemotherapy*, *59*(9), 5203–5212. https://doi.org/10.1128/AAC.00019-15

Verheijen, M., Lienhard, M., Schrooders, Y., Clayton, O., Nudischer, R., Boerno, S., Timmermann, B., Selevsek, N., Schlapbach, R., Gmuender, H., Gotta, S., Geraedts, J., Herwig, R., Kleinjans, J., & Caiment, F. (2019). DMSO induces drastic changes in human cellular processes and epigenetic landscape in vitro. *Scientific Reports*, *9*(1), 4641. https://doi.org/10.1038/s41598-019-40660-0

Vieira, C., Gomes, A. T. P. C., Mesquita, M. Q., Moura, N. M. M., Neves, M. G. P. M. S., Faustino, M. A. F., & Almeida, A. (2018). An Insight Into the Potentiation Effect of Potassium Iodide on aPDT Efficacy. *Frontiers in Microbiology*, *9*, 2665. https://doi.org/10.3389/fmicb.2018.02665

Vilhunen, S., Särkkä, H., & Sillanpää, M. (2009). Ultraviolet light-emitting diodes in water disinfection. *Environmental Science and Pollution Research*, *16*(4), 439–442. https://doi.org/10.1007/s11356-009-0103-y

Vollmerhausen, T. L., Conneely, A., Bennett, C., Wagner, V. E., Victor, J. C., & O'Byrne, C. P. (2017). Visible and UVA light as a potential means of preventing *Escherichia coli* biofilm formation in urine and on materials used in urethral catheters. *Journal of Photochemistry and Photobiology B: Biology*, *170*(April), 295–303. https://doi.org/10.1016/j.jphotobiol.2017.04.018

Wang, D., Kyere, E., & Sadiq, F. A. (2021). New trends in photodynamic inactivation (Pdi) combating biofilms in the food industry—A review. *Foods*, *10*(11), 1–20. https://doi.org/10.3390/foods10112587

Wang, F., Wang, R., Pan, Y., Du, M., Zhao, Y., & Liu, H. (2022). Gelatin/Chitosan Films Incorporated with Curcumin Based on Photodynamic Inactivation Technology for Antibacterial Food Packaging. *Polymers*, *14*(8). https://doi.org/10.3390/polym14081600

Wang, Y., Ferrer-Espada, R., Baglo, Y., Goh, X. S., Held, K. D., Grad, Y. H., Gu, Y., Gelfand, J. A., & Dai, T. (2019). Photoinactivation of *Neisseria gonorrhoeae*: A Paradigm-Changing Approach for Combating Antibiotic-Resistant Gonococcal Infection. *The Journal of Infectious Diseases*, *220*(5), 873–881. https://doi.org/10.1093/infdis/jiz018

Wang, Y., Wang, Y., Wang, Y., Murray, C. K., Hamblin, M. R., Hooper, D. C., & Dai, T. (2017). Antimicrobial blue light inactivation of pathogenic microbes: State of the art. *Drug Resistance Updates*, *33–35*(June), 1–22. https://doi.org/10.1016/j.drup.2017.10.002

Weber, D. J., Rutala, W. A., Sickbert-Bennett, E. E., Kanamori, H., & Anderson, D. (2019). Continuous room decontamination technologies. *American Journal of Infection Control*, *47*, A72–A78. https://doi.org/10.1016/j.ajic.2019.03.016

Weber, M. M., French, C. L., Barnes, M. B., Siegele, D. A., & McLean, R. J. C. (2010). A previously uncharacterized gene, yjfO (bsmA), influences *Escherichia coli* biofilm formation and stress response. *Microbiology*, *156*(1), 139–147. https://doi.org/10.1099/mic.0.031468-0

Wolcott, R., Costerton, J. W., Raoult, D., & Cutler, S. J. (2013). The polymicrobial nature of biofilm infection. *Clinical Microbiology and Infection*, *19*(2), 107–112. https://doi.org/10.1111/j.1469-0691.2012.04001.x

World Health Organization. (2015). Food-Borne Disease Burden Epidemiology Reference Group. *WHO Library Cataloguing-in-Publication Data*, 1–1. https://doi.org/10.1007/978-3-642-27769-6_3884-1

Wu, S., Ross, C., Hadi, J., & Brightwell, G. (2021). In vitro inactivation effect of blue light emitting diode (LED) on Shiga-toxin-producing *Escherichia coli* (STEC). *Food Control*, *125*(November 2020), 107990. https://doi.org/10.1016/j.foodcont.2021.107990

Würtele, M. A., Kolbe, T., Lipsz, M., Külberg, A., Weyers, M., Kneissl, M., & Jekel, M. (2011). Application of GaN-based ultraviolet-C light emitting diodes—UV LEDs—For water disinfection. *Water Research*, *45*(3), 1481–1489. https://doi.org/10.1016/j.watres.2010.11.015

Xu, F., Hu, J., Sriboonvorakul, N., & Lin, S. (2024). Evaluation of antimicrobial photodynamic activity of CuminUP60®- A commercially-available high-soluble curcumin. *LWT*, *205*, 116490. https://doi.org/10.1016/j.lwt.2024.116490

Xu, X., Li, P., Zhong, Y., Yu, J., Miao, C., & Tong, G. (2023). Review on the oxidative catalysis methods of converting lignin into vanillin. *International Journal of Biological Macromolecules*, *243*, 125203. https://doi.org/10.1016/j.ijbiomac.2023.125203

Yagi, N., Mori, M., Hamamoto, A., Nakano, M., Akutagawa, M., Tachibana, S., Takahashi, A., Ikehara, T., & Kinouchi, Y. (2007). Sterilization Using 365 nm UV-LED. *2007 29th Annual International Conference of the IEEE Engineering in Medicine and Biology Society*, 5841–5844. https://doi.org/10.1109/IEMBS.2007.4353676

Yang, P., Wang, N., Wang, C., Yao, Y., Fu, X., Yu, W., Cai, R., & Yao, M. (2017). 460 nm visible light irradiation eradicates MRSA via inducing prophage activation. *Journal of Photochemistry and Photobiology B: Biology*, *166*, 311–322. https://doi.org/10.1016/j.jphotobiol.2016.12.001

Yang, R., Xu, Y., Xu, J., Li, Y., Wan, X., Kong, R., Ding, C., Tao, H., & Wang, H.-L. (2024). The transcriptional changes of LrgA discriminates the responsiveness of *Staphylococcus aureus* towards blue light from that of photodynamic inactivation. *Journal of Photochemistry and Photobiology B: Biology*, *258*, 112967. https://doi.org/10.1016/j.jphotobiol.2024.112967

Yang, S. M., Lee, D. W., Park, H. J., Kwak, M. H., Park, J. M., & Choi, M. (2019). Hydrogen Peroxide Enhances the Antibacterial Effect of Methylene Blue-based Photodynamic Therapy on Biofilm-forming Bacteria. *Photochemistry and Photobiology*, *95*(3), 833–838. https://doi.org/10.1111/php.13056

Yin, R., Dai, T., Avci, P., Jorge, A. E. S., De Melo, W. C. M. A., Vecchio, D., Huang, Y. Y., Gupta, A., & Hamblin, M. R. (2013). Light based anti-infectives: Ultraviolet C irradiation, photodynamic

therapy, blue light, and beyond. *Current Opinion in Pharmacology*, *13*(5), 731–762. https://doi.org/10.1016/j.coph.2013.08.009

Yuan, L., Lyu, P., Huang, Y.-Y., Du, N., Qi, W., Hamblin, M. R., & Wang, Y. (2020). Potassium iodide enhances the photobactericidal effect of methylene blue on *Enterococcus faecalis* as planktonic cells and as biofilm infection in teeth. *Journal of Photochemistry and Photobiology B: Biology*, *203*, 111730. https://doi.org/10.1016/j.jphotobiol.2019.111730

Zaffina, S., Camisa, V., Lembo, M., Vinci, M. R., Tucci, M. G., Borra, M., Napolitano, A., & Cannatã, V. (2012). Accidental exposure to UV radiation produced by germicidal lamp: Case report and risk assessment. *Photochemistry and Photobiology*, *88*(4), 1001–1004. https://doi.org/10.1111/j.1751-1097.2012.01151.x

Zenichowski, K., Gothe, M., & Saalfrank, P. (2007). Exciting flavins: Absorption spectra and spin–orbit coupling in light–oxygen–voltage (LOV) domains. *Journal of Photochemistry and Photobiology A: Chemistry*, 190(2–3). https://doi.org/10.1016/j.jphotochem.2007.02.007.

Zhang, J., Zhang, F., Tang, Q., Xu, C., & Meng, X. (2018). Effect of photodynamic inactivation of *Escherichia coli* by hypericin. *World Journal of Microbiology and Biotechnology*, *34*(7), 100. https://doi.org/10.1007/s11274-018-2464-1

Zhang, L., Li, Y., Lintian, Yuan, Qianyi, Zhang, Yuqing, Yan, Fan, Dong, Jun, Tang, & Yuguang, Wang. (2023). Advanced and Readily-Available Wireless-Powered Blue-Light-Implant for Non-Invasive Peri-ImplantDisinfection. *Advanced Science*, *10*(2203472), 1–12. https://doi.org/10.1002/advs.202203472

Zhang, X.-S., García-Contreras, R., & Wood, T. K. (2007). YcfR (BhsA) Influences *Escherichia coli* Biofilm Formation through Stress Response and Surface Hydrophobicity. *Journal of Bacteriology*, *189*(8), 3051–3062. https://doi.org/10.1128/JB.01832-06

Zhang, Y., Zhu, Y., Gupta, A., Huang, Y., Murray, C. K., Vrahas, M. S., Sherwood, M. E., Baer, D. G., Hamblin, M. R., & Dai, T. (2014). Antimicrobial blue light therapy for multidrug-resistant *Acinetobacter baumannii* infection in a mouse burn model: Implications for prophylaxis and treatment of combat-related wound infections. *Journal of Infectious Diseases*, *209*(12), 1963–1971. https://doi.org/10.1093/infdis/jit842

Zhao, B., Lv, L.-P., Ma, P., Zhang, Y.-Y., Deng, J., & Zhang, Y.-Y. (2023). A novel exposure mode based on UVA-LEDs for bacterial inactivation. *Journal of Photochemistry and Photobiology B: Biology*, *239*, 112641. https://doi.org/10.1016/j.jphotobiol.2022.112641

Zhao, X., & Drlica, K. (2014). Reactive oxygen species and the bacterial response to lethal stress. *Current Opinion in Microbiology*, *21*, 1–6. https://doi.org/10.1016/j.mib.2014.06.008

Ziege, R., Tsirigoni, A.-M., Large, B., Serra, D. O., Blank, K. G., Hengge, R., Fratzl, P., & Bidan, C. M. (2021). Adaptation of *Escherichia coli* Biofilm Growth, Morphology, and Mechanical

Properties to Substrate Water Content. *ACS Biomaterials Science & Engineering*, *7*(11), 5315–5325. https://doi.org/10.1021/acsbiomaterials.1c00927

Zwinkels, J. (2015). Encyclopedia of Color Science and Technology. In *Encyclopedia of Color Science and Technology* (pp. 1–8). https://doi.org/10.1007/978-3-642-27851-8